universität wien

MASTERARBEIT | MASTER'S THESIS

Titel | Title

Evaluation of a qPCR-based telomere sequence variant detection assay on several ALT model cell lines

verfasst von | submitted by

Nicolai Valentin Hörstke B.Sc.

angestrebter akademischer Grad | in partial fulfilment of the requirements for the degree of

Master of Science (MSc)

Wien | Vienna, 2024

Studienkennzahl lt. Studienblatt | Degree programme code as it appears on the student record sheet:	UA 066 834
Studienrichtung lt. Studienblatt | Degree programme as it appears on the student record sheet:	Masterstudium Molekulare Biologie
Betreut von | Supervisor:	Dipl.-Ing. Dr. Klaus Holzmann

Acknowledgments

First, I want to thank Ao. Univ.-Prof. Dipl.-Ing. Dr. Klaus Holzmann for his support, his advice and for giving me the opportunity to perform the research described in this thesis in his lab.

My gratitude also goes to Doris Mejri for always being present in the lab and providing training for the methods and help when it was needed and to Judith Heininger, BSc. for assisting me with some of the experiments and especially for supporting me performing the cell culture.

Additionally, I want to thank the team at the imaging core facility of the Center for Cancer Research of the Medical University of Vienna for assisting me while performing the FISH experiments described in this thesis.

I am deeply grateful for the support of my family and friends, especially Ines Munker, BA. and Marle Poppelaars, MSc. for providing me feedback for this thesis.

Table of contents

1. Zusammenfassung 5
2. Abstract 6
3. Abbreviations and symbols 7
4. Introduction 9
   4.1. ALT-activity detection 9
      4.1.1. C-circle assay 10
      4.1.2. Native ALT-FISH 11
   4.2. qPCR-based variant detection 11
   4.3. Telomere-variant FISH 13
   4.4. Aim of this work 14
5. Material and Methods 15
   5.1. Cell culture 15
      5.1.1. Cell lines 15
      5.1.1. Defrosting of cells from cryo stocks 15
      5.1.2. Trypsinization of adherent cells 19
      5.1.3. Cell counting 19
      5.1.4. Cell pellet preparation 20
      5.1.5. Cryo vial preparation 20
      5.1.6. Cytospin 20
      5.1.7. Microscopic analysis of cell culture 21
   5.2. DNA isolation 21
   5.3. C-circle assay 22
   5.4. Native ALT-FISH 24
   5.5. qPCR assays 26
      5.5.1. CCA qPCR 29
      5.5.2. Telomere sequence-variant qPCR 31
      5.5.3. TCAGGG cluster oligo variant qPCR 35

5.6. Restriction enzyme digest for TGAGGG and TCAGGG telomere sequence variants in genomic DNA 35
5.7. Telomere-variant FISH 36
5.8. Analysis and quantification of FISH images 41
5.9. Establishment of monoclonal cell lines 44
5.10. Statistical analysis 45
5.10.1. Native ALT-FISH 45
5.10.2. Telomere sequence-variant qPCR 45
5.10.3. Telomere-variant FISH 47
6. Results 48
6.1. ALT activity detection 48
6.1.1. ALT activity detection by C-circle assay 48
6.1.2. ALT activity detection by Native ALT-FISH 50
6.2. qPCR-based variant detection 65
6.2.1. NCTR variants in gDNA samples 65
6.2.2. Correlation with whole genome sequencing data 84
6.2.3. NCTR variants in C-circle assay products 86
6.2.4. qPCR of TCAGGG and TGAGGG restriction digest products 96
6.2.5. TCAGGG cluster variant DNA oligomer qPCR 100
6.3. Telomere-variant FISH 104
6.4. Establishment of monoclonal cell lines 115
7. Discussion 116
7.1. ALT activity detection 116
7.2. qPCR-based variant detection 118
7.2.1. gDNA samples 118
7.2.2. Correlation with whole genome sequencing data 118
7.2.1. C-circle assay products 119
7.2.2. TCAGGG and TGAGGG restriction digest products 120
7.2.3. TCAGGG cluster oligo variant qPCR 120

7.3. Telomere-variant FISH 120
7.4. Conclusion 121
8. References 123
9. List of Tables 128
10. List of Figures 133
11. Annex 135
11.1. STR-Marker profiles 135
11.2. ALT activity detection 135
11.2.1. C-circle assay 135
11.2.2. Native ALT-FISH 150
11.3. qPCR-based variant detection 157
11.3.1. gDNA samples 157
11.3.2. Correlation with whole genome sequencing data 162
11.3.1. C-circle assay products 163
11.3.2. TCAGGG and TGAGGG restriction digest products 166
11.3.3. TCAGGG cluster variant DNA oligomer qPCR 166
11.4. Telomere-variant FISH 167

1. Zusammenfassung

Die alternative Verlängerung der Telomere (ALT) ist ein Telomererhaltungsmechanismus (TMM), der bei etwa 10-15 Prozent der Krebsarten vorliegt. ALT führt zu heterogenen Telomerlängen und Variantenwiederholungen (NCTRs) in den distalen Telomerregionen, was zu einer verringerten Shelterinfunktion führt. Bislang wurden diese Varianten hauptsächlich durch Sequenzierung des gesamten Genoms (WGS) nachgewiesen. In dieser Studie wurde ein qPCR-basierter Nachweis von Telomervarianten evaluiert.

Zelllinienmodelle mit definiertem TMM wurden mit C-Circle-Assays (CCA) und quantitativem ALT-FISH auf ihre ALT-Aktivität hin überprüft, welche bei fünf von sechs ALT-Zelllinien gezeigt wurde. Außerdem wurde das das Vorhandensein von NCTRs in C-Circles, indem der Variantennachweis-Assay auf die Produkte der CCAs angewendet wurde.

Im Anschluss wurden Telomersequenzvarianten (TCAGGG, TGAGGG, TAAGGG) durch einen qPCR-basierten Assay sowie durch quantitative FISH (nur TCAGGG und TGAGGG) nachgewiesen. Der Vergleich der Ergebnisse untereinander und mit publizierten WGS-Daten zeigte statistisch signifikante, starke Korrelationen zwischen qPCR- und WGS-Daten für die TCAGGG- und TGAGGG-Varianten. Zusätzlich wurde die Fähigkeit des Assays Cluster mit mehreren Variantenwiederholungen zu erkennen an verschiedenen TCAGGG-Variantenoligonukleotiden getestet sowie seine Spezifität ermittelt, indem er an mit für TCAGGG- und TGAGGG-Varianten spezifischen Restriktionsenzymen verdauten DNA angewandt wurde. Bei diesen Experimenten wurde die abnehmende Nachweisbarkeit mit zunehmender Clusterlänge sowie, die zunehmende Nachweisbarkeit von Varianten, die näher am 5'-Ende der von Primern flankierten Region liegen und eine signifikante Verringerung der TGAGGG-, aber nicht der TCAGGG-Häufigkeit nach dem Restriktionsverdau gezeigt.

In dieser Arbeit wurde gezeigt, dass NCTRs durch qPCR mit einer hohen Sensitivität und Spezifität in validierten ALT-Zelllinien nachgewiesen werden können. Dies ermöglicht den potenziellen Einsatz von qPCR-basierten NCTR-Detektionsmethoden im klinischen Screening.

2. Abstract

Alternative lengthening of telomeres (ALT) is a telomere maintenance mechanism (TMM) used by around 10-15 percent of cancers. ALT leads to heterogeneous telomere lengths and variant repeats (NCTRs) in telomeres' distal regions reducing shelterin functions. For now, these variants have been mainly detected by whole genome sequencing (WGS). In this study, a qPCR-based assay for NCTR-detection was evaluated.

Cell lines with a defined TMM state were validated for ALT activity by C-circle assays (CCA) and quantitative ALT-FISH confirming the ALT activity of five out of six ALT cell lines. Additionally, the presence of NCTRs in C-Circles was shown by applying the variant detection assay to the CCA-products.

Subsequently, telomere sequence variants were detected by a qPCR-based assay and quantitative FISH. Comparisons of the results with each other and with published WGS data showed statistically significant, strong correlations between qPCR and WGS data for the TCAGGG and TGAGGG variants. Furthermore, the assay's ability to detect clusters of multiple variant repeats and its specificity was assessed by applying it to different TCAGGG variant-oligonucleotides and to DNA digested by TCAGGG and TGAGGG variant-specific restriction enzymes, respectively. These experiments showed decreasing detectability of longer clusters and increasing detectability of variants closer to the 5' end of the primer-flanked region and a significant decrease of TGAGGG- but not of TCAGGG-variants upon digestion.

This thesis shows that NCTRs can be detected by qPCR with a high sensitivity and specificity in validated ALT cell lines. This enables the potential usage of qPCR-based NCTR-detection assays in clinical screening.

3. Abbreviations and symbols

ALT	Alternative lengthening of telomers
ANOVA	Analysis of Variance
CCA	C-circle assay
CT	Cycle threshold value
CV	Coefficient of variation (= SD/average)
D_{10} P/S	DMEM (Dulbecco's Modified Eagle's Medium) + 10% heat-inactivated fetal calf serum (FCS) + 1% Penicillin, 1% Streptomycin
dCT	Delta CT value
dH_2O	distilled water
ddH_2O	double distilled water
ECTR	extra-chromosomal telomeric repeat DNA
MNP_{10}	Minimum Essential Medium Eagle + 10% FCS + 1% non-essential amino acids + 1 mM pyruvate + 1% Penicillin and 1% Streptomycin
NCTR	Non-canonical telomere repeat
norm. TC	normalized telomeric content
NTC	Non-template control
phi+	phi-polymerase positive
phi-	phi-polymerase negative
R_{10} P/S	RPMI 1640 Medium (Roswell Park Memorial Institute 1640 Medium) with 10% FCS and 1% Streptomycin
RCA	Roling-circle amplification
SC	standard curve
SCG	single-copy gene
SD	Standard deviation
SEM	Standard error of the mean

SQ	starting quantity value
Std.	Standard dilution
TE (1x)	Tris (10 mM) EDTA (1 mM), pH 8
TERRA	Telomeric repeat-containing RNA
TMM	Telomere maintenance mechanism
v/v	volume for volume
WGS	whole genome sequencing

4. Introduction

Alternative lengthening of telomeres (ALT) is a telomerase-independent telomere maintenance mechanism (TMM) that is present in 10 to 15% of all cancers in humans (Dilley & Greenberg, 2015). The abundance varies across different tumor types, influencing patient outcome and prognosis. (Henson & Reddel, 2010). Additionally, it was found to be present in canine sarcomas (Kreilmeier-Berger et al., 2023; Kreilmeier et al., 2017). Similar to telomerase activity, ALT maintains the length of telomeres to prevent the cancer cells from reaching the so-called *Hayflick limit* and preventing senescence (Hayflick, 1965). This enables the cells to become immortal, which was described to be one of the hallmarks of cancer (Hanahan, 2022; Hanahan & Weinberg, 2000, 2011). The mechanisms of ALT have been unclear up until recently. The lengthening of the telomeres is based on homologous recombination-related Break-induced replication caused by replication stress at the telomeres (Zhang & Zou, 2020). During this process, it is hypothesized that non-canonical telomere repeat (NCTR) variants are introduced, indicated by their presence in telomeres elongated by ALT (Conomos et al., 2012; Marzec et al., 2015). The introduction of these NCTRs leads to reduced binding of the shelterin complex, consequently abbreviating telomere stability (Conomos et al., 2012) and thereby increasing genetic instability, an enabling characteristic of cancer (Hanahan, 2022; Hanahan & Weinberg, 2011). This is why the NCTR content of the telomeres could have a substantial impact on the characteristics of cancer and would be of interest to screen in larger numbers. Up until now, this has been hampered by the availability of only the expensive and time-consuming method of whole genome sequencing (WGS), which has been the go-to method for NCTR detection (Conomos et al., 2012; Lee et al., 2014). Potential solutions for these limitations are qPCR-based assays for the detection of the NCTRs TCAGGG, TGAGGG and TAAGGG which will be tested and presented in this study on the subject of established ALT cell lines.

4.1. ALT-activity detection

The main challenge with ALT is its reliable detection. For a long time, only the survival of cells of hundreds of population doublings with a constant telomere length upon telomerase inactivity was the definitive marker for ALT (Henson & Reddel, 2010). The solution to this problem was the detection of ALT-specific markers, the partially single-stranded C- or G-circles (Henson & Reddel, 2010). These extra-chromosomal telomeric repeat DNA (ECTR) molecules are generated during the ALT-specific telomere elongation (Zhang & Zou, 2020). In this study, two methods will be used for ALT activity detection to validate the ALT status of the cell lines used for the evaluation of the NCTR variant detection qPCR assay. First, the C-circle assay (Henson et al., 2009, 2017), the current gold standard for ALT detection (Frank et al., 2022), which

detects the C-circles and second, native ALT-FISH using two DNA probes, a G-rich and a C-rich probe detecting C- and G-rich single stranded DNA, respectively (Frank et al., 2022). Based on this work, the ALT-FISH experiment in this study was conducted using the C-rich probe (TelC, see Table 6), with some modifications which are described in more detail below (Chapter 4.1.2). Additionally, Claude et al. presented a similar method under native conditions using a G-rich LNA probe for detecting C-rich single stranded telomeric DNA in 2021, which was not regarded in more detail here.

4.1.1. C-circle assay

The C-circle assay, which was first described by Henson et al. in 2009 and optimized by the same group in 2017 (Henson et al., 2017), is a rolling-circle amplification (RCA) based, self-primed ALT detection method. This assay detects the ALT-specific partially single-stranded C-circles by qPCR-based detection of the rolling-circle processivity of the ϕ29 DNA polymerase (Figure 1). As described by Henson et al. (2017), the resulting C-circle levels are the product of the calculation comparing the CCA qPCR results of each sample's polymerase-containing and polymerase-free reactions after normalization on the DNA content of both reactions with their respective single-copy gene (SCG) content. To ease comparability and data presentation, the C-circle levels were normalized with the C-circle levels of the positive control, the cell line U2OS. This will be described in more detail in chapter 5.5.1

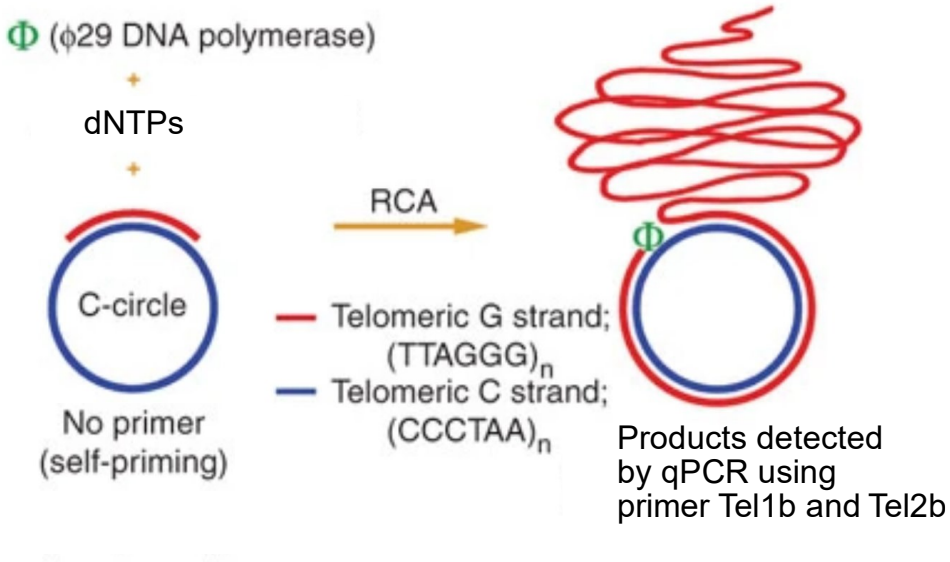

Figure 1: Scheme of the CCA process used in this study. Adapted from (Henson et al. (2009)

This method will be used in this study to validate the ALT activity of the cell lines SAOS-2, U2OS, WI38-VA13/2RA, YTBO and IIICF/c.

4.1.2. Native ALT-FISH

Native ALT-FISH is a fairly new method for quantitative ALT detection established by Frank et al. (2022). It uses C-rich oligomer DNA probes labeled with a fluorophore, in this case, ATTO633, to stain the ALT-specific G-circle ECTRs under native conditions to quantify ALT via the number of G-circle signals per cell. The choice of the G-circles is interesting since these ECTRs are described to be substantially less abundant than C-circles in ALT cells (Henson et al., 2009; Henson & Reddel, 2010). Yet, Frank et al. (2022) showed that using the C-rich probe yielded a higher number of signals per cell while treating the cells with RNase to exclude telomeric repeat-containing RNA (TERRA) without discussing this result in detail and thus leaving open questions. Contrary to Frank et al. (2022), the data analysis of a range of 102-802 cells per sample in this study will be performed using an AI-based method with a neural network specifically trained for this application. Using this adapted method, I will determine the ALT activity in the cell lines SAOS-2, U2OS, WI38-VA13/2RA, YTBO and IIICF/c in this study with slight methodical modifications in the staining and washing processes. For an instance, 1.5 x 10^4 cells were inoculated instead of 2.5 x 10^4 cells. And the cells were fixed into chamber slides instead of 12 mm round glass coverslips. Additional adaptions can be found when comparing the detailed description of the method used in this study, as shown in chapter 5.4, with the methods described by Frank et al. (2022).

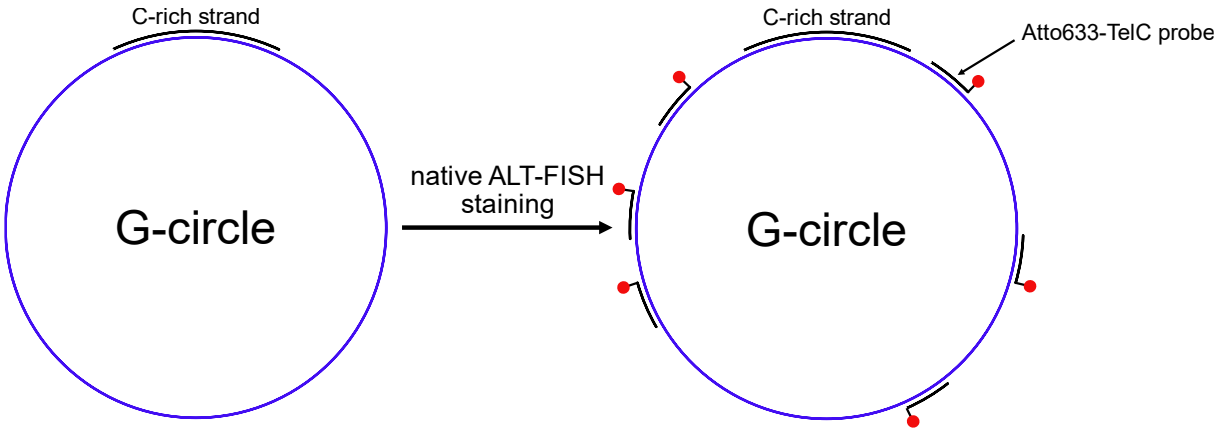

Figure 2: Scheme of the probe locations on G-circles of the native ALT-FISH method.

4.2. qPCR-based variant detection

Quantitative PCR (qPCR)-based detection has been used for relative- (Cawthon, 2002, 2009) and absolute (O'Callaghan & Fenech, 2011) telomere length (TL) measurements for over two decades and are a crucial tool in this field. A novelty, however, is the detection of NCTR

variants using qPCR, instead of using the expensive and labor-intensive WGS which was the single option up until now. NCTR variants have an impact on genetic instability due to their hampering of shelterin binding (Conomos et al., 2012). Therefore, detecting their presence in a faster and cheaper way is of interest to learn more about potential implications for tumor biology and as a promising screening tool in the clinic. To achieve this, the primer design by Cawthon (2009) was adapted by adding a base, e.g. a cytosine to the TCAGGG forward primers and by exchanging a base, e.g. an adenine with a guanine in the TCAGGG reverse primers, respectively (Figure 3). By that, the special characteristics of Cawthon's primers remained: First, a minimization of primer hybridization by mismatches and 3' overhangs when the two primers bind to each other; Second, the inability of the Telc-A, Telc-T, Telc-G and Telc-C primers to prime the replication of the G-rich strand as well as the configuration of the two primers that the amplification product is fixed in length (Cawthon, 2009). All of these characteristics enable tighter control over the replication process, thus increasing the assays' specificity. This technique was combined with the usage of standard curves for each NCTR variant comprised of standard concentrations with known numbers of target molecules and thus with a known length of telomere sequence for each standard point as described by O'Callaghan & Fenech (2011) for absolute quantification of the variant repeats to enable better comparability between experiments. In this study, this assay will be used to determine the NCTR variant content for the cell lines IIICF/c, SAOS-2, HeLa, U2OS, WI38-VA13/2RA, HT-1080, HT-1080 hTR wt and YTBO to compare the resulting NCTR contents of the cell lines with available WGS data (Lee et al., 2014) and telomere-variant FISH results to ensure the validity of the qPCR-generated data. Additionally, the specificity of the qPCR-based TCAGGG and TGAGGG detection assays by conducting restriction enzyme digestions of the gDNAs of WI38-VA13/2RA and YTBO cells will be evaluated. To gain insight into the resolution of the NCTR variant detection assays, the ability to detect clusters of multiple variant repeats in series as well as the influence of their orientation in the primer-flanked region will be tested exemplary on the TCAGGG detection assay by using DNA oligomer templates with different length, variant content and -orientations.

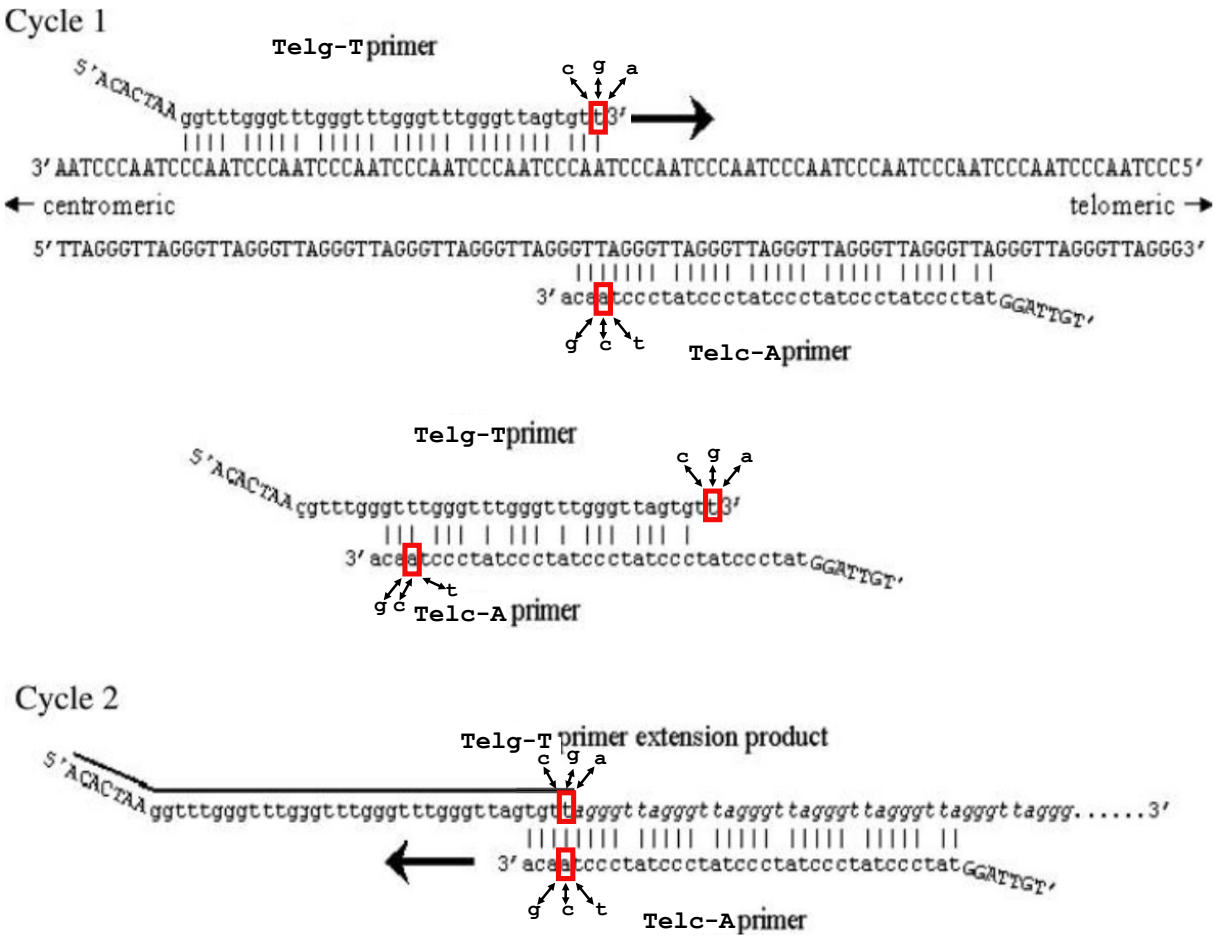

Figure 3: Scheme of the adapted primer design used for qPCR-based NCTR detection in this study. The positions where the base addition (Telg-primers) or exchange (Telc-primers) for the NCTR variant detection was performed are indicated by the red boxes. The first base indicated over or under the red box seen from left to right was exchanged for the TCAGGG assay, the second base for the TGAGGG assay and the third for the TAAGGG assay (see Table 6). Adapted from Cawthon (2009)

4.3. Telomere-variant FISH

Fluorescence in-situ hybridization (FISH) developed into one of the crucial methods in molecular biology over its four decades of existence (Levsky & Singer, 2003). Its quantitative variant became a regularly used tool in cancer research (Ikeda et al., 2014; Romero et al., 2011) and is also used for telomere length measurements (Canela et al., 2007) and, as mentioned and applied in this study, for the determination of ALT (Frank et al., 2022). Fittingly, one of its applications is the detection of NCTR variants (Lee et al., 2014) and more specifically the TCAGGG and TGAGGG variants (Conomos et al., 2012) that will also be detected by

qPCR in this study. This enables a supplementary layer of comparison and validation of the qPCR data generated by the novel NCTR variant detection assays in addition to WGS data reported by Lee et al. (2014). To implement this, the cell lines IIICF/c, SAOS-2, HeLa, U2OS, WI38-VA13/2RA, HT-1080, HT-1080 hTR wt and YTBO will be assayed for their TCAGGG and TGAGGG content by telomere-variant FISH.

4.4. Aim of this work

This work aims to validate qPCR-based NCTR variant detection assays by experimentally generating qPCR and telomere-variant FISH data on cell lines with defined TMM.

First, cell lines were chosen based on availability of WGS data from Lee et al. (2014) and TMM status (Table 1). Based on that, the ALT positive cell lines IIICF/c, Saos-2, WI38-VA13/2RA, *GM847** (identified as the telomerase positive the telomerase positive HCT 116 subline Luc2 by STR marker analysis) and YTBO as well as the telomerase positive cell lines HeLa, HT-1080 and a HT-1080 subline with hTR wt overexpression.

In the next step cell lines will be verified for their ALT status by CCA and native ALT-FISH (chapter 6.1) followed by the detection of their TCAGGG, TGAGGG and TAAGGG content with qPCR-based NCTR variant detection assays (chapter 6.2). Additionally, telomere-variant FISH experiments with these cell lines will be performed (chapter 6.3) to confirm the NCTR content detected by qPCR, so the validity can be ensured by an independent method in addition to the publicly available WGS data. The resulting qPCR-based data will be compared to the telomere-variant FISH results and WGS data from Lee et al. (2014) (chapter 6.2.2) to ensure the validity of the data created by performing the qPCR-based NCTR variant detection assays.

Furthermore, to ensure the sensitivity and specificity of the qPCR assay, it will be applied to restriction enzyme digestion products (chapter 6.2.4) and TCAGGG cluster variant DNA oligomers (chapter 6.2.5).

Unrelated to the validation, the qPCR-based NCTR variant detection assays will be applied to CCA products to gain insight into the location and propagation of NCTR variants in the C-circles of ALT-positive cell lines (chapter 6.2.3).

In addition, monoclonal cell lines from the HT-1080 cell line and its sublines with hTR wt and variant overexpression as well as with a retroviral *gfp* insertion (Table 1) will be established for a separate project (chapter 6.4).

5. Material and Methods

5.1. Cell culture

5.1.1. Cell lines

All cell lines used in this work, their respective media and origin are listed in Table 1. These cell lines, excepts for YTBO were selected due to the availability of WGS data (Lee et al., 2014). The ALT positive YTBO was selected to have an additional cell line for the comparison of qPCR and Telomere-variant FISH results. The cell line used and assumed to be GM847 in this work was identified instead as the telomerase positive HCT 116 subline Luc2 (Samad et al., 2021). However, this cell line will still be called G*M847** in order to be consistent with the data created in the experimental processes.

All cells were grown at 37°C, 5 % CO_2.

5.1.1. Defrosting of cells from cryo stocks

Before cell culture was started, cell lines used in previous works from -80°C and liquid nitrogen storage had to be defrosted to be used in the experiments. First, 5 ml of appropriate medium (see Table 1) were prepared in a T25 flask followed by taking the cryo vails from the desired cell line out of liquid N_2 storage. The cryo vials were held in lukewarm water for slow defrosting without putting the O-ring seal below the water's surface to minimize contamination risks. Directly after the last parts were molten, the complete content of the cryo vial was transferred into the prepared T25 flask using a Pasteur pipette. The flasks were incubated for 24 h at 37°C, 5 % CO_2. The medium that still contained traces of DMSO was changed to the appropriate medium the next day.

Table 1: List of all cell lines and clones used in this work.

Cell line/clone	Origin	Characteristic	Reference	Medium	STR Marker (see Table 40) analysis using CLASTR (Robin et al., 2020)
IIICF/c	Thomas Aschenbacher from Bergmann Lab, Department for Oncology and Inflammation, Medical University of Vienna	Spontaneous immortalization in cells from human patients with Li-Fraumeni syndrome, breast tissue, female, ALT-positive	Bryan et al (1995); Rogan et al. (1995), Lee et al. (2014)	DMEM (Dulbecco's Modified Eagle's Medium, Cat# D5648, Merck KgaA, Darmstadt, Germany) + 10% heat-inactivated fetal calf serum (FCS; Cat# S181H, Batch S00FG1, VWR international LLC., Radnor, PA, USA) + 1% Penicillin, 1% Streptomycin (Cat# P4333, Merck KgaA, Darmstadt, Germany) (D_{10} P/S)	No 100% identity with available marker profiles, no existing IIICF/c profile in CLASTR
*GM847**	Thomas Aschenbacher from Bergmann Lab, Department for Oncology and Inflammation, Medical University of Vienna	SV-40 transformed cell line from human patient with Lesch-Nyham syndrome, skin fibroblasts, male, ALT-positive	Named LN-SV in Koprowski & Croce (1977); Bryan et al. (1997); Lee et al. (2014)	D_{10} P/S	Identified as HCT 116-Luc2 cell line
HeLa	ATCC (HeLa S3, CCL-2.2)	Cells form a Human papillomavirus-related endocervical adenocarcinoma, female, telomerase-positive	Puck & Marcus (1955), Lee et al. (2014)	RPMI 1640 Medium (Roswell Park Memorial Institute 1640 Medium, Cat# R6504 Merck KgaA, Darmstadt, Germany) with 10% FCS + 1% Penicillin and 1% Streptomycin (R_{10} P/S)	Identity verified

HT-1080	ATCC (CCL121)	Cells from a human fibrosarcoma, male, telomerase-positive, Parental cell line [PTL]	Rasheed et al. (1974), Lee et al. (2014)	D_{10} P/S	Identity verified
HT-1080 hTR wt	Hammerl (2021) based on HT-1080 PTL	Retroviral insert of wild-type *hTR* and *puro* (Puromycin resistance) genes	Hammerl, (2021)	D_{10} P/S + 1 µg/ml puromycin	Not done (ND)
HT-1080 hTR TCA	Hammerl (2021) based on HT-1080 PTL	Retroviral insert of *hTR* with TCAGGG template and *puro* (Puromycin resistance) genes	Hammerl, (2021)	D_{10} P/S + 1 µg/ml puromycin	ND
HT-1080 hTR wt rv2	Hammerl (2021) based on HT-1080 PTL	Retroviral insert of wild type *hTR* and *puro* (Puromycin resistance) genes, biological replicate of HT-1080 hTR wt	Hammerl, (2021)	D_{10} P/S + 1 µg/ml puromycin	ND
HT-1080 hTR TCA rv2	Hammerl (2021) based on HT-1080 PTL	Retroviral insert of *hTR* with TCAGGG template and *puro* (Puromycin resistance) genes, biological replicate of HT-1080 hTR TCA	Hammerl, (2021)	D_{10} P/S + 1 µg/ml puromycin	ND
HT-1080 GFP rv2	Hammerl (2021) based on HT-1080 PTL	Retroviral insert of *gfp* and *puro* (Puromycin resistance) genes	Hammerl, (2021)	D_{10} P/S + 1 µg/ml puromycin	ND
Saos-2	VetBioBank, University of Veterinary Medicine Vienna	Cells from human osteosarcoma, female, ALT-positive	Wright et al. (1981), Lee et al. (2014)	D_{10} P/S	Identity verified

Saos-2 2022	Identical to Saos-2, exclusively thawed and used as a positive control for C-circle assays. Stock established in 2022				
U2OS	VetBioBank, University of Veterinary Medicine Vienna	Cells from human osteosarcoma, female, ALT-positive	Wright et al. (1981), Lee et al. (2014)	D_{10} P/S	Identity verified
U2OS 2022	Identical to U2OS, exclusively thawed and used as a positive control for C-circle assays. Stock established in 2022				
WI38-VA13/2RA	ATCC (CCL75 VA13 subline 2RA)	SV-40 transformed lung fibroblast cell line, human male, ALT-positive	Ehmann et al. (1978), Lee et al. (2014)	MNP_{10}P/S (Minimum Essential Medium Eagle, Cat# M0268, Merck KgaA, Darmstadt, Germany + 10% FCS + 1% non-essential amino acids, #M7145, Merck KgaA, Darmstadt, Germany + 1 mM pyruvate, Cat# P2256, Merck KgaA, Darmstadt, Germany) + 1% Penicillin and 1% Streptomycin	Identity verified
YTBO	Facility Cellculture, Center for Cancer Research, Medical University of Vienna	Cells from an astrocytoma, human, male, ALT-positive	Chen et al. (2021); Sampl et al. (2012)	R_{10} P/S	Identity verified in 2017 based on a not published marker profile from tissue

5.1.2. Trypsinization of adherent cells

First, the density of the cells was estimated with a microscope. If a sufficient confluency (>70 %) was reached the media was suctioned with Pasteur pipettes and a vacuum pump followed by a washing step with 1 ml (T25 flask) or 1.5 (T75 flask) trypsin. Following the removal of the trypsin from the washing step the same amount of trypsin was added again with a subsequent incubation at 37°C and 5 % CO_2 for 3-5 min (T75 flask) or 3 min (T25 flask). After checking the success of the detachment under the microscope, the trypsinization was stopped by adding 3,5 ml (T75) or 2-4 ml (T25) of the appropriate media for the cultured cell line (see Table 1). The resulting cell suspension was pipetted up and down and used to rinse the flask to dissolve cell aggregations and suspend all cells. The content of the T75 flasks was exclusively and completely used for cryo vail preparation (see 5.1.5). The content of T25 was split in ratios of 1:3 or 1:5. One part remained in the same flask, which was filled up to 3-5 ml using the fitting media. The remaining parts were used to inoculate additional T25 flasks, to prepare cell pellets (see 5.1.4) or to prepare slides for microscopy experiments (see 5.1.6 or 5.4).

5.1.3. Cell counting

Cell counting was exclusively performed using a CASY cell counter (OMNI Life Science GmbH & Co KG, Bremen, Germany). For counting, 50 µl cell suspension were added to 10 ml CASY buffer in an appropriate flask. To ensure the cleanliness of the device, only CASY buffer was measured before the cell suspension was measured three times. After the measurement, the device was cleaned using the same-named function twice. The cleaning was ensured by measuring blank CASY buffer.

For measuring a setup, the following parameters were used:

- Capillary: 150 µl
- Sample volume: 400 µl
- X-Axis: 50 µm
- Cell suspension dilution: 1:200
- Evaluation cursor: 10.75 - 50µm
- Normalization cursor: 6.00 - 50µm
- %Calculation: %Viable
- Debris: Off

5.1.4. Cell pellet preparation

For the preparation of cell pellets for DNA, RNA or protein isolation in future studies, approximately 1 million suspended cells were added into a screw tube followed by centrifuging at 800 g, 4° C for 10 minutes (Centrifuge 5427 R, Eppendorf SE, Hamburg, Germany). The resulting supernatant was discarded and the cells were resuspended in 500 µl phosphate-buffered saline (PBS). After resuspension, the cells were centrifuged at 800 g, 4°C for 10 minutes again with a subsequent discarding of the supernatant. For the preparation of pellets for protein isolation, the second centrifuging step was followed by snap freezing of the pellets using dry ice. Pellets for protein- and RNA isolation were prepared from cultures with < 95 % density to prevent altered expression patterns due to contact inhibition. The cell pellets were stored at -80° C.

5.1.5. Cryo vial preparation

Cryo vials were prepared by counting the trypsinized cells with the CASY cell counter (see 5.1.3) and transferring the cells into a 50 ml falcon tube followed by centrifuging at 188 g for 5 min at room temperature. The supernatant was discarded and 4 µl FCS + 10 % dimethyl sulfoxide (DMSO) was added and used to resuspend the cells. Approximately 1 Mio cells each were transferred to cryo vials and stored at -80°C for one to 14 days followed by a transfer into liquid nitrogen storage.

5.1.6. Cytospin

Trypsinized cells were diluted to a concentration of approximately 250 000 cells/ml and stored on ice. Fisherbrand Superfrost Plus microscope slides (Thermo Fisher Scientific Inc., Waltham, MA, USA) were put in the metal centrifugation frame of the Cytospin 4 centrifuge (Thermo Fisher Scientific Inc.) with the labeling side facing away from the frame. The slide was overlayed with a filter card for cytology centrifuges (VWR international LLC., Radnor, PA, USA) and fixed with the funnel for the cell suspension. This is done in a way that the funnel's hole is positioned over the filter card's hole on the lower half of the slide seen from the label. This setup is finally locked with the metal frame's bar and put in the centrifuge with the funnel facing the rotor's center with the opening facing to the top. Before starting the centrifugation, 0.4 ml of cell suspension were added to each filter. Centrifugation was performed at 300 g at room temperature for 5 min at medium acceleration. After the centrifugation, the cells were fixed by adding -20°C cold 100% methanol overnight at 4°C. After the fixation, the slides were stored at -20°C and used for telomere-variant FISH (see 5.7).

5.1.7. Microscopic analysis of cell culture

Growth of the cultivated cell lines was observed on a Nikon Eclipse Ti2 microscope (Nikon Corp., Tokyo, Japan) using phase contrast with 40x and 100x magnification.

Adjustments and cropping of the images as well as insertions of scale bars were performed using the program ImageJ Fiji (Schindelin et al., 2012).

5.2. DNA isolation

DNA extraction was performed as described by Henson et al. (2017). It is an straight-forward, one-tube method requiring Qiagen Protease (Qiagen N.V., Venlo, Netherlands), a Vortex shaker for mixing, a microcentrifuge, a cooling centrifuge (Centrifuge 5427 R, Eppendorf SE, Hamburg, Germany), a heating block with shaking function (HeatingThermoMixer MHR 13, Andreas Hettich GmbH & Co. KG, Tuttlingen, Germany) and QCP lysis buffer, which components are described in Table 2.

Table 2: Components and concentrations for 50 ml QCP lysis buffer (1x).

Stock solution	Volume	Final concentration
1 M KCl (autoclaved)	2.5 ml	50 mM
1 M Tris-HCl (pH 8.5, autoclaved)	0.5 ml	10 mM
1 M $MgCl_2$ (autoclaved)	100 µl	2 mM
IGEPAL CA-360 detergent	225 µl	0.5 % v/v
Tween-20 detergent	225 µl	0.5 %v/v
Ultrapure water (autoclaved)	46.45.ml	

For the extraction, the heating block was preheated to 56°C and the centrifuge was cooled down to 4°C. The protease was thawed on ice, mixed and kept on ice until use. 50 µl x the number of samples x 1.2 were added to a 1.5 ml reaction tube and pre-warmed to 56°C. In the next step, the cell pellets (see 5.1.4) were removed from frozen storage and placed on ice followed by a quick spin in the centrifuge (13 000 rpm, 4°C). The protease was added to the QCP buffer at a 1:20 ratio followed by mixing and a quick spin. Next, 50 µl of the QCP buffer-protease mixture was added to each tube. All tubes were tightly closed, which was double-checked followed by vortexing at 2 000 rpm for 15 s. After being mixed, the tubes were shaken at 1 400 rpm, 56°C for 1 h. This was followed up by a temperature increase to 70°C during which the samples were spun down shortly to return evaporated water. The samples were shaken at 1 400 rpm, 70°C for 20 min then allowed to cool down to room temperature. The

cooled samples were spun down shortly, vortexed for 15 s at 2 000 rpm and spun quickly again. After the extraction, the samples were stored at -20 (short term) to -80°C (long term) without a defrost cycle until use.

5.3. C-circle assay

For the C-circle assay, the isolated DNA (see 5.2) was quantified using a Qubit 1X dsDNA BR kit (Cat# Q33265, Invitrogen AG, Carlsbad CA, USA) according to the kit's manual. The working solution (199 µl x number of samples x 1.2) was prepared in a 15 ml falcon tube followed by the addition of the DNA sensing dye (1 µl x number of samples x 1.2), finalizing the working solution. For the quantification, a 1:2 dilution series of the kit's Standard #2 was prepared in 1xTE buffer. 190 µl of the working solution was added in wells of a 96-well plate used for the standard series. For the samples, 198 µl of the solution was added into the wells. In the final pipetting step, 10 µl of the standards and 2 µl of the DNA samples were added to the respective wells. The DNA samples were heated to 56°C for 10 min followed by vortexing at 1 800 rpm for 15 s and briefly spun down every time they were taken out of storage. The samples were kept on ice all the time. The finalized 96-well plate was incubated for 2 min at RT in the dark followed by fluorescence measurement with an initial shaking step for 5 s before measuring the samples at 485 nm excitation and 530 nm emission in a blade reader (Tecan Infinite 200 Pro, Tecan Group AG, Männerdorf, Schweiz). The resulting concentrations were used to calculate a dilution to a concentration of 3.2 ng/µl over three steps. For the first step, QCP lysis buffer (Table 2) was used to dilute the samples to 32 ng/µl. For step 2 (dilution to 16 ng/µl) and 3 (to the final 3.2 ng/µl), 10 mM TrisHCl pH 7.6 was used. From the final dilution, 10 µl each were put into two PCR-reaction tubes, one for the polymerase negative- (phi -) and one for the polymerase positive (phi +) reaction. The PCR tubes were put on ice. For multiple samples PCR tube stripes were used. As a negative control 1:3 10mM TrisHCl pH 7.6 in nuclease free H_2O was used.

In the next step, the master mix was prepared in a 1.5 ml reaction tube. The components and volumes of the master mix for twelve samples are shown in Table 3. The final volume was calculated in the following way: Number of samples (12 in this case) x 9.25 µl x 1.2. The components' volumes were calculated according to their final concentration. The components were pipetted on ice.

Table 3: Components and volumes of the CCA master mix for twelve reactions

Component	Volume [µl]
Nuclease-free H_2O (Promega Corp., Fitchburg, WI, USA)	182.1
1 M Dithiothreitol (DTT)	2.5
10x phi 29 buffer (New England Biolabs GmbH (NEB), Frankfurt am Main, Germany)	63.1
0.2 mg/ml BSA (NEB, Frankfurt am Main, Germany)	12.6
10% Tween-20	6.3
100 mM dATP	6.3
100 mM dTTP	6.3
100 mM dGTP	6.3
100 mM dCTP	6.3
Total	291.8

133.2 µl of the master mix was transferred to another reaction tube. In the first one, 10.8 µl (number of samples (12) x 0.75 µl x 1.2) nuclease-free H_2O was added. From this tube, 10 µl were added to each polymerase-negative PCR reaction tube and the PCR tubes were closed tightly to prevent polymerase contamination. In the second reaction tube, 10.8 µl (number of samples (12) x 0.75 µl x 1.2) Phi29 Polymerase (7.5 U) (NEB, Frankfurt am Main, Germany) were added to the remaining 132.2 µl master mix. The polymerase must be kept cold and must be put at -20°C directly after usage. 10 µl of the polymerase-positive master mix were added to each polymerase-positive PCR reaction tube. After closing the polymerase-positive PCR tube tightly, all PCR reaction tubes were vortexed at 1 800 for 5 s and spun quickly twice before being put in a PCR cycler (peqSTAR Thermocycler, VWR International LLC., Radnor, PA, USA). The program stated in Table 4 was started and run overnight. The final DNA concentration in each reaction was 1.6 ng/µl, so every reaction contained 32 ng DNA.

The resulting samples were stored at -20°C until used for CCA-qPCRs (see 5.5.1) or telomere sequence variant-qPCRs (see 5.5.2) for CCA quantification and further analysis of the samples.

Table 4: CCA-cycler program

Temperature [°C]	Time
30	1 min
Pause: 30	Until continued manually
30	8 h
Heat lid: 110	
70	20 min
Hold: 4	

5.4. Native ALT-FISH

For the native ALT-FISH experiments, 500 µl per well of cell suspensions (see 5.1.2) with a concentration of 30 000 cells/ml were added in chamber slides (Millicell EZ slide 8-Well, Glass, sterile. Merck KGaA, Darmstadt, Germany). For every cell line, three wells were inoculated: one for each of the three treatments. After 24 h incubation at 37°C and 2% CO_2, the cells were fixed with -20°C cold 70% Ethanol for 30 min at 4°C followed by the aspiration of the ethanol. The cells were air-dried for 1 h at RT and then 0.5 ml PBS was added into each well for storage for up to three months.

The chemicals that were needed for the FISH experiment are listed in Table 5.

For the staining, the cells were washed with ALT-FISH washing buffer (500 µl/well) twice for two minutes. Excess buffer was carefully removed by softly knocking the chamber slides on a paper towel. This was followed by RNase treatment, which was performed by adding 500 µl/well of RNase treatment solution with subsequent incubation for 30 min at 37°C. Thereafter, another two-minute ALT-FISH washing buffer wash was performed. Again, the excess buffer was removed by knocking. The RNase treatment and the following wash were omitted in the preliminary experiment. The hybridization was performed by adding 500 µl/well of ALT-FISH staining solution with subsequent incubation at 37°C for 30 min in the dark. Afterwards, the slides were washed twice with 2x SSC for two min and stained with 500 µl/well DAPI staining solution for 15 min at RT in the dark. For the final wash series, the slides were washed three times in PBS at RT for 5 min. For dehydration the slides were rinsed with 500 µl/well dH_2O, then the same amount of 70% and 100% ethanol was added for 2 min each. The liquids were aspirated between each step. After dehydration, the well structure was removed and the slides were air-dried for 5-10 min on a clean paper towel. Finally, the cells were mounted with a clean coverslip using 20-40 µl of Vectashield while preventing air bubble formation. The coverslips were sealed with nail polish and stored in the dark, overnight at RT to let the nail polish harden.

The slides were stored at 4°C until microscopical imaging was performed as described further down.

Table 5: Chemicals/solutions needed for native ALT-FISH

Chemical/Solution	Composition
ALT-FISH washing buffer	100 mM Tris-HCl pH8, 150 mM NaCl, 0.05% Tween-20
RNase treatment solution	5 µl/ml RNase A (Cat# EN0531, Thermo Fisher Scientific Inc., Waltham, MA, USA) + 2 µl/ml RNase H (Cat# M0297S, NEB, Frankfurt am Main, Germany) in PBS
20x SSC	3 M NaCl and 0.3 M sodium citrate in dH_2O, pH 7
2x SSC	0.3 M NaCl and 0.03 M sodium citrate in dH_2O, pH 7
Hybridization solution	0.5 ml 20x SSC + 0.4 ml de-ionized paraformaldehyde + 4.1 ml nuclease-free H_2O
ALT-FISH staining solution	5 ml hybridization buffer + 5 nM Atto633-TelC-probe (5´-Atto633$(CCCTAA)_5$-3´ (Eurofins Genomics AT GmbH, Vienna, Austria)
DAPI staining solution	5 ml PBS + 5 µM DAPI (Cat# MBD0015-1ML, Merck KGaA, Darmstadt, Germany)
Vectashield mounting medium	Vectashield (H-1000) without DAPI (Vector Laboratories, Newark CA, USA)

Microscopical imaging of the slides was performed using an Olympus IX83P2ZF spinning disk confocal microscope (Evident Corporation, Tokyo, Japan) at 400x magnification using an UPLXAPO 40x / 0.95 objective (Evident Corporation, Tokyo, Japan) designed for use without immersion media. For the DAPI channel, an excitation laser at 345 nm with an intensity of 100% for the preliminary experiment and 80% for the main experiment was used. The dye emitted light at 455 nm. The exposure time was 100 ms in both experiments. For the ALT spots, the signals of the ATTO633 dye were detected at 670 nm. The excitation happened at 625 nm with a laser intensity of 100% for the preliminary experiment and 80% for the main experiment. The exposure time was 500 ms.

The analysis of the resulting images is described in 5.8.

For presentation, adjustments and cropping of the images as well as insertions of scale bars were performed using the program ImageJ Fiji (Schindelin et al., 2012).

5.5. qPCR assays

All qPCRs were performed using CFX Connect Real-Time PCR detection systems (Bio-Rad Laboratories GmbH, Feldkirchen, Germany) with the corresponding Hard-Shell 96-Well PCR plates (Cat# HSP9601, Bio-Rad Laboratories GmbH, Feldkirchen, Germany) which were sealed with Microseal 'B' PCR Plate Sealing Film (Cat# MSB1001, Bio-Rad Laboratories GmbH, Feldkirchen, Germany). Regarding the chemicals, the GoTaq qPCR Master Mix (Cat# A6001, Promega GmbH, Walldorf, Germany) was used. Primer and DNA oligomers (see Table 6) were sourced from Eurofins Genomics AT GmbH, Vienna, Austria. For experimental planning and analysis, CFX Maestro 4.1.2433 (Bio-Rad Laboratories GmbH, Feldkirchen, Germany) was used. A detailed protocol for every experiment is described below.

Table 6: List of DNA-Oligomers used in this study

DNA-oligomer name	Purpose	Sequence	Source and modifications
Telg-T	TTAGGG forward primer	ACACTAAGGTTTGGGTTTGGGTTTGGGTTTGGGTTAGTGTT	Cawthon (2009) with an additional thymine at the 3' end
Telc-A	TTAGGG reverse primer	TGTTAGGTATCCCTATCCCTATCCCTATCCCTATCCCTAACA	Cawthon (2009)
Tel1b	CCA qPCR forward primer	CGGTTTGTTTGGGTTTGGGTTTGGGTTTGGGTTTGGGTT	Henson et al. (2017)
Tel2b	CCA qPCR reverse primer	GGCTTGCCTTACCCTTACCCTTACCCTTACCCTTACCCT	Henson et al. (2017)
36B4u	36B4 forward primer	CAGCAAGTGGGAAGGTGTAATCC	Cawthon (2002)
36B4d	36B4 reverse primer	CCCATTCTATCATCAACGGGTACAA	Cawthon (2002)
Telg-C	TCAGGG forward primer	ACACTAAGGTTTGGGTTTGGGTTTGGGTTTGGGTTAGTGT**C**	Adapted from Telg-T (changed base in **bold**)
Telc-G	TCAGGG reverse primer	TGTTAGGTATCCCTATCCCTATCCCTATCCCTATCCCT**G**ACA	Adapted from Telc-A (changed base in **bold**)
Telg-G	TGAGGG forward primer	ACACTAAGGTTTGGGTTTGGGTTTGGGTTTGGGTTAGTGT**G**	Adapted from Telg-T (changed base in **bold**)
Telc-C	TGAGGG reverse Primer	TGTTAGGTATCCCTATCCCTATCCCTATCCCTATCCCT**C**ACA	Adapted from Telc-A (changed base in **bold**)
Telg-A	TAAGGG forward primer	ACACTAAGGTTTGGGTTTGGGTTTGGGTTTGGGTTAGTGT**A**	Adapted from Telg-T (changed base in **bold**)
Telc-T	TAAGGG reverse primer	TGTTAGGTATCCCTATCCCTATCCCTATCCCTATCCCT**T**ACA	Adapted from Telc-A (changed base in **bold**)
36B4 (SCG) Standard	Standard for absolute qPCR calculations	CAGCAAGTGGGAAGGTGTAATCCGTCTCCACAGACAAGGCCAGGA CTCGTTTGTACCCGTTGATGATAGAATGGG	O'Callaghan & Fenech (2011)
TTAGGG (canonical) standard	Standard for absolute qPCR calculations	CCCTAACCCTAACCCTAACCCTAACCCTAACCCTAACCCTAACCC TAACCCTAACCCTAACCCTAACCCTAACCCTAA	Reverse complementary sequence to the standard used by O'Callaghan & Fenech (2011) shortened by six bases
TCAGGG standard/ Telg-C_1x	Standard for absolute qPCR calculations/ TCAGGG cluster oligo variant PCR template	CCCTAACCCTAACCCTAACCCTAACCCTAACCCTAACCCT**G**ACCC TAACCCTAACCCTAACCCTAACCCTAACCCTAA	Changed base from canonical in **bold**

TGAGGG standard	Standard for absolute qPCR calculations	CCCTAACCCTAACCCTAACCCTAACCCTAACCCTAACCCT**C**ACCC TAACCCTAACCCTAACCCTAACCCTAACCCTAA	Changed base from canonical in **bold**
TAAGGG standard	Standard for absolute qPCR calculations	CCCTAACCCTAACCCTAACCCTAACCCTAACCCTAACCCT**T**ACCC TAACCCTAACCCTAACCCTAACCCTAACCCTAA	Changed base from canonical in **bold**
Telg-C_2x	TCAGGG cluster oligo variant PCR template	CCCTAACCCTAACCCTAACCCTAACCCTAACCCTAACCCT**G**ACCC T**G**ACCCTAACCCTAACCCTAACCCTAACCCTAACCCTAA	Added CCCTGA to Telg-C 1x in 3' direction
Telg-C_4x	TCAGGG cluster oligo variant PCR template	CCCTAACCCTAACCCTAACCCTAACCCTAACCCTAACCCT**G**ACCC T**G**ACCCT**G**ACCCT**G**ACCCTAACCCTAACCCTAACCCTAACCCTAA CCCTAA	Added 3x CCCTGA to Telg-C 1x in 3' direction
Telg-C_8x	TCAGGG cluster oligo variant PCR template	CCCTAACCCTAACCCTAACCCTAACCCTAACCCTAACCCT**G**ACCC T**G**ACCCT**G**ACCCT**G**ACCCT**G**ACCCT**G**ACCCT**G**ACCCTAA CCCTAACCCTAACCCTAACCCTAACCCTAA	Added 7x CCCTGA to Telg-C 1x in 3' direction
Telg-C_7xL	TCAGGG cluster oligo variant PCR template	CCCT**G**ACCCT**G**ACCCT**G**ACCCT**G**ACCCT**G**ACCCT**G**ACCCT**G**ACCC TAACCCTAACCCTAACCCTAACCCTAACCCTAA	Replaced 6x CCCTAA with CCCTGA in Telg-C_1x in 5' direction
Telg-C_7xR	TCAGGG cluster oligo variant PCR template	CCCTAACCCTAACCCTAACCCTAACCCTAACCCTAACCCT**G**ACCC T**G**ACCCT**G**ACCCT**G**ACCCT**G**ACCCT**G**A	Replaced 6x CCCTAA with CCCTGA in Telg-C_1x in 3' direction

5.5.1. CCA qPCR

For the quantification of the CCAs, the products of the reactions described in 5.3 were analyzed by qPCR as described by Henson et al. (2017). To do this, the plate layout was planned according to the number of samples. For every cell line tested, 12 wells needed to be calculated consisting of phi-polymerase positive (phi+) and phi-polymerase negative (phi-)CCA samples for telomere length (Tel) and single copy gene (36B4), all of which were performed in triplicates. The CCA samples were taken from -20°C storage and thawed at RT followed by transfer of 5 µl of the CCA reactions into a new 1.5 ml reaction tube where they were diluted with 15 µl 10 mM TrisHCl pH 7.6 and 30 µl nuclease-free H_2O resulting in a volume of 50 µl. This was vortexed at 1 800 rpm for 5 s followed by a quick-spin. For quantification purposes, two standard curves were prepared using U2OS gDNA with a starting concentration of 32 ng/µl. For the 36B4 curve, a serial two-fold dilution was prepared with the DNA quantities of 8, 4, 2, 1, 0.5 and 0.25 ng DNA in 5 µl. The Tel curve consisted of a serial three-fold dilution containing the DNA quantities of 5.33, 1.77, 0.59, 0.2, 0.07 and 0.02 ng DNA in 5 µl. The master mix was prepared using the components listed in Table 7.

Table 7: Components & volumes of the CCA-qPCR master mixes

Components	Volume/reaction Tel [µl]	Volume/reaction 36B4 [µl]
Master mix preparation (5 µl used per well)		
Promega GoTaq Master Mix	5	
10 pmol/µl Primer mix (fwd + rev) 1:10 (200nM/primer)	0.2 (Tel1b and Tel2b)	0.2 (36B4u and 36B4d)
Volume per well		
CCA sample, negative control (1:3 10 mM TrisHCl pH 7.6 and nuclease-free H_2O) or standard curve dilution	5	
Total	10	

For the qPCR reaction, 5 µl master mix were pipetted into all wells planned for samples in a Hard-Shell 96-Well PCR plate using low retention tips followed by adding 5 µl of the diluted CCA samples or the standard curve dilutions into the appropriate well, also while using low retention tips. A pipette only used for qPCRs was used for these two steps. When all samples were added, the plate was sealed and spun up to 1 000 rpm to remove air bubbles from the wells' bottom. The plate was put into the cycler and the program shown in Table 8 was run.

Table 8: Program for CCA-qPCR

Temperature [°C]	Time
Holding stage	
95	2 min
Cycling stage (repeated 40 times)	
95	15 s
58	30 s including plate read
Melting curve (continuous)	
58	5 s
Increase to 95 in 0.5 increments	5 s including plate read

Before exporting the results from the CFX Maestro software version 4.1.2433 (Bio-Rad Laboratories GmbH, Feldkirchen, Germany) for further analysis, the threshold for CT evaluation was set to an arbitrary value of 300 for the Tel and the 36B4 (SCG) results to enable comparability to other CCA experiments. Additionally, it was checked if all data points were lying in the range of their respective standard curve (SC), which was calculated by the CFX Maestro software by plotting the CT values of the standards against their DNA concentration. These curves should have good linearity with an R^2> 0.99 and a slope of -3.3±0.1 with an efficiency of close to 100%. The exported results were analyzed further using Microsoft Excel (Redmond, WA, USA).

The first step of the Excel calculations was to calculate the relative Tel and SCG quantity of each replicate by using the following formula: ($CT_{Tel\ or\ SCG}$ – Y-Intercept of corresponding SC) / slope of corresponding SC.

In the second step the average relative Tel-, SCG quantities, SD and CV of the samples' replicates were calculated. For quality control, the CV for the relative Tel averages of the phi+ reactions should not exceed 15%. For the relative Tel phi- and relative SCG averages the CV should be less than 10%.

The third step of the analysis consisted of dividing the average relative Tel by the average relative SCG from the same sample and phi treatment to obtain the normalized Tel content ($TC_{norm.}$). The CV for the $TC_{norm.}$ was calculated by adding the CV of the relative Tel and the relative SCG for each sample and phi treatment. The $TC_{norm.}$ error bars in this step were calculated by adding the $TC_{norm.}$ multiplied by the respective CV to the $TC_{norm.}$ ($TC_{norm.}$ +

$TC_{norm.}$ x CV) for the upper $TC_{norm.}$ error bar and by subtracting the $TC_{norm.}$ multiplied by the respective CV from the $TC_{norm.}$ ($TC_{norm.}$ – $TC_{norm.}$ x CV) for the lower $TC_{norm.}$ error bar.

To calculate the CCA levels in the fourth step, the normalized Tel content of each sample's phi- treatment was subtracted from the normalized Tel content of the same sample's phi+ treatment (CCA level= norm. Tel_{phi+} content – norm. Tel_{phi-} content). The error bars depict the worst-case scenario and were calculated by subtracting the in step four calculated lower error bar of the sample's phi- $TC_{norm.}$ from the upper error bar of the respective phi+ $TC_{norm.}$ for the upper CCA level error bar (= upper $TC_{norm.}$ error bar phi+ - lower $TC_{norm.}$ error bar phi-). The lower CCA level error bar was calculated by subtracting the upper error bar of the sample's phi+ $TC_{norm.}$ from the lower error bar of the respective phi- $TC_{norm.}$ error bar (= lower $TC_{norm.}$ error bar phi+ - upper $TC_{norm.}$ error bar phi-).

Based on these calculations, a sample is considered ALT+ if its lower CCA level error bar is >0 and if its CCA level is > 1% of the CCA level of U2OS. To be able to display this, the CCA levels were normalized to U2OS. To do this, the sample cell line U2OS (Figure 6, Panel A) respectively, the positive control U2OS cell line (Figure 6, Panel B) were assigned with an arbitrary norm. CCA level of 100. This was done by dividing the CCA level by the CCA level of the same U2OS cell line which was firstly divided by 100 (=CCA $level_{U2OS}$ / (CCA $level_{U2OS}$ / 100)). To normalize the error bars, the respective U2OS CCA level error bar was divided by the same error bar multiplied by 100 (=CCA level error bar_{U2OS} / CCA level error bar_{U2OS} x 100). By this, the same ratio between the normalized CCA level and the error bar is maintained compared to the raw CCA levels.

To normalize the CCA levels of all samples, their CCA level was divided by the CCA level of an U2OS cell line firstly divided by 100 (CCA $level_{cell\ line}$ / (CCA $level_{U2OS}$ / 100)). The samples' error bars were normalized by dividing the respective sample's CCA level error bar by the corresponding U2OS CCA level error bar multiplied by 100 (=CCA level error $bar_{cell\ line}$ / CCA level error bar_{U2OS} x 100). The raw and normalized CCA level values with their respective error bar were transferred to GraphPad Prism 8 for better visualization.

5.5.2. Telomere sequence-variant qPCR

For the telomere sequence variant-qPCRs, the isolated DNAs (see 5.2) were quantified using a Qubit 1X dsDNA BR kit (Invitrogen AG, Carlsbad CA, USA) as described in the first paragraph of 5.3. Based on the measured concentrations, the DNA samples were diluted to 2 ng/µl using 0.1x TE buffer. Based on these dilutions, a first 36B4 qPCR was run to adjust all samples to a 36B4 CT value of 20, so an equal SCG content was ensured. Each sample was analyzed in triplicates. For that, a master mix was prepared according to Table 9 and the samples were taken from storage (-20°C long term, 4°C short term), heated up to 56°C for 10

min followed by vortexing at 1 800 rpm for 10 s and a quick-spin, every time they were taken from storage. Afterwards, the samples were kept on ice.

Table 9: Components of telomere sequence variant-qPCR reaction

Components	Volume
Master mix preparation (5 µl used per well)	
Promega GoTaq Master Mix	5 x number of samples x 1.1
10 pmol/µl respective Primer mix (fwd + rev, see Table 10) 1:10 (200nM/primer)	0.2 x number of samples x 1.1
Volume per well	
DNA sample, NTC (0.1x TE or 1:3 10 mM TrisHCl pH 7.6 and nuclease-free H_2O for the CCA-products) or standard curve dilution	5
Total	10

Table 10: Primer used for telomere sequence variant qPCRs

Target	Primer pair
36B4 (SCG)	36B4u and 36B4d
TTAGGG	Telg-T and Telc-A
TCAGGG	Telg-C and Telc-G
TGAGGG	Telg-G and Telc-C
TAAGGG	Telg-A and Telc-T

For the PCR, 5 µl of the master mix were added to wells of a Hard-Shell 96-well PCR plate, layout was planned in the CFX Maestro before. Every plate needed to contain at least one non-template control (NTC) and it had to be considered that every sample and standard had to be analyzed in triplicates. Following the master mix, 5 µl of the DNA samples and standard dilutions were added according to the layout. The standard dilutions (see

Table 13 for Std. content) were added to have the opportunity for the quantifications of absolute numbers of diploid gene copies (SCG) and kb of telomere sequence. All pipetting steps were performed, using low retention tips and a pipette only used for qPCRs. When all samples, standards and NTCs were added, the plate was sealed and spun up to 1 000 rpm to remove air bubbles from the wells' bottom. The plate was put into the cycler and the program shown

in Table 11 was run. For the evaluation of the results, an arbitrary threshold of 100 was set in CFX Maestro to have comparability to other SCG qPCR experiments. Based on the samples' CT deviation from 20, they were diluted again, whereas for every deviation of a size of 1 CT, a further step of a two-fold dilution was added. This means that a sample with e.g., a CT of 22 was diluted four-fold using 0.1x TE.

Table 11: 36B4 (SCG) qPCR program

Temperature [°C]	Time
Polymerase heat activation	
95	2 min
Cycling stage (repeated 40 times)	
95	15
60	1 min with signal acquisition
Melting curve	
60 to 95 in 0.5 increments	5 s with signal acquisition

Based on these dilutions, qPCRs to detect the SCG, the canonical telomere repeat TTAGGG and the variant repeats TCAGGG, TGAGGG and TAAGGG were performed. These assays were performed analogous to the SCG concentration detection qPCR but with the respective primer pairs (see Table 10) and standards (see

Table 13). For the telomere repeats including the variants, the program shown in Table 12 was used. For the CCA products, the same dilution as for the CCA-qPCR (see 5.5.1) was used for the assays mentioned above.

For the data analysis, the threshold for the evaluation of all qPCRs was set to an arbitrary value of 100 to ensure comparability and it was checked if all data points were laying in the range of their respective standard curve before exporting the results to Excel. From the Excel sheets, the values were sorted and transferred to GraphPad Prism 8 for statistical analyses. These are described in 5.10.2.

Table 12: TTAGGG and NCTR qPCR program

Temperature [°C]	Time
	Polymerase heat activation
95	2 min
	Initiation cycle (repeated twice)
94	15 s
49	15 s
	Cycling stage (repeated 40 times)
94	15 s
62	10 s
75	15 s with signal acquisition
	Melting curve
65 to 95 in 0.5 increments	30 s with signal acquisition

Table 13: Absolute copy- respectively telomere kb numbers of the standard DNA oligomer dilutions used for absolute quantification

qPCR assy:	36B4 (SCG)	TTAGGG	TCAGGG	TGAGGG	TAAGGG
Standard dilution:	Diploid genome copies/well	kb of telomere sequence/well			
Std. 1	2.00×10^{7}	1.38×10^{9}	1.37×10^{7}	1.36×10^{7}	1.37×10^{7}
Std. 2	1.98×10^{6}	1.38×10^{8}	1.35×10^{6}	1.35×10^{6}	1.35×10^{6}
Std. 3	1.96×10^{5}	1.37×10^{7}	1.34×10^{5}	1.34×10^{5}	1.34×10^{5}
Std. 4	1.94×10^{4}	1.36×10^{6}	1.32×10^{4}	1.32×10^{4}	1.33×10^{4}
Std. 5	1.92×10^{3}	1.34×10^{5}	1.31×10^{3}	1.31×10^{3}	1.31×10^{3}
Std. 6	1.90×10^{2}	1.33×10^{4}	1.30×10^{2}	1.30×10^{2}	1.30×10^{2}

5.5.3. TCAGGG cluster oligo variant qPCR

The TCAGGG cluster oligo variant qPCR was performed analogously to the TCAGGG variant qPCR described in 5.5.2 with the difference that six different DNA oligomers in different concentrations were used as templates. The final number of molecules per reaction of these templates is listed in Table 14.

Table 14: Number of molecules of the TCAGGG cluster oligo variants in each reaction

	Name of Oligonucleotide (number of hexamers)					
Order of magnitude	Telg-C 1x (13)	Telg-C 2x (14)	Telg-C 4x (16)	Telg-C 8x (20)	Telg-C 7xL (13)	Telg-C 7xR (13)
10^8	1.75	1.77	1.70	1.17	1.87	2.19
10^7	1.73	1.71	1.65	1.13	1.81	2.12
10^6	1.72	1.66	1.59	1.09	1.75	2.05
10^5	1.70	1.61	1.54	1.06	1.70	1.99
10^4	1.68	1.56	1.50	1.03	1.64	1.92

5.6. Restriction enzyme digest for TGAGGG and TCAGGG telomere sequence variants in genomic DNA

For the restriction enzyme digest, a dilution containing 100 ng of gDNA solved in 0.1xTE (quantified as described in 5.5.1) was added up to 5 µl with nuclease-free H_2O. This DNA in this dilution was digested with telomere sequence variant-specific restriction enzymes in the following step. For the TCAGGG variant, WI38-VA13/2RA gDNA was digested in a mixture containing 0.2 µl LpnPI (Cat# R0663S, 5 000 units/ml, New England Biolabs GmbH (NEB), Frankfurt am Main, Germany), 0.5 µl enzyme activator solution (NEB, Frankfurt am Main, Germany), 1.5 µl rCutSmart buffer (Cat# B6004S, NEB, Frankfurt am Main, Germany) and 7.8 µl nuclease-free H_2O. For the TGAGGG variant, YTBO gDNA was digested in a mixture containing 0.3 µl MnlI (Cat# R0163S, 5 000 units/ml, NEB, Frankfurt am Main, Germany) or 0.3 µl HphI (Cat# R0158S, 5 000 units/ml, NEB, Frankfurt am Main, Germany) respectively, 1.5 µl rCutSmart buffer and 8.2 µl nuclease-free H_2O. For the uncut controls, the enzymes and activators were replaced with the respective volume of nuclease-free H_2O.

Before the reaction mixtures were prepared, the gDNAs were heated to 56°C, 10 min followed by vortexing at 1 800 rpm, 5 s and a quick-spin. The reaction mixtures missing the enzymes

were heated to 37°C for 5 min before the restriction enzymes were added. The enzyme addition started the digest, which was run at 37°C for 1 h followed by heating the samples to 80°C, 20 min, for heat inactivation. The resulting products were aliquoted in volumes of 5 µl and stored at -20°C. Additionally, one of the aliquots of each digest was diluted 1:10 with 1xTE and the specific telomere sequence-variant qPCR as well as the qPCR for the canonical telomere sequence (TTAGGG) was run (see 5.5.2). For that, 5 µl of the 1:10 dilution were directly used in the PCRs, analogous to normal gDNA samples.

5.7. Telomere-variant FISH

The execution of the telomere-variant FISH experiment exposed itself to be a severe problem. Over a period of three months, six telomere-variant FISH experiments under different conditions were conducted, of which only two yielded useful results and that only for the TCAGGG variant. These were Experiment B (designated first Experiment in the Results) and Experiment E (designated second Experiment). Even correspondence with the authors of the papers which these experiments were based on (Conomos et al., 2012; Lee et al., 2014) and with the probe manufacturer (PNA Bio Inc., Newbury Park, CA, USA) did not solve the problems with the TGAGGG variant detection. For the sake of completeness, the process of all experiments will be described in the following section.

For the chamber slides (See Table 15, Exp. A) 15 000 cells/well were inoculated in six wells per cell line and incubated at 37°C, 2% CO_2 for 24 h followed by fixation with -20°C cold 100% Methanol overnight at 4°C. The cells on the cytospin slides were treated as described in 5.1.6. If the slides were stored between the fixation and the hybridization, the slides were dehydrated prior to the staining by submerging them in 70% and 100% ethanol (for Exp. B: 1x 2 min in 90% ethanol in between) for 2 min each followed by airdrying for 10 min. The ethanol was reused for multiple experiments.

To improve readability, only the general steps will be listed in the following paragraph, the details about used temperatures, durations and chemicals for each experiment are listed in Table 15. For the hybridization, the probes (and chamber slides) were preheated followed by the addition of 15 µl (100 µl/well for chamber slides) of the respective probe directly on the cells. The cells and probes were covered with coverslips and sealed using glue (Fixogum, MARABU GmbH & Co. KG, Tamm, Germany). For the chamber slides, only the chamber cover was added. The covered and sealed slides were placed on a heating plate for denaturation followed by hybridization in a humid container for 2 h, RT in the dark. Consequently, the glue and the coverslips were removed and the first and second wash series were carried out. After the washes, the slides were dried carefully without touching the cells. A pap pen was used to draw a hydrophobic circle around the cells, which were stained with DAPI subsequently. Per

slide 40 µl (200 µl/well for chamber slides) of DAPI staining solution was used and the slides were incubated for 15 min in a humid container at RT in the dark. The slides were washed in two to three series before being mounted with mounting medium and a coverslip without adding air bubbles and finally sealed using nail polish. The sealed slides were dried overnight in the dark, so the nail polish could harden and microscopical analysis could be conducted.

Table 15: Conditions of all telomere-variant FISH experiments

	Exp. A	Exp. B (First Exp. in Results)	Exp. C	Exp. D	Exp. E (Second Exp. in Results)	Exp. F
cell line:	Chamber slides (Millicell EZ slide 8-Well, Glass, sterile. Merck KGaA, Darmstadt, Germany) with WI38-VA13/2RA and YTBO	Cytospin slides of WI38-VA13/2RA and YTBO	Cytospin slides of WI38-VA13/2RA	Cytospin slides of WI38-VA13/2RA and YTBO	Cytospin slides of WI38-VA13/2RA and YTBO	Cytospin slides of YTBO
PNA probes used (+ means both probes in combination)	TelC-FITC (50 nM), CY3-TCA (50 nM), TelC-FITC (50 nM) + CY3-TCA (50 nM), CY3-TGA (50 nM), TelC-FITC (50 nM) + CY3-TGA (50 nM)	TelC-FITC (66 nM), TelC-FITC (66 nM) + CY3-TCA (22 nM), CY3-TCA (22 nM), TelC-FITC (66 nM) + CY3-TGA (22 nM), CY3-TGA (22 nM)	TelC-FITC (66 nM) + CY3-TCA (22 nM) from Exp. B and a new dilution, CY3-TGA (33, 16.6, 8 and 4 nM)	TelC-FITC (66 nM) + CY3-TCA (22 nM) from Exp. B, CY3-TGA (66, 200 and 600 nM)	TelC-FITC (66 nM) + CY3-TCA (22 nM) from Exp. B, CY3-TGA (500 nM)	TelC-FITC (66 nM) + CY3-TCA (22 nM) from Exp. B, CY3-TGA (500 nM), TelC-FITC (50 nM) + CY3-TGA (50 nM and 500 nM)
Cell line treatment combination	Both cell lines got all treatments	WI38-VA13/2RA: all YTBO: only combinations	Only WI38/VA13	Both cell lines got all treatments	Both cell lines got all treatments	Both cell lines got both treatments

Probes preheat temperature [°C]	85	85	85	90	95	99
Denaturation/ Hybridization temperature [°C] and time	85, 5 min	85, 5 min	85, 5 min	90, 5 min	95, 10 min	99, 10 min
First wash series	PNA wash buffer, 2x 10 min, different containers for each wash				Wash solution, 2x 10 min, 55-60°C, different container for each wash	
Second wash series	TBST, 2x 5min				Wash solution, 10 min RT	
First wash series after DAPI staining	TBST, 3x 5 min				2xSSC 2 min	
Second wash series after DAPI staining	ddH_2O, 2x 5 min				1x SSC 2 min	
Third wash series after DAPI staining					ddH_2O 2 min	

Table 16: Chemicals/Components used for telomere-variant FISH

Chemical/component	Composition
Hybridization buffer	20 mM TrisCl, pH 7.5; 60% deionized formamide (Cat# F5786, Merck KGaA, Darmstadt, Germany), 0.25% blocking reagent (Cat# 11096176001, Roche Austria GmbH, Vienna, Austria), in ddH_2O
PNA-Wash buffer	70% deionized formamide (Cat# F5786, Merck KGaA, Darmstadt, Germany), 10 mM TrisCl pH 7.5, in ddH_2O
2x SSC	0.3 M NaCl and 0.03 M sodium citrate in dH_2O, pH 7
Wash solution	2xSSC, 0.1% Tween20
1xTBST	20 mM Tris pH 7.5, 150 mM NaCl, 0.1% Tween20
DAPI staining solution	1 µg/ml DAPI (Cat# D9542, Merck KGaA, Darmstadt, Germany) in 1xTBST
TelC-FITC probe	Cat# F1009, PNA Bio Inc., Newbury Park, CA, USA; solved in deionized formamide
CY3-TCA probe	`Cy3-OO-TCAGGGTCAGGGTCAGGG`, PNA Bio Inc., Newbury Park, CA, USA; solved in deionized formamide
CY3-TGA probe	`Cy3-OO-TGAGGGTGAGGGTGAGGG`, PNA Bio Inc., Newbury Park, CA, USA; solved in deionized formamide
Vectashield mounting medium	Vectashield (H-1000) without DAPI (Vector Laboratories, Newark CA, USA)

Microscopical imaging of the slides was performed using an Olympus IX83P2ZF spinning disk confocal microscope (Evident Corporation, Tokyo, Japan) at 400x magnification, using an UPLXAPO 40x / 0.95 objective (Evident Corporation, Tokyo, Japan) designed for use without immersion media and at 600x magnification, using an UPLXAPO 60x / 1.42 objective (Evident Corporation, Tokyo, Japan) designed for use with oil immersion. For the DAPI channel an excitation laser at 345 nm, with an intensity of 80% for the first experiment and 88% for the second experiment was used. The dye emitted light at 455 nm. The exposure time was 200 ms in both experiments. The FITC dye of the telomere repeat probe was excited at 495 nm

with a laser intensity of 80% for the first experiment and 88% for the second experiment. The detection took place at a wavelength of 519 nm with an exposure time of 100 ms for both experiments. For the telomere variant spots, the signals of the Cy3 dye were detected at 576 nm. The excitation happened at 551 nm with a laser intensity of 80% for the first experiment and 88% for the second experiment. The exposure time was 100 ms for both experiments.

The analysis of the resulting images is described in 5.8.

For presentation, adjustments and cropping of the images as well as insertions of scale bars were performed using the program ImageJ Fiji (Schindelin et al., 2012).

5.8. Analysis and quantification of FISH images

For the detection and quantification of the foci in all FISH experiments, the software Olympus cellSens Dimension (Evident Corporation, Tokyo, Japan) with its TruAI functionality. For the analysis, two neural networks were trained. The first was used for nucleus detection. For this, the training data was prepared according to the manufacturer's tutorial (Evident Corporation, n.d.-b). The second network was trained for foci detection. Here the training data was prepared analog to a tutorial (Evident Corporation, n.d.-a) provided by the manufacturer. For that, the areas of the cells' nuclei were labeled as background in the same channel the foci were detected in while the DAPI channel also was displayed to show the nuclei's outlines. This was followed by the labeling of every single focus as such in the area of the nuclei, which were labeled as background in the previous step. For this process, the DAPI channel was not displayed. An exemplary presentation of the process is shown in Figure 4 but with all channels displayed. The training was done using microscopical images of the Native ALT-FISH experiments (see 5.4) but the resulting neural network was also applicable to the Telomer variant FISH experiments (see 5.7). In total, 304 nuclei and 2 194 foci from four different cell lines were labeled for the training. After the labeling, both training data sets were used to train their respective neural networks according to a manufacturer's tutorial (Evident Corporation, n.d.-c).

The trained networks were used for the analysis of the FISH experiments following the procedures described here. Firstly, a maximum intensity (called *Maximum Z projection* in cellSens) was performed. Secondly, all nuclei were detected using the neural network described above. Here nuclei, which were truncated by the images' borders were excluded. Based on the detected nuclei, regions of interest (ROIs) were created and counted. In these ROIs, the foci were detected using the second neural network. For the Telomere-variant FISH experiments, this was done in two steps, one for the TTAGGG foci and the other for the variant foci. Foci truncated by the ROI's border were included in the foci analysis. The detected foci

were counted and measured for size, intensity of their respective channel and intensity of the DAPI signal in their area. Also, the number of foci per nucleus was counted. These data were used for statistical analyses (See 5.10.1 and 5.10.3). Exemplary results are shown in Figure 5.

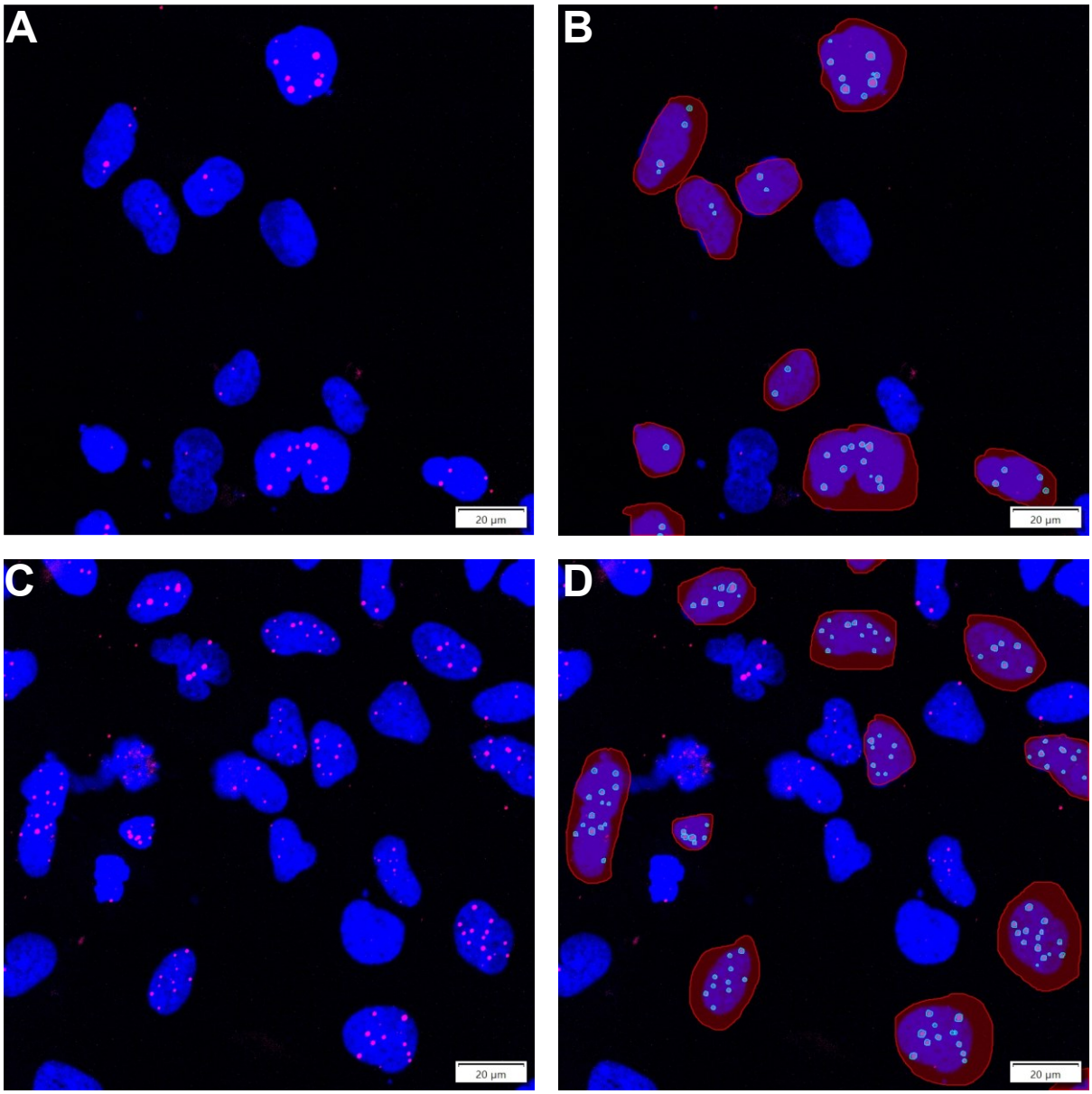

Figure 4: Microscopical confocal spinning disc images at 400x magnification of the cell lines Saos-2 (A and B) and U2OS (C and D) stained using Atto 633 labeled TelC probes for ALT-spot detection and DAPI for nuclear staining used for neural network training. The red labels in Panel B and D depict the background label whereas the blue label shows labeled foci. Panel A and C shows the same images without training labels. Scale bar: 20 µm.

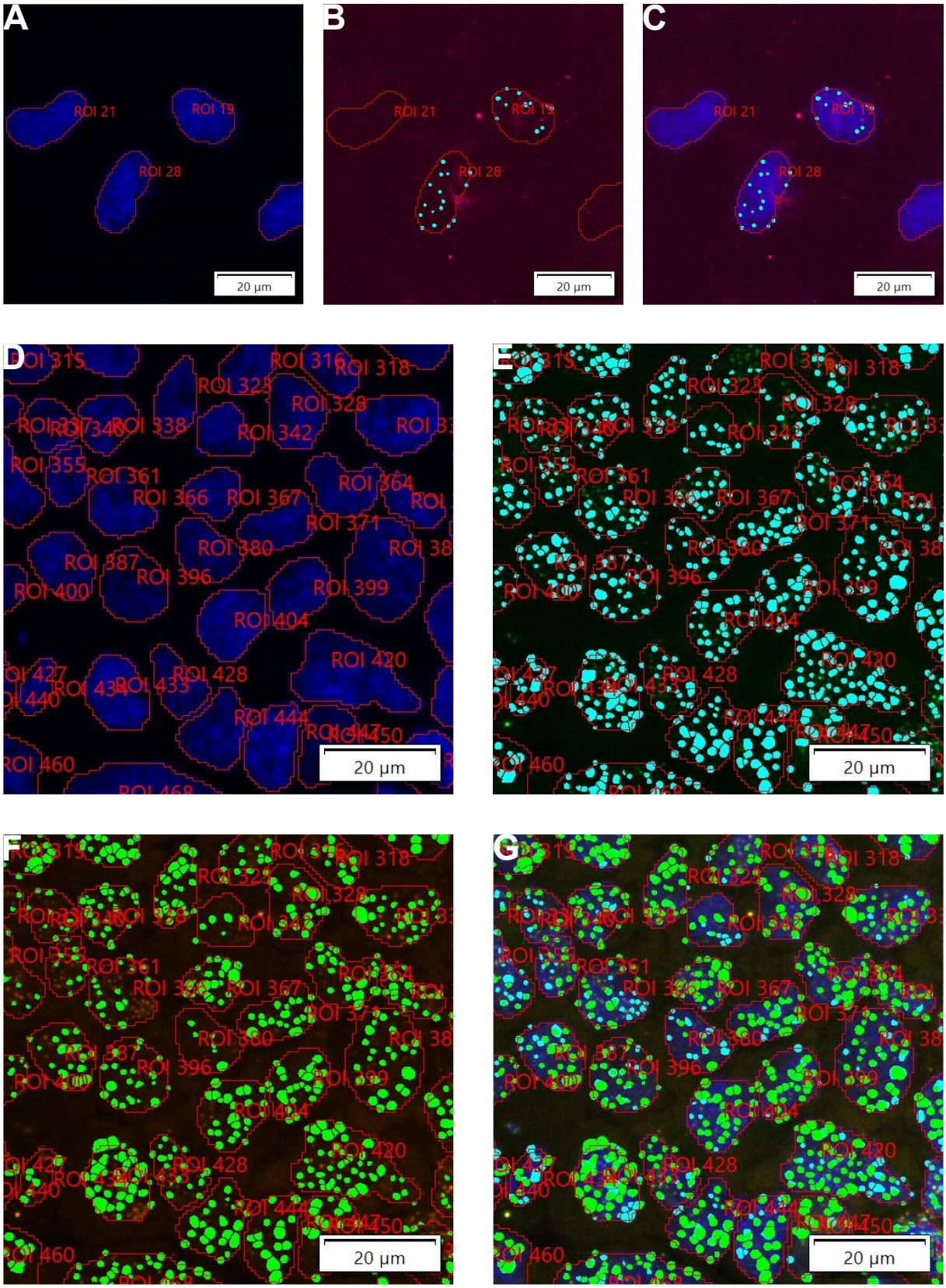

Figure 5: Microscopical confocal spinning disc images at 400x magnification of the cell line WI38-VA13/2RA from the main native ALT-FISH experiment (Figure 7, Panel A-C) and second telomere-variant FISH experiment (Figure 19, Panel D-G) stained using Atto 633 labeled TelC probes for ALT-spot detection (A) or FITC labeled TelC PNA probes for

canonical telomere repeat detection (E) and ATTO-633 labeled PNA probes for TCAGGG detection (F) and DAPI for nuclear staining (A and D) as well as the respective channels merged (C and G). The red frames in all panels depict the AI-based nuclear detection. The cyan labels show detected ALT-foci (B and C), respectively TTAGGG detection foci (E and G). The yellow labels show the detected telomere variant (TCAGGG) foci (F and G) which superimpose the cyan labels in these images. Scale bar: 20 µm.

5.9. Establishment of monoclonal cell lines

For the establishment of monoclonal cell lines, conditioned medium was needed. This was prepared by growing the cell line from which a monoclonal cell line should be established, in its respective medium for 24 h. Here the cells must not grow to a density higher than 90%. After the incubation, the medium was transferred into a 50 ml centrifugation tube. Repeat this process until enough medium is collected. A minimum of 10 ml will be needed for a 96-well plate. When a sufficient amount of medium was collected, it was sterile filtrated using a 0.45 µm pore filter into a new 50 ml centrifugation tube. Before the conditioned medium was used, FCS was added to a concentration of 20%. The conditioned medium was stored at 4°C until used.

For the cell line establishment, sterile PBS and Acutase (Cat# A6964, Merck KGaA, Darmstadt, Germany) were pre-warmed to 37°C. A 96-well plate was prepared with 100 µl conditioned medium per well and stored at 4°C for use later down the line. In order to prepare the cells, which were grown in T25 flasks, they were washed using 1 ml PBS. This was aspirated before 2.5 ml Acutase was added. Afterwards, the flasks were incubated at 37°C for 3 min to detach the cells. 2 ml of the cell suspension was transferred into a new 50 ml centrifugation tube, and the remaining 1.5 ml in the flask were filled up to 3 ml with the cells' respective medium. The cells in the centrifugation tube were centrifuged at 188 g for 5 min. The supernatant was aspirated and the cells were resuspended in 1 ml FACS buffer (PBS with 0.5 % BSA and 2 mM EDTA) and transferred into a FACS tube afterwards. Based on this suspension, one cell per well was sorted in all wells of the previously prepared 96-well plate using a FACSMelody Cell Sorter (Becton Dickinson GmbH, Heidelberg, Germany) followed by an incubation at 37°C, 2% CO_2 for seven days. After this incubation, another 100 µl of conditioned medium was added using a multichannel pipette followed by an additional incubation for seven days. Two weeks after the FACS sorting, the first cell clusters should be visible under the microscope. If sufficient cells (80-100% density) were observed, the cells from at least three different wells were transferred into separate T25 flasks, which were previously prepared with 3 ml of the appropriate conditioned medium. The transfer was done by aspirating the wells' medium and washing them with 50 µl trypsin once. After the wash, 50 µl trypsin were added and the plate was incubated at 37°C for 2 to 3 min. The trypsin's reaction then was stopped with 100 µl

medium followed by a gentle mix using a pipette with genomic pipette tips. The mixed content of the well was finally transferred to the T25 flasks.

5.10. Statistical analysis

All statistical analyses were performed using GraphPad Prism 8.0.1 (GraphPad Software, Boston, MA, USA). The following parameters were used for all statistical analyses: Alpha: 0.05, P-value symbols: >0.05 = ns, 0.05≥ p < 0.01 = *, 0.01≥ p < 0.001 = **, 0.001≥ p ≤ 0.0001 = ***, p< 0.0001 = ****. Correlations were categorized in the following way: r > 0.75 = strong correlation, 0.5 < r > 0.75 = moderate correlation, 0.25 < r > 0.5 = weak correlation and r < 0.25 was deemed as not correlating.

5.10.1. Native ALT-FISH

For the statistical analysis of the native ALT-FISH experiments, the foci count per cell, the area of the foci, their signal intensity and the DAPI signal intensity in the focal area each were combined into separate grouped data tables for all images of each treatment and cell line. From the combined data “descriptive statistics” were created. Based on these, the mean, SD and quantity of nuclei and foci were transferred to new data tables while maintaining a link to the source tables. Each cell line was represented as a separate line while the treatments were represented as separate data sets. The tables were used to create bar graphs for the four metrics, comparing the cell lines and treatments, as well as performing statistical analyses. For the main experiment two-way ANOVAs with Tukey’s multiple comparisons follow-up tests were used. For the preliminary experiment, the data tables were x-y transposed to enable an analysis with Brown-Forsythe and Welch ANOVA tests with Games-Howell’s multiple comparison tests.

In the comparison of both experiments, the data tables of the DAPI + TelC treatment of both experiments were combined in a way that each experiment was represented as a data set. Based on the combined data tables two-way ANOVAs with Sidak’s multiple comparisons follow-up tests were performed and bar graphs were created.

5.10.2. Telomere sequence-variant qPCR

5.10.2.1. Telomere sequence-variant qPCR of gDNAs

Based on the Excel tables created in 5.5.2 the SQ of the cell lines and CT values including the NTC of the cell lines and standards were transferred into three separate grouped data tables in GraphPad Prism, with each cell line or standard dilution level represented as separate lines and the different qPCR targets (36B4, TTAGGG and the variants) represented as separate data sets. The creation of the data tables was followed by the calculation of “Row stats” containing the mean, the SEM and the n of all data sets in all tables. The row stats of the cell

line CT table were x-y transposed to enable statistical analysis. The transposed row stat cell line CT table and the row stat standard cell line were used to create bar graphs to compare the cell line and standard values to the NTC. The standard values were also compared to each other. The statistical analyses of these comparisons were done in form of two-way ANOVAs with Tukey's multiple comparisons follow-up tests.

Based on the row stats of the SQ values, a "Remove Baseline and Column Math" analysis was performed to calculate the percentage of the variants compared to TTAGGG repeat (=100 x Mean SQ Variant ± SEM / Mean SQ TTAGGG±SEM). The resulting table was x-y transposed. From the transposed data table, the percentages of the separate variants were transferred into the y column of xy-tables to calculate a correlation to the whole genome sequencing data (in the x column) from Lee et al. (2014). The values of these resulting xy-tables were carried over into a new grouped data table, in which the number of technical replicates were added again to enable a statistical analysis via a two-way ANOVA with Tukey's multiple comparisons follow-up test.

The correlation tables were tested for normality and, in case no normality was shown, transformed by calculating the decadic logarithm of both columns to create normality. This was confirmed by an additional normality test. Since all tables showed normality, the correlation between the qPCR and WGS data was calculated using Pearson's correlation. Additionally, a linear regression analysis was performed, to present the data.

For the reproducibility analysis, the cell line qPCR results were normalized by the SCG content by subtracting the CT of the SCG from the CT of the canonic telomere repeat and the variants, respectively. This was done using GraphPad Prism's "Remove Baseline and Column Math" function. These dCT values were compared to dCT values of preliminary qPCR telomere variant detection experiments. The statistical analyses of these comparisons were done in form of two-way ANOVAs with Sidak's multiple comparisons follow-up tests. For the comparison of the variant percentages, these were calculated as stated above. For the statistical analysis a two-way ANOVA with Tukey's multiple comparisons follow-up test was used.

5.10.2.2. Restriction digest products

The SQ data of every qPCR target (TTAGGG and TCAGGG) of both cell lines (see 5.6 and 5.5.2) was transferred into a separate grouped data table resulting in four distinct tables. In these tables, the resulting SQ values of the separate digests were displayed as distinct data sets. Of all these data tables "row stats" analyses were performed including the SQs mean, SEM and n. These tables were used to create bar graphs as well as the basis of statistical analyses. For the YTBO digests Brown-Forsythe and Welch ANOVA tests with Games-

Howell's multiple comparison tests were used. The WI38-VA13/2RA digest data was analyzed using unpaired t-tests with Welch's correction.

5.10.2.3. C-circle assay products

For the analysis of the C-circle assay products, the SQ values of their telomere sequence variant qPCRs (see 5.5.2) were transferred to a grouped data table where the single targets are represented as separate lines and the cell lines and their polymerase positive and negative treatments are represented as separate data sets. First, the mean, the SEM and n of the SQs were calculated followed by a "Remove Baseline and Column Math" analysis. Here the percentage of the mean ± SEM of the polymerase positive reaction compared to the mean ± SEM of the polymerase negative reaction (100 x Phi+ SQ mean ± SEM / Phi- SQ mean ± SEM) was calculated to present the increase of the respective qPCR target. These results were used to create bar graphs and were transferred into a newly grouped data table, in which the number of technical replicates was added again followed by a xy-transpose to enable statistical analyses via two two-way ANOVAs with Tukey's multiple comparisons follow-up test to compare the cell lines and variants.

5.10.2.4. TCAGGG cluster variant DNA oligomer qPCR

For the analysis of the results from the TCAGGG cluster variant DNA oligomer qPCR, the resulting CT values (see 5.5.3) were transferred into a grouped data table where the dilution levels (i.e., number of molecules) and NTCs were represented as separate lines and the different oligomer templates as separate data sets. This table was used to calculate two two-way ANOVAs, one with a Dunnett's multiple comparison follow-up test to compare the dilution levels of every oligomer template to the NTC and a second one with a Tukey's multiple comparisons follow-up test to compare the separate dilution levels of all oligomer templates. The table was also used to calculate "row stats" (mean, SEM and n) of all CTs, which were used to create bar graphs.

5.10.3. Telomere-variant FISH

The statistical analysis of both Telomere-variant FISH experiments followed a similar path as the native ALT-FISH analysis. First, the data of the TTAGGG and TCAGGG foci count per cell, the respective foci area and intensity as well as the DAPI signal intensity in the respective foci area was combined for all images of each cell line whereas the TTAGGG and TCAGGG data were transferred into one data table but as separate data sets. The separate cell lines were represented as separate lines in the data tables. These data tables were used as the basis for bar graphs of the different metrics as well as the source for statistical analyses in form of two-way ANOVAs with Sidak's multiple comparison tests comparing the cell lines and probe targets with each other. In addition to the metrics, which were also used in the native ALT-FISH

analysis, a “Remove Baseline and Column Math” analysis was performed to calculate the percentage of the TCAGGG foci per cell compared to TTAGGG foci per cell (=100 x TCAGGG foci per cell / TTAGGG foci per cell) to enable comparability to the qPCR analyses. For these analyses, statistical differences cannot be calculated.

In the comparison of both experiments, the data tables of both experiments were combined in a way that each experiment’s target was represented as a separate data set (e.g., TTAGGG Exp.1, TCAGGG Exp. 1, TTAGGG Exp. 2, TCAGGG Exp. 2). Based on the combined data tables two-way ANOVAs with Sidak’s multiple comparisons follow-up tests were performed and bar graphs were created.

6. Results

6.1. ALT activity detection

To verify that all cell lines described as such (Table 1) were ALT-positive, I used two distinct methods to ensure their TMM. First, the gold-standard C-circle assay was used and second, a recently developed method called native ALT-FISH. The results of these two methods are described in the following section, starting with the C-circle assays’ results.

6.1.1. ALT activity detection by C-circle assay

First, I applied the C-circle assay in two experiments to measure the CCA levels in each cell line (Table 1). In the first experiment using previously isolated gDNA which were already used for other qPCR experiments, (Figure 6A; Table 43) I observed very high standard deviations for all cell lines in their triplicates (Table 41 and Table 42), leading to enormous error bars in the graph. The highest normalized CCA level was observed in the Saos-2 2022 positive control, followed by Saos-2, U2OS, U2OS positive control, IIICF/c, *GM847**, HT-1080 PTL, WI38-VA13/2RA, HeLa, the negative control, YTBO and HT-1080 hTR wt. Additionally, the positive control cell line U2OS 2022 typically used for normalization, was deemed ALT negative due to its lower error bar (for classification guidelines see 5.5.1) and unexpectedly, several usually ALT-positive cell lines were not detected as such (*GM847**, IIICF/C, WI38-VA13/2RA and YTBO). Also, due to the negativity of the U2OS positive control cell line, a biological replicate of this cell line, technically a test subject, was used for normalization in this experiment. It showed an unnormalized C-circle level of 0.59 (Figure 23, Table 43). The Saos-2 cell line and the Saos-2 positive control were detected as ALT-positive and showed high ALT activities. The telomerase-positive cell lines (HeLa and HT-1080) as well as the negative control were ALT negative, following the expectations that telomerase positive cell lines and the negative control do not show ALT activity.

In consequence of these results, the experiment was repeated with freshly isolated DNAs from freshly grown cell lines. These DNAs were used for the second C-circle assay directly without additional freeze-thaw cycles and without prolonged storage at 4°C. The results of the repeated experiment are depicted in Figure 6B. Here the standard deviations were much lower (Table 45 and Table 46). Misleadingly, the error bars in Panel B seem to be of similar range as in Panel A which is due to the different scaling of the graphs' X-axes. In this case, the normalized errors were much smaller in the second experiment. The highest normalized CCA level in the second experiment was observed in the Saos-2 2022 positive control followed by the U2OS 2022 positive control, YTBO, U2OS, IIICF/c, WI38-VA13/2RA, HeLa, HT-1080 PTL, the negative control, *GM847** and HT-1080 hTR wt. Here, the positive control U2OS cell line could be used for normalization. It had a C-circle level of 1.5 (See Figure 23 and Table 47), which was three times as high as in experiment one, leading to a reduction of the normalized CCA levels in experiment two compared to experiment one. All canonically ALT-positive cell lines, except *GM847** and WI38-VA13/2RA, showed a positive CCA result. However, all ALT-positive cell lines except IIICF/c and YTBO showed a lower level in the second experiment. The telomerase-positive cell lines as well as *GM847**, WI38-VA13/2RA and the negative control were ALT negative.

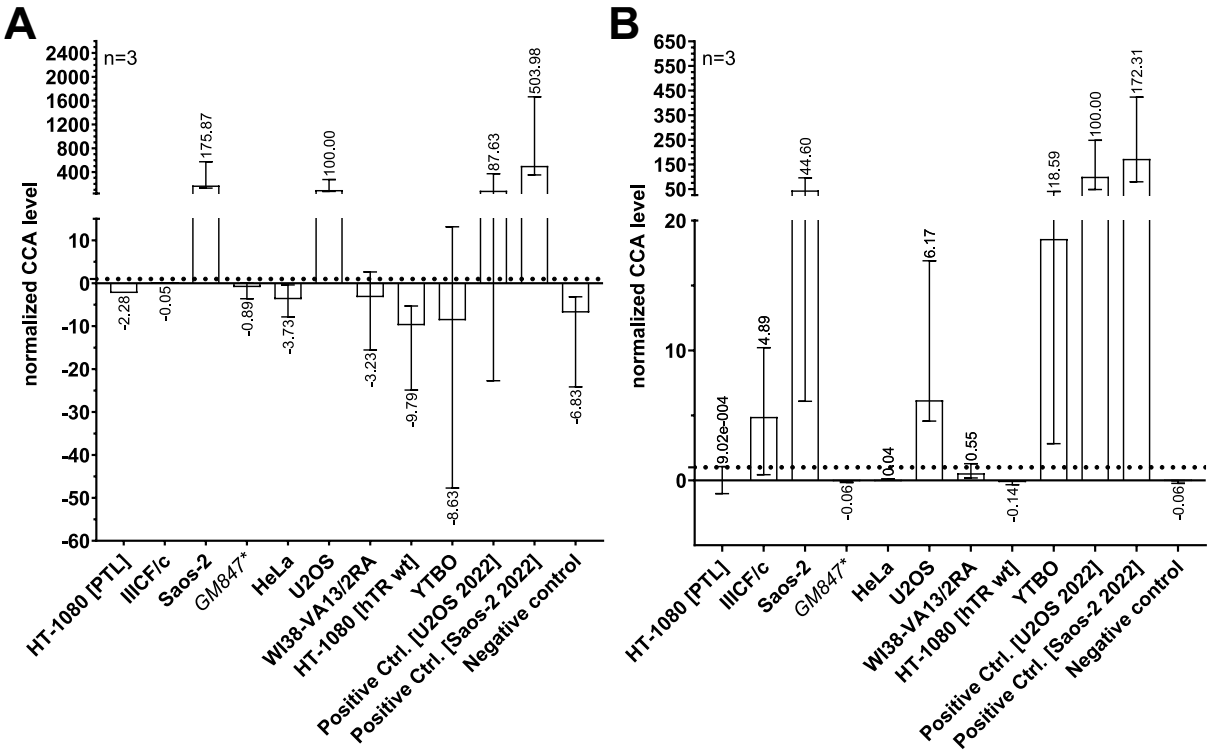

Figure 6: Normalized C-circle levels detected by qPCR. A: Normalized C-circle levels of the first C-circle experiment. Here the cell line U2OS was used for normalization, not the positive control U2OS cell line. B: Normalized C-circle levels of biological replicates from cells

tested in A. These graphs depict the averaged, normalized C-circle levels of two independent C-circle assay experiments. The CCA-qPCR experiments were performed in technical triplicates. Raw data can be found in 11.2.1. The error bars were calculated as stated in 5.5.1. The dotted line depicts 1% of the C-circle levels of the positive control U2OS cell line used as the threshold for positive C-circle assay results.

6.1.2. ALT activity detection by Native ALT-FISH

In order to validate the ALT status of the cell lines and to see if the representatives of *GM847** and WI38-VA13/2RA cells used in this work were just C-circle negative but showed ALT-activity, experiments were conducted using a more recent ALT-detection method called native ALT-FISH. This analysis included the canonically ALT-positive cell lines *GM847**, IIICF/c, Saos-2, U2OS, WI38-VA13/2RA and YTBO. The telomerase-positive cell line HeLa was used as a negative control.

In summary, all cell lines except *GM847** and WI38-VA13/2RA which were described as ALT-positive in the literature also showed ALT activity in the second CCA (Figure 6B) and the ALT FISH experiments (Figure 7), although deviations between the two detection methods were observed. WI38-VA13/2RA for an instance, contrary to the CCA results was ALT-positive in the ALT FISH experiment. In the CCA, Saos-2 cell lines showed the highest ALT activity (Figure 6) while in the ALT FISH, it had the second lowest number of ALT spots per cell in the "DAPI + TelC" treatment and the lowest number following RNase treatment (Figure 7A). These spots, however, were the biggest of all cell lines (Figure 7B). This may compensate for the difference in number to be more consistent with the CCA results. The second strongest activity in the CCA was shown by YTBO cells (Figure 6B), which had the lowest and second lowest amount of ALT signals per cell in the "DAPI + TelC" and "DAPI + TelC + RNase" treatments respectively (Figure 7A). Here the spots had intermediate to small sizes and were on the lower end in terms of signal strength (Figure 7B and C). This did not fit the CCA results. The experimental U2OS cell line had the next lower CCA activity (Figure 6) and also was the third cell line in terms of ALT spot number per cell with intermediate sizes and signal intensities (Figure 7A, B and C). This is consistent with the CCA experiment whereas the deviation to the positive control U2OS cell line has to be noted there. IIICF/c had the lowest CCA level in the second assay (Figure 6B) but the highest amount of ALT spots per cell with intermediate to high spot sizes and average signal intensities (Figure 7A, B and C), so a substantial deviation between the two ALT detection methods could be observed with this cell line. The same was also true for the WI38-VA13/2RA cell line, which did not show CCA levels high enough to be

counted as ALT-positive (Figure 6A and B) but the third highest amount of ALT spots per cell could be observed here (Figure 7A). Whereas the standard deviation in the ALT spot numbers was very high and their size and signal intensities were on the lower end of the cell lines tested (Figure 7B and C). More detailed descriptions of the results can be found in the following paragraphs.

In the negative control treatment (DAPI only), none of the cell lines showed any significantly elevated number of ALT-spots, as expected (Figure 7A, Table 17). In this treatment, the number of signals per cell line ranged from 33 in U2OS to one in Saos-2 and YTBO while more than 100 cells were analyzed for each cell line. These signals were probably due to noise or contamination with small fluorescent particles during preparation. They also showed high variability in size (Figure 7B, Table 19) and signal intensity (Figure 7C, Table 21), which also speaks for random occurrences. Only U2OS showed significantly smaller ALT spot sizes compared to the cell lines with the biggest spots *GM847** and Wi38-VA13/2RA. No significant difference in size was observed compared to all other cell lines. Only in U2OS, the signal intensity (430.9±351.1) was significantly higher compared to all other cell lines in the DAPI-only treatment.

In the DAPI + TelC treatment, all ALT-positive cell lines except *GM847** showed significantly more ALT spots compared to the negative control treatment (Table 18) and significantly more compared to the telomerase-positive cell lines (Figure 7A, Table 17). Analog to the CCA experiments, *GM847** showed no ALT activity. Its mean number of ALT spots/cell did not significantly differ from the negative control cell line HeLa. All other cell lines, except YTBO crossed the threshold to be determined ALT-positive in this experiment and fell in the “ALT” category. YTBO was categorized as “low ALT” based on the classification of Frank et al. (2022). IIICF/c showed the highest number of mean ALT spots/cell followed by a significantly lower amount in WI38-VA13/2RA. The results from this cell line showed a very high standard deviation. The cell lines with the next smaller number of average spots per cell were Saos-2 and YTBO. These two cell lines did not significantly differ from each other. For this treatment, the size of the ALT spots differed significantly from one ALT-positive cell line to the other (Table 19) except for WI38-VA13/2RA and YTBO. Saos-2 cells contained the biggest spots but also had the biggest standard deviation. The next smaller sizes were observed in IIICF/c followed by U2OS. The smallest signals were found in WI38-VA13/2RA and YTBO cells. The ALT spot size did not differ significantly in these two cell lines. When looking at the signal intensity of the ALT spots, a more uniform pattern could be observed in the ALT-positive classified cell lines (Figure 7C, Table 21). The negative control HeLa showed the highest intensity, which was only attributed to two signals, probably caused by fluorescent debris or probe accumulations.

*GM847** spots' signal intensity did not significantly differ from all other cell lines except the negative control.

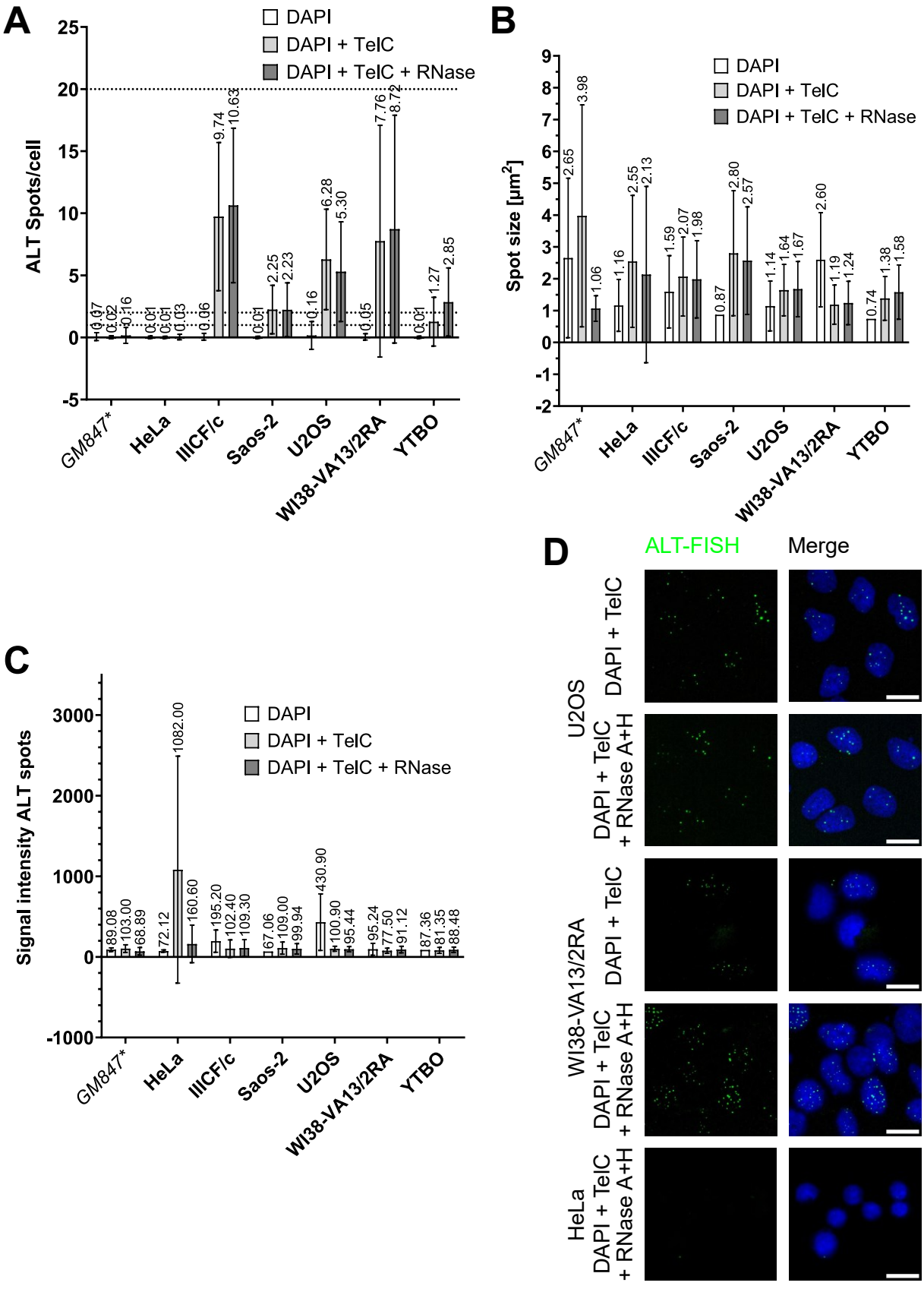

Figure 7: Quantification of the main ALT-FISH experiment (no technical replicates). A: Comparison of the mean ALT spots per cell ± SD of seven different cell lines at three different treatments. The dotted lines depict thresholds for ALT levels: 1-2: low ALT, 2-20 ALT, >20

super ALT. Statistics are shown in Table 17 and Table 18. B: Comparison of the mean area of ALT-spots ± SD in the analyzed cell lines at three different treatments. Statistics can be found in Table 19 and Table 20. C: Comparison of the mean ALT-Spot signal intensity ± SD of the analyzed cell lines at three different treatments. Statistics are presented in Table 21 and Table 22. D: Microscopical confocal spinning disc images at 400x magnification of two ALT-positive cell lines (WI38-VA13/2RA and U2OS) with and without combined RNase A+H treatment and the negative control HeLa stained using Atto 633 labeled TelC probes for ALT-spot detection and DAPI for nuclear staining. Scale bar: 20 µm

Of the cell lines classified as ALT-positive, Saos-2 had the strongest ALT spot signals, which was significantly different compared to HeLa, U2OS, Wi38-VA13/2RA and YTBO but did not show a significant difference in contrast to *GM847** and IIICF/c. The next weaker signal was that of IIICF/c, which was significantly different compared to Hela, WI38-VA13/2RA and YTBO but did not differ significantly from the rest of the cell lines. Following in line was U2OS. This was significantly different from all other cell lines except IIICF/c and *GM847**. The lowest intensities could be observed in YTBO and WI38-VA13/2RA cells. These values differed significantly from all other cell lines except *GM847** and each other.

In the cells that were treated with RNase A + H, the order of cell lines in terms of mean ALT spots/cell numbers ± SD from high to low numbers nearly stayed the same (Figure 7A, Table 17). Here, only Saos-2 and YTBO swapped places but without showing a significant difference anymore. The increase of YTBO's spot amount shifted the cell line to the "ALT" classification in this treatment. All other cell lines significantly differed from each other in this regard with one exception, which was *GM847**. Here the difference compared to the negative control HeLa was not significant. This was analog to the previous treatment. In terms of mean ALT spot sizes (Figure 7 Panel B, Table 19), the sequence from big to small stayed the same as in the treatment without adding RNase. Only differences in significance occurred. From the cell lines classified ALT-positive, only YTBO and U2OS, the two cell lines with the smallest spots, did not show a significant difference here. Compared to the previous treatment, the range of different signal intensities decreased here (Figure 7C, Table 21). The highest average ALT spot signal intensity was observed in IIICF/c cells which was significantly higher than the intensity of all other cells classified ALT-positive followed by Saos-2. This value only showed significant differences to IIICF/c, WI38-VA13/2RA, YTBO. The three lowest average signal intensities of U2OS, WI38-VA13/2RA and YTBO only were significantly different compared to IIICF/c and in case of U2OS to Saos-2 but not compared to each other.

To see how much of a difference the RNase treatment made, the data from the three treatments was compared for each cell line. In the case of the average number of ALT spots per cell (Table 18), *GM847** and the negative control HeLa did not show any significant differences comparing all three treatments. The cell lines IIICF/c and Saos-2 showed a significant difference comparing the “DAPI + TelC” and “DAPI + TelC +RNase” treatments to the “DAPI only” negative control but not when comparing these two treatments with each other. For the cell lines U2OS and WI38-VA13/2RA, all the treatments made a significant difference in the number of ALT spots per cell, albeit the difference between the two TelC probe-including treatments was much smaller and had a much bigger p-value. For YTBO, all three treatments made a significant difference but the variation between the “DAPI only” control compared to the “DAPI + TelC” treatment was lower and less significant (P value= 0.0218) than when comparing the “DAPI + TelC” treatment with the “DAPI + TelC + RNase” treatment with a P value <0.0001. When comparing the size of the ALT spots between the treatments (Table 20), HeLa did not show any significant changes. For *GM847** only the spots in the “DAPI + TelC + RNase” treatment were significantly smaller than the ones in the other treatments. In IIICF/c cells, only this treatment significantly differed from the others in terms of ALT spot size, with their value being in the middle of the two others. The same pattern could also be observed in Saos-2 cells but with a higher level of significance. In the U2OS cell line, the spot size in the TelC probe containing treatments only significantly diverged from the “DAPI only” control but not from each other. The same could be seen in WI38-VA13/2RA cells but with a higher level of significance. In YTBO cells the ALT spot sizes only differed significantly from another when comparing the “DAPI + TelC” and “DAPI + TelC + RNase” treatment. When assessing the ALT spot signal intensities of the three treatments (Table 22), no significant differences could be observed in the cell lines *GM847** and YTBO. In HeLa cells, the signals observed in the “DAPI + TelC” treatment were significantly stronger than in the two other treatments, which did not significantly differ from each other. The signals from the “DAPI only” treatment were the significantly strongest in IIICF/c cells followed by the intensity of the “DAPI + TelC + RNase” signals. In these cells, the significantly weakest signals could be observed in the “DAPI + TelC” treatment. In Saos-2 cells, the intensity of the one ALT spot signal in the “DAPI only” treatment did not significantly differ from the signal intensity of cells in the two remaining treatments. These two significantly differed from each other. The signals in cells treated with “DAPI + TelC” were stronger than in cells that additionally underwent RNase treatment. In U2OS cells the cells only treated with DAPI contained the significantly strongest signals, albeit only being 33 in number compared to >2000 in the other treatments. The signals of the other two treatments significantly differed from each other in intensity. The “DAPI + TelC” treatment showed a slightly higher signal intensity. In WI38-VA13/2RA cells, only the signal intensity in the “DAPI + TelC” treatment was significantly lower than in the other two remaining ones.

To check if the ALT FISH results are reproducible, the results of the HeLa, Saos-2 and U2OS cell lines from the main experiment were compared with the results of biological replicates of the same cell lines from a preliminary experiment.

When comparing the mean amount of ALT spots per cell (Figure 8A, Table 23) no significant differences between the preliminary and main experiment could be observed. In terms of mean ALT spot size (see Figure 8B; Table 24), only the U2OS cell line showed significantly smaller spots in the main experiment. When taking a look at the mean signal intensities (Figure 8C, Table 25), HeLa showed a striking difference of nearly two orders of magnitude between the two experiments. As mentioned above, the high signal in the main experiment was probably due to some fluorescence debris or other artifacts since there only were two signals with a very high standard deviation. Saos-2 cells did not show significant differences between the two experiments. In U2OS, there were only small differences in mean signal intensity but significant ones, nonetheless. All in all, the ALT fish experiments were reproducible, especially compared to the C-circle assay experiments (see 0).

Table 17: Statistics (two-way ANOVA with Tukey's multiple comparisons follow-up test) of the ALT-spots per cell quantification of the main ALT-FISH experiment (See Figure 7, Panel A) comparing the cell lines.

DAPI only

		*GM847**	HeLa	IIICF/c	Saos-2	U2OS	WI38-VA13/2RA	YTBO
n Cells		102	265	103	123	201	119	114
Mean ALT spots/cell		0.07	0.01	0.06	0.01	0.16	0.05	0.01
SD ALT spots/cell		0.32	0.11	0.27	0.09	1.12	0.26	0.09
Range		2	1	2	1	10	2	1
*GM847**	P values		ns (>0.9999)	ns (>0.9999)	ns (>0.9999)	ns (>0.9999)	ns (>0.9999)	ns (>0.9999)
HeLa	P values	ns (>0.9999)		ns (>0.9999)	ns (>0.9999)	ns (0.9997)	ns (>0.9999)	ns (>0.9999)
IIICF/c	P values	ns (>0.9999)	ns (>0.9999)		ns (>0.9999)	ns (>0.9999)	ns (>0.9999)	ns (>0.9999)
SAOS-2	P values	ns (>0.9999)	ns (>0.9999)	ns (>0.9999)		ns (>0.9999)	ns (>0.9999)	ns (>0.9999)
U2OS	P values	ns (>0.9999)	ns (>0.9999)	ns (>0.9999)	ns (>0.9999)		ns (>0.9999)	ns (>0.9999)
WI38-VA13/2RA	P values	ns (>0.9999)	ns (>0.9999)	ns (>0.9999)	ns (>0.9999)	ns (>0.9999)		ns (>0.9999)
YTBO	P values	ns (>0.9999)	ns (>0.9999)	ns (>0.9999)	ns (>0.9999)	ns (>0.9999)	ns (>0.9999)	

TelC

		*GM847**	HeLa	IIICF/c	Saos-2	U2OS	WI38-VA13/2RA	YTBO
n Cells		260	244	181	442	419	270	233
Mean ALT Spots/cell		0.02	0.01	9.74	2.25	6.28	7.76	1.27
SD ALT spots/cell		0.12	0.09	5.97	1.95	4.04	9.33	1.96
Range		1	1	36	10	20	95	11
*GM847**	P values		ns (>0.9999)	**** (<0.0001)	**** (<0.0001)	**** (<0.0001)	**** (<0.0001)	* (0.0145)
HeLa	P values	ns (>0.9999)		**** (<0.0001)	**** (<0.0001)	**** (<0.0001)	**** (<0.0001)	* (0.0162)
IIICF/c	P values	**** (<0.0001)	**** (<0.0001)		**** (<0.0001)	**** (<0.0001)	**** (<0.0001)	**** (<0.0001)
SAOS-2	P values	**** (<0.0001)	**** (<0.0001)	**** (<0.0001)		**** (<0.0001)	**** (<0.0001)	ns (0.0571)
U2OS	P values	**** (<0.0001)	**** (<0.0001)	**** (<0.0001)	**** (<0.0001)		*** (0.0001)	**** (<0.0001)
WI38-VA13/2RA	P values	**** (<0.0001)	**** (<0.0001)	**** (<0.0001)	**** (<0.0001)	*** (0.0001)		**** (<0.0001)
YTBO	P values	* (0.0145)	* (0.0162)	**** (<0.0001)	ns (0.0571)	**** (<0.0001)	**** (<0.0001)	

TelC + RNase treatment

		*GM847**	HeLa	IIICF/c	Saos-2	U2OS	WI38-VA13/2RA	YTBO
n Cells		268	287	300	802	435	460	375
Mean ALT Spots/cell		0.16	0.03	10.63	2.23	5.30	8.72	2.85
SD ALT spots/cell		0.64	0.22	6.23	2.17	4.02	9.17	2.75
Range		6	2	38	15	19	41	15
*GM847**	P values		ns (0.9998)	**** (<0.0001)	**** (<0.0001)	**** (<0.0001)	**** (<0.0001)	**** (<0.0001)
HeLa	P values	ns (0.9998)		**** (<0.0001)	**** (<0.0001)	**** (<0.0001)	**** (<0.0001)	**** (<0.0001)
IIICF/c	P values	**** (<0.0001)	**** (<0.0001)		**** (<0.0001)	**** (<0.0001)	**** (<0.0001)	**** (<0.0001)
SAOS-2	P values	**** (<0.0001)	**** (<0.0001)	**** (<0.0001)		**** (<0.0001)	**** (<0.0001)	ns (0.2056)
U2OS	P values	**** (<0.0001)	**** (<0.0001)	**** (<0.0001)	**** (<0.0001)		**** (<0.0001)	**** (<0.0001)
WI38-VA13/2RA	P values	**** (<0.0001)	**** (<0.0001)	**** (<0.0001)	**** (<0.0001)	**** (<0.0001)		**** (<0.0001)
YTBO	P values	**** (<0.0001)	**** (<0.0001)	**** (<0.0001)	ns (<0.0001)	**** (<0.0001)	**** (<0.0001)	

Table 18: Statistics (two-way ANOVA with Tukey's multiple comparisons follow-up test) of the ALT-spots per cell quantification of the main ALT-FISH experiment (See Figure 7, Panel A) comparing the treatments.

	DAPI	DAPI + TelC	DAPI + TelC + RNase treatment
		*GM847**	
n Cells	102	260	268
Mean ALT Spots/cell	0.07	0.02	0.16
Standard deviation	0.32	0.12	0.64
		P values	
DAPI only		ns (0.9934)	ns (0.9804)
DAPI + TelC	ns (0.9934)		ns (0.9153)
DAPI + TelC + RNase treatment	ns (0.9804)	ns (0.9153)	
		HeLa	
n Cells	265	244	287
Mean ALT Spots/cell	0.01	0.01	0.03
Standard deviation	0.11	0.09	0.22
		P values	
DAPI only		ns (>0.9999)	ns (0.9976)
DAPI + TelC	ns (>0.9999)		ns (0.997)
DAPI + TelC + RNase treatment	ns (0.9976)	ns (0.997)	
		IIICF/c	
n Cells	103	181	300
Mean ALT Spots/cell	0.06	9.74	10.63
Standard deviation	0.27	5.97	6.23
		P values	
DAPI only		**** (<0.0001)	**** (<0.0001)
DAPI + TelC	**** (<0.0001)		ns (0.0577)
DAPI + TelC + RNase treatment	**** (<0.0001)	ns (0.0577)	
		Saos-2	
n Cells	123	442	802
Mean ALT Spots/cell	0.01	2.25	2.23
Standard deviation	0.09	1.95	2.17
		P values	
DAPI only		**** (<0.0001)	**** (<0.0001)
DAPI + TelC	**** (<0.0001)		ns (0.9977)
DAPI + TelC + RNase treatment	**** (<0.0001)	ns (0.9977)	
		U2OS	
n Cells	201	419	435
Mean ALT Spots/cell	0.16	6.28	5.30
Standard deviation	1.12	4.04	4.02
		P values	
DAPI only		**** (<0.0001)	**** (<0.0001)
DAPI + TelC	**** (<0.0001)		** (0.0015)
DAPI + TelC + RNase treatment	**** (<0.0001)	** (0.0015)	
		WI38-VA13/2RA	
n Cells	119	270	460
Mean ALT Spots/cell	0.05	7.76	8.72
Standard deviation	0.26	9.33	9.17
		P values	
DAPI only		**** (<0.0001)	**** (<0.0001)
DAPI + TelC	**** (<0.0001)		** (0.0068)
DAPI + TelC + RNase treatment	**** (<0.0001)	** (0.0068)	
		YTBO	
n Cells	114	233	375
Mean ALT Spots/cell	0.01	1.27	2.85
Standard deviation	0.09	1.96	2.75
		P values	
DAPI only		* (0.0218)	**** (<0.0001)
DAPI + TelC	* (0.0218)		**** (<0.0001)
DAPI + TelC + RNase treatment	**** (<0.0001)	**** (<0.0001)	

Table 19: Statistics (two-way ANOVA with Tukey's multiple comparisons follow-up test) of the ALT-spot area quantification of the main ALT-FISH experiment (See Figure 7, Panel B) comparing the cell lines.

DAPI only

		*GM847**	HeLa	IIICF/c	Saos-2	U2OS	WI38-VA13/2RA	YTBO
n ALT spots		7	3	6	1	33	6	1
Mean Area [µm²]		2.65	1.16	1.59	0.87	1.14	2.60	0.74
SD Area		2.51	0.82	1.14	0.00	0.78	1.48	0.00
*GM847**	P values		ns (0.4132)	ns (0.5673)	ns (0.7164)	* (0.0134)	ns (>0.9999)	ns (0.6434)
HeLa		ns (0.4132)		ns (0.9978)	ns (>0.9999)	ns (>0.9999)	ns (0.4933)	ns (0.9999)
IIICF/c		ns (0.5673)	ns (0.9978)		ns (0.9963)	ns (0.9668)	ns (0.6711)	ns (0.9908)
SAOS-2		ns (0.7164)	ns (>0.9999)	ns (0.9963)		ns (>0.9999)	ns (0.7554)	ns (>0.9999)
U2OS		* (0.0134)	ns (>0.9999)	ns (0.9668)	ns (>0.9999)		* (0.0382)	ns (0.9998)
WI38-VA13/2RA		ns (>0.9999)	ns (0.4933)	ns (0.6711)	ns (0.7554)	* (0.0382)		ns (0.6861)
YTBO		ns (0.6434)	ns (0.9999)	ns (0.9908)	ns (>0.9999)	ns (0.9998)	ns (0.6861)	

TelC

		*GM847**	HeLa	IIICF/c	Saos-2	U2OS	WI38-VA13/2RA	YTBO
n ALT spots		4	2	1762	993	2633	2094	296
Mean Area [µm²]		3.98	2.55	2.07	2.80	1.64	1.19	1.38
SD Area		3.49	2.07	1.24	1.96	0.81	0.61	0.69
*GM847**	P values		ns (0.072)	** (<0.0001)	ns (<0.0001)	*** (0.0045)	**** (0.9416)	**** (0.0349)
HeLa		ns (0.072)		ns (0.9995)	ns (0.861)	ns (0.8345)	ns (0.1213)	ns (0.6752)
IIICF/c		** (<0.0001)	ns (0.9995)		**** (<0.0001)	**** (<0.0001)	**** (<0.0001)	**** (<0.0001)
SAOS-2		ns (<0.0001)	ns (0.861)	**** (<0.0001)		**** (<0.0001)	**** (<0.0001)	**** (<0.0001)
U2OS		*** (0.0045)	ns (0.8345)	**** (<0.0001)	**** (<0.0001)		**** (<0.0001)	** (0.2074)
WI38-VA13/2RA		**** (0.9416)	ns (0.1213)	**** (<0.0001)	**** (<0.0001)	**** (<0.0001)		ns (0.0532)
YTBO		**** (0.0349)	ns (0.6752)	**** (<0.0001)	**** (<0.0001)	** (0.2074)	ns (0.0532)	

TelC + RNase treatment

		*GM847**	HeLa	IIICF/c	Saos-2	U2OS	WI38-VA13/2RA	YTBO
n ALT spots		43	10	3188	1789	2296	4013	1069
Mean Area [µm²]		1.06	2.13	1.98	2.57	1.67	1.24	1.58
SD Area		0.40	2.77	1.21	1.69	0.87	0.68	0.85
*GM847**	P values		ns (0.726)	**** (0.0075)	**** (0.3093)	** (0.0003)	ns (<0.0001)	* (<0.0001)
HeLa		ns (0.726)		ns (0.996)	ns (0.9999)	ns (0.901)	ns (0.5608)	ns (0.7329)
IIICF/c		**** (0.0075)	ns (0.996)		**** (<0.0001)	**** (<0.0001)	**** (<0.0001)	**** (<0.0001)
SAOS-2		**** (0.3093)	ns (0.9999)	**** (<0.0001)		**** (<0.0001)	**** (<0.0001)	**** (<0.0001)
U2OS		** (0.0003)	ns (0.901)	**** (<0.0001)	**** (<0.0001)		**** (<0.0001)	ns (0.0015)
WI38-VA13/2RA		ns (<0.0001)	ns (0.5608)	**** (<0.0001)	**** (<0.0001)	**** (<0.0001)		**** (0.0532)
YTBO		* (<0.0001)	ns (0.7329)	**** (<0.0001)	**** (<0.0001)	ns (0.0015)	**** (0.0532)	

Table 20: Statistics (two-way ANOVA with Tukey's multiple comparisons follow-up test) of the ALT-spots area quantification of the main ALT-FISH experiment (See Figure 7, Panel B) comparing the treatments.

	DAPI	DAPI + TelC	DAPI + TelC + RNase treatment
		*GM847**	
n ALT spots	7	4	43
Mean Area [µm2]	2.65	3.98	1.06
SD Area	2.51	3.49	0.40
		P values	
DAPI only		ns (0.1234)	*** (0.0009)
DAPI + TelC	ns (0.1234)		**** (<0.0001)
DAPI + TelC + RNase treatment	*** (0.0009)	**** (<0.0001)	
		HeLa	
n ALT spots	3	2	10
Mean Area [µm2]	1.16	2.55	2.13
SD Area	0.82	2.07	2.77
		P values	
DAPI only		ns (0.3389)	ns (0.3602)
DAPI + TelC	ns (0.3389)		ns (0.8734)
DAPI + TelC + RNase treatment	ns (0.3602)	ns (0.8734)	
		IIICF/c	
n ALT spots	6	1762	3188
Mean Area [µm2]	1.59	2.07	1.98
SD Area	1.14	1.24	1.21
		P values	
DAPI only		ns (0.5255)	ns (0.6441)
DAPI + TelC	ns (0.5255)		* (0.0258)
DAPI + TelC + RNase treatment	ns (0.6441)	* (0.0258)	
		Saos-2	
n ALT spots	1	993	1789
Mean Area [µm2]	0.87	2.80	2.57
SD Area	0.00	1.96	1.69
		P values	
DAPI only		ns (0.1733)	ns (0.2565)
DAPI + TelC	ns (0.1733)		**** (<0.0001)
DAPI + TelC + RNase treatment	ns (0.2565)	**** (<0.0001)	
		U2OS	
n ALT spots	33	2633	2296
Mean Area [µm2]	1.14	1.64	1.67
SD Area	0.78	0.81	0.87
		P values	
DAPI only		* (0.0218)	* (0.0136)
DAPI + TelC	* (0.0218)		ns (0.5726)
DAPI + TelC + RNase treatment	* (0.0136)	ns (0.5726)	
		WI38-VA13/2RA	
n ALT spots	6	2094	4013
Mean Area [µm2]	2.60	1.19	1.24
SD Area	1.48	0.61	0.68
		P values	
DAPI only		** (0.0039)	** (0.0058)
DAPI + TelC	** (0.0039)		ns (0.1734)
DAPI + TelC + RNase treatment	** (0.0058)	ns (0.1734)	
		YTBO	
n ALT spots	1	296	1069
Mean Area [µm2]	0.74	1.38	1.58
SD Area	0.00	0.69	0.85
		P values	
DAPI only		ns (0.8232)	ns (0.7168)
DAPI + TelC	ns (0.8232)		* (0.015)
DAPI + TelC + RNase treatment	ns (0.7168)	* (0.015)	

Table 21: Statistics (two-way ANOVA with Tukey's multiple comparisons follow-up test) of the ALT-spot intensity quantification of the main ALT-FISH experiment (See Figure 7, Panel C) comparing the cell lines.

DAPI only

		*GM847**	HeLa	IIICF/c	Saos-2	U2OS	WI38-VA13/2RA	YTBO
Mean ALT spot Intensity		89.08	72.12	195.20	67.06	430.90	95.24	87.36
SD ALT spot Intensity		23.52	14.91	138.50	0.00	351.10	74.03	0.00
n ALT spots		7	3	6	1	33	6	1
*GM847**			ns (0.9998)	ns (0.0656)	ns (>0.9999)	**** (<0.0001)	ns (>0.9999)	ns (>0.9999)
HeLa		ns (0.9998)		ns (0.125)	ns (>0.9999)	**** (<0.0001)	ns (0.999)	ns (>0.9999)
IIICF/c	P values	ns (0.0656)	ns (0.125)		ns (0.5658)	**** (<0.0001)	ns (0.1293)	ns (0.7492)
SAOS-2		ns (>0.9999)	ns (>0.9999)	ns (0.5658)		**** (<0.0001)	ns (0.9997)	ns (>0.9999)
U2OS		**** (<0.0001)	**** (<0.0001)	**** (<0.0001)	**** (<0.0001)		**** (<0.0001)	**** (<0.0001)
WI38-VA13/2RA		ns (>0.9999)	ns (0.999)	ns (0.1293)	ns (0.9997)	**** (<0.0001)		ns (>0.9999)
YTBO		ns (>0.9999)	ns (>0.9999)	ns (0.7492)	ns (>0.9999)	**** (<0.0001)	ns (>0.9999)	

TelC

		*GM847**	HeLa	IIICF/c	Saos-2	U2OS	WI38-VA13/2RA	YTBO
Mean ALT spot Intensity		103.00	1082.00	102.40	109.00	100.90	77.50	81.35
SD ALT spot Intensity		47.53	1408.00	108.80	75.45	30.75	31.06	37.06
n ALT spots		4	2	1762	993	2633	2094	296
*GM847**			**** (<0.0001)	ns (>0.9999)	ns (>0.9999)	ns (>0.9999)	ns (0.9884)	ns (0.9954)
HeLa		**** (<0.0001)		**** (<0.0001)	**** (<0.0001)	**** (<0.0001)	**** (<0.0001)	**** (<0.0001)
IIICF/c	P values	ns (>0.9999)	**** (<0.0001)		ns (0.1639)	ns (0.9909)	**** (<0.0001)	**** (<0.0001)
SAOS-2		ns (>0.9999)	**** (<0.0001)	ns (0.1639)		* (0.0197)	**** (<0.0001)	**** (<0.0001)
U2OS		ns (>0.9999)	**** (<0.0001)	ns (0.9909)	* (0.0197)		**** (<0.0001)	**** (<0.0001)
WI38-VA13/2RA		ns (0.9884)	**** (<0.0001)	**** (<0.0001)	**** (<0.0001)	**** (<0.0001)		ns (0.9683)
YTBO		ns (0.9954)	**** (<0.0001)	**** (<0.0001)	**** (<0.0001)	**** (<0.0001)	ns (0.9683)	

TelC + RNase treatment

		*GM847**	HeLa	IIICF/c	Saos-2	U2OS	WI38-VA13/2RA	YTBO
Mean ALT spot Intensity		68.89	160.60	109.30	99.94	95.44	91.12	88.48
SD ALT spot Intensity		46.96	233.30	104.00	65.12	32.82	40.94	33.03
n ALT spots		43	10	3188	1789	2296	4013	1069
*GM847**			** (0.0018)	** (0.0016)	* (0.042)	ns (0.1323)	ns (0.313)	ns (0.4914)
HeLa		** (0.0018)		ns (0.1893)	ns (0.0641)	* (0.0345)	* (0.0179)	* (0.0122)
IIICF/c	P values	** (0.0016)	ns (0.1893)		**** (<0.0001)	**** (<0.0001)	**** (<0.0001)	**** (<0.0001)
SAOS-2		* (0.042)	ns (0.0641)	**** (<0.0001)		ns (0.3327)	**** (<0.0001)	*** (0.0002)
U2OS		ns (0.1323)	* (0.0345)	**** (<0.0001)	ns (0.3327)		ns (0.1708)	ns (0.0734)
WI38-VA13/2RA		ns (0.313)	* (0.0179)	**** (<0.0001)	**** (<0.0001)	ns (0.1708)		ns (0.9134)
YTBO		ns (0.4914)	* (0.0122)	**** (<0.0001)	*** (0.0002)	ns (0.0734)	ns (0.9134)	

Table 22: Statistics (two-way ANOVA with Tukey's multiple comparisons follow-up test) of the ALT-spot intensity quantification of the main ALT-FISH experiment (See Figure 7, Panel C) comparing the treatments.

	DAPI	DAPI + TelC	DAPI + TelC + RNase treatment
		*GM847**	
Mean ALT spot Intensity	89.08	103.00	68.89
SD ALT spot Intensity	23.52	47.53	46.96
n ALT spots	7	4	43
		P values	
DAPI only		ns (0.941)	ns (0.7392)
DAPI + TelC	ns (0.941)		ns (0.5922)
DAPI + TelC + RNase treatment	ns (0.7392)	ns (0.5922)	
		HeLa	
Mean ALT spot Intensity	72.12	1082.00	160.60
SD ALT spot Intensity	14.91	1408.00	233.30
n ALT spots	3	2	10
		P values	
DAPI only		**** (<0.0001)	ns (0.1098)
DAPI + TelC	**** (<0.0001)		**** (<0.0001)
DAPI + TelC + RNase treatment	ns (0.1098)	**** (<0.0001)	
		IIICF/c	
Mean ALT spot Intensity	195.20	102.40	109.30
SD ALT spot Intensity	138.50	108.80	104.00
n ALT spots	6	1762	3188
		P values	
DAPI only		** (0.002)	** (0.0048)
DAPI + TelC	** (0.002)		** (0.0015)
DAPI + TelC + RNase treatment	** (0.0048)	** (0.0015)	
		Saos-2	
Mean ALT spot Intensity	67.06	109	99.94
SD ALT spot Intensity	0	75.45	65.12
n ALT spots	1	993	1789
		P values	
DAPI only		ns (0.8054)	ns (0.8753)
DAPI + TelC	ns (0.8054)		** (0.0018)
DAPI + TelC + RNase treatment	ns (0.8753)	** (0.0018)	
		U2OS	
Mean ALT spot Intensity	430.90	100.90	95.44
SD ALT spot Intensity	351.10	30.75	32.82
n ALT spots	33	2633	2296
		P values	
DAPI only		**** (<0.0001)	**** (<0.0001)
DAPI + TelC	**** (<0.0001)		* (0.0118)
DAPI + TelC + RNase treatment	**** (<0.0001)	* (0.0118)	
		WI38-VA13/2RA	
Mean ALT spot Intensity	95.24	77.50	91.12
SD ALT spot Intensity	74.03	31.06	40.94
n ALT spots	6	2094	4013
		P values	
DAPI only		ns (0.793)	ns (0.9875)
DAPI + TelC	ns (0.793)		**** (<0.0001)
DAPI + TelC + RNase treatment	ns (0.9875)	**** (<0.0001)	
		YTBO	
Mean ALT spot Intensity	87.36	81.35	88.48
SD ALT spot Intensity	0	37.06	33.03
n ALT spots	1	296	1069
		P values	
DAPI only		ns (0.9956)	ns (0.9998)
DAPI + TelC	ns (0.9956)		ns (0.2358)
DAPI + TelC + RNase treatment	ns (0.9998)	ns (0.2358)	

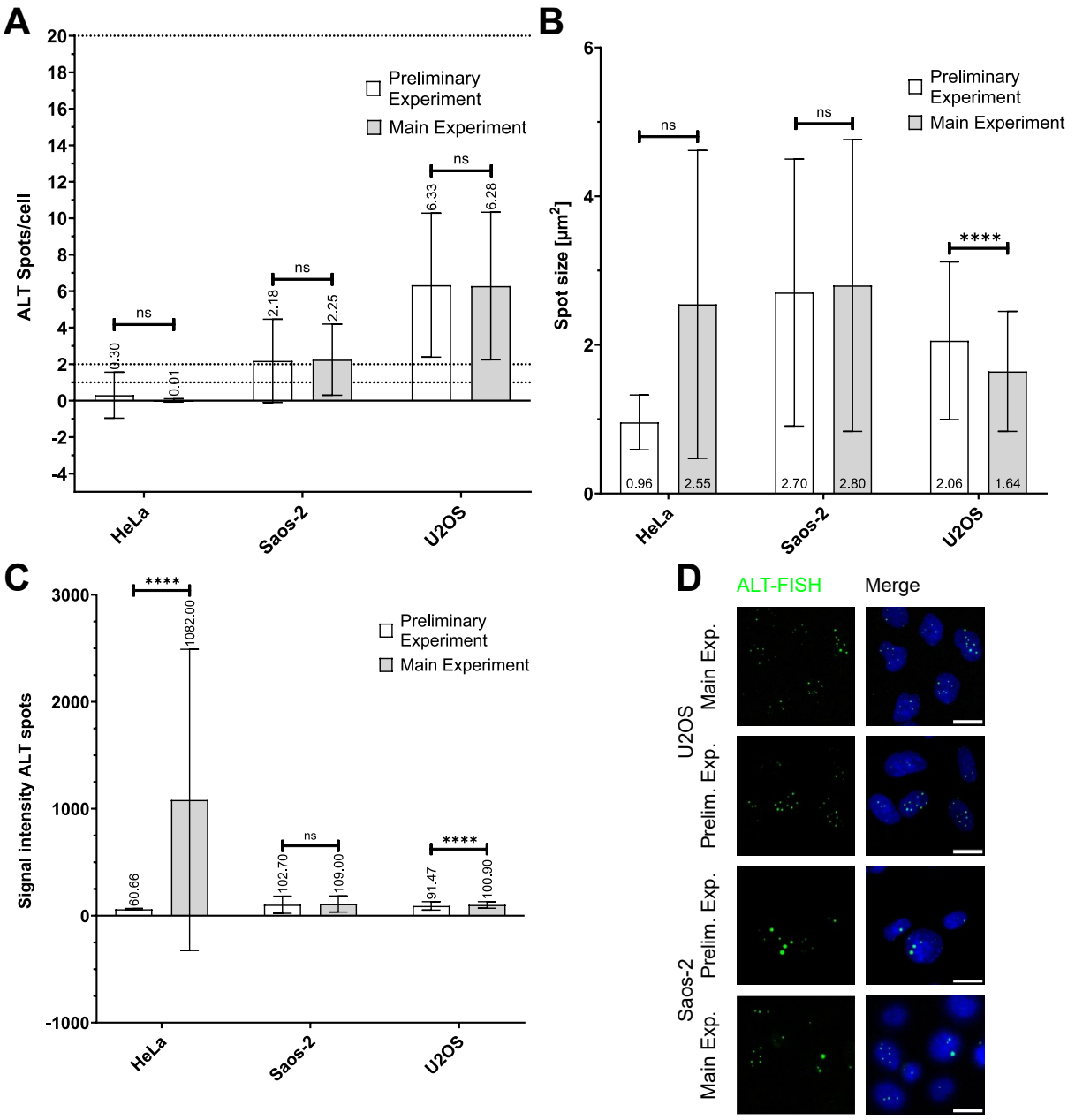

Figure 8: Comparison of the main and the preliminary ALT-FISH experiment. A: Comparison of the mean ALT-spots per cell ± SD of three different cell lines stained using Atto 633 labeled TelC probes without RNase treatment of the main and the preliminary ALT-FISH experiment. The dotted lines depict thresholds for ALT levels: 1-2: low ALT, 2-20 ALT, >20 super ALT. Both experiments are biological replicates of each other (no technical replicates each). Statistics are shown in Table 23. B: Depiction of the mean area of ALT-spots ± SD in the analyzed cell lines of the main and the preliminary experiment. Statistics can be found in Table 24. C: Portrayal of the mean ALT-Spot signal intensity ± SD of the analyzed cell lines of the main and the preliminary experiment. Statistics are presented in Table 25. D: Representative microscopical confocal spinning disc images at 400x magnification of two ALT-positive cell lines (Saos-2 and U2OS) of the main and preliminary experiment stained using

Atto 633 labeled TelC probes for ALT-spot detection and DAPI for nuclear staining. Scale bar: 20 µm.

Table 23: Statistics (two-way ANOVA with Sidak's multiple comparisons follow-up test) of the ALT-spots per cell quantification comparing the main and the preliminary ALT-FISH experiments (See Figure 8, Panel A).

				DAPI + TelC			
					HeLa Prelim. Exp.	Saos-2 Prelim. Exp.	U2OS Prelim. Exp.
				n cells	249	238	570
				Mean ALT spots/cell	0.30	2.18	6.33
				SD spots/cell	1.26	2.29	3.95
	n cells	Mean ALT spot/cell	SD spots/cell	Range	11	15	20
						P values	
HeLa Main Exp.	244	0.01	0.09	1	ns (0.6166)		
Saos-2 Main Exp.	442	2.25	1.95	10		ns (0.9897)	
U2OS Main Exp.	419	6.28	4.04	20			ns (0.9917)

Table 24: Statistics (two-way ANOVA with Sidak's multiple comparisons follow-up test) of the ALT-spot area quantification comparing the main and the preliminary ALT-FISH experiments (See Figure 8, Panel B).

			DAPI + TelC			
				HeLa Prelim Exp.	Saos-2 Prelim. Exp.	U2OS Prelim Exp.
			n ALT spots	75	519	3610
			Mean Area [µm^2]	0.96	2.70	2.06
	n ALT spots	Mean Area [µm^2]	SD Area	0.37	1.80	1.06
					P values	
HeLa Main Exp.	2	2.55	2.07	ns (0.183)		
Saos-2 Main Exp.	993	2.80	1.96		ns (0.364)	
U2OS Main Exp.	2633	1.64	0.81			**** (<0.0001)

Table 25: Statistics (two-way ANOVA with Sidak's multiple comparisons follow-up test) of the ALT-spot signal intensity quantification comparing the main and the preliminary ALT-FISH experiments (See Figure 8, Panel C).

			DAPI + TelC			
				HeLa Prelim. Exp.	Saos-2 Prelim. Exp.	U2OS Prelim Exp.
			n ALT spots	75	519	3610
			Mean ALT spot Intensity	60.66	102.7	91.47
	n ALT spots	Mean ALT spot Intensity	SD ALT spot Intensity	7.37	79.92	39.43
					P values	
HeLa Main Exp.	2	1082.00	1408.00	**** (<0.0001)		
Saos-2 Main Exp.	993	109.00	75.45		ns (0.0542)	
U2OS Main Exp.	2633	100.90	30.75			**** (<0.0001)

6.2. qPCR-based variant detection

After confirming the ALT activity of all but one cell line, the qPCR-based variant detection experiments were started. At first, the genomic DNAs of the cell lines were examined.

6.2.1. NCTR variants in gDNA samples

Combined, the results of this chapter show that the cell lines used in this study have different amounts of the three variants tested for, although the differences are only significant in a single cell line and for one variant (Figure 9, Table 26). Also, it was shown that the results of all cell lines are in the detectable range (Figure 10) and that the ranges used in the qPCR experiments are above the detection limit or are just reaching them (Figure 11). In addition, it was observed that the assays are very sensitive to changes in the abundance of telomeric and variant repeats which limits the assay's reproducibility on the raw data (Figure 12). However, when the data is normalized to show the percentages of each variant, no limitations to reproducibility were observed (Figure 13). More detailed descriptions of the results can be found it the following paragraphs.

For the comparison of this qPCR-based variant detection with whole genome sequencing data, first, the percentages of the telomere sequence variants TCAGGG, TGAGGG and TAAGGG compared to the canonical repeat TTAGGG were calculated. These results were based on absolute SQ values. The results of the calculations are depicted in Figure 9 with their statistical analysis in Table 26. In panel A, the baseline i.e., the TTAGGG average percentages ± SEM are depicted to show the corresponding high error. There were no significant differences between the cell lines here. Also, it has to be noted that these values do not give information about the value of the baseline i.e., the telomere lengths. For a relative comparison of telomere lengths between the cell lines, the TTAGGG CT values depicted in Figure 10 can be used. For the TCAGGG variant (Figure 9B) WI38-VA13/2RA showed the highest average percentage followed by YTBO. The third highest average TCAGGG percentage was observed in *GM847** cells. The remaining cell lines had an average TCAGGG percentage smaller than one, with HeLa having the highest of this group followed by HT-1080 [PTL], Saos-2, HT-1080 hTR wt, IIICF/c and U2OS. All the differences in TCAGGG percentage between the cell lines were not of statistical significance. However, for TGAGGG (Figure 9C) the overall level was higher. YTBO cells had the highest average TGAGGG percentage ± SEM, which was significantly higher than all cell lines except HT-1080 [PTL] and *GM847**. The remaining cell lines did not significantly differ from each other in terms of TGAGGG percentage. The second highest percentage was found in *GM847** cells followed by HT-1080 [PTL], HeLa, HT-1080 hTR wt, Saos-2, WI38-VA13/2RA and U2OS. The overall level of TAAGGG percentages (Figure 9D) was low compared to the other variants, with the highest value found in *GM847** cells followed by HeLa, YTBO, HT-1080 [PTL], Saos-2, HT-1080 hTR wt, IIICF/c, WI38-VA13/2RA and U2OS without showing significant differences.

In order to check if these results are inside the detectable range for these assays, the CT values of the cell lines were compared to the non-template control (NTC). The results are shown in Figure 10 and Table 27.

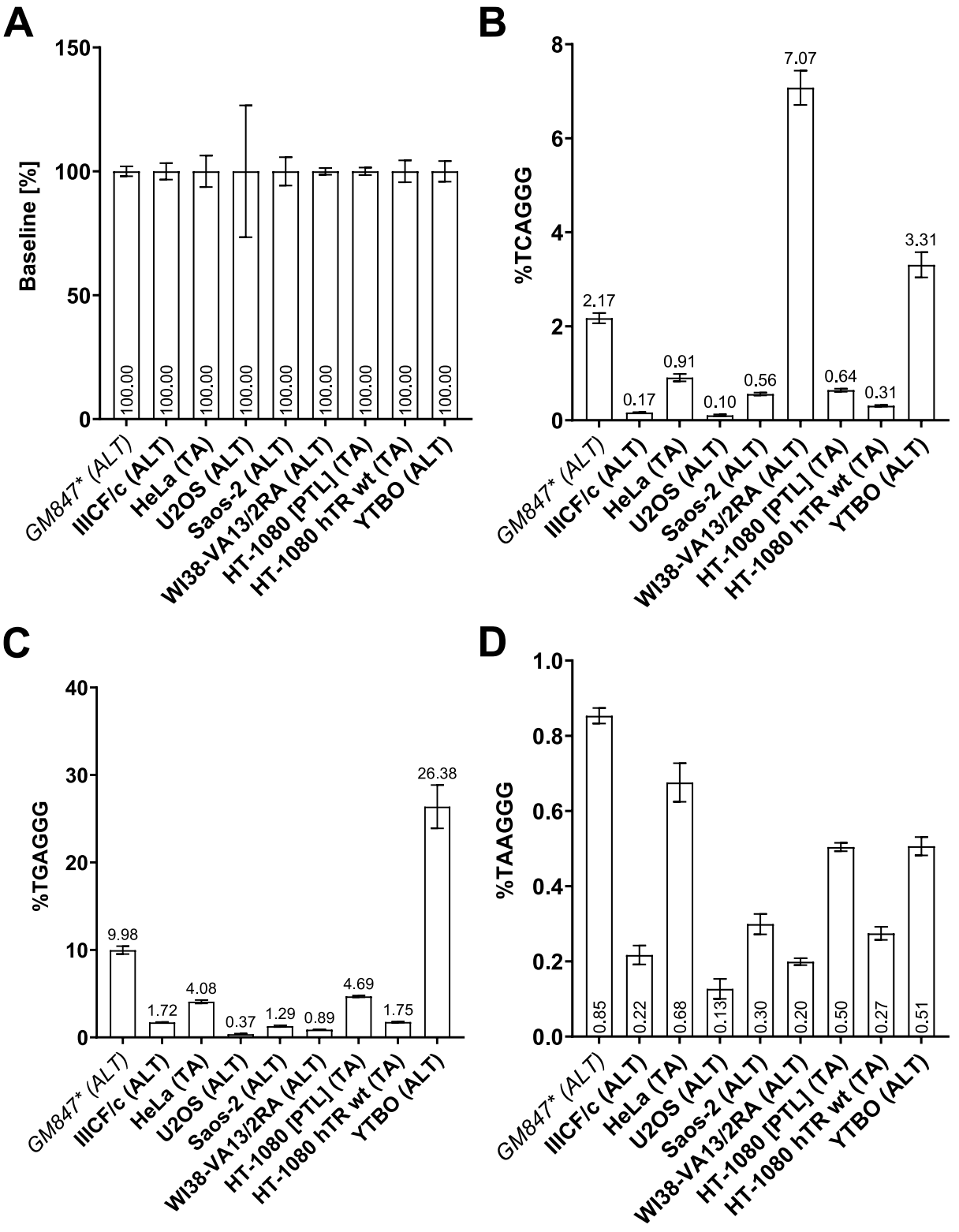

Figure 9: Average SQ-based percentage ± SEM of the analyzed NCTRs compared to the telomeric repeat SQ detected by qPCR of multiple cell lines. A: Percentage of the baseline (TTAGGG repeat). B: Percentage of the TCAGGG repeat. C: Percentage of the TGAGGG

repeat. D: Percentage of the TAAGGG repeat. N = 3 technical replicates. Statistics can be found in Table 26 and. Raw data can be found in Table 56 and Table 57.

With a very high level of significance, it was shown that the CT values of all cell lines were lower than the NTCs' CT values, so all cell line values were in the detectable range.

The same analysis also was conducted for the standard dilution series to check what the limit for absolute detection is. The results of this analysis are portrayed in Figure 11 and Table 28. It was observed that only the highest dilutions of the TTAGGG and TCAGGG standard dilutions did not significantly differ from the NTC. This means that the detection limit for the TTAGGG variant is somewhere between 10^5 and 10^4 kb of telomere sequence and for the TCAGGG variant, the limit lies between 10^3 and 10^2 kb of variant sequence. For the remaining variants and the SCG, all dilution CTs differed from the NTC with very high levels of significance which means that the detection limit was lower than the lowest dilution for these assays.

For examination of the assays' reproducibility average dCT values ± SEM of a preliminary qPCR variant detection experiment and the experiment described in Figure 9 were compared (Figure 12, Table 29). The preliminary experiments were conducted with gDNAs isolated by a technician and previous students. For the canonical telomere repeat, the average dCT values were significantly lower in the main experiment. The most severe difference was observed in *GM847**. The results of all other cell lines had a difference below 3 CTs. The results for all variants were consistent with this pattern with a few exceptions. The differences between the dCT values of the preliminary and main experiment for the TCAGGG variant were not significant for the cell lines U2OS, HT-1080 PTL and YTBO. Additionally, the variant percentages were compared between the main and the preliminary experiments (Figure 13, Table 30). Here, no significant differences between the two experiments were observed in any case.

After evaluation of the qPCR results, I correlated the results with whole genome sequencing data for validation in the next chapter.

Table 26: Statistics (two-way ANOVA with Tukey's multiple comparisons follow-up test) of the percentual NCTR content detected by qPCR (See Figure 9) comparing the cell lines.

Baseline

	*GM847** (ALT)	IIICF/c (ALT)	HeLa (TA)	U2OS (ALT)	Saos-2 (ALT)	WI38-VA13/2RA (ALT)	HT-1080 [PTL] (TA)	HT-1080 hTR wt (TA)	YTBO (ALT)
Mean % [TTAGGG/TTAGGG]	100.00	100.00	100.00	100.00	100.00	100.00	100.00	100.00	100.00
SEM [%TTAGGG]	1.98	3.31	6.37	26.59	5.73	1.37	1.50	4.41	4.18
n	3	3	3	3	3	3	3	3	3
					P values				
*GM847** (ALT)		ns (>0.9999)	ns (>0.9999)	ns (>0.9999)	ns (>0.9999)	ns (>0.9999)	ns (>0.9999)	ns (>0.9999)	ns (>0.9999)
IIICF/c (ALT)	ns (>0.9999)		ns (>0.9999)	ns (>0.9999)	ns (>0.9999)	ns (>0.9999)	ns (>0.9999)	ns (>0.9999)	ns (>0.9999)
HeLa (TA)	ns (>0.9999)	ns (>0.9999)		ns (>0.9999)	ns (>0.9999)	ns (>0.9999)	ns (>0.9999)	ns (>0.9999)	ns (>0.9999)
U2OS (ALT)	ns (>0.9999)	ns (>0.9999)	ns (>0.9999)		ns (>0.9999)	ns (>0.9999)	ns (>0.9999)	ns (>0.9999)	ns (>0.9999)
Saos-2 (ALT)	ns (>0.9999)	ns (>0.9999)	ns (>0.9999)	ns (>0.9999)		ns (>0.9999)	ns (>0.9999)	ns (>0.9999)	ns (>0.9999)
WI38-VA13/2RA (ALT)	ns (>0.9999)	ns (>0.9999)	ns (>0.9999)	ns (>0.9999)	ns (>0.9999)		ns (>0.9999)	ns (>0.9999)	ns (>0.9999)
HT-1080 [PTL] (TA)	ns (>0.9999)	ns (>0.9999)	ns (>0.9999)	ns (>0.9999)	ns (>0.9999)	ns (>0.9999)		ns (>0.9999)	ns (>0.9999)
HT-1080 hTR wt (TA)	ns (>0.9999)	ns (>0.9999)	ns (>0.9999)	ns (>0.9999)	ns (>0.9999)	ns (>0.9999)	ns (>0.9999)		ns (>0.9999)
YTBO (ALT)	ns (>0.9999)	ns (>0.9999)	ns (>0.9999)	ns (>0.9999)	ns (>0.9999)	ns (>0.9999)	ns (>0.9999)	ns (>0.9999)	

%TCAGGG

	*GM847** (ALT)	IIICF/c (ALT)	HeLa (TA)	U2OS (ALT)	Saos-2 (ALT)	WI38-VA13/2RA (ALT)	HT-1080 [PTL] (TA)	HT-1080 hTR wt (TA)	YTBO (ALT)
Mean % [TCAGGG/TTAGGG]	2.17	0.17	0.91	0.10	0.56	7.07	0.64	0.31	3.31
SEM [%TCAGGG]	0.11	0.01	0.08	0.02	0.03	0.36	0.03	0.02	0.27
n	3	3	3	3	3	2	3	3	3
					P values				
*GM847** (ALT)		ns (>0.9999)	ns (>0.9999)	ns (>0.9999)	ns (>0.9999)	ns (0.9993)	ns (>0.9999)	ns (>0.9999)	ns (>0.9999)
IIICF/c (ALT)	ns (>0.9999)		ns (>0.9999)	ns (>0.9999)	ns (>0.9999)	ns (0.9925)	ns (>0.9999)	ns (>0.9999)	ns (>0.9999)
HeLa (TA)	ns (>0.9999)	ns (>0.9999)		ns (>0.9999)	ns (>0.9999)	ns (0.9965)	ns (>0.9999)	ns (>0.9999)	ns (>0.9999)
U2OS (ALT)	ns (>0.9999)	ns (>0.9999)	ns (>0.9999)		ns (>0.9999)	ns (0.992)	ns (>0.9999)	ns (>0.9999)	ns (>0.9999)
Saos-2 (ALT)	ns (>0.9999)	ns (>0.9999)	ns (>0.9999)	ns (>0.9999)		ns (0.9949)	ns (>0.9999)	ns (>0.9999)	ns (>0.9999)
WI38-VA13/2RA (ALT)	ns (0.9993)	ns (0.9925)	ns (0.9965)	ns (0.992)	ns (0.9949)		ns (0.9953)	ns (0.9935)	ns (>0.9999)
HT-1080 [PTL] (TA)	ns (>0.9999)	ns (>0.9999)	ns (>0.9999)	ns (>0.9999)	ns (>0.9999)	ns (0.9953)		ns (>0.9999)	ns (>0.9999)
HT-1080 hTR wt (TA)	ns (>0.9999)	ns (>0.9999)	ns (>0.9999)	ns (>0.9999)	ns (>0.9999)	ns (0.9935)	ns (>0.9999)		ns (>0.9999)
YTBO (ALT)	ns (>0.9999)	ns (>0.9999)	ns (>0.9999)	ns (>0.9999)	ns (>0.9999)	ns (>0.9999)	ns (>0.9999)	ns (>0.9999)	

%TGAGGG

	*GM847** (ALT)	IIICF/c (ALT)	HeLa (TA)	U2OS (ALT)	Saos-2 (ALT)	WI38-VA13/2RA (ALT)	HT-1080 [PTL] (TA)	HT-1080 hTR wt (TA)	YTBO (ALT)
Mean % [TGAGGG/TTAGGG]	9.98	1.72	4.08	0.37	1.29	0.89	4.69	1.75	26.38

SEM [%TGAGGG]	0.46	0.04	0.19	0.07	0.10	0.03	0.10	0.06	2.47
n	3	3	3	3	3	3	3	3	3
					P values				
*GM847** (ALT)		ns (0.9524)	ns (0.9942)	ns (0.8928)	ns (0.9368)	ns (0.9193)	ns (0.9973)	ns (0.9536)	ns (0.3019)
IIICF/c (ALT)	ns (0.9524)		ns (>0.9999)	ns (>0.9999)	ns (>0.9999)	ns (>0.9999)	ns (>0.9999)	ns (>0.9999)	* (0.0158)
HeLa (TA)	ns (0.9942)	ns (>0.9999)		ns (0.9998)	ns (>0.9999)	ns (>0.9999)	ns (>0.9999)	ns (>0.9999)	* (0.0425)
U2OS (ALT)	ns (0.8928)	ns (>0.9999)	ns (0.9998)		ns (>0.9999)	ns (>0.9999)	ns (0.9994)	ns (>0.9999)	** (0.0086)
Saos-2 (ALT)	ns (0.9368)	ns (>0.9999)	ns (>0.9999)	ns (>0.9999)		ns (>0.9999)	ns (0.9999)	ns (>0.9999)	* (0.0131)
WI38-VA13/2RA (ALT)	ns (0.9193)	ns (>0.9999)	ns (>0.9999)	ns (>0.9999)	ns (>0.9999)		ns (0.9998)	ns (>0.9999)	* (0.0109)
HT-1080 [PTL] (TA)	ns (0.9973)	ns (>0.9999)	ns (>0.9999)	ns (0.9994)	ns (0.9999)	ns (0.9998)		ns (>0.9999)	ns (0.0539)
HT-1080 hTR wt (TA)	ns (0.9536)	ns (>0.9999)	ns (>0.9999)	ns (>0.9999)	ns (>0.9999)	ns (>0.9999)	ns (>0.9999)		* (0.0161)
YTBO (ALT)	ns (0.3019)	* (0.0158)	* (0.0425)	** (0.0086)	* (0.0131)	* (0.0109)	ns (0.0539)	* (0.0161)	

%TAAGGG

	*GM847** (ALT)	IIICF/c (ALT)	HeLa (TA)	U2OS (ALT)	Saos-2 (ALT)	WI38-VA13/2RA (ALT)	HT-1080 [PTL] (TA)	HT-1080 hTR wt (TA)	YTBO (ALT)
Mean % [TAAGGG/TTAGGG]	0.85	0.22	0.68	0.13	0.30	0.20	0.50	0.27	0.51
SEM [%TAAGGG]	0.02	0.02	0.05	0.03	0.03	0.01	0.01	0.02	0.02
n	3	3	3	3	3	3	3	3	3
					P values				
*GM847** (ALT)		ns (>0.9999)	ns (>0.9999)	ns (>0.9999)	ns (>0.9999)	ns (>0.9999)	ns (>0.9999)	ns (>0.9999)	ns (>0.9999)
IIICF/c (ALT)	ns (>0.9999)		ns (>0.9999)	ns (>0.9999)	ns (>0.9999)	ns (>0.9999)	ns (>0.9999)	ns (>0.9999)	ns (>0.9999)
HeLa (TA)	ns (>0.9999)	ns (>0.9999)		ns (>0.9999)	ns (>0.9999)	ns (>0.9999)	ns (>0.9999)	ns (>0.9999)	ns (>0.9999)
U2OS (ALT)	ns (>0.9999)	ns (>0.9999)	ns (>0.9999)		ns (>0.9999)	ns (>0.9999)	ns (>0.9999)	ns (>0.9999)	ns (>0.9999)
Saos-2 (ALT)	ns (>0.9999)	ns (>0.9999)	ns (>0.9999)	ns (>0.9999)		ns (>0.9999)	ns (>0.9999)	ns (>0.9999)	ns (>0.9999)
WI38-VA13/2RA (ALT)	ns (>0.9999)	ns (>0.9999)	ns (>0.9999)	ns (>0.9999)	ns (>0.9999)		ns (>0.9999)	ns (>0.9999)	ns (>0.9999)
HT-1080 [PTL] (TA)	ns (>0.9999)	ns (>0.9999)	ns (>0.9999)	ns (>0.9999)	ns (>0.9999)	ns (>0.9999)		ns (>0.9999)	ns (>0.9999)
HT-1080 hTR wt (TA)	ns (>0.9999)	ns (>0.9999)	ns (>0.9999)	ns (>0.9999)	ns (>0.9999)	ns (>0.9999)	ns (>0.9999)		ns (>0.9999)
YTBO (ALT)	ns (>0.9999)	ns (>0.9999)	ns (>0.9999)	ns (>0.9999)	ns (>0.9999)	ns (>0.9999)	ns (>0.9999)	ns (>0.9999)	

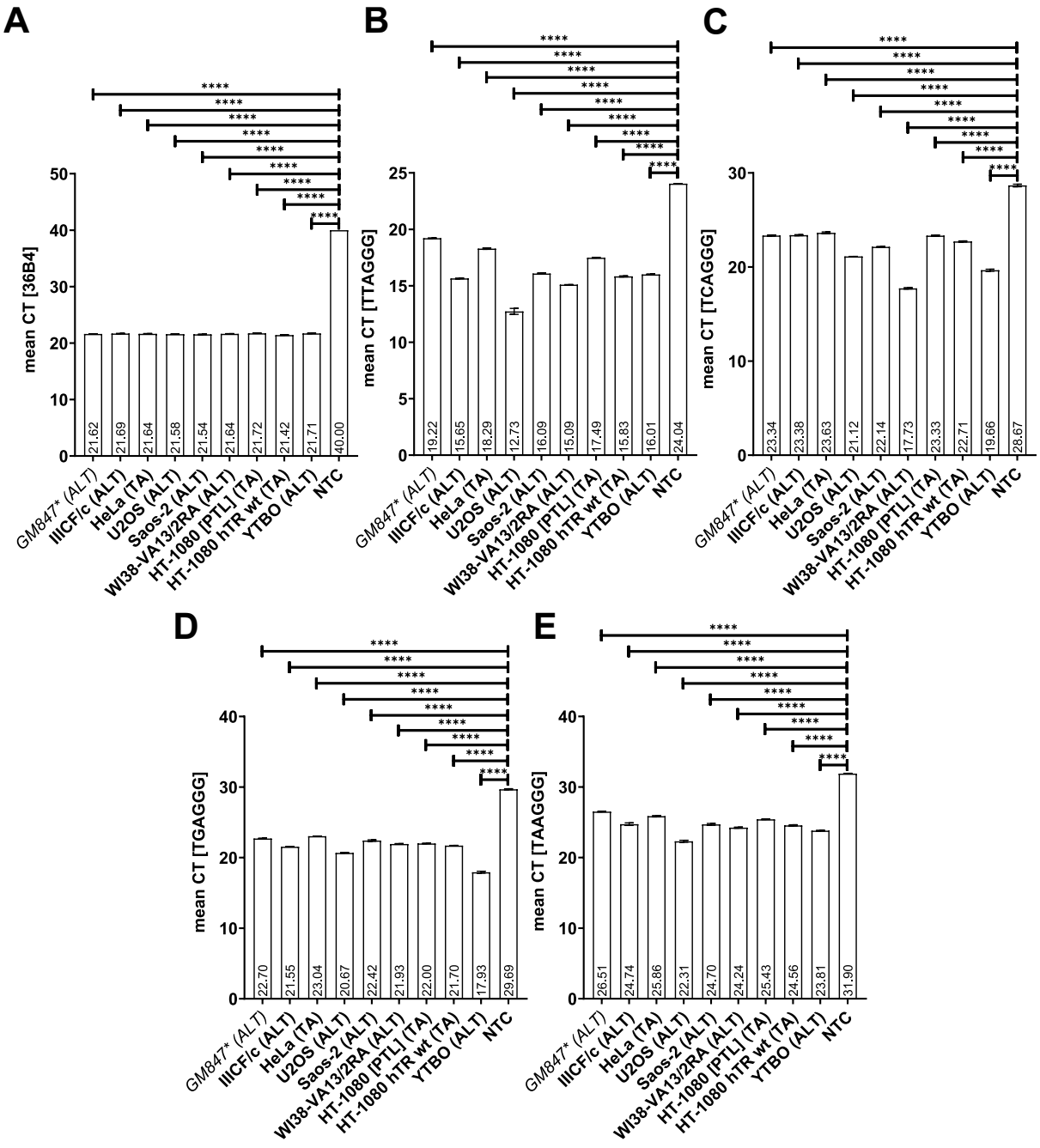

Figure 10: Comparison of the CTs ± SEM of the analyzed NCTRs and the SCG of several cell lines with the NTC CTs ± SEM. A: SCG CTs compared to respective NTC, the NTC CTs were not detectable (>40) so the value 40 was used for the analysis. B: TTAGGG CTs compared to respective NTC CTs. C: TCAGGG CTs compared to respective NTC CTs. D: TGAGGG CTs compared to the respective NTC CTs. E: TAAGGG CTs compared to the respective NTC CTs. N = 3 technical replicates. Statistics can be found in Table 27. Raw data can be found in Table 57.

Table 27: Statistics (two-way ANOVA with Tukey's multiple comparisons follow-up test) of the NCTRs CT of each cell line detected by qPCR compared with the NTC (See Figure 10). For CT >40 the value 40 was used for the analysis.

*GM847** (ALT)					
	36B4	TTAGGG	TCAGGG	TGAGGG	TAAGGG
n	3	3	3	3	3
Mean CT	21.62	19.22	23.34	22.70	26.51
SEM CT	0.04	0.02	0.06	0.06	0.03
P values vs. NTC	**** (<0.0001)	**** (<0.0001)	**** (<0.0001)	**** (<0.0001)	**** (<0.0001)
Mean NTC CT	40.00	24.04	28.67	29.69	31.90
SEM NTC CT	0.00	0.02	0.13	0.06	0.04
n NTC	3	3	3	3	3
IIICF/c (ALT)					
	36B4	TTAGGG	TCAGGG	TGAGGG	TAAGGG
n	3	3	3	3	3
Mean CT	21.69	15.65	23.38	21.55	24.74
SEM CT	0.03	0.03	0.05	0.01	0.18
P values vs. NTC	**** (<0.0001)	**** (<0.0001)	**** (<0.0001)	**** (<0.0001)	**** (<0.0001)
Mean NTC CT	40.00	24.04	28.67	29.69	31.90
SEM NTC CT	0.00	0.02	0.13	0.06	0.04
n NTC	3	3	3	3	3
HeLa (TA)					
	36B4	TTAGGG	TCAGGG	TGAGGG	TAAGGG
n	3	3	3	3	3
Mean CT	21.64	18.29	23.63	23.04	25.86
SEM CT	0.05	0.06	0.10	0.02	0.09
P values vs. NTC	**** (<0.0001)	**** (<0.0001)	**** (<0.0001)	**** (<0.0001)	**** (<0.0001)
Mean NTC CT	40.00	24.04	28.67	29.69	31.90
SEM NTC CT	0.00	0.02	0.13	0.06	0.04
n NTC	3	3	3	3	3
U2OS (ALT)					
	36B4	TTAGGG	TCAGGG	TGAGGG	TAAGGG
n	3	3	3	3	3
Mean CT	21.58	12.73	21.12	20.67	22.31
SEM CT	0.01	0.27	0.01	0.03	0.14
P values vs. NTC	**** (<0.0001)	**** (<0.0001)	**** (<0.0001)	**** (<0.0001)	**** (<0.0001)
Mean NTC CT	40.00	24.04	28.67	29.69	31.90
SEM NTC CT	0.00	0.02	0.13	0.06	0.04
n NTC	3	3	3	3	3
Saos-2 (ALT)					
	36B4	TTAGGG	TCAGGG	TGAGGG	TAAGGG
n	3	3	3	3	3
Mean CT	21.54	16.09	22.14	22.42	24.70
SEM CT	0.06	0.06	0.05	0.10	0.13
P values vs. NTC	**** (<0.0001)	**** (<0.0001)	**** (<0.0001)	**** (<0.0001)	**** (<0.0001)
Mean NTC CT	40.00	24.04	28.67	29.69	31.90
SEM NTC CT	0.00	0.02	0.13	0.06	0.04
n NTC	3	3	3	3	3
WI38-VA13/2RA (ALT)					
	36B4	TTAGGG	TCAGGG	TGAGGG	TAAGGG
n	3	3	2	3	3
Mean CT	21.64	15.09	17.73	21.93	24.24
SEM CT	0.03	0.01	0.07	0.05	0.07
P values vs. NTC	**** (<0.0001)	**** (<0.0001)	**** (<0.0001)	**** (<0.0001)	**** (<0.0001)
Mean NTC CT	40.00	24.04	28.67	29.69	31.90
SEM NTC CT	0.00	0.02	0.13	0.06	0.04
n NTC	3	3	3	3	3
HT-1080 [PTL] (TA)					

	36B4	TTAGGG	TCAGGG	TGAGGG	TAAGGG
n	3	3	3	3	3
Mean CT	21.72	17.49	23.33	22.00	25.43
SEM CT	0.02	0.02	0.07	0.03	0.03
P values vs. NTC	**** (<0.0001)	**** (<0.0001)	**** (<0.0001)	**** (<0.0001)	**** (<0.0001)
Mean NTC CT	40.00	24.04	28.67	29.69	31.90
SEM NTC CT	0.00	0.02	0.13	0.06	0.04
n NTC	3	3	3	3	3

HT-1080 hTR wt (TA)

	36B4	TTAGGG	TCAGGG	TGAGGG	TAAGGG
n	3	3	3	3	3
Mean CT	21.42	15.83	22.71	21.70	24.56
SEM CT	0.03	0.04	0.06	0.02	0.09
P values vs. NTC	**** (<0.0001)	**** (<0.0001)	**** (<0.0001)	**** (<0.0001)	**** (<0.0001)
Mean NTC CT	40.00	24.04	28.67	29.69	31.90
SEM NTC CT	0.00	0.02	0.13	0.06	0.04
n NTC	3	3	3	3	3

YTBO (ALT)

	36B4	TTAGGG	TCAGGG	TGAGGG	TAAGGG
n	3	3	3	3	3
Mean CT	21.71	16.01	19.66	17.93	23.81
SEM CT	0.04	0.04	0.11	0.14	0.06
P values vs. NTC	**** (<0.0001)	**** (<0.0001)	**** (<0.0001)	**** (<0.0001)	**** (<0.0001)
Mean NTC CT	40.00	24.04	28.67	29.69	31.90
SEM NTC CT	0.00	0.02	0.13	0.06	0.04
n NTC	3	3	3	3	3

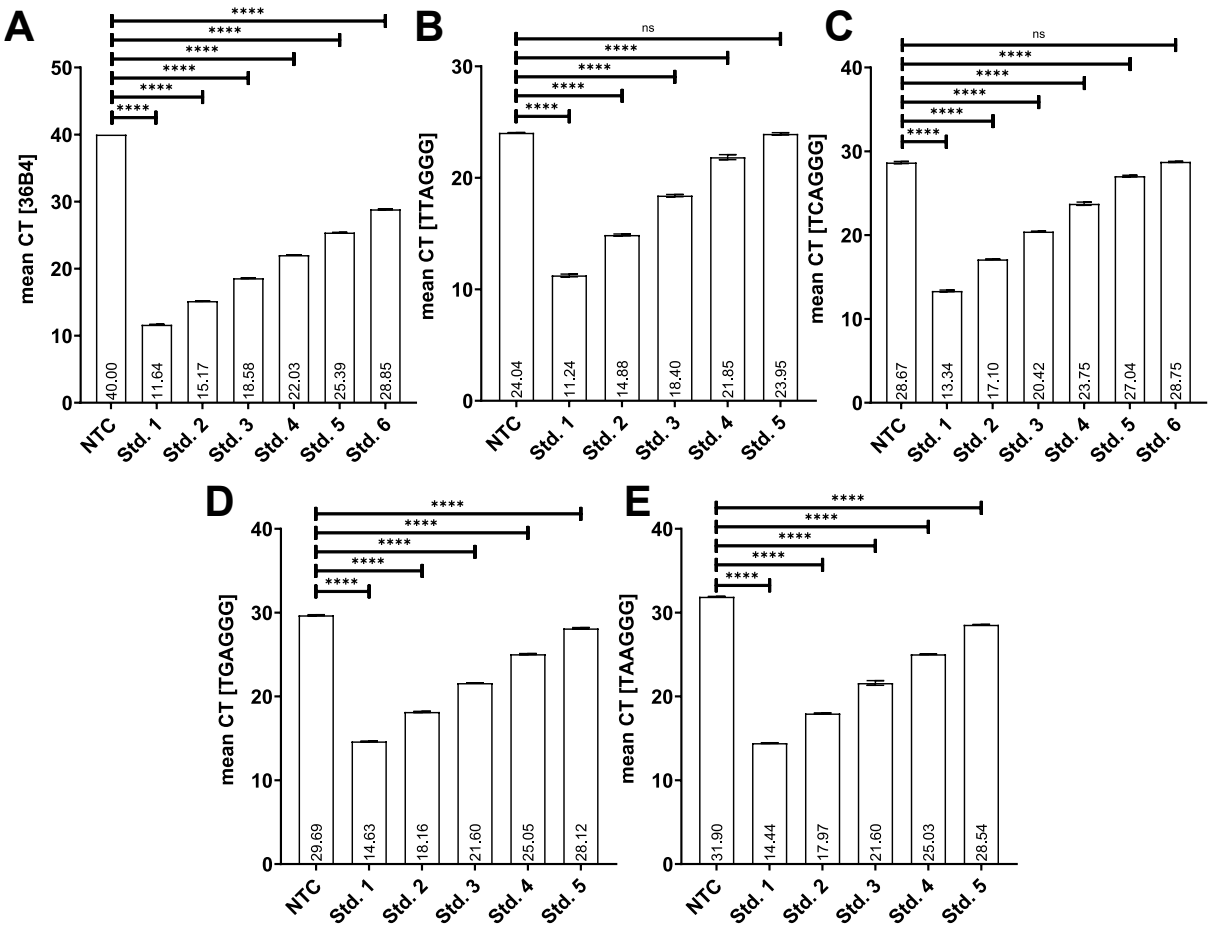

Figure 11: Comparison of the CTs ± SEM of the used NCTR- and the SCG standard curve dilutions with the NTC CTs ± SEM. A: SCG standard CTs compared to respective NTC, the NTC CTs were not detectable (>40) so the value 40 was used for the analysis. B: TTAGGG standard CTs compared to respective NTC CTs. C: TCAGGG standard CTs compared to respective NTC CTs. D: TGAGGG standard CTs compared to the respective NTC CTs. E: TAAGGG standard CTs compared to the respective NTC CTs. N = 3 technical replicates. Statistics can be found in Table 28. Raw data can be found in Table 57.

Table 28: Statistics (two-way ANOVA with Tukey's multiple comparisons follow-up test) of the SCG and NCTR standard curve concentration CTs detected by qPCR compared with the NTC (See Figure 11). For CT >40 the value 40 was used for the analysis.

36B4 standard

					Std. 1	Std. 2	Std. 3	Std. 4	Std. 5	Std. 6
			diploid copies		10^7	10^6	10^5	10^4	10^3	10^2
			Mean CT		11.64	15.17	18.58	22.03	25.39	28.85
			SEM CT		0.08	0.04	0.05	0.02	0.04	0.09
	Mean CT	SEM CT	n		3	3	3	3	3	3
NTC	40	0	3	P values	**** (<0.0001)	**** (<0.0001)	**** (<0.0001)	**** (<0.0001)	**** (<0.0001)	**** (<0.0001)

TTAGGG standard

					Std. 1	Std. 2	Std. 3	Std. 4	Std. 5
			kb of telomere sequence		10^8	10^7	10^6	10^5	10^4
			Mean CT		11.24	14.88	18.40	21.85	23.95
			SEM CT		0.13	0.08	0.10	0.23	0.11
	Mean CT	SEM CT	n		3	3	3	3	3
NTC	24.04	0.02	3	P values	**** (<0.0001)	**** (<0.0001)	**** (<0.0001)	**** (<0.0001)	ns (0.9602)

TCAGGG standard

					Std. 1	Std. 2	Std. 3	Std. 4	Std. 5	Std. 6
			kb of variant sequence		10^7	10^6	10^5	10^4	10^3	10^2
			Mean CT		13.34	17.10	20.42	23.75	27.04	28.75
			SEM CT		0.10	0.02	0.06	0.19	0.10	0.06
	Mean CT	SEM CT	n		3	3	3	3	3	3
NTC	28.67	0.13	3	P values	**** (<0.0001)	**** (<0.0001)	**** (<0.0001)	**** (<0.0001)	**** (<0.0001)	ns (0.9651)

TGAGGG standard

					Std. 1	Std. 2	Std. 3	Std. 4	Std. 5
			kb of variant sequence		10^7	10^6	10^5	10^4	10^3
			Mean CT		14.63	18.16	21.60	25.05	28.12
			SEM CT		0.05	0.07	0.03	0.06	0.10
	Mean CT	SEM CT	n		3	3	3	3	3
NTC	29.69	0.06	3	P values	**** (<0.0001)	**** (<0.0001)	**** (<0.0001)	**** (<0.0001)	**** (<0.0001)

TAAGGG standard

					Std. 1	Std. 2	Std. 3	Std. 4	Std. 5
			kb of variant sequence		10^7	10^6	10^5	10^4	10^3
			Mean CT		14.44	17.97	21.60	25.03	28.54
			SEM CT		0.04	0.07	0.28	0.02	0.05
	Mean CT	SEM CT	n		3	3	3	3	3
NTC	31.90	0.04	3	P values	**** (<0.0001)	**** (<0.0001)	**** (<0.0001)	**** (<0.0001)	**** (<0.0001)

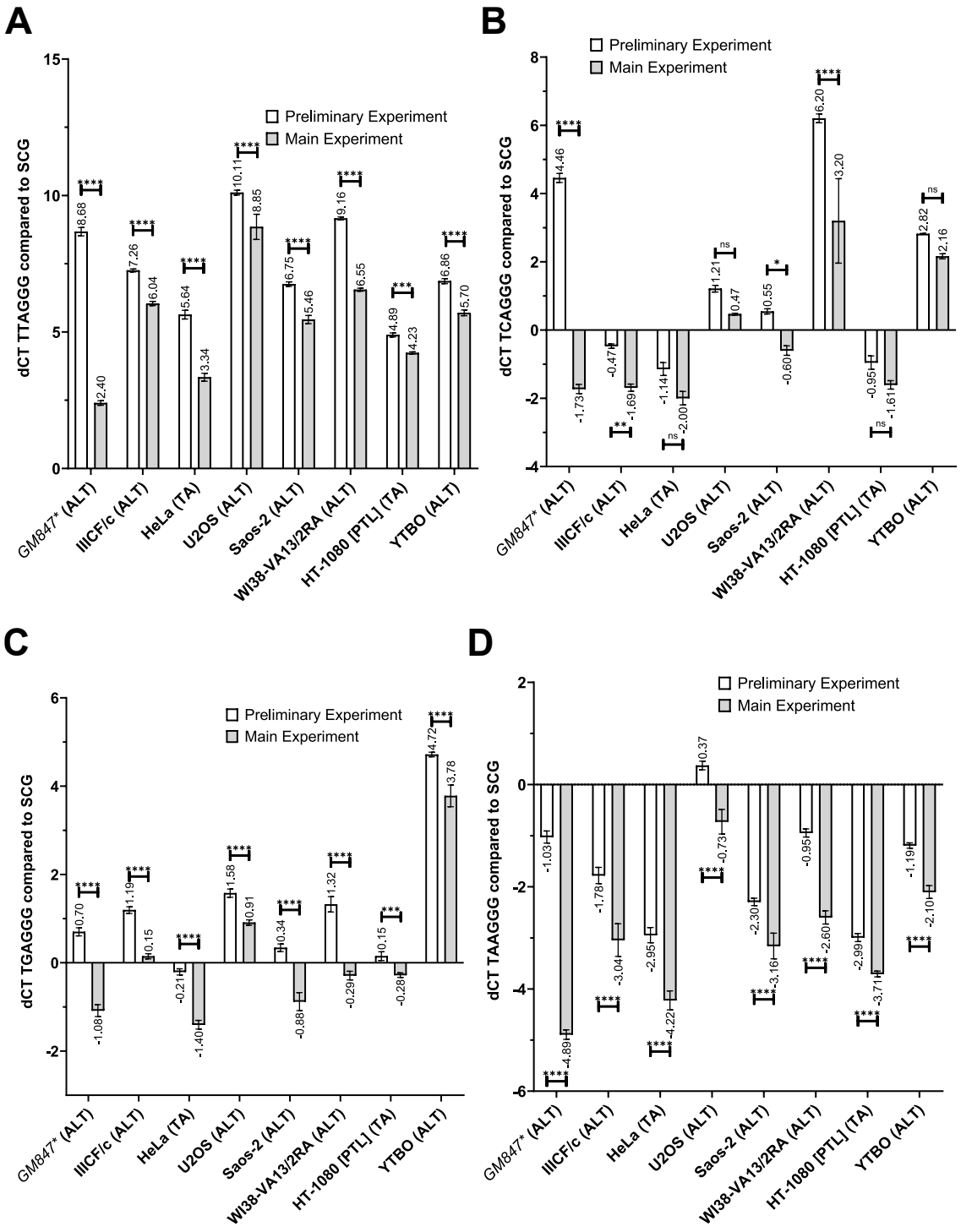

Figure 12: Average dCT values of telomeric repeats and NCTRs compared to the SCG detected by qPCR of the preliminary and main experiment in contrast to each other. A: Comparison of average dCTs of the telomeric repeat TTAGGG. B: Comparison of the average dCTs of TCAGGG repeats. C: Comparison of the average dCTs of the TGAGGG repeats. D: Comparison of the average dCTs of the TAAGGG repeats. dCT values >0 symbolize abundance higher than SCG. Statistics can be found in Table 29. Raw data can be found in

Table 56 and Table 57. N = 3 technical replicates for both experiments. Both experiments are biological replicates of each other.

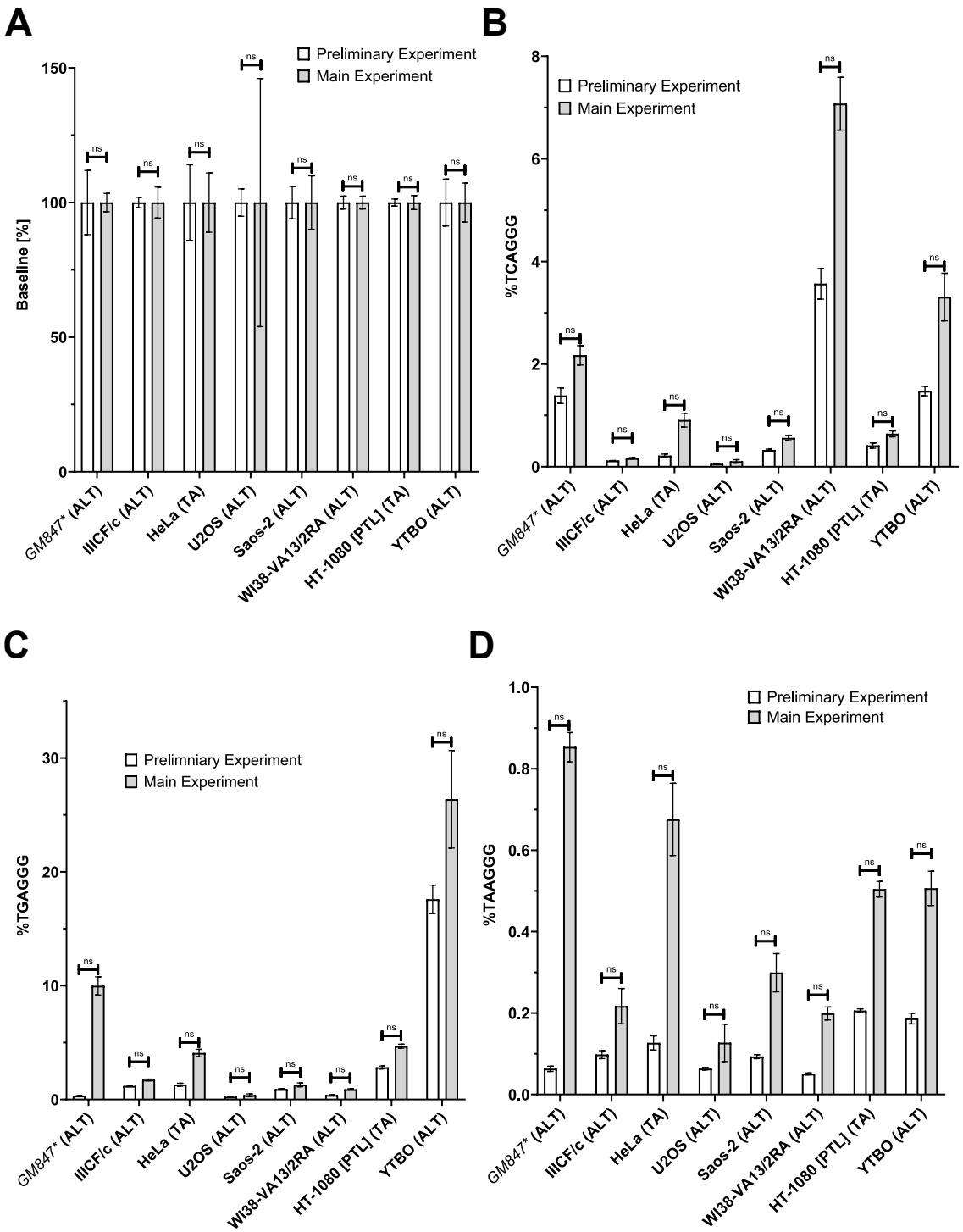

Figure 13: Average SQ-based percentage ± SEM of the analyzed NCTRs compared to the telomeric repeat SQ detected by qPCR of the preliminary and main experiment in contrast to each other. A: Comparison of average percentages of the telomeric repeat

TTAGGG. B: Comparison of average percentages of TCAGGG repeats. C: Comparison of average percentages of the TGAGGG repeats. D: Comparison of average percentages of the TAAGGG repeats. Statistics can be found in Table 30. Raw data can be found in Table 56 and Table 57. N = 3 technical replicates for both experiments. Both experiments are biological replicates of each other.

Table 29: Statistics (two-way ANOVA with Sidak's multiple comparisons follow-up test) of the comparison of dCT values from the main and the preliminary NCTR detection qPCR experiment in gDNAs. (See Figure 12)

dCT TTAGGG

					Main Experiment							
					*GM847** (ALT)	IIICF/c (ALT)	HeLa (TA)	U2OS (ALT)	Saos-2 (ALT)	WI38-VA13/2RA (ALT)	HT-1080 [PTL] (TA)	YTBO (ALT)
				n	3	3	3	3	3	3	3	3
				Mean dCT	2.40	6.04	3.34	8.85	5.46	6.55	4.23	5.70
		n	Mean dCT	SEM dCT	0.05	0.05	0.08	0.27	0.09	0.03	0.02	0.06
					P values							
Preliminary Experiment	*GM847** (ALT)	3	8.68	0.09	**** (<0.0001)							
	IIICF/c (ALT)	3	7.26	0.03		**** (<0.0001)						
	HeLa (TA)	3	5.64	0.09			**** (<0.0001)					
	U2OS (ALT)	3	10.11	0.05				**** (<0.0001)				
	Saos-2 (ALT)	3	6.75	0.05					**** (<0.0001)			
	WI38-VA13/2RA (ALT)	3	9.16	0.03						**** (<0.0001)		
	HT-1080 [PTL] (TA)	3	4.89	0.04							**** (<0.0001)	
	YTBO (ALT)	3	6.86	0.05								**** (<0.0001)

dCT TCAGGG

					Main Experiment							
					*GM847** (ALT)	IIICF/c (ALT)	HeLa (TA)	U2OS (ALT)	Saos-2 (ALT)	WI38-VA13/2RA (ALT)	HT-1080 [PTL] (TA)	YTBO (ALT)
				n	3	3	3	3	3	3	3	2
				Mean dCT	-1.73	-1.69	-2.00	0.47	-0.60	3.20	-1.61	2.16
		n	Mean dCT	SEM dCT	0.08	0.06	0.11	0.01	0.08	0.72	0.07	0.05
					P values							
Preliminary Experiment	*GM847** (ALT)	3	4.46	0.08	**** (<0.0001)							
	IIICF/c (ALT)	3	-0.47	0.04		*** (0.0009)						
	HeLa (TA)	3	-1.14	0.11			* (0.0329)					
	U2OS (ALT)	3	1.21	0.06				ns (0.0843)				
	Saos-2 (ALT)	3	0.55	0.04					** (0.0019)			

	WI38-VA13/2RA (ALT)	3	6.20	0.07						**** (<0.0001)		
	HT-1080 [PTL] (TA)	3	-0.95	0.11							ns (0.1785)	
	YTBO (ALT)	3	2.82	0.01								ns (0.2806)

dCT TGAGGG

					Main Experiment							
					*GM847** (ALT)	IIICF/c (ALT)	HeLa (TA)	U2OS (ALT)	Saos-2 (ALT)	WI38-VA13/2RA (ALT)	HT-1080 [PTL] (TA)	YTBO (ALT)
				n	3	3	3	3	3	3	3	3
				Mean dCT	-1.08	0.15	-1.40	0.91	-0.88	-0.29	-0.28	3.78
		n	Mean dCT	SEM dCT	0.08	0.03	0.06	0.03	0.12	0.06	0.03	0.14
					P values							
Preliminary Experiment	*GM847** (ALT)	3	0.70	0.05	**** (<0.0001)							
	IIICF/c (ALT)	3	1.19	0.04		**** (<0.0001)						
	HeLa (TA)	3	-0.21	0.04			**** (<0.0001)					
	U2OS (ALT)	3	1.58	0.05				**** (<0.0001)				
	Saos-2 (ALT)	3	0.34	0.05					**** (<0.0001)			
	WI38-VA13/2RA (ALT)	3	1.32	0.10						**** (<0.0001)		
	HT-1080 [PTL] (TA)	3	0.15	0.06							*** (0.0009)	
	YTBO (ALT)	3	4.72	0.03								**** (<0.0001)

dCT TAAGGG

					Main Experiment							
					*GM847** (ALT)	IIICF/c (ALT)	HeLa (TA)	U2OS (ALT)	Saos-2 (ALT)	WI38-VA13/2RA (ALT)	HT-1080 [PTL] (TA)	YTBO (ALT)
				n	3	3	3	3	3	3	3	3
				Mean dCT	-4.89	-3.04	-4.22	-0.73	-3.16	-2.60	-3.71	-2.10
		n	Mean dCT	SEM dCT	0.05	0.18	0.11	0.14	0.14	0.07	0.03	0.07
					P values							
Preliminary	*GM847** (ALT)	3	-1.03	0.07	**** (<0.0001)							
	IIICF/c (ALT)	3	-1.78	0.09		**** (<0.0001)						
	HeLa (TA)	3	-2.95	0.09			**** (<0.0001)					
	U2OS (ALT)	3	0.37	0.05				**** (<0.0001)				

Saos-2 (ALT)	3	-2.30	0.04					**** (<0.0001)				
WI38-VA13/2RA (ALT)	3	-0.95	0.05						**** (<0.0001)			
HT-1080 [PTL] (TA)	3	-2.99	0.05							**** (<0.0001)		
YTBO (ALT)	3	-1.19	0.03									**** (<0.0001)

Table 30: Statistics (two-way ANOVA with Tukey's multiple comparisons follow-up test) of the comparison of variant percentages of the main and the preliminary NCTR detection qPCR experiments in gDNAs. (See Figure 12)

					Baseline							
					Main Experiment							
					GM847 (ALT)	IIICF/c (ALT)	HeLa (TA)	U2OS (ALT)	Saos-2 (ALT)	WI38-VA13/2RA (ALT)	HT-1080 [PTL] (TA)	YTBO (ALT)
				n	3	3	3	3	3	3	3	3
				Mean % [TTAGGG/TTAGGG]	100.00	100.00	100.00	100.00	100.00	100.00	100.00	100.00
		n	Mean % [TTAGGG/TTAGGG]	SEM [%TTAGGG]	1.98	3.31	6.37	26.59	5.73	1.37	1.50	4.18
Preliminary Experiment	GM847 (ALT)	3	100.00	6.88	ns (>0.9999)							
	IIICF/c (ALT)	3	100.00	1.12		ns (>0.9999)						
	HeLa (TA)	3	100.00	8.09			ns (>0.9999)					
	U2OS (ALT)	3	100.00	2.94				ns (>0.9999)				
	Saos-2 (ALT)	3	100.00	3.48					ns (>0.9999)			
	WI38-VA13/2RA (ALT)	3	100.00	1.38						ns (>0.9999)		
	HT-1080 [PTL] (TA)	3	100.00	0.76							ns (>0.9999)	
	YTBO (ALT)	3	100.00	5.03								ns (>0.9999)

					%TCAGGG							
					Main Experiment							

					GM847 (ALT)	IIICF/c (ALT)	HeLa (TA)	U2OS (ALT)	Saos-2 (ALT)	WI38-VA13/2RA (ALT)	HT-1080 [PTL] (TA)	YTBO (ALT)
Preliminary Experiment				n	3	3	3	3	3	2	3	3
				Mean % [TCAGGG/TTAGGG]	2.17	0.17	0.91	0.10	0.56	7.07	0.64	3.31
		n	Mean % [TCAGGG/TTAGGG]	SEM [%TCAGGG]	0.11	0.01	0.08	0.02	0.03	0.36	0.03	0.27
	GM847 (ALT)	3	1.38	0.09	ns (>0.9999)							
	IIICF/c (ALT)	3	0.12	0.00		ns (>0.9999)						
	HeLa (TA)	3	0.21	0.02			ns (>0.9999)					
	U2OS (ALT)	3	0.05	0.00				ns (>0.9999)				
	Saos-2 (ALT)	3	0.32	0.01					ns (>0.9999)			
	WI38-VA13/2RA (ALT)	3	3.56	0.17						ns (0.9992)		
	HT-1080 [PTL] (TA)	3	0.41	0.03							ns (>0.9999)	
	YTBO (ALT)	3	1.48	0.05								ns (>0.9999)

%TGAGGG

Main Experiment

					GM847 (ALT)	IIICF/c (ALT)	HeLa (TA)	U2OS (ALT)	Saos-2 (ALT)	WI38-VA13/2RA (ALT)	HT-1080 [PTL] (TA)	YTBO (ALT)
Preliminary Experiment				n	3	3	3	3	3	3	3	3
				Mean % [TGAGGG/TTAGGG]	9.98	1.72	4.08	0.37	1.29	0.89	4.69	26.38
		n	Mean % [TGAGGG/TTAGGG]	SEM [%TGAGGG]	0.46	0.04	0.19	0.07	0.10	0.03	0.10	2.47
	GM847 (ALT)	3	0.32	0.02	ns (0.6661)							
	IIICF/c (ALT)	3	1.18	0.03		ns (>0.9999)						
	HeLa (TA)	3	1.30	0.08			ns (0.9996)					
	U2OS (ALT)	3	0.22	0.01				ns (>0.9999)				

	Saos-2 (ALT)	3	0.89	0.03					ns (>0.9999)			
	WI38-VA13/2RA (ALT)	3	0.38	0.03						ns (>0.9999)		
	HT-1080 [PTL] (TA)	3	2.81	0.07							ns (>0.9999)	
	YTBO (ALT)	3	17.58	0.72								ns (0.7626)

%TAAGGG

					Main Experiment							
					GM847 (ALT)	IIICF/c (ALT)	HeLa (TA)	U2OS (ALT)	Saos-2 (ALT)	WI38-VA13/2RA (ALT)	HT-1080 [PTL] (TA)	YTBO (ALT)
				n	3	3	3	3	3	3	3	3
				Mean % [TAAGGG/TTAGGG]	0.85	0.22	0.68	0.13	0.30	0.20	0.50	0.51
		n	Mean % [TAAGGG/TTAGGG]	SEM [%TAAGGG]	0.02	0.02	0.05	0.03	0.03	0.01	0.01	0.02
Preliminary Experiment	GM847 (ALT)	3	0.06	0.00	ns (>0.9999)							
	IIICF/c (ALT)	3	0.10	0.01		ns (>0.9999)						
	HeLa (TA)	3	0.13	0.01			ns (>0.9999)					
	U2OS (ALT)	3	0.06	0.00				ns (>0.9999)				
	Saos-2 (ALT)	3	0.09	0.00					ns (>0.9999)			
	WI38-VA13/2RA (ALT)	3	0.05	0.00						ns (>0.9999)		
	HT-1080 [PTL] (TA)	3	0.21	0.00							ns (>0.9999)	
	YTBO (ALT)	3	0.19	0.01								ns (>0.9999)

6.2.2. Correlation with whole genome sequencing data

In order to compare the qPCR and the WGS data, correlations of the variant percentages were performed. The cell line *GM847** was omitted from these analyses since there was the suspicion that the cells were not originating from the assumed cell line due to the results of the ALT activity detection experiments, which was confirmed by the STR marker analysis. In the following chapter, the variant percentages of the remaining seven cell lines were compared for the two methods.

For both the TCAGGG variant (Figure 14A) and the TGAGGG variant (Figure 14B), there was a very strong correlation between qPCR and WGS variant detection assays ($r = 0.94$, $p = 0.0019$ and $r = 0.85$, $p = 0.0157$, respectively). While the percentages detected by qPCR for the TCAGGG variant were lower than those of the WGS, they were more similar for the TGAGGG variant, except for the WI38/VA13/2RA cell line, which had a substantially lower percentage in the qPCR results (Table 58).

For the TAAGG variant, there was no correlation ($r = 0.52$, $p = 0.2318$). The values of the two methods were similar except for the cell lines IIICF/c and WI38-VA13/2RA. Here the percentages were substantially lower in the qPCR assay (Table 58).

In summary, there were strong, significant correlations between qPCR and WGS variant detection assays for two variants and one moderate but insignificant correlation for the least represented variant.

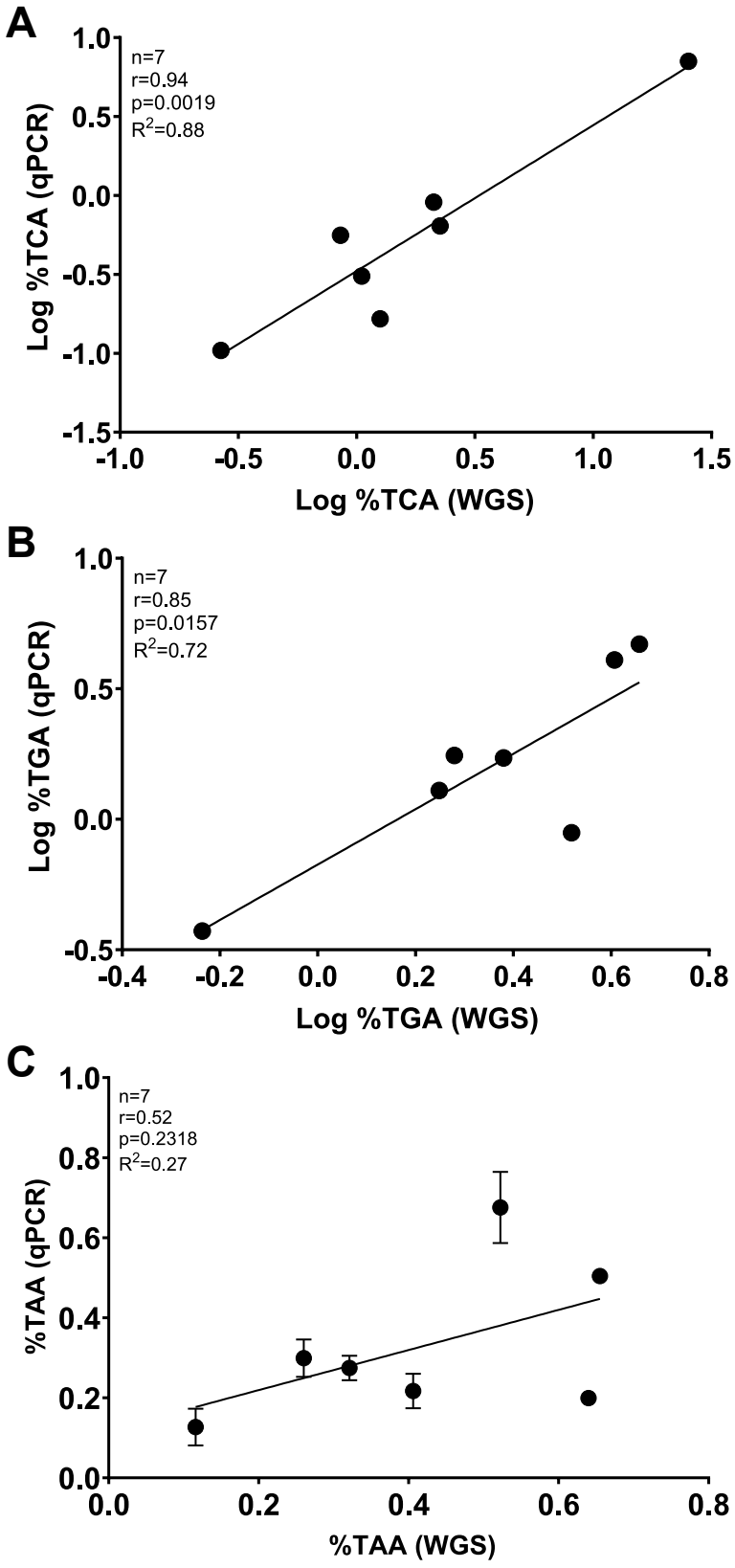

Figure 14: Correlation of qPCR detected NCTR percentages shown in Figure 9 (3 technical replicates for each dot) with NCTR percentages from WGS data produced by Lee et al. (2014). A: Correlation of TCAGGG percentages. All values were logarithmized to create a normal distribution. Due to a limitation in GraphPad Prism 8, the transformation of the

SEM was impossible. B: Correlation of TGAGGG percentages. All values were logarithmized to create a normal distribution. Due to a limitation in GraphPad Prism 8, the transformation of the SEM was impossible. C: Correlation of TAAGGG percentages. Error bars: SEM. N = 7 cell lines, r = Pearson's correlation coefficient. Plotted values can be found in Table 58.

6.2.3. NCTR variants in C-circle assay products

After the detection of the telomere sequence variants, it was also of interest to know where these variants are coming from or how they get amplified. To check a potential origin of variants in ALT-positive cell lines, the products of the second CCA from 0 were used as templates for the variant detection qPCR assays. The results of these assays are shown in Figure 15 with the corresponding statistics portrayed in Table 31 and Table 32.

In summary, it was observed that the variants increased the most in cell lines with high ALT activity i.e., a high increase of the canonical repeat (Figure 15). So, there are variants present in the ALT-specific C-circles and these variants are multiplied by high C-circle activity. The variant with the highest percentual increase, in general, was TAAGGG (Figure 15E), but this variant also is the least abundant in the cell lines in the polymerase negative reactions (Table 32). The TCAGGG percentage was observed to increase at the second-highest rate (Figure 15C). This variant also was the second highest in abundance in the polymerase negative reactions (Table 32). The TGAGGG variant percentage showed the lowest increase in the polymerase-positive reactions (Figure 15D), but it also was the most abundant variant in the polymerase-negative reactions (Table 32). When comparing the percentual variant increases with each other in the single cell lines, I observed that different cell lines have different patterns of variant increases (Figure 15 and Table 32). More detailed descriptions of the results follow in the next sections.

For the single copy gene (36B4) there were no significant differences in the average percentual differences comparing the polymerase positive and negative treatments between all cell lines (Figure 15A). Values above 100 mean an increase of the target in the polymerase-positive treatment compared to the negative one. The cell lines ranged from an average percentage ± SEM of 106.43%±3.8 (*GM847**) to 225.55%±3.01 (Saos-2) with the majority of the cell line percentages sitting below 150. This was due to the low average SCG quantity in both treatments so even the small difference in SQs of 3.4 (see Table 59) leads to a high percentual increase.

The canonical repeat in the polymerase positive reactions (Figure 15B) only significantly increased compared to the negative control in the ALT-positive (see 0 and 6.1.2) Saos-2 2022 positive control cell line, Saos-2 and YTBO. The average percentage of the Saos-2 positive control and the Saos-2 cell line were the significantly highest and second highest, respectively. YTBO ranged in the third place, differing significantly from all cell lines except IIICF/c. The ALT-positive control U2OS cell line and IIICF/c also showed a high average percentual, although without significant differences compared to the negative control. The CCA and ALT-FISH positive cell lines WI38-VA13/2RA and U2OS had average percentages in a similar scope to the ALT negative cell lines *GM847** HT-1080 PTL, HeLa, HT-1080 hTR wt and the negative control (see Table 31).

The TCAGGG variant (Figure 15C) only was significantly elevated in the polymerase-positive treatment of the Saos-2 positive control and of the Saos-2 cell line compared to the negative control and all other cell lines except for YTBO. Only the positive control Saos-2 had a significantly higher average percentage than YTBO but not the Saos-2 cell line. The positive control Saos-2 and the Saos-2 cell line did not significantly differ from each other. The remaining cell lines did not significantly differ from the negative control and each other. But it has to be mentioned that from these cell lines, some showed high average percentages ± SEM like YTBO, U2OS positive control, IIICF/c and U2OS.

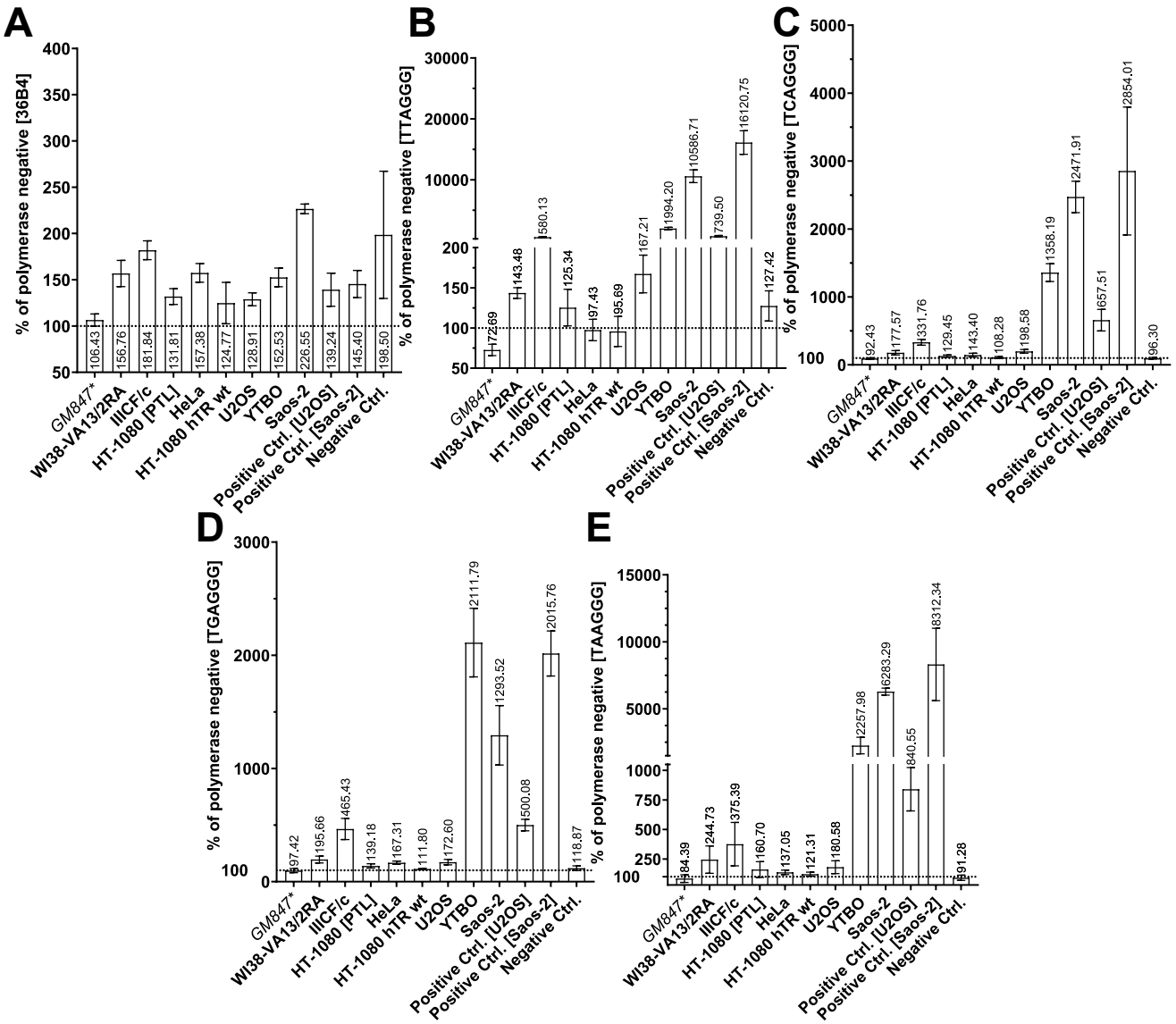

Figure 15: Average SQ-based percentage ± SEM of the by qPCR detected SCG, telomere repeats and NCTRs in the polymerase positive reactions compared to the SCG, telomere repeats and NCTRs in the polymerase negative reactions of the CCA products of multiple cell lines. A: Percentage of the SCG 36B4. B: Percentage of the canonical telomere repeat TTAGGG. C: Percentage of the TCAGGG repeat. D: Percentage of the TGAGGG repeat. E: Percentage of the TAAGGG repeat. N = 3 technical replicates. Statistics can be found in Table 31 and Table 32. Raw data can be found in Table 60.

The TGAGGG variant percentage was significantly enriched in the polymerase positive reaction of YTBO and the Saos-2 positive control (Figure 15D). In the case of YTBO, the percentage was significantly higher than the negative control and all cell lines except the Saos-2 positive control and the Saos-2 cell line. For the Saos-2 positive control, the TGAGGG percentage was significantly higher than the negative control and all other cell lines except

YTBO and the Saos-2. Similar to the TCAGGG variant, the remaining cell lines did not significantly differ from the negative control and each other but there were cases with high average percentages ± SEM, nonetheless. These were Saos-2, the U2OS positive control, IIICF/c and WI38-VA13/2RA.

For the TAAGGG variant (Figure 15E), the pattern of significant differences was nearly the same as for the TGAGGG variant. The only deviation was that the average TAAGGG percentage of the Saos-2 positive control was significantly higher than that of the Saos-2 cell line. For this NCTR, the cell lines with high but not significantly increased percentages were the U2OS positive control, IIICF/c and WI38-VA13/2RA.

When comparing the average percentage increases of the SCG, canonical repeat and NCTR with each other in every cell line (Table 32) there were only significant differences in Saos-2, Saos-2 positive control and YTBO. In Saos-2 the percentages of all targets significantly differed from each other except for TGAGGG. This variant did not significantly differ from the SCG but from all other variants. The variant with the highest percentual increase in this cell line was TCAGGG followed by TAAGGG and TGAGGG. In the Saos-2 positive control, the percentages of all targets, except two, significantly differed from each other. These two targets were TCAGGG and TGAGGG. Their percentages were not significantly different from each other but significantly differed from the remaining targets. The variant which increased the most was TAAGGG followed by TCAGGG and TGAGGG. In YTBO, all the telomeric targets significantly differed from the SCG but not from each other. Here, the variant with the highest increase was TAAGGG followed by TGAGGG and TCAGGG.

Table 31: Statistics (two-way ANOVA with Tukey's multiple comparisons follow-up test) of the percentual SCG, TTAGGG repeat and NCTR content of the polymerase-positive reaction compared to the polymerase-negative reaction detected by qPCR (See Figure 15) comparing the CCA products of all cell lines of the second CCA.

36B4 [% Phi+/Phi-]

	*GM847**	WI38-VA13/2RA	IIICF/c	HT-1080 PTL	HeLa	HT-1080 hTR wt	U2OS	YTBO	Saos-2	+ Ctrl. [U2OS]	+ Ctrl. [Saos-2]	- Ctrl.
Mean % Phi+/Phi-	106.43	156.76	181.84	131.81	157.38	124.77	128.91	152.53	226.55	139.24	145.40	198.50
SEM % Phi+/Phi-	3.80	8.18	5.88	4.92	5.83	12.95	4.04	5.79	3.01	10.33	8.48	68.77
n	3	3	3	3	3	3	3	3	3	3	3	1
						P values						
*GM847**		ns (>0.9999)	ns (>0.9999)	ns (>0.9999)	ns (>0.9999)	ns (>0.9999)	ns (>0.9999)	ns (>0.9999)	ns (>0.9999)	ns (>0.9999)	ns (>0.9999)	ns (>0.9999)
WI38-VA13/2RA	ns (>0.9999)		ns (>0.9999)	ns (>0.9999)	ns (>0.9999)	ns (>0.9999)	ns (>0.9999)	ns (>0.9999)	ns (>0.9999)	ns (>0.9999)	ns (>0.9999)	ns (>0.9999)
IIICF/c	ns (>0.9999)	ns (>0.9999)		ns (>0.9999)	ns (>0.9999)	ns (>0.9999)	ns (>0.9999)	ns (>0.9999)	ns (>0.9999)	ns (>0.9999)	ns (>0.9999)	ns (>0.9999)
HT-1080 PTL	ns (>0.9999)	ns (>0.9999)	ns (>0.9999)		ns (>0.9999)	ns (>0.9999)	ns (>0.9999)	ns (>0.9999)	ns (>0.9999)	ns (>0.9999)	ns (>0.9999)	ns (>0.9999)
HeLa	ns (>0.9999)	ns (>0.9999)	ns (>0.9999)	ns (>0.9999)		ns (>0.9999)	ns (>0.9999)	ns (>0.9999)	ns (>0.9999)	ns (>0.9999)	ns (>0.9999)	ns (>0.9999)
HT-1080 hTR wt	ns (>0.9999)	ns (>0.9999)	ns (>0.9999)	ns (>0.9999)	ns (>0.9999)		ns (>0.9999)	ns (>0.9999)	ns (>0.9999)	ns (>0.9999)	ns (>0.9999)	ns (>0.9999)
U2OS	ns (>0.9999)	ns (>0.9999)	ns (>0.9999)	ns (>0.9999)	ns (>0.9999)	ns (>0.9999)		ns (>0.9999)	ns (>0.9999)	ns (>0.9999)	ns (>0.9999)	ns (>0.9999)
YTBO	ns (>0.9999)	ns (>0.9999)	ns (>0.9999)	ns (>0.9999)	ns (>0.9999)	ns (>0.9999)	ns (>0.9999)		ns (>0.9999)	ns (>0.9999)	ns (>0.9999)	ns (>0.9999)
Saos-2	ns (>0.9999)	ns (>0.9999)	ns (>0.9999)	ns (>0.9999)	ns (>0.9999)	ns (>0.9999)	ns (>0.9999)	ns (>0.9999)		ns (>0.9999)	ns (>0.9999)	ns (>0.9999)
+ Ctrl. [U2OS]	ns (>0.9999)	ns (>0.9999)	ns (>0.9999)	ns (>0.9999)	ns (>0.9999)	ns (>0.9999)	ns (>0.9999)	ns (>0.9999)	ns (>0.9999)		ns (>0.9999)	ns (>0.9999)
+ Ctrl. [Saos-2]	ns (>0.9999)	ns (>0.9999)	ns (>0.9999)	ns (>0.9999)	ns (>0.9999)	ns (>0.9999)	ns (>0.9999)	ns (>0.9999)	ns (>0.9999)	ns (>0.9999)		ns (>0.9999)
- Ctrl.	ns (>0.9999)	ns (>0.9999)	ns (>0.9999)	ns (>0.9999)	ns (>0.9999)	ns (>0.9999)	ns (>0.9999)	ns (>0.9999)	ns (>0.9999)	ns (>0.9999)	ns (>0.9999)	

TTAGGG [% Phi+/Phi-]

	*GM847**	WI38-VA13/2RA	IIICF/c	HT-1080 PTL	HeLa	HT-1080 hTR wt	U2OS	YTBO	Saos-2	+ Ctrl. [U2OS]	+ Ctrl. [Saos-2]	- Ctrl.
Mean % Phi+/Phi-	72.69	143.48	580.13	125.34	97.43	95.69	167.21	1994.20	10586.71	739.50	16120.75	127.42
SEM % Phi+/Phi-	4.07	3.89	65.81	13.17	7.70	10.83	13.50	118.06	607.43	73.38	1120.09	10.84

n	3	3	2	3	3	3	3	3	3	3	3	3
P values												
*GM847**		ns (>0.9999)	ns (0.9918)	ns (>0.9999)	ns (>0.9999)	ns (>0.9999)	ns (>0.9999)	*** (0.0002)	**** (<0.0001)	ns (0.8721)	**** (<0.0001)	ns (>0.9999)
WI38-VA13/2RA	ns (>0.9999)		ns (0.9977)	ns (>0.9999)	ns (>0.9999)	ns (>0.9999)	ns (>0.9999)	*** (0.0005)	**** (<0.0001)	ns (0.9365)	**** (<0.0001)	ns (>0.9999)
IIICF/c	ns (0.9918)	ns (0.9977)		ns (0.9968)	ns (0.9946)	ns (0.9944)	ns (0.9986)	ns (0.0739)	**** (<0.0001)	ns (>0.9999)	**** (<0.0001)	ns (0.9969)
HT-1080 PTL	ns (>0.9999)	ns (>0.9999)	ns (0.9968)		ns (>0.9999)	ns (>0.9999)	ns (>0.9999)	*** (0.0004)	**** (<0.0001)	ns (0.9227)	**** (<0.0001)	ns (>0.9999)
HeLa	ns (>0.9999)	ns (>0.9999)	ns (0.9946)	ns (>0.9999)		ns (>0.9999)	ns (>0.9999)	*** (0.0003)	**** (<0.0001)	ns (0.8978)	**** (<0.0001)	ns (>0.9999)
HT-1080 hTR wt	ns (>0.9999)	ns (>0.9999)	ns (0.9944)	ns (>0.9999)	ns (>0.9999)		ns (>0.9999)	*** (0.0003)	**** (<0.0001)	ns (0.8962)	**** (<0.0001)	ns (>0.9999)
U2OS	ns (>0.9999)	ns (>0.9999)	ns (0.9986)	ns (>0.9999)	ns (>0.9999)	ns (>0.9999)		*** (0.0006)	**** (<0.0001)	ns (0.9518)	**** (<0.0001)	ns (>0.9999)
YTBO	*** (0.0002)	*** (0.0005)	ns (0.0739)	*** (0.0004)	*** (0.0003)	*** (0.0003)	*** (0.0006)		**** (<0.0001)	ns (0.0791)	**** (<0.0001)	*** (0.0004)
Saos-2	**** (<0.0001)	**** (<0.0001)	**** (<0.0001)	**** (<0.0001)	**** (<0.0001)	**** (<0.0001)	**** (<0.0001)	**** (<0.0001)		**** (<0.0001)	**** (<0.0001)	**** (<0.0001)
+ Ctrl. [U2OS]	ns (0.8721)	ns (0.9365)	ns (>0.9999)	ns (0.9227)	ns (0.8978)	ns (0.8962)	ns (0.9518)	ns (0.0791)	**** (<0.0001)		**** (<0.0001)	ns (0.9244)
+ Ctrl. [Saos-2]	**** (<0.0001)	**** (<0.0001)	**** (<0.0001)	**** (<0.0001)	**** (<0.0001)	**** (<0.0001)	**** (<0.0001)	**** (<0.0001)	**** (<0.0001)	**** (<0.0001)		**** (<0.0001)
- Ctrl.	ns (>0.9999)	ns (>0.9999)	ns (0.9969)	ns (>0.9999)	ns (>0.9999)	ns (>0.9999)	ns (>0.9999)	*** (0.0004)	**** (<0.0001)	ns (0.9244)	**** (<0.0001)	

TCAGGG [% Phi+/Phi-]

	*GM847**	WI38-VA13/2RA	IIICF/c	HT-1080 PTL	HeLa	HT-1080 hTR wt	U2OS	YTBO	Saos-2	+ Ctrl. [U2OS]	+ Ctrl. [Saos-2]	- Ctrl.
Mean % Phi+/Phi-	92.43	177.57	331.76	129.45	143.40	108.28	198.58	1358.19	2471.91	657.51	2854.01	96.30
SEM % Phi+/Phi-	6.24	18.67	24.72	9.04	15.83	7.71	15.60	76.30	133.62	91.13	543.61	6.34
n	3	3	3	3	3	3	3	3	3	3	3	3
P values												
*GM847**		ns (>0.9999)	ns (>0.9999)	ns (>0.9999)	ns (>0.9999)	ns (>0.9999)	ns (>0.9999)	ns (0.0734)	**** (<0.0001)	ns (0.9559)	**** (<0.0001)	ns (>0.9999)
WI38-VA13/2RA	ns (>0.9999)		ns (>0.9999)	ns (>0.9999)	ns (>0.9999)	ns (>0.9999)	ns (>0.9999)	ns (0.1274)	**** (<0.0001)	ns (0.9871)	**** (<0.0001)	ns (>0.9999)
IIICF/c	ns (>0.9999)	ns (>0.9999)		ns (>0.9999)	ns (>0.9999)	ns (>0.9999)	ns (>0.9999)	ns (0.2964)	**** (<0.0001)	ns (0.9996)	**** (<0.0001)	ns (>0.9999)
HT-1080 PTL	ns (>0.9999)	ns (>0.9999)	ns (>0.9999)		ns (>0.9999)	ns (>0.9999)	ns (>0.9999)	ns (0.0939)	**** (<0.0001)	ns (0.9729)	**** (<0.0001)	ns (>0.9999)

HeLa	ns (>0.9999)	ns (>0.9999)	ns (>0.9999)	ns (>0.9999)		ns (>0.9999)	ns (>0.9999)	ns (0.1028)	**** (<0.0001)	ns (0.9779)	**** (<0.0001)	ns (>0.9999)
HT-1080 hTR wt	ns (>0.9999)	ns (>0.9999)	ns (>0.9999)	ns (>0.9999)	ns (>0.9999)		ns (>0.9999)	ns (0.0816)	**** (<0.0001)	ns (0.9639)	**** (<0.0001)	ns (>0.9999)
U2OS	ns (>0.9999)	ns (>0.9999)	ns (>0.9999)	ns (>0.9999)	ns (>0.9999)	ns (>0.9999)		ns (0.1447)	**** (<0.0001)	ns (0.991)	**** (<0.0001)	ns (>0.9999)
YTBO	ns (0.0734)	ns (0.1274)	ns (0.2964)	ns (0.0939)	ns (0.1028)	ns (0.0816)	ns (0.1447)		ns (0.1885)	ns (0.8311)	* (0.0127)	ns (0.0753)
Saos-2	**** (<0.0001)	**** (<0.0001)	**** (<0.0001)	**** (<0.0001)	**** (<0.0001)	**** (<0.0001)	**** (<0.0001)	ns (0.1885)		*** (0.0007)	ns (0.9981)	**** (<0.0001)
+ Ctrl. [U2OS]	ns (0.9559)	ns (0.9871)	ns (0.9996)	ns (0.9729)	ns (0.9779)	ns (0.9639)	ns (0.991)	ns (0.8311)	*** (0.0007)		**** (<0.0001)	ns (0.9579)
+ Ctrl. [Saos-2]	**** (<0.0001)	**** (<0.0001)	**** (<0.0001)	**** (<0.0001)	**** (<0.0001)	**** (<0.0001)	**** (<0.0001)	* (0.0127)	ns (0.9981)	**** (<0.0001)		**** (<0.0001)
- Ctrl.	ns (>0.9999)	ns (>0.9999)	ns (>0.9999)	ns (>0.9999)	ns (>0.9999)	ns (>0.9999)	ns (>0.9999)	ns (0.0753)	**** (<0.0001)	ns (0.9579)	**** (<0.0001)	

TGAGGG [% Phi+/Phi-]

	*GM847**	WI38-VA13/2RA	IIICF/c	HT-1080 PTL	HeLa	HT-1080 hTR wt	U2OS	YTBO	Saos-2	+ Ctrl. [U2OS]	+ Ctrl. [Saos-2]	- Ctrl.
Mean % Phi+/Phi-	97.42	195.66	465.43	139.18	167.31	111.80	172.60	2111.79	1293.52	500.08	2015.76	118.87
SEM % Phi+/Phi-	10.63	17.50	54.06	10.83	8.36	3.12	14.03	174.80	151.58	29.16	115.04	12.10
n	3	3	3	3	3	3	3	3	3	3	3	3

P values

*GM847**		ns (>0.9999)	ns (0.9987)	ns (>0.9999)	ns (>0.9999)	ns (>0.9999)	ns (>0.9999)	**** (<0.0001)	ns (0.1157)	ns (0.997)	*** (0.0002)	ns (>0.9999)
WI38-VA13/2RA	ns (>0.9999)		ns (>0.9999)	ns (>0.9999)	ns (>0.9999)	ns (>0.9999)	ns (>0.9999)	*** (0.0002)	ns (0.2057)	ns (0.9998)	*** (0.0006)	ns (>0.9999)
IIICF/c	ns (0.9987)	ns (>0.9999)		ns (0.9996)	ns (0.9998)	ns (0.9991)	ns (0.9998)	** (0.0034)	ns (0.6301)	ns (>0.9999)	** (0.008)	ns (0.9992)
HT-1080 PTL	ns (>0.9999)	ns (>0.9999)	ns (0.9996)		ns (>0.9999)	ns (>0.9999)	ns (>0.9999)	*** (0.0001)	ns (0.1493)	ns (0.9989)	*** (0.0004)	ns (>0.9999)
HeLa	ns (>0.9999)	ns (>0.9999)	ns (0.9998)	ns (>0.9999)		ns (>0.9999)	ns (>0.9999)	*** (0.0002)	ns (0.1757)	ns (0.9995)	*** (0.0005)	ns (>0.9999)
HT-1080 hTR wt	ns (>0.9999)	ns (>0.9999)	ns (0.9991)	ns (>0.9999)	ns (>0.9999)		ns (>0.9999)	**** (<0.0001)	ns (0.1265)	ns (0.9979)	*** (0.0003)	ns (>0.9999)
U2OS	ns (>0.9999)	ns (>0.9999)	ns (0.9998)	ns (>0.9999)	ns (>0.9999)	ns (>0.9999)		*** (0.0002)	ns (0.1811)	ns (0.9996)	*** (0.0005)	ns (>0.9999)
YTBO	**** (<0.0001)	*** (0.0002)	** (0.0034)	*** (0.0001)	*** (0.0002)	**** (<0.0001)	*** (0.0002)		ns (0.6474)	** (0.0047)	ns (>0.9999)	*** (0.0001)
Saos-2	ns (0.1157)	ns (0.2057)	ns (0.6301)	ns (0.1493)	ns (0.1757)	ns (0.1265)	ns (0.1811)	ns (0.6474)		ns (0.6902)	ns (0.8017)	ns (0.1321)

+ Ctrl. [U2OS]	ns (0.997)	ns (0.9998)	ns (>0.9999)	ns (0.9989)	ns (0.9995)	ns (0.9979)	ns (0.9996)	** (0.0047)	ns (0.6902)		* (0.0108)	ns (0.9982)
+ Ctrl. [Saos-2]	*** (0.0002)	*** (0.0006)	** (0.008)	*** (0.0004)	*** (0.0005)	*** (0.0003)	*** (0.0005)	ns (>0.9999)	ns (0.8017)	* (0.0108)		*** (0.0003)
- Ctrl.	ns (>0.9999)	ns (>0.9999)	ns (0.9992)	ns (>0.9999)	ns (>0.9999)	ns (>0.9999)	ns (>0.9999)	*** (0.0001)	ns (0.1321)	ns (0.9982)	*** (0.0003)	

TAAGGG [% Phi+/Phi-]

	*GM847**	WI38-VA13/2RA	IIICF/c	HT-1080 PTL	HeLa	HT-1080 hTR wt	U2OS	YTBO	Saos-2	+ Ctrl. [U2OS]	+ Ctrl. [Saos-2]	- Ctrl.
Mean % Phi+/Phi-	84.39	244.73	375.39	160.70	137.05	121.31	180.58	2257.98	6283.29	840.55	8312.34	91.28
SEM % Phi+/Phi-	18.73	66.82	105.99	38.48	10.79	9.90	31.15	357.96	150.69	105.98	1560.17	12.76
n	3	3	3	3	3	3	3	3	3	3	3	3
P values												
*GM847**		ns (>0.9999)	ns (0.9999)	ns (>0.9999)	ns (>0.9999)	ns (>0.9999)	ns (>0.9999)	**** (<0.0001)	**** (<0.0001)	ns (0.7511)	**** (<0.0001)	ns (>0.9999)
WI38-VA13/2RA	ns (>0.9999)		ns (>0.9999)	ns (>0.9999)	ns (>0.9999)	ns (>0.9999)	ns (>0.9999)	**** (<0.0001)	**** (<0.0001)	ns (0.9366)	**** (<0.0001)	ns (>0.9999)
IIICF/c	ns (0.9999)	ns (>0.9999)		ns (>0.9999)	ns (>0.9999)	ns (>0.9999)	ns (>0.9999)	*** (0.0003)	**** (<0.0001)	ns (0.9899)	**** (<0.0001)	ns (0.9999)
HT-1080 PTL	ns (>0.9999)	ns (>0.9999)	ns (>0.9999)		ns (>0.9999)	ns (>0.9999)	ns (>0.9999)	**** (<0.0001)	**** (<0.0001)	ns (0.857)	**** (<0.0001)	ns (>0.9999)
HeLa	ns (>0.9999)	ns (>0.9999)	ns (>0.9999)	ns (>0.9999)		ns (>0.9999)	ns (>0.9999)	**** (<0.0001)	**** (<0.0001)	ns (0.8274)	**** (<0.0001)	ns (>0.9999)
HT-1080 hTR wt	ns (>0.9999)	ns (>0.9999)	ns (>0.9999)	ns (>0.9999)	ns (>0.9999)		ns (>0.9999)	**** (<0.0001)	**** (<0.0001)	ns (0.806)	**** (<0.0001)	ns (>0.9999)
U2OS	ns (>0.9999)	ns (>0.9999)	ns (>0.9999)	ns (>0.9999)	ns (>0.9999)	ns (>0.9999)		**** (<0.0001)	**** (<0.0001)	ns (0.8795)	**** (<0.0001)	ns (>0.9999)
YTBO	**** (<0.0001)	**** (<0.0001)	*** (0.0003)	**** (<0.0001)	**** (<0.0001)	**** (<0.0001)	**** (<0.0001)		**** (<0.0001)	* (0.0241)	**** (<0.0001)	**** (<0.0001)
Saos-2	**** (<0.0001)	**** (<0.0001)	**** (<0.0001)	**** (<0.0001)	**** (<0.0001)	**** (<0.0001)	**** (<0.0001)	**** (<0.0001)		**** (<0.0001)	**** (<0.0001)	**** (<0.0001)
+ Ctrl. [U2OS]	ns (0.7511)	ns (0.9366)	ns (0.9899)	ns (0.857)	ns (0.8274)	ns (0.806)	ns (0.8795)	* (0.0241)	**** (<0.0001)		**** (<0.0001)	ns (0.7618)
+ Ctrl. [Saos-2]	**** (<0.0001)	**** (<0.0001)	**** (<0.0001)	**** (<0.0001)	**** (<0.0001)	**** (<0.0001)	**** (<0.0001)	**** (<0.0001)	**** (<0.0001)	**** (<0.0001)		**** (<0.0001)
- Ctrl.	ns (>0.9999)	ns (>0.9999)	ns (0.9999)	ns (>0.9999)	ns (>0.9999)	ns (>0.9999)	ns (>0.9999)	**** (<0.0001)	**** (<0.0001)	ns (0.7618)	**** (<0.0001)	

Table 32: Statistics (two-way ANOVA with Tukey's multiple comparisons follow-up test) of the percentual SCG, TTAGGG repeat and NCTR content of the polymerase-positive reaction compared to the polymerase-negative reaction detected by qPCR (See Figure 15) comparing the qPCR assay results of each cell line of the second CCA.

*GM847**					
	36B4	TTAGGG	TCAGGG	TGAGGG	TAAGGG
n	3	3	3	3	3
Mean SQ Phi+	2685.43	46172.55	1501.06	4243.96	140.23
SEM SQ Phi+	92.26	2139.28	99.44	451.20	29.51
Mean SQ Phi-	2523.21	63522.13	1624.05	4356.15	166.16
SEM SQ Phi-	24.51	2003.32	20.70	106.14	11.74
Mean % phi+/phi-	106.43	72.69	92.43	97.42	84.39
SEM Mean %phi+/phi-	3.80	4.07	6.24	10.63	18.73
			P values		
36B4		ns (>0.9999)	ns (>0.9999)	ns (>0.9999)	ns (>0.9999)
TTAGGG	ns (>0.9999)		ns (>0.9999)	ns (>0.9999)	ns (>0.9999)
TCAGGG	ns (>0.9999)	ns (>0.9999)		ns (>0.9999)	ns (>0.9999)
TGAGGG	ns (>0.9999)	ns (>0.9999)	ns (>0.9999)		ns (>0.9999)
TAAGGG	ns (>0.9999)	ns (>0.9999)	ns (>0.9999)	ns (>0.9999)	

IIICF/c					
	36B4	TTAGGG	TCAGGG	TGAGGG	TAAGGG
n	3	3	3	3	3
Mean SQ Phi+	2414.48	4716473.55	4960.83	28001.68	1027.04
SEM SQ Phi+	35.17	186591.46	353.71	3203.10	288.96
Mean SQ Phi-	1327.84	812997.58	1495.29	6016.32	273.59
SEM SQ Phi-	38.37	86437.76	32.35	121.32	6.45
Mean % phi+/phi-	181.84	580.13	331.76	465.43	375.39
SEM Mean %phi+/phi-	5.88	65.81	24.72	54.06	105.99
			P values		
36B4		ns (>0.9999)	ns (>0.9999)	ns (>0.9999)	ns (>0.9999)
TTAGGG	ns (>0.9999)		ns (>0.9999)	ns (>0.9999)	ns (>0.9999)
TCAGGG	ns (>0.9999)	ns (>0.9999)		ns (>0.9999)	ns (>0.9999)
TGAGGG	ns (>0.9999)	ns (>0.9999)	ns (>0.9999)		ns (>0.9999)
TAAGGG	ns (>0.9999)	ns (>0.9999)	ns (>0.9999)	ns (>0.9999)	

HeLa					
	36B4	TTAGGG	TCAGGG	TGAGGG	TAAGGG
n	3	3	3	3	3
Mean SQ Phi+	4351.23	158408.39	2678.02	6581.76	305.44
SEM SQ Phi+	125.91	12420.28	293.06	285.35	9.64
Mean SQ Phi-	2764.76	162593.79	1867.49	3933.84	222.87
SEM SQ Phi-	63.89	1575.70	26.65	97.75	16.08
Mean % phi+/phi-	157.38	97.43	143.40	167.31	137.05
SEM Mean %phi+/phi-	5.83	7.70	15.83	8.36	10.79
			P values		
36B4		ns (0.9999)	ns (>0.9999)	ns (>0.9999)	ns (>0.9999)
TTAGGG	ns (0.9999)		ns (>0.9999)	ns (0.9998)	ns (>0.9999)
TCAGGG	ns (>0.9999)	ns (>0.9999)		ns (>0.9999)	ns (>0.9999)
TGAGGG	ns (>0.9999)	ns (0.9998)	ns (>0.9999)		ns (>0.9999)
TAAGGG	ns (>0.9999)	ns (>0.9999)	ns (>0.9999)	ns (>0.9999)	

U2OS					
	36B4	TTAGGG	TCAGGG	TGAGGG	TAAGGG
n	3	3	3	3	3
Mean SQ Phi+	1936.69	7391712.77	5783.35	13951.62	1786.77
SEM SQ Phi+	36.37	474553.61	425.74	1059.84	300.15
Mean SQ Phi-	1502.40	4420640.54	2912.31	8083.07	989.45
SEM SQ Phi-	37.75	216353.19	79.88	233.57	38.69
Mean % phi+/phi-	128.91	167.21	198.58	172.60	180.58
SEM Mean %phi+/phi-	4.04	13.50	15.60	14.03	31.15
			P values		
36B4		ns (>0.9999)	ns (0.9998)	ns (>0.9999)	ns (>0.9999)
TTAGGG	ns (>0.9999)		ns (>0.9999)	ns (>0.9999)	ns (>0.9999)
TCAGGG	ns (0.9998)	ns (>0.9999)		ns (>0.9999)	ns (>0.9999)
TGAGGG	ns (>0.9999)	ns (>0.9999)	ns (>0.9999)		ns (>0.9999)
TAAGGG	ns (>0.9999)	ns (>0.9999)	ns (>0.9999)	ns (>0.9999)	

Saos-2

	36B4	TTAGGG	TCAGGG	TGAGGG	TAAGGG
n	3	3	3	3	3
Mean SQ Phi+	5396.57	65947162.01	63303.28	48046.20	20179.32
SEM SQ Phi+	56.04	3348067.53	3240.18	5400.92	226.76
Mean SQ Phi-	2382.07	622923.87	2560.91	3714.37	321.16
SEM SQ Phi-	19.72	16652.56	44.52	122.99	6.80
Mean % phi+/phi-	226.55	10586.71	2471.91	1293.52	6283.29
SEM Mean %phi+/phi-	3.01	607.43	133.62	151.58	150.69
			P values		
36B4		**** (<0.0001)	**** (<0.0001)	ns (0.0608)	**** (<0.0001)
TTAGGG	**** (<0.0001)		**** (<0.0001)	**** (<0.0001)	**** (<0.0001)
TCAGGG	**** (<0.0001)	**** (<0.0001)		* (0.0287)	**** (<0.0001)
TGAGGG	ns (0.0608)	**** (<0.0001)	* (0.0287)		**** (<0.0001)
TAAGGG	**** (<0.0001)	**** (<0.0001)	**** (<0.0001)	**** (<0.0001)	

Positive Ctrl. [Saos-2]

	36B4	TTAGGG	TCAGGG	TGAGGG	TAAGGG
n	3	3	3	3	3
Mean SQ Phi+	4790.96	132985581.25	103673.21	95874.31	29093.97
SEM SQ Phi+	161.53	7860540.37	14230.52	3709.63	4766.62
Mean SQ Phi-	3295.11	824934.35	3632.54	4756.23	350.01
SEM SQ Phi-	156.74	30128.70	479.70	199.52	32.05
Mean % phi+/phi-	145.40	16120.75	2854.01	2015.76	8312.34
SEM Mean %phi+/phi-	8.48	1120.09	543.61	115.04	1560.17
			P values		
36B4		**** (<0.0001)	**** (<0.0001)	**** (<0.0001)	**** (<0.0001)
TTAGGG	**** (<0.0001)		**** (<0.0001)	**** (<0.0001)	**** (<0.0001)
TCAGGG	**** (<0.0001)	**** (<0.0001)		ns (0.2199)	**** (<0.0001)
TGAGGG	**** (<0.0001)	**** (<0.0001)	ns (0.2199)		**** (<0.0001)
TAAGGG	**** (<0.0001)	**** (<0.0001)	**** (<0.0001)	**** (<0.0001)	

WI38-VA13/2RA

	36B4	TTAGGG	TCAGGG	TGAGGG	TAAGGG
n	3	3	3	3	3
Mean SQ Phi+	5310.52	2063961.22	132608.78	11057.78	1334.17
SEM SQ Phi+	197.54	53911.78	11928.50	762.92	185.73
Mean SQ Phi-	3387.63	1438479.92	74680.65	5651.42	545.15
SEM SQ Phi-	123.95	10407.74	4068.74	321.52	128.04
Mean % phi+/phi-	156.76	143.48	177.57	195.66	244.73
SEM Mean %phi+/phi-	8.18	3.89	18.67	17.50	66.82
			P values		
36B4		ns (0.8965)	ns (0.9956)	ns (0.9524)	ns (0.9883)
TTAGGG	ns (0.8965)		ns (0.9804)	ns (0.999)	ns (0.9905)
TCAGGG	ns (0.9956)	ns (0.9804)		ns (0.9972)	ns (>0.9999)
TGAGGG	ns (0.9524)	ns (0.999)	ns (0.9972)		ns (0.9994)
TAAGGG	ns (0.9883)	ns (0.9905)	ns (>0.9999)	ns (0.9994)	

HT-1080 [PTL]

	36B4	TTAGGG	TCAGGG	TGAGGG	TAAGGG
n	3	3	3	3	3
Mean SQ Phi+	3988.33	234921.92	2360.99	9015.05	346.71
SEM SQ Phi+	137.89	23149.33	57.94	93.04	45.04
Mean SQ Phi-	3025.76	187422.32	1823.92	6477.12	215.76
SEM SQ Phi-	42.56	6822.41	119.32	499.37	43.41
Mean % phi+/phi-	131.81	125.34	129.45	139.18	160.70
SEM Mean %phi+/phi-	4.92	13.17	9.04	10.83	38.48
			P values		
36B4		ns (>0.9999)	ns (>0.9999)	ns (>0.9999)	ns (>0.9999)
TTAGGG	ns (>0.9999)		ns (>0.9999)	ns (>0.9999)	ns (>0.9999)
TCAGGG	ns (>0.9999)	ns (>0.9999)		ns (>0.9999)	ns (>0.9999)
TGAGGG	ns (>0.9999)	ns (>0.9999)	ns (>0.9999)		ns (>0.9999)
TAAGGG	ns (>0.9999)	ns (>0.9999)	ns (>0.9999)	ns (>0.9999)	

HT-1080 hTR wt

	36B4	TTAGGG	TCAGGG	TGAGGG	TAAGGG
n	3	3	3	3	3
Mean SQ Phi+	4060.92	866152.19	2783.82	8108.61	518.24
SEM SQ Phi+	352.97	72667.81	98.52	190.26	25.14
Mean SQ Phi-	3254.85	905153.20	2571.00	7252.92	427.22
SEM SQ Phi-	184.66	68761.54	158.96	109.82	28.05

Mean % phi+/phi-	124.77	95.69	108.28	111.80	121.31
SEM Mean %phi+/phi-	12.95	10.83	7.71	3.12	9.90
			P values		
36B4		ns (>0.9999)	ns (>0.9999)	ns (>0.9999)	ns (>0.9999)
TTAGGG	ns (>0.9999)		ns (>0.9999)	ns (>0.9999)	ns (>0.9999)
TCAGGG	ns (>0.9999)	ns (>0.9999)		ns (>0.9999)	ns (>0.9999)
TGAGGG	ns (>0.9999)	ns (>0.9999)	ns (>0.9999)		ns (>0.9999)
TAAGGG	ns (>0.9999)	ns (>0.9999)	ns (>0.9999)	ns (>0.9999)	

YTBO

	36B4	TTAGGG	TCAGGG	TGAGGG	TAAGGG
n	3	3	3	3	3
Mean SQ Phi+	3945.35	12104128.15	162736.10	1991927.38	11519.49
SEM SQ Phi+	133.54	666065.45	8096.46	52430.82	1710.11
Mean SQ Phi-	2586.61	606967.30	11981.88	94324.17	510.17
SEM SQ Phi-	44.52	13252.18	312.56	7402.41	28.37
Mean % phi+/phi-	152.53	1994.20	1358.19	2111.79	2257.98
SEM Mean %phi+/phi-	5.79	118.06	76.30	174.80	357.96
			P values		
36B4		**** (<0.0001)	* (0.0236)	**** (<0.0001)	**** (<0.0001)
TTAGGG	**** (<0.0001)		ns (0.4966)	ns (0.9983)	ns (0.9632)
TCAGGG	* (0.0236)	ns (0.4966)		ns (0.3215)	ns (0.1613)
TGAGGG	**** (<0.0001)	ns (0.9983)	ns (0.3215)		ns (0.996)
TAAGGG	**** (<0.0001)	ns (0.9632)	ns (0.1613)	ns (0.996)	

Positive Ctrl. [U2OS]

	36B4	TTAGGG	TCAGGG	TGAGGG	TAAGGG
n	3	3	3	3	3
Mean SQ Phi+	9034.22	113447201.30	47443.11	150382.16	24830.89
SEM SQ Phi+	87.77	8697483.86	4999.10	7421.97	2407.09
Mean SQ Phi-	6488.14	15341059.79	7215.56	30071.88	2954.13
SEM SQ Phi-	477.31	966500.47	649.71	933.50	238.19
Mean % phi+/phi-	139.24	739.50	657.51	500.08	840.55
SEM Mean %phi+/phi-	10.33	73.38	91.13	29.16	105.98
			P values		
36B4		ns (0.5544)	ns (0.6864)	ns (0.8921)	ns (0.3954)
TTAGGG	ns (0.5544)		ns (0.9996)	ns (0.9741)	ns (0.9991)
TCAGGG	ns (0.6864)	ns (0.9996)		ns (0.9947)	ns (0.9905)
TGAGGG	ns (0.8921)	ns (0.9741)	ns (0.9947)		ns (0.9109)
TAAGGG	ns (0.3954)	ns (0.9991)	ns (0.9905)	ns (0.9109)	

Negative Ctrl.

	36B4	TTAGGG	TCAGGG	TGAGGG	TAAGGG
n	1 [Phi -] \ 3 [Phi +]	3	3	3	3
Mean SQ Phi+	6.86	2137.36	1022.85	1141.72	58.62
SEM SQ Phi+	2.38	142.18	30.28	27.20	6.22
Mean SQ Phi-	3.46	1677.47	1062.12	960.51	64.21
SEM SQ Phi-	0.00	88.89	62.49	95.08	5.84
Mean % phi+/phi-	198.50	127.42	96.30	118.87	91.28
SEM Mean %phi+/phi-	68.77	10.84	6.34	12.10	12.76
			P values		
36B4		ns (0.9998)	ns (0.999)	ns (0.9996)	ns (0.9988)
TTAGGG	ns (0.9998)		ns (>0.9999)	ns (>0.9999)	ns (>0.9999)
TCAGGG	ns (0.999)	ns (>0.9999)		ns (>0.9999)	ns (>0.9999)
TGAGGG	ns (0.9996)	ns (>0.9999)	ns (>0.9999)		ns (>0.9999)
TAAGGG	ns (0.9988)	ns (>0.9999)	ns (>0.9999)	ns (>0.9999)	

6.2.4. qPCR of TCAGGG and TGAGGG restriction digest products

In order to validate the specificity of the TCAGGG and TGAGGG detection assays, restriction digests were conducted of gDNAs of the cell lines that contained these variants in the highest abundance, WI38-VA13/2RA and YTBO respectively. The used restriction enzymes were

specific for the TCAGGG (LpnPI) and TGAGGG (MnlI and HpHI). Following the digests, their products were used as templates for the respective telomere-variant qPCR assays.

The absolute content of the canonic telomere repeat (TTAGGG) was not significantly changed by the digests in both cell lines (Figure 16A and C). For the absolute TCAGGG variant content in WI38-VA13/2RA the digest with LpnPI did not make a significant difference (Figure 16B) as well. The absolute TGAGGG content was significantly reduced by both digestions, whereas the MnlI digest significantly reduced the absolute variant even more than the HpHI digest (Figure 16D).

To sum this up, the restriction enzymes were specific for their respective variant and did not lead to a reduction in TTAGGG content. The TCAGGG assay did not react to a reduction in variant content, or the restriction digest did not work. The TGAGGG assay specifically reacted to a reduction in variant content and the restriction enzyme MnlI was the most potent enzyme for the digestion of this variant.

The assays' abilities to detect clusters of variant repeats will be tested in the next chapter.

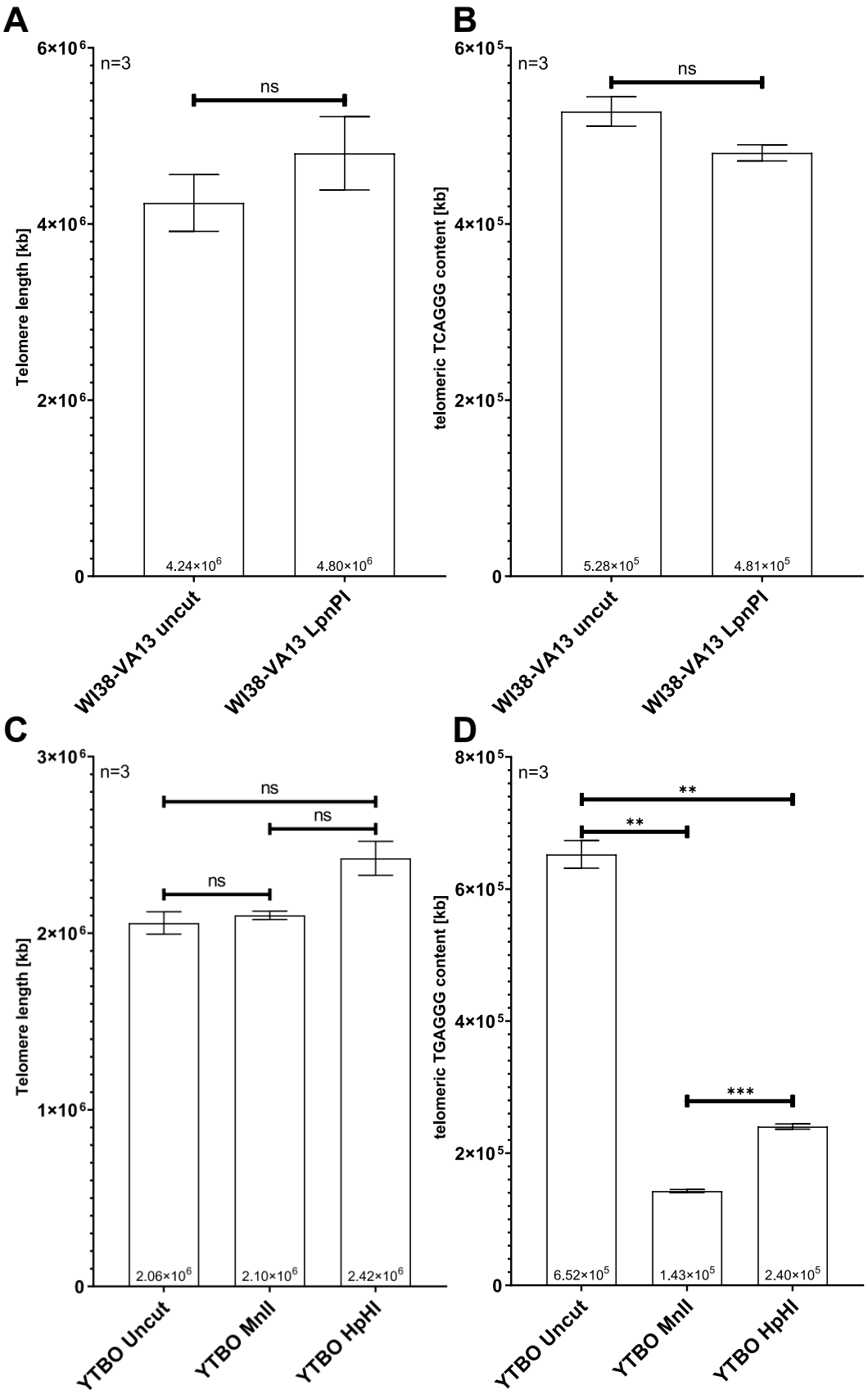

Figure 16: Comparison of the telomere repeat and NCTR SQs ± SEM from qPCRs of gDNAs of two ALT-positive cell lines after digestion with restriction enzymes specific for two NCTRs. A: Comparison of telomeric repeat SQs of WI38-VA13/2RA gDNA after

TCAGGG-specific LpnPI digestion and undigested WI38-VA12/2RA gDNA. B: Comparison of TCAGGG repeat SQs of WI38-VA13/2RA gDNA after TCAGGG-specific LpnPI digestion and undigested WI38-VA12/2RA gDNA. C: Comparison of telomeric repeat SQs of YTBO gDNA after TGAGGG-specific MnlI or HpHI digestion and undigested YTBO gDNA. D: Comparison of TGAGGG repeat SQs of YTBO gDNA after TGAGGG-specific MnlI or HpHI digestion and of undigested YTBO gDNA. N = 3 technical replicates. Statistics can be found in Table 33 and Table 34. Raw data can be found in Table 61.

Table 33: Statistics (Unpaired t-tests with Welch's correction) comparing the TTAGGG and TCAGGG SQs of uncut and LpnPI digested WI38-VA13/2RA gDNA (See Figure 16, Panel A and B).

WI38-VA13/2RA TTAGGG		
	Uncut	LpnPI
Mean SQ	4 239 192.55	4 802 940.84
SEM SQ	322 814.91	415 914.32
n	3	3
	P values	
Uncut		ns (0.7519)

WI38-VA13/2RA TCAGGG		
	Uncut	LpnPI
Mean SQ	527 707.76	480 813.57
SEM SQ	16 759.31	9 193.31
n	3	3
	P values	
Uncut		ns (0.0886)

Table 34: Statistics (Brown-Forsythe and Welch ANOVA test with Games-Howell's multiple comparisons follow-up test) comparing the TTAGGG and TGAGGG SQs of uncut, MnlI and HpHI digested YTBO gDNA (See Figure 16, Panel C and D).

YTBO TTAGGG			
	Uncut	MnlI	HpHI
Mean SQ TTAGGG	2 057 965.98	2 101 097.47	2 424 143.84
SEM SQ	63 345.25	23 761.16	96 327.58
n	3	3	3
		P values	
Uncut		ns (0.1298)	ns (0.8137)
MnlI	ns (0.1298)		ns (0.0839)
HpHI	ns (0.8137)	ns (0.0839)	

YTBO TGAGGG			
	Uncut	MnlI	HpHI
Mean SQ TGAGGG	652 441.38	142 714.16	240 414.77
SEM SQ	20 823.76	2 424.75	3 982.84
n	3	3	3
		P values	
Uncut		** (0.0021)	** (0.0034)
MnlI	** (0.0021)		*** (0.0003)
HpHI	** (0.0034)	*** (0.0003)	

6.2.5. TCAGGG cluster variant DNA oligomer qPCR

After probing the specificity of the TCAGGG and TGAGGG detection assays, the ability of the TCAGGG assay was tested to detect variant clusters. For this several DNA oligomers with different TCAGGG content and orientation (see Table 6) were used as templates for the qPCR assay.

In summary, it was shown that the longer the variant cluster is, the harder it gets to detect by the assay. Only clusters with a length of two are as easy to detect as single hexamers. However, the assay can still detect clusters of up to eight variant repeats down to 1000 molecules when the variants are in the middle of the primer-flanked DNA region (Figure 17A and Table 35). It also was shown that it is easier for the assay to detect variant repeats when they are closer to the 5' end of the probed strand. Variants closer to the 3' end get harder to detect (Figure 17B and Table 36). The results will be described in more detail in the following section.

The cluster length (Figure 17A) made a significant difference in detectability for all molecule amounts. In the highest molecule amount (10^8) all clusters except the one containing two hexamers were significantly harder to detect than the single variant. The detectability got significantly worse for every step of TCAGGG hexamer addition. At 10^7 molecules the same was observed. For 10^6 molecules, a similar result as in the previous two groups was observed. For 10^5 molecules all clusters were harder to detect than a single variant repeat. Clusters with a length of two hexamers were not significantly easier to detect than clusters containing four hexamers. At 10^4 molecules, the same pattern as at 10^6 molecules was observed.

The cluster orientation made a significant difference for all molecule amounts (Figure 17B). The oligo with the seven variants closer to the 5' end (Telg-C_7xL) was significantly easier to detect in all cases. When comparing the orientation oligos with those of different lengths (See Table 35), the Telg-C_7xL oligo was as easy to detect as the Telg-C_4x oligo for all molecule amounts. For the lowest molecule amount (10^4), the Telg-C_7xL mean CT was also not significantly different from the mean CT of Telg-C_8x in addition to the CTs of Telg-C_4x, so the Telg-C_7xL detectability was in between the detectability of these two oligos without a distinct differentiation. Telg-C_7xR was as hard to detect as the Telg-C_8x oligo in all molecule amounts except for 10^5 molecules where its detectability was significantly worse.

In order to see, if the oligos were all in the assay's detectable range, the CTs of all oligos at all molecule amounts were compared to the NTC CTs (Figure 17 and Table 36). It was observed that the CTs of all oligos at all molecule amounts significantly differed from the NTC except the average CT of the Telg-C_7xR oligo at the lowest molecule amount. Thus, it was just at the

border of the detectable range with an average CT ± SD of 28.49±0.74 vs. the NTC's 28.75±0.16.

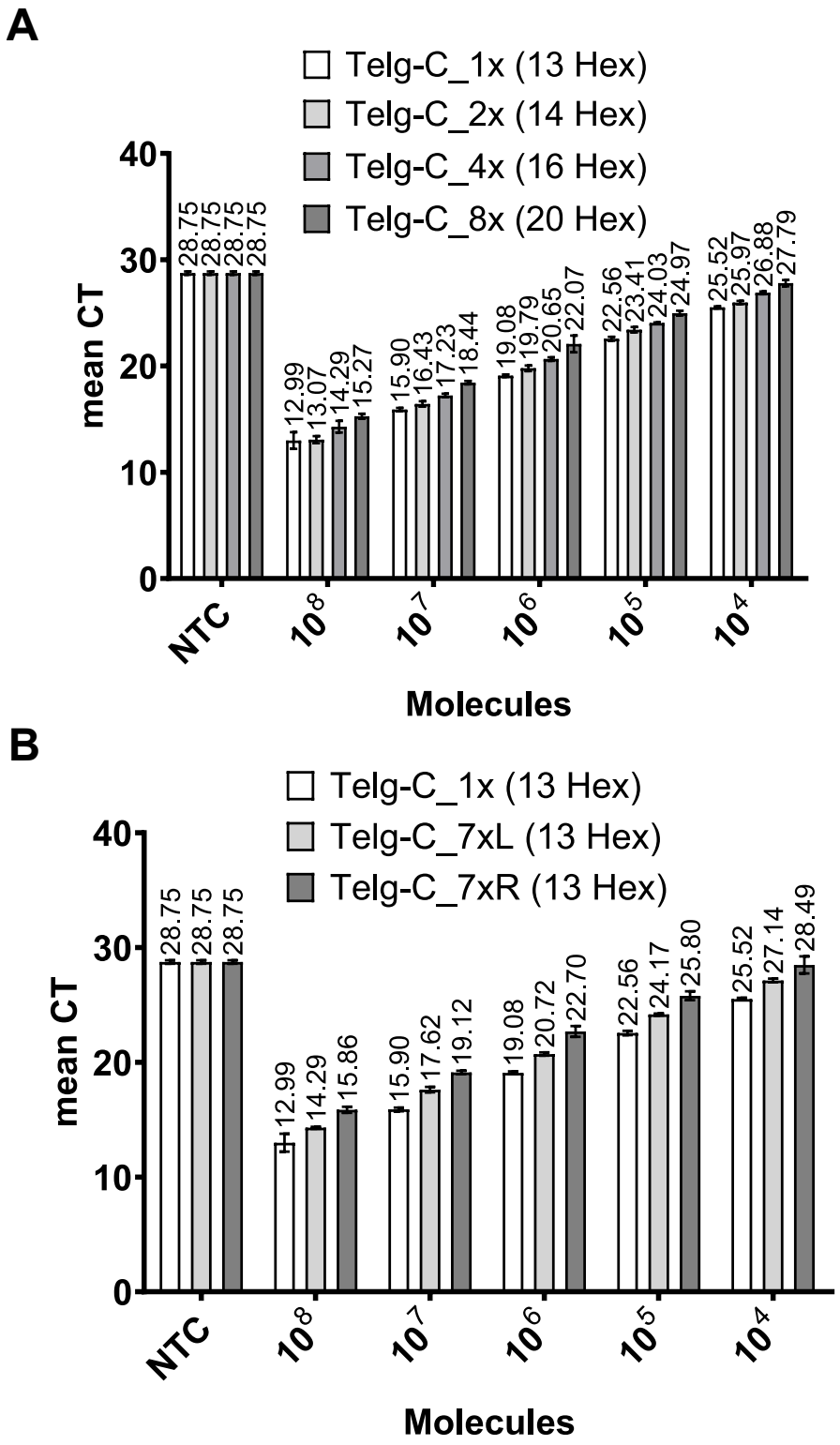

Figure 17: Average CT ± SD of TCAGGG cluster variant DNA oligomers and the NTC detected by qPCR. A: Comparison of TCAGGG cluster variant DNA oligomers of different cluster lengths. B: Comparison of TCAGGG cluster variant DNA oligomers of different

orientations. N = 3 technical replicates, Statistics can be found in Table 35 and Table 36. Raw data can be found in Table 62.

Table 35: Statistics (two-way ANOVA with Tukey's multiple comparisons follow-up test) of the CTs of TCAGGG cluster variant DNA oligomers detected by qPCR (See Figure 17) comparing the CTs of all variants.

10^8 molecules						
	Telg-C_1x	Telg-C_2x	Telg-C_4x	Telg-C_8x	Telg-C_7xL	Telg-C_7xR
n	3	3	3	3	3	3
Mean CT	12.99	13.07	14.29	15.27	14.29	15.86
SD	0.78	0.34	0.55	0.23	0.08	0.26
Telg-C_1x		ns (0.9996)	**** (<0.0001)	**** (<0.0001)	**** (<0.0001)	**** (<0.0001)
Telg-C_2x	ns (0.9996)		**** (<0.0001)	**** (<0.0001)	**** (<0.0001)	**** (<0.0001)
Telg-C_4x	**** (<0.0001)	**** (<0.0001)		** (0.0021)	ns (>0.9999)	**** (<0.0001)
Telg-C_8x	**** (<0.0001)	**** (<0.0001)	** (0.0021)		** (0.0023)	ns (0.1795)
Telg-C_7xL	**** (<0.0001)	**** (<0.0001)	ns (>0.9999)	** (0.0023)		**** (<0.0001)
Telg-C_7xR	**** (<0.0001)	**** (<0.0001)	**** (<0.0001)	ns (0.1795)	**** (<0.0001)	

10^7 molecules						
	Telg-C_1x	Telg-C_2x	Telg-C_4x	Telg-C_8x	Telg-C_7xL	Telg-C_7xR
n	3	3	3	3	3	3
Mean CT	15.90	16.43	17.23	18.44	17.62	19.12
SD	0.09	0.15	0.10	0.09	0.13	0.09
Telg-C_1x		ns (0.2702)	**** (<0.0001)	**** (<0.0001)	**** (<0.0001)	**** (<0.0001)
Telg-C_2x	ns (0.2702)		* (0.0227)	**** (<0.0001)	*** (0.0001)	**** (<0.0001)
Telg-C_4x	**** (<0.0001)	* (0.0227)		**** (<0.0001)	ns (0.615)	**** (<0.0001)
Telg-C_8x	**** (<0.0001)	**** (<0.0001)	**** (<0.0001)		* (0.0167)	ns (0.0778)
Telg-C_7xL	**** (<0.0001)	*** (0.0001)	ns (0.615)	* (0.0167)		**** (<0.0001)
Telg-C_7xR	**** (<0.0001)	**** (<0.0001)	**** (<0.0001)	ns (0.0778)	**** (<0.0001)	

10^6 molecules						
	Telg-C_1x	Telg-C_2x	Telg-C_4x	Telg-C_8x	Telg-C_7xL	Telg-C_7xR
n	3	3	3	3	3	2
Mean CT	19.08	19.79	20.65	22.07	20.72	22.70
SD	0.07	0.15	0.10	0.46	0.08	0.34
Telg-C_1x		ns (0.0618)	**** (<0.0001)	**** (<0.0001)	**** (<0.0001)	**** (<0.0001)
Telg-C_2x	ns (0.0618)		* (0.0104)	**** (<0.0001)	** (0.0043)	**** (<0.0001)
Telg-C_4x	**** (<0.0001)	* (0.0104)		**** (<0.0001)	ns (0.9997)	**** (<0.0001)
Telg-C_8x	**** (<0.0001)	**** (<0.0001)	**** (<0.0001)		**** (<0.0001)	ns (0.2285)
Telg-C_7xL	**** (<0.0001)	** (0.0043)	ns (0.9997)	**** (<0.0001)		**** (<0.0001)
Telg-C_7xR	**** (<0.0001)	**** (<0.0001)	**** (<0.0001)	ns (0.2285)	**** (<0.0001)	

10^5 molecules						
	Telg-C_1x	Telg-C_2x	Telg-C_4x	Telg-C_8x	Telg-C_7xL	Telg-C_7xR
n	3	3	3	3	3	3
Mean CT	22.56	23.41	24.03	24.97	24.17	25.80
SD	0.11	0.15	0.04	0.13	0.05	0.22
Telg-C_1x		* (0.0117)	**** (<0.0001)	**** (<0.0001)	**** (<0.0001)	**** (<0.0001)
Telg-C_2x	* (0.0117)		ns (0.1315)	**** (<0.0001)	* (0.0341)	**** (<0.0001)
Telg-C_4x	**** (<0.0001)	ns (0.1315)		** (0.0041)	ns (0.9936)	**** (<0.0001)
Telg-C_8x	**** (<0.0001)	**** (<0.0001)	** (0.0041)		* (0.0219)	* (0.0161)
Telg-C_7xL	**** (<0.0001)	* (0.0341)	ns (0.9936)	* (0.0219)		**** (<0.0001)
Telg-C_7xR	**** (<0.0001)	**** (<0.0001)	**** (<0.0001)	* (0.0161)	**** (<0.0001)	

10^4 molecules						
	Telg-C_1x	Telg-C_2x	Telg-C_4x	Telg-C_8x	Telg-C_7xL	Telg-C_7xR
n	2	3	3	3	3	2
Mean CT	25.52	25.97	26.88	27.79	27.14	28.49
SD	0.07	0.09	0.08	0.17	0.09	0.53
Telg-C_1x		ns (0.5783)	**** (<0.0001)	**** (<0.0001)	**** (<0.0001)	**** (<0.0001)
Telg-C_2x	ns (0.5783)		** (0.0053)	**** (<0.0001)	*** (0.0002)	**** (<0.0001)
Telg-C_4x	**** (<0.0001)	** (0.0053)		** (0.0058)	ns (0.9077)	**** (<0.0001)
Telg-C_8x	**** (<0.0001)	**** (<0.0001)	** (0.0058)		ns (0.0972)	ns (0.137)
Telg-C_7xL	**** (<0.0001)	*** (0.0002)	ns (0.9077)	ns (0.0972)		**** (<0.0001)
Telg-C_7xR	**** (<0.0001)	**** (<0.0001)	**** (<0.0001)	ns (0.137)	**** (<0.0001)	

Table 36: Statistics (two-way ANOVA with Dunnett's multiple comparisons follow-up test) of the CTs of TCAGGG cluster variant DNA oligomers detected by qPCR (See Figure 17) comparing the CTs of each variant to the NTC.

				Telg-C_1x (13 Hex)				
				10^8	10^7	10^6	10^5	10^4
			n	3	3	3	3	2
			Mean CT	12.99	15.90	19.08	22.56	25.52
	n	Mean CT	SD	0.78	0.16	0.12	0.19	0.11
NTC	3	28.75	0.16	**** (<0,0001)	**** (<0,0001)	**** (<0,0001)	**** (<0,0001)	**** (<0,0001)
				Telg-C_2x (14 Hex))				
				10^8	10^7	10^6	10^5	10^4
			n	3	3	3	3	3
			Mean CT	13.07	16.43	19.79	23.41	25.97
	n	Mean CT	SD	0.34	0.26	0.27	0.25	0.16
NTC	3	28.75	0.16	**** (<0,0001)	**** (<0,0001)	**** (<0,0001)	**** (<0,0001)	**** (<0,0001)
				Telg-C_4x (16 Hex)				
				10^8	10^7	10^6	10^5	10^4
			n	3	3	3	3	3
			Mean CT	14.29	17.23	20.65	24.03	26.88
	n	Mean CT	SD	0.55	0.17	0.17	0.08	0.14
NTC	3	28.75	0.16	**** (<0,0001)	**** (<0,0001)	**** (<0,0001)	**** (<0,0001)	**** (<0,0001)
				Telg-C_8x (20 Hex)				
				10^8	10^7	10^6	10^5	10^4
			n	3	3	3	3	3
			Mean CT	15.27	18.44	22.07	24.97	27.79
	n	Mean CT	SD	0.23	0.16	0.79	0.23	0.30
NTC	3	28.75	0.16	**** (<0,0001)	**** (<0,0001)	**** (<0,0001)	**** (<0,0001)	** (0,0012)
				Telg-C_7xL (13 Hex)				
				10^8	10^7	10^6	10^5	10^4
			n	3	3	3	3	3
			Mean CT	14.29	17.62	20.72	24.17	27.14
	n	Mean CT	SD	0.08	0.23	0.14	0.09	0.16
NTC	3	28.75	0.09	**** (<0,0001)	**** (<0,0001)	**** (<0,0001)	**** (<0,0001)	**** (<0,0001)
				Telg-C_7x R (13 Hex)				
				10^8	10^7	10^6	10^5	10^4
			n	3	3	2	3	2
			Mean CT	15.86	19.12	22.70	25.80	28.49
	n	Mean CT	SD	0.26	0.15	0.47	0.39	0.74
NTC	3	28.75	0.16	**** (<0,0001)	**** (<0,0001)	**** (<0,0001)	**** (<0,0001)	ns (0,8192)

In order to complement and validate the qPCR variant detection assay results, telomer-variant FISH experiments were conducted. The results of these experiments are presented in the next chapter.

6.3. Telomere-variant FISH

For validation of the qPCR results, multiple telomere-variant FISH experiments were conducted with varying success. It was only possible to detect the TCAGGG variant because there were no specific signals for the TGAGGG variant (Figure 18E). The results of the two more or less successful experiments for TCAGGG detection are presented in this chapter. Due to those struggles, the method was not applied to the remaining cell lines.

In summary, it must be said, that the application of this method was not successful. It was only possible to quantify the TCAGGG variant (Figure 18, Figure 19, Table 37 and Table 38) but with poor reproducibility (Figure 19 and Table 39). These quantifications offered results that greatly diverged from qPCR and WGS data. The results will be described in detail in the next sections.

In the first experiment (Figure 18, Table 37), WI38-VA13/2RA cells showed the most and significantly less TCAGGG spots/cell. YTBO cells contained significantly more TTAGGG spots/cell which was significantly higher than their TCAGGG content but also significantly fewer than in WI38-VA13/2RA. The TCAGGG content was substantially and significantly lower in YTBO compared to WI38-VA13/2RA (Figure 18A). The spot sizes of TTAGGG and TCAGGG were significantly different from each other in both cell lines (Figure 18B), although the difference in WI38-VA13/2RA was much smaller than in YTBO. The differences comparing the average spot size for the two separate targets between the two cell lines were also significant. The smaller size of the TCAGGG signals in YTBO could also be seen while inspecting the microscopical images by eye in Figure 18E. When looking at the signal intensity of the spots, the average intensity ± SD was nearly the same for TTAGGG in WI38-VA13/2RA, although the difference was still statistically significant but with a comparably high p-value of 0.0151. All the other differences in intensity had p-values <0.0001. In YTBO the statistically significant difference in signal intensity was more striking, with the TTAGGG spots having an average intensity ± SD of 126.50±88.34 and TCAGGG spots' average intensity being 183.80±70.70. When comparing the targets' spot intensity between the two cell lines statistical differences were found in all four cases. To have a comparable metric to the two other methods of variant detection mentioned in this study, WGS and the qPCR assay, the percentages of the TCAGGG spots compared to the TTAGGG spots, the baseline, were calculated. These are presented in Figure 18D. The TCAGGG percentages were much higher in this FISH experiment than in the qPCR (Figure 9B) and WGS data (Lee et al., 2014: WI38-VA13/2RA

only). To test the reproducibility of this data, a second telomere-variant FISH experiment was conducted which is described below.

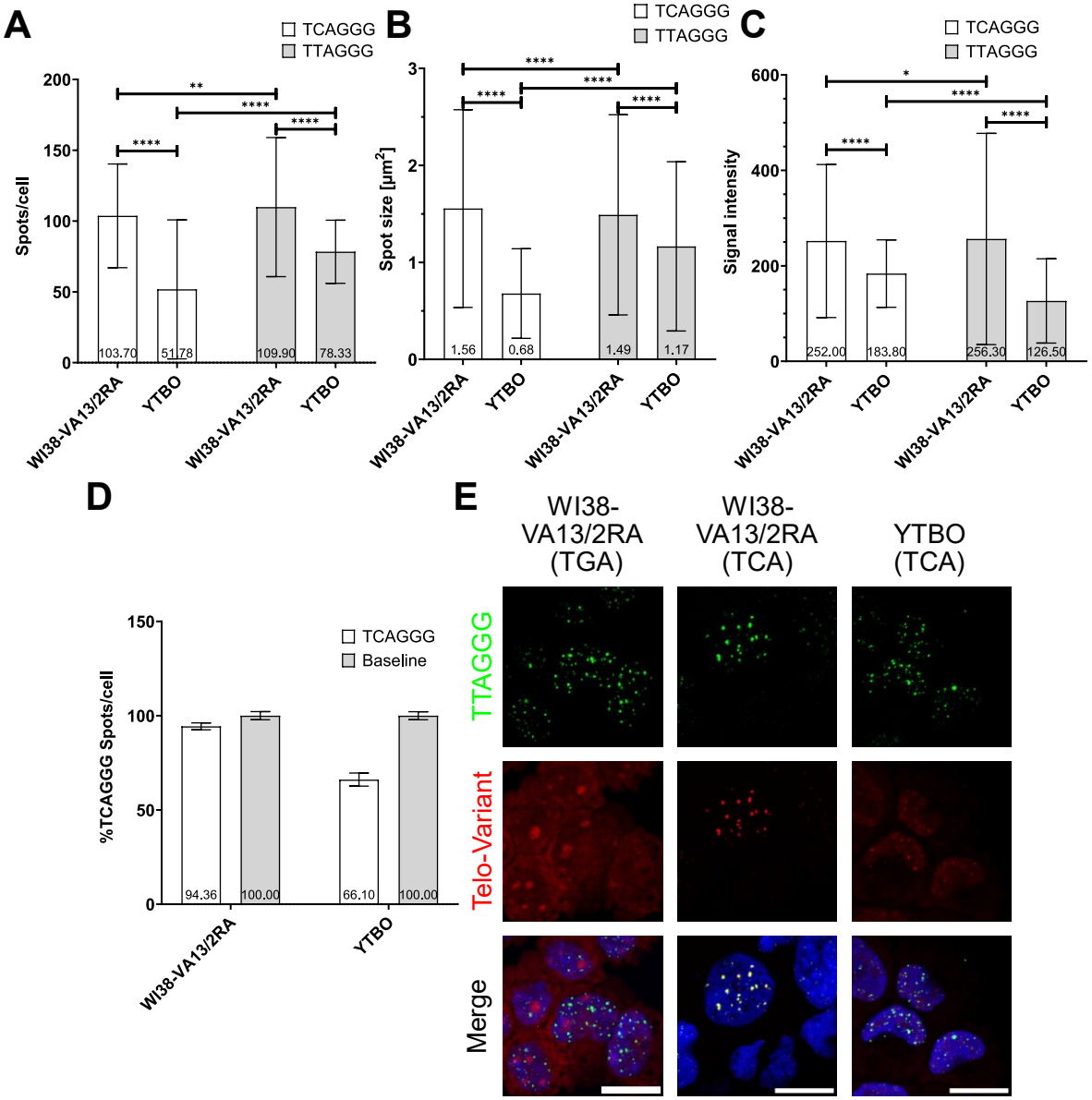

Figure 18: Quantification of the first telomere-variant FISH experiment (no technical replicates). A: Comparison of the mean TTTAGGG- and TCAGGG-spots per cell ± SD of the cell lines WI38-VA13/2RA and YTBO. B: Comparison of the mean area of TTTAGGG- and TCAGGG-spots ± SD in the analyzed cell lines. C: Comparison of the mean TTAGGG- and TCAGGG-Spot signal intensity ± SD of the analyzed cell line. D: Microscopical confocal spinning disc images at 600x magnification of two ALT-positive cell lines (WI38-VA13/2RA and YTBO) stained using FITC labeled TelC PNA probes for canonical telomere repeat detection,

one of two different ATTO-633 labeled PNA probes for TGAGGG, respectively TCAGGG detection and DAPI for nuclear staining. Scale bar: 20 µm. Statistics can be found in Table 37.

Table 37: Statistics (two-way ANOVA with Sidak's multiple comparisons follow-up tests) of the TTAGGG and TCAGGG-spots per cell, spot size and spot signal intensity quantification of the first telomere variant-FISH experiment (See Figure 18) comparing the cell lines and the targets.

Spots/cell					
		Wi-38-VA13/2RA		YTBO	
	Target	TCAGGG	TTAGGG	TCAGGG	TTAGGG
	Mean Spots/cell	103.70	109.90	51.78	78.33
	SD	36.61	49.10	49.07	22.29
	n	857	857	356	356
	Range	316.50	382.40	179.20	166.60
	Target	p-values			
Wi-38-VA13/2RA	TCAGGG		** (0.0044)	**** (<0.0001)	
	TTAGGG	** (0.0044)			**** (<0.0001)
YTBO	TCAGGG	**** (<0.0001)			**** (<0.0001)
	TTAGGG		**** (<0.0001)	**** (<0.0001)	

Spot size					
		Wi-38-VA13/2RA		YTBO	
	Target	TCAGGG	TTAGGG	TCAGGG	TTAGGG
	Mean Spot size [µm2]	1.56	1.49	0.68	1.17
	SD	1.02	1.03	0.46	0.87
	n	22418	30541	1117	10255
	Target	p-values			
Wi-38-VA13/2RA	TCAGGG		**** (<0.0001)	**** (<0.0001)	
	TTAGGG	**** (<0.0001)			**** (<0.0001)
YTBO	TCAGGG	**** (<0.0001)			**** (<0.0001)
	TTAGGG		**** (<0.0001)	**** (<0.0001)	

Signal intensity spots					
		Wi-38-VA13/2RA		YTBO	
	Target	TCAGGG	TTAGGG	TCAGGG	TTAGGG
	Mean Signal intensity spots	252.00	256.30	183.80	126.50
	SD	160.40	221.20	70.70	88.34
	n	22418	30541	1117	10255
	Target	p-values			
Wi-38-VA13/2RA	TCAGGG		* (0.0151)	**** (<0.0001)	
	TTAGGG	* (0.0151)			**** (<0.0001)
YTBO	TCAGGG	**** (<0.0001)			**** (<0.0001)
	TTAGGG		**** (<0.0001)	**** (<0.0001)	

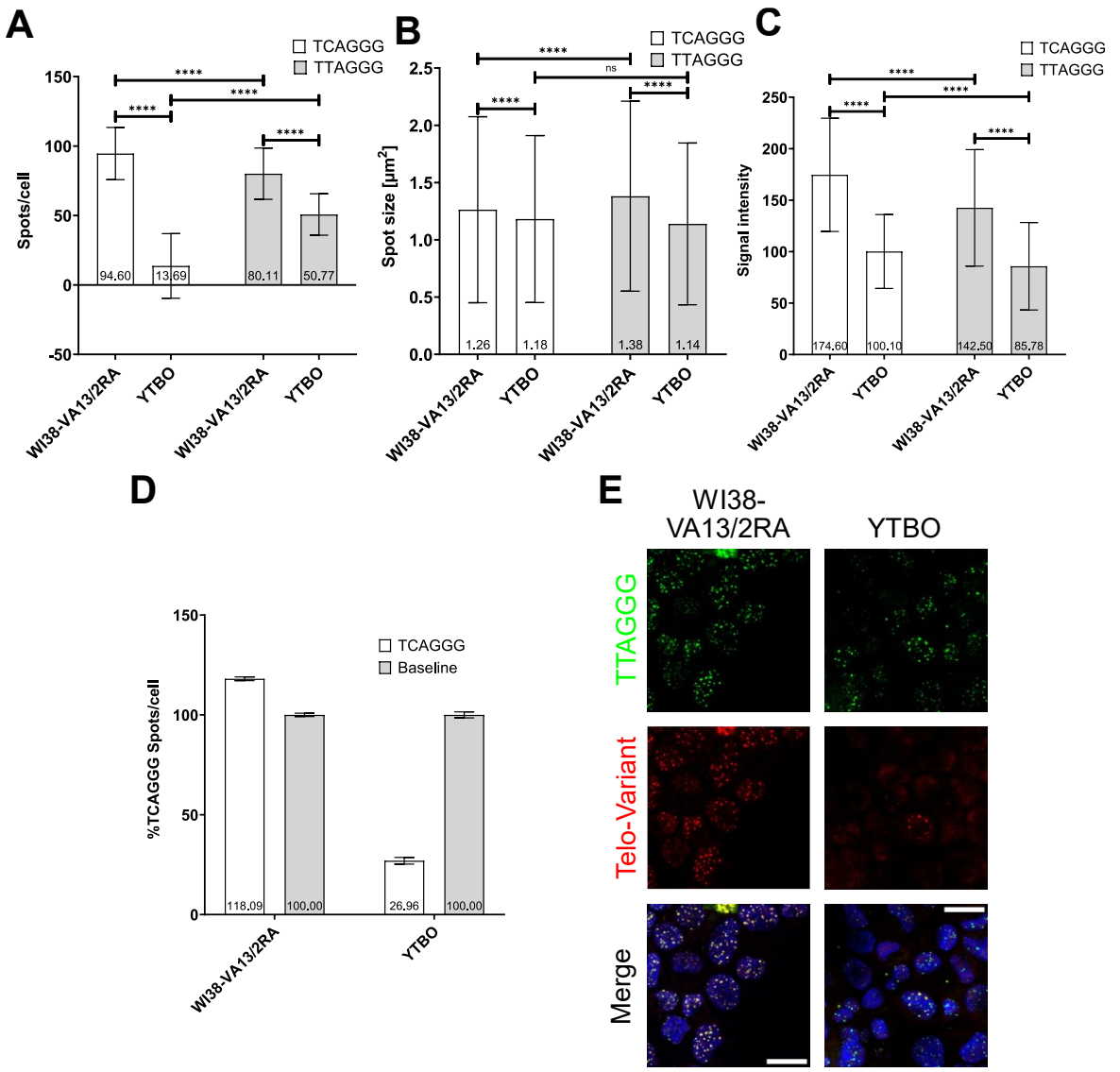

Figure 19: Quantification of the second telomere-variant FISH experiment (no technical replicates). A: Comparison of the mean TTTAGGG- and TCAGGG-spots per cell ± SD of the cell lines WI38-VA13/2RA and YTBO. B: Comparison of the mean area of TTTAGGG- and TCAGGG-spots ± SD in the analyzed cell lines. C: Comparison of the mean TTAGGG- and TCAGGG-Spot signal intensity ± SD of the analyzed cell line. D: Microscopical confocal spinning disc images at 400x magnification of two ALT-positive cell lines (WI38-VA13/2RA and YTBO) stained using FITC labeled TelC PNA probes for canonical telomere repeat detection, Cy3 labeled PNA probes for TCAGGG detection and DAPI for nuclear staining. Scale bar: 20 µm. Statistics can be found in Table 38.

In the second telomere-variant FISH experiment (Figure 19, Table 38), surprisingly, the number of average TCAGGG spots per cell was significantly higher than the number of TTAGGG spots in WI38-VA13/2RA cells. In YTBO cells TTAGGG spots were significantly more abundant than TCAGGG spots. When comparing the two cell lines, WI38-VA13/2RA

contained significantly more spots of both kinds than YTBO (Figure 19A). When looking at the average spot sizes (Figure 19B), the results were more uniform than in the first experiment, but there still were significant differences between the TTAGGG and TCAGGG spots in WI38-VA13/2RA. In YTBO the difference between the average sizes of TTAGGG and TCAGGG spots was not significant. The average sizes of both kinds of spots were significantly larger in WI38-VA13/2RA. In terms of average signal intensity (Figure 19C), there were significant differences between both kinds of spots in both cell lines and when comparing them between the cell lines. The highest average intensity ± SD was observed in TCAGGG spots followed by TTAGGG spots in WI38-VA13/2RA. Next in line, there were the TCAGGG spots in YTBO. The weakest average signals were observed in TTAGGG spots in YTBO. When looking at the TCAGGG spot percentages in this experiment (Figure 19D), it was observed that it was even higher in WI38-VA13/2RA cells than compared to the first experiment with a value of 118.09%. In YTBO the percentage of TCAGGG spots was 26.96%, which is closer to the qPCR results than in the first experiment.

When comparing both experiments (Figure 20, Table 39) the average number of spots/cell (Panel A) was significantly higher in the first experiment for both kinds of spots in both cell lines. In terms of spot size (Panel B), the only kind of spots that did not differ in average size significantly between the two experiments were the TCAGGG spots in YTBO. The TTAGGG spots were on average significantly smaller in the first experiment in this cell line. In WI38-VA13/2RA both species of spots were on average significantly larger in the first experiment. Regarding signal intensity, the same pattern as in the amounts of spots/cell was observed. The intensities of both kinds of spots were significantly higher in the first experiment in both cell lines. As mentioned before, the percentage of the TCAGGG spots compared to TTAGGG was higher in the second experiment in WI38-VA13/2RA. In YTBO it was the other way around.

Table 38: Statistics (two-way ANOVA with Sidak's multiple comparisons follow-up tests) of the TTAGGG and TCAGGG-spots per cell, spot size and spot signal intensity quantification of the second telomere variant-FISH experiment (See Figure 19) comparing the cell lines and the targets.

Spots/cell					
		Wi-38-VA13/2RA		YTBO	
	Target	TCAGGG	TTAGGG	TCAGGG	TTAGGG
	Mean Spots/cell	94.60	80.11	13.69	50.77
	SD	18.81	18.45	23.27	14.93
	n	1526	1526	771	771
	Range	170.00	195.50	107.20	138.40
	Target	p-values			
Wi-38-VA13/2RA	TCAGGG		**** (<0.0001)	**** (<0.0001)	
	TTAGGG	**** (<0.0001)			**** (<0.0001)
YTBO	TCAGGG	**** (<0.0001)			**** (<0.0001)
	TTAGGG		**** (<0.0001)	**** (<0.0001)	

Spot size					
		Wi-38-VA13/2RA		YTBO	
	Target	TCAGGG	TTAGGG	TCAGGG	TTAGGG
	Mean Spot size [µm2]	1.38	1.26	1.14	1.18
	SD	0.83	0.81	0.71	0.73
	n	27053	29353	608	10922
	Target	p-values			
Wi-38-VA13/2RA	TCAGGG		**** (<0.0001)	**** (<0.0001)	
	TTAGGG	**** (<0.0001)			**** (<0.0001)
YTBO	TCAGGG	**** (<0.0001)			ns (0.3771)
	TTAGGG		**** (<0.0001)	ns (0.3771)	

Signal intensity spots					
		Wi-38-VA13/2RA		YTBO	
	Target	TCAGGG	TTAGGG	TCAGGG	TTAGGG
	Mean Signal intensity spots	174.60	142.50	100.10	85.78
	SD	55.03	56.60	35.86	42.47
	n	27053	29353	608	10922
	Target	p-values			
Wi-38-VA13/2RA	TCAGGG		**** (<0.0001)	**** (<0.0001)	
	TTAGGG	**** (<0.0001)			**** (<0.0001)
YTBO	TCAGGG	**** (<0.0001)			**** (<0.0001)
	TTAGGG		**** (<0.0001)	**** (<0.0001)	

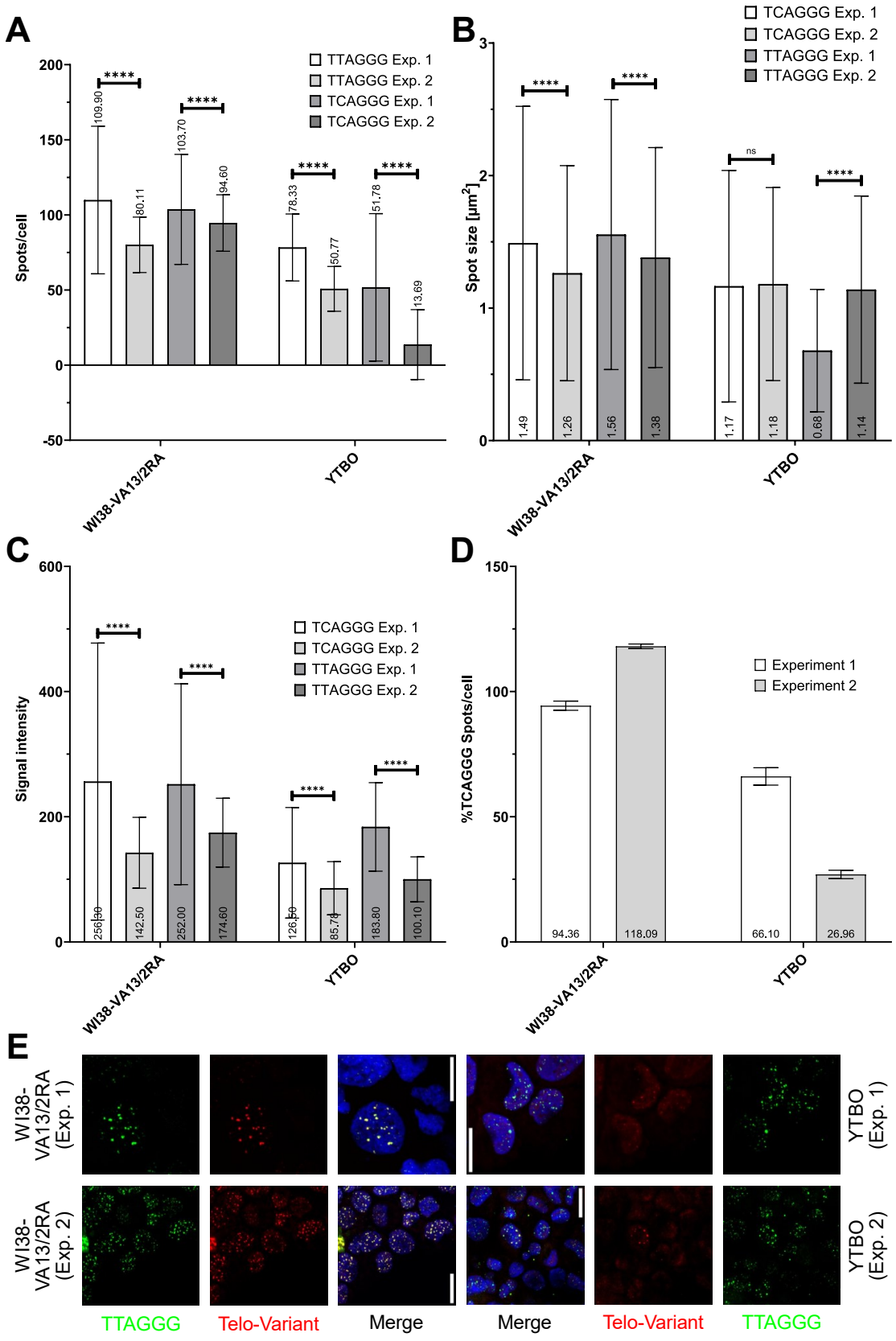

Figure 20: Comparison of the first and second telomere-variant FISH experiment. A: Comparison of the mean TTTAGGG- and TCAGGG-spots per cell ± SD of the cell lines WI38-VA13/2RA and YTBO from both experiments. B: Comparison of the mean area of TTTAGGG- and TCAGGG-spots ± SD in the analyzed cell lines from both experiments. C: Comparison of

the mean TTAGGG- and TCAGGG-Spot signal intensity ± SD of the analyzed cell lines from both experiments. D: Microscopical confocal spinning disc images at 600x (Exp.1.), respectively 400x (Exp. 2.) magnification of two ALT-positive cell lines (WI38-VA13/2RA and YTBO) from Experiment 1 and 2, stained using FITC labeled TelC PNA probes for canonical telomere repeat detection, Cy3 labeled PNA probes for TCAGGG detection and DAPI for nuclear staining. Scale bar: 20 µm. Statistics can be found in Table 39.

Table 39: Statistics (two-way ANOVA with Tukey's multiple comparisons follow-up tests) of the TTAGGG and TCAGGG-spots per cell, spot size and spot signal intensity quantification of the first and second telomere variant-FISH experiment (See Figure 20) comparing the cell lines and the targets of the two experiments.

Spots/cell

			Wi-38-VA13/2RA				YTBO			
		Experiment	1		2		1		2	
		Target	TCAGGG	TTAGGG	TCAGGG	TTAGGG	TCAGGG	TTAGGG	TCAGGG	TTAGGG
		Mean Spots/cell	103.70	109.90	94.60	80.11	51.78	78.33	13.69	50.77
		SD	36.61	49.10	18.81	18.45	49.07	22.29	23.27	14.93
		n	857	857	1526	1526	356	356	771	771
	Experiment	Target	p-values							
Wi-38-VA13/2RA	1	TCAGGG		**** (<0.0001)	**** (<0.0001)	**** (<0.0001)				
		TTAGGG	**** (<0.0001)		**** (<0.0001)	**** (<0.0001)				
	2	TCAGGG	**** (<0.0001)	**** (<0.0001)		**** (<0.0001)				
		TTAGGG	**** (<0.0001)	**** (<0.0001)	**** (<0.0001)					
YTBO	1	TCAGGG						**** (<0.0001)	**** (<0.0001)	ns (0.9482)
		TTAGGG					**** (<0.0001)		**** (<0.0001)	**** (<0.0001)
	2	TCAGGG					**** (<0.0001)	**** (<0.0001)		**** (<0.0001)
		TTAGGG					ns (0.9482)	**** (<0.0001)	**** (<0.0001)	

Spot size

			Wi-38-VA13/2RA				YTBO			
		Experiment	1		2		1		2	
		Target	TCAGGG	TTAGGG	TCAGGG	TTAGGG	TCAGGG	TTAGGG	TCAGGG	TTAGGG
		Mean Spot size [µm2]	1.56	1.49	1.26	1.38	0.68	1.17	1.18	1.14
		SD	1.02	1.03	0.81	0.83	0.46	0.87	0.73	0.71
		n	22418	30541	29353	27053	1117	10255	10922	608
	Experiment	Target	p-values							
Wi-38-VA13/2RA	1	TCAGGG		**** (<0.0001)	**** (<0.0001)	**** (<0.0001)				
		TTAGGG	**** (<0.0001)		**** (<0.0001)	**** (<0.0001)				

YTBO	2	TCAGGG		**** (<0.0001)	**** (<0.0001)		**** (<0.0001)			
		TTAGGG		**** (<0.0001)	**** (<0.0001)	**** (<0.0001)				
	1	TCAGGG						**** (<0.0001)	**** (<0.0001)	**** (<0.0001)
		TTAGGG					**** (<0.0001)		ns (0.9011)	ns (0.5705)
	2	TCAGGG					**** (<0.0001)	ns (0.9011)		ns (0.6798)
		TTAGGG					**** (<0.0001)	ns (0.5705)	ns (0.6798)	

Signal intensity spots

		Experiment	Wi-38-VA13/2RA				YTBO			
			1		2		1		2	
		Target	TCAGGG	TTAGGG	TCAGGG	TTAGGG	TCAGGG	TTAGGG	TCAGGG	TTAGGG
		Mean Signal intensity spots	252.00	256.30	174.60	142.50	183.80	126.50	100.10	85.78
		SD	160.40	221.20	55.03	56.60	70.70	88.34	35.86	42.47
		n	22418	30541	27053	29353	1117	10255	608	10922
	Experiment	Target	p-values							
Wi-38-VA13/2RA	1	TCAGGG		** (0.0014)	**** (<0.0001)	**** (<0.0001)				
		TTAGGG	** (0.0014)		**** (<0.0001)	**** (<0.0001)				
	2	TCAGGG	**** (<0.0001)	**** (<0.0001)		**** (<0.0001)				
		TTAGGG	**** (<0.0001)	**** (<0.0001)	**** (<0.0001)					
YTBO	1	TCAGGG						**** (<0.0001)	**** (<0.0001)	**** (<0.0001)
		TTAGGG					**** (<0.0001)		**** (<0.0001)	**** (<0.0001)
	2	TCAGGG					**** (<0.0001)	**** (<0.0001)		* (0.049)
		TTAGGG					**** (<0.0001)	**** (<0.0001)	* (0.049)	

Signal intensity DAPI

	Experiment	Wi-38-VA13/2RA				YTBO			
		1		2		1		2	
	Target	TCAGGG	TTAGGG	TCAGGG	TTAGGG	TCAGGG	TTAGGG	TCAGGG	TTAGGG
	Mean Signal intensity DAPI	582.60	570.90	361.50	360.00	597.20	601.20	229.40	229.40

	Experiment	Target	SD n	254.60 22418	254.60 30541	187.20 29353	186.10 27053	220.40 1117	218.20 10255	108.90 608	108.90 10922
							p-values				
Wi-38-VA13/2RA	1	TCAGGG			**** (<0.0001)	**** (<0.0001)	**** (<0.0001)				
		TTAGGG		**** (<0.0001)		**** (<0.0001)	**** (<0.0001)				
	2	TCAGGG		**** (<0.0001)	**** (<0.0001)		ns (0.8401)				
		TTAGGG		**** (<0.0001)	**** (<0.0001)	ns (0.8401)					
YTBO	1	TCAGGG							ns (0.9345)	**** (<0.0001)	**** (<0.0001)
		TTAGGG						ns (0.9345)		**** (<0.0001)	**** (<0.0001)
	2	TCAGGG						**** (<0.0001)	**** (<0.0001)		ns (>0.9999)
		TTAGGG						**** (<0.0001)	**** (<0.0001)	ns (>0.9999)	

6.4. Establishment of monoclonal cell lines

For a separate project, 18 monoclonal (three/clone) cell lines were established from the six HT-1080 clones shown in Table 1. The stages of establishment of the cell line HT-1080 hTR wt are shown as an example for the 18 established cell lines (Figure 21). The results and procedures were similar for the remaining cell lines ± one or two days.

Thirteen days after seeding a single cell by FACS, 20% of the surface of a 96-well plate's well was covered by cells. During these thirteen days, the plates were not inspected to ensure successful seeding. The next day the coverage was around 50%. After 17 days, 100% of the surface was covered and the cells were transferred into a T25 flask. Following four days of incubation (21 days after seeding), the density in the T25 flask was around 10%. On this day, the cells were reseeded. Another three days later (24 days after seeding), the density reached 80%. This density was sufficient to split the cells the first time and to prepare a T75 for cryo vial preparation, which happened four days later (28 days after seeding) completing the monoclonal cell line establishment. Additionally, multiple cell pellets for DNA, RNA or protein extraction were prepared.

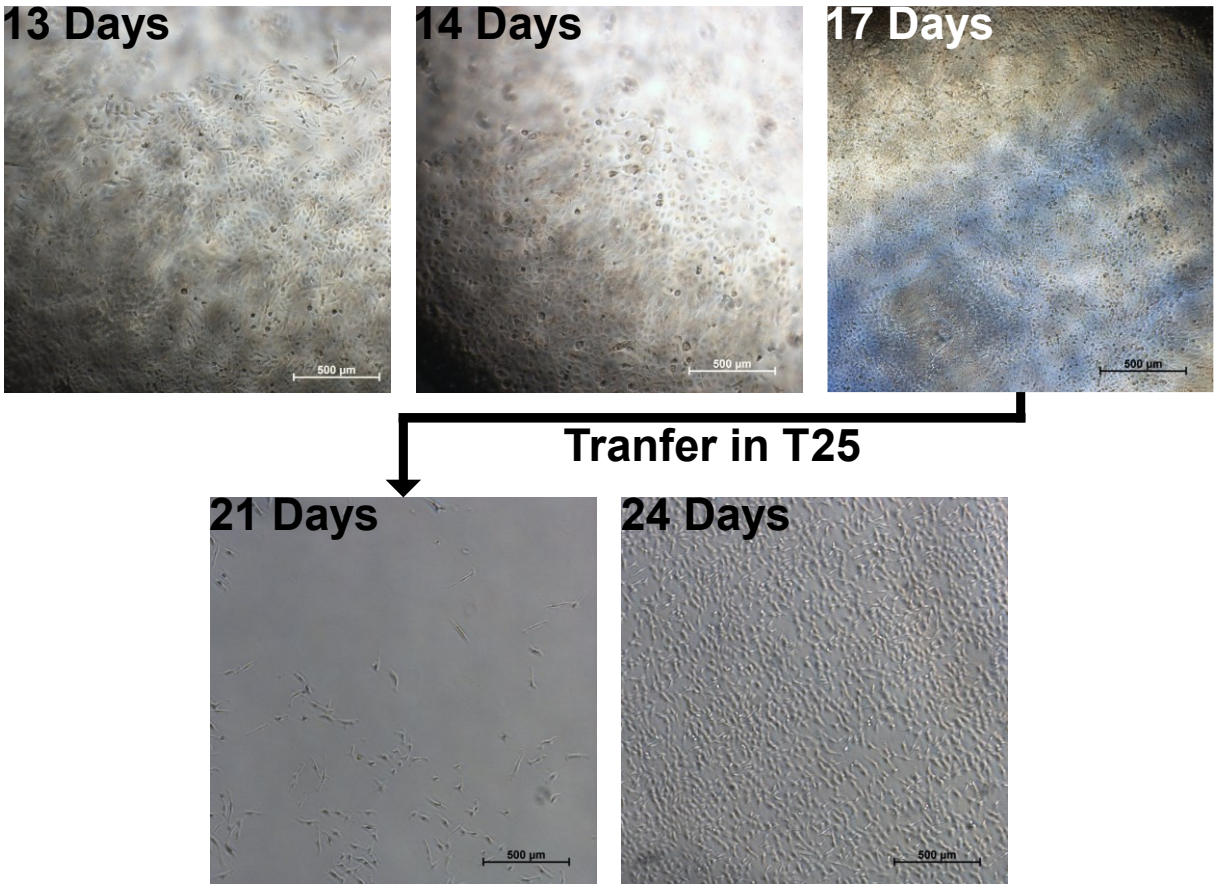

Figure 21: Microscopical images of the cell line HT-1080 hTR wt at 400x magnification on different days after starting the monoclonal cell line establishment shown as an example of the process. One of three technical replicates. The process was performed for

18 different cell lines in total originating from 6 clones. For each clone, the isolation was done in triplicates. On Day 0 single cells were seeded into wells of 96-well plates using FACS. After 17 days the cells were transferred into a T25 flask. Scale bar: 500 µm.

7. Discussion

This study aimed to validate qPCR-based assays to detect NCTR variants on the example of several ALT-positive cell lines. First, the TMM status of the used cell lines was successfully validated using C-circle assays or native ALT-FISH.

7.1. ALT activity detection

The ALT activity detection via C-circle assay was more error-prone than using the native ALT-FISH methods. With the C-circle assay, STR-marker analysis verified cell lines that are ALT-positive, IIICF/C, WI38-VA13/2RA and U2OS (Alhendi & Royle, 2020; Conomos et al., 2012; Henson et al., 2009; Lee et al., 2014), were not detected as such in at least one of the C-circle experiments. Additionally, this assay showed to be susceptible to changes in sample handling and storage as seen by the difference between the two C-circle experiments. Although Henson et al. (2009) stated that rapid freeze-thaw cycles may influence the assay results, the influence of prolonged storage at 4°C was not previously discussed. This seemed to be the issue here since multiple freeze-thaw cycles were minimized but the results between the two assays were still substantial. These issues also hamper reproducibility. To enable further processibility, e.g. testing the CCA products for NCTR variant content, and to prevent the radiation work needed to perform the C-circle assay's dot blots (Henson et al., 2017) within the frame of a master's thesis, the qPCR-based CCA (Henson et al., 2017) was chosen in this work which minimized comparability to the literature since there were no papers found that use this variant of the assay on any of the cell lines used in this study.

The native ALT-FISH method proved to be more reliable in sensing ALT as it detected ALT activity in all STR-marker verified, canonically ALT-positive cell lines (Alhendi & Royle, 2020; Conomos et al., 2012; Henson et al., 2009; Lee et al., 2014) as well as in YTBO. A comparison to the numbers of ALT spots reported by Frank et al. (2022) for the cell lines U2OS and HeLa (Figure 22) indicated that the number of ALT spots detected in this study was substantially lower for the cell line U2OS indicating that the here adapted method is underreporting the number of ALT spots per cell. This could be due to a plethora of reasons, for example, the different ways of data analysis, different ways of sample handling or alterations in the staining process. These differences need to be investigated in the future to spot the cause of the signal reduction. Since there were no coherent indicators for its influence over all cell lines in all

metrics, the RNase treatment's influence on the results of the ALT detection was inconclusive. This may be due to differences in levels of telomeric repeat-containing RNA (TERRA) expression which explains the reduction of the metrics upon RNase treatment but not their increase in some cell lines. The causes for that must be investigated in the future. The significant reduction in ALT spots upon RNase treatment shown by Frank et al. (2022) could be replicated. The native ALT-FISH method appeared to be better suited for ALT detection in terms of reproducibility since no significant differences were found between the preliminary and the main experiment in the ALT determining factor as it was defined by Frank et al. (2022). The significant differences in ALT-spot size and -intensity that were found in the ALT-positive cell lines were of intermediate to low percentages and were determined as statistically significant due to the high number of signals showing a substantial statistical power.

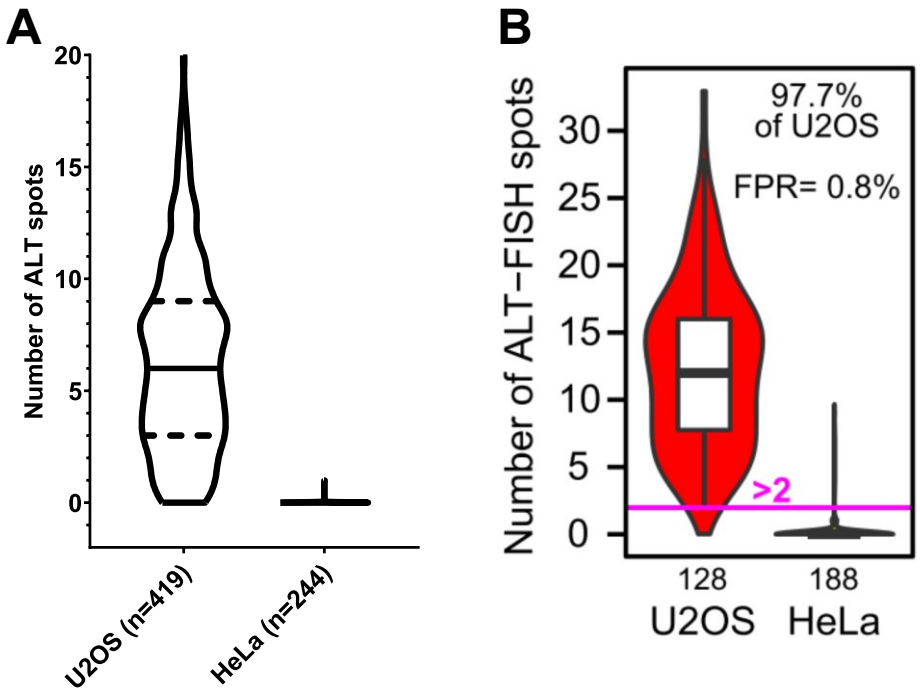

Figure 22: Comparison of the Number of ALT spots of U2OS and HeLa cells to data reported by Frank et al. (2022). A: Number of ALT spots of U2OS and HeLa cells of the "DAPI + TelC" treatment of the main ALT-FISH experiment. Full line: Median. Dashed lines: Quartiles. B: Number of ALT spots of U2OS and HeLa cells adapted from Figure 2C from Frank et al. (2022). Full line: Median, Box: Quartiles.

All in all, the detection of ALT in the cell lines used in this study was successful whereas the ALT-FISH method was more reliable even though it is more complex to perform. In the future, C-circle assays should be verified by ALT FISH experiments where it is possible. The STR marker-validated cell lines in this study that were suspected to be ALT-positive were verified

as such so in the results of the remaining experiments their TMM status is valid. After ensuring the validity of the cell lines' TMM, their content of the NCTR variants TCAGGG, TGAGGG and TAAGGG was detected using the respective qPCR-based assay. Additionally, I successfully showed the assays' reproducibility.

7.2. qPCR-based variant detection

7.2.1. gDNA samples

The detection of telomere sequence variants by qPCR was successful. The values of all cell line samples ranged in the detectable limit of the assay. Depending on the variant this limit was as low as 10^3 kb of variant sequence. Due to the high sensitivity of the qPCR method (Koskinen et al., 2009; Mackay et al., 2002; Nutz et al., 2011) and the variability of NCTR content as seen when comparing the results reported by Lee et al. (2014) and Conomos et al. (2012), the inter-assay reproducibility seemed to be flawed when looking at the raw data. The intra-assay reproducibility was acceptable, as seen by the standard deviations of the replicates. The concerns about inter-assay reproducibility decreased when the normalized data for the NCTR percentages was considered. Here, no concerns about reproducibility were raised. However, it has to be stressed that the statistical reliability of the presented results is limited due to the small number of technical replicates for each sample. Measuring samples with a higher number of technical replicates should be the subject of further validation of this assay.

Following the qPCR-based detection of the relative abundance of the NCTR variants TCAGGG, TGAGGG and TAAGGG, I compared the results to WGS data reported by Lee et al. (2014).

7.2.2. Correlation with whole genome sequencing data

The validation of the qPCR-based NCTR detection assay was a success for the most represented variants TCAGGG and TGAGGG (Conomos et al., 2012; Lee et al., 2014) since the correlation with the variant percentages detected by whole genome sequencing reported by Lee et al. (2014) showed very strong and statistically significant correlations. For these variants, it can be said that the qPCR-based NCTR detection assays yield reliable data, although with a tendency to underestimate the variant percentages. In the case of these variants, the qPCR-based assays could be used for low-cost screening to detect anomalies in variant content which could be verified by WGS if needed to gather more information about their potential biological impact. For the TAAGGG variant, no significant correlation to the WGS

data (Lee et al., 2014) was shown so for this variant no reliable statements for its abundance can be made with this qPCR-based assay. Moreover, the importance of this variant is questionable since it usually is part of the least represented NCTRs (Conomos et al., 2012; Lee et al., 2014). Due to the limited number of samples in this study (n=7 cell lines), a higher number of different cell lines should be tested for their TCAGGG, TGAGGG and TAAGGG variant content while collecting qPCR-based and WGS data of the same samples in parallel to further validate the qPCR-based assays' variant detection capabilities.

To test one origin and way of propagation of NCTR variants in ALT cell lines, I used the qPCR-based assays to probe C-circle assay products for their variants.

7.2.1. C-circle assay products

It was successfully shown, that NCTRs are present in C-circles and that they are propagated with the C-circles by ALT activity. Since this experiment was built on the C-circle assay products, cells with higher C-circle levels, and thus the highest increase in TTAGGG content showed a higher increase in NCTR content. Cell lines that were ALT-positive but were not CCA-positive or had aberrantly low CCA levels did not show a clear increase in NCTR content. For the other cell lines, the increase of the NCTRs did not show statistical significance when comparing the variants but similar to the gDNA assay results, the statistics are not very reliable here due to the low number of technical replicates. Of the strong CCA-positive cell lines, only in IIICF/c, the variant with the highest increase in the CCA products was the most abundant NCTR in the gDNAs as well. In Saos-2 and YTBO, the TAAGGG variant percentage increased the most in the CCA products comparing the polymerase-negative and polymerase-positive reactions, which was due to the low amount of this variant in the polymerase-negative reaction. When looking at the absolute values of the polymerase-positive reaction, in both cases the TGAGGG variant was the most abundant NCTR which was consistent with the NCTR content of the gDNAs. This could be addressed with a different way of normalization in the future. Since no data of an analysis of this kind has been published yet, no verdict about validity and reproducibility can be made about the respective results presented in this study. To change this, it should be the subject of future research. However, the results showing different NCTR content in the C-circles of different cell lines could be one of the reasons for the different telomere variant distributions in ALT cell lines (Alhendi & Royle, 2020; Conomos et al., 2012; Lee et al., 2014).

In the next step, the sensibility of the qPCR-based assays was tested on the example of the TGAGGG variant detection assay by applying it to restriction enzyme digest products.

7.2.2. TCAGGG and TGAGGG restriction digest products

The validation of the qPCR-based NCTR assay's specificity was successful for the TGAGGG variant. As shown previously, the restriction enzymes MnlI and HphI were used on telomeres and to specifically digest the TGAGGG variant (Baird et al., 2006; Kimura et al., 2008; Kimura & Aviv, 2011) as done in this study. The reduction of this specific NCTR was successfully detected by the TGAGGG detection assay, proving its specificity. For the LpnPI restriction enzyme, no data for its application on telomeric DNA was found, hinting toward an unsuited use of this enzyme in this context. This could be a potential reason for the failure of this experiment with the TCAGGG NCTR. To verify this, experiments with the TCAGGG NCTR need to be repeated with the addition of suited restriction enzyme activity controls clarifying if the problem was the assay's inability to detect the reduction in TCAGGG content or if none of this reduction took place.

After the assays' specificity was assessed. their high sensitivity was shown by applying the TCAGGG assay on cluster oligo variants of the respective variant in different concentrations.

7.2.3. TCAGGG cluster oligo variant qPCR

With the data presented in this study, it was demonstrated that the qPCR-based TCAGGG detection assay senses single repeats with higher sensitivity and that the sensitivity goes down with the increase of TCAGGG cluster length. Additionally, it was shown that variant repeats closer to the 5' end of the primer-flanked region are easier to detect than variants closer to the 3' end. Since the assays for the detection of the TGAGGG and TAAGGG variants are based on the same principle and use virtually identical primers with only one base being different per primer, the results of the TCAGGG assay can be extrapolated to the remaining variants with substantial confidence. To verify this, this experiment should be repeated with the respectable variant cluster DNA-oligomers for each assay The findings discussed in this chapter could be the reason for the underrepresentation of the NCTR percentages detected by qPCR in the correlation with the WGS data (see 6.2.2 and 7.2.2), whereas the WGS data was already filtered to show the reads of only 7 non-consecutive variant repeats (Lee et al., 2014) which hampers the comparability in this regard. A remedy for this would be to perform the qPCR-based NCTR detection assays in parallel with WGS of the same samples in the future so different sequencing settings can be compared to the qPCR-based data.

7.3. Telomere-variant FISH

For an additional way of validating the qPCR-based NCTR variant detection results, six telomere-variant FISH experiments were conducted on the cell lines WI-38VA13/2RA and

YTBO. Contrary to the variant detection by qPCR, the detection using Telomere-variant FISH was not successful. In all the conducted experiments, the results for the TGAGGG variant presented by Conomos et al. (2012) could not be replicated even after correspondence with the authors of the paper and the manufacturer of the probes. In this study, no specific signals for this probe could be observed. The causes for this can only be speculated about. Either the probe was not working from the beginning due to a manufacturing defect, the sample preparation did not work even after five experiments with variation in sample preparation (see 5.7) or the probe-target combination was not working from the beginning. For the TCAGGG variant, specific signals were observed and detected but the results did not make sense as the WI38-VA13/2RA cell line showed extremely high TCAGGG percentages in both experiments compared to the qPCR and WGS data. In the second experiment, the variant was shown to be more abundant than the canonical TTAGGG repeat. In the YTBO cell line, abnormally high TCAGGG percentages were particularly observed in the first experiment. In the second experiment, this percentage was lower but still substantially higher than in the qPCR data. For YTBO no WGS data was available. These fluctuations in TCAGGG percentages also showed that the reproducibility of this method is limited and thus not suited for application and comparison to the qPCR and WGS data. This was the reason why only the cell lines WI38-VA13/2RA and YTBO were used to validate the method, which was not successful. The reasons for this unsuccessful application of the method for this variant are again elusive. One potential reason is that the high percentages of the variant could be caused by unoptimized data analysis which could be improved. The Telomere-variant method could also just not be suited for quantitative analyses as it was only used as a method to validate the presence of the variants by Conomos et al. (2012) but not to quantify them. The failed attempt to apply this method to detect NCTR variants in two cell lines led to the change of focus to the other experiments in this study. This is why this method was not applied to the remaining ALT cell lines to save time and resources.

7.4. Conclusion

This study showed that the NCTR variants TCAGGG and TGAGGG can be detected and quantified by qPCR in the cell lines IIICF/c, Saos-2, U2OS, WI38-VA13/2RA and YTBO validated as ALT-positive by CCA and ALT-FISH. This was validated by correlations with WGS data (Lee et al., 2014) for all cell lines except YTBO. For the less abundant TAAGGG variant, no significant correlation to the WGS data was shown. The validation of the qPCR detected NCTR variant abundances by Telomere-variant FISH was not successful.

Additionally, I showed that the variants TCAGGG, TGAGGG and TAAGGG are present in the ALT-specific C-circles and that these variants are propagated with these C-circles.

On the example of the TGAGGG variant, I validated the qPCR assay's specificity by conducting a restriction enzyme digestion experiment and applying the assay to the products.

It was shown on the example of the TCAGGG variant that the ability of the assay to detect the variants decreases with the cluster lengths of these variants and that variants closer to the 5' end of the primer-flanked region are easier to detect.

The limitations of this study were the low numbers of technical replicates in the qPCR assays and the correlation to WGS data from non-paired biological replicates of the respective cell lines from a different lab. These limitations should be used as a basis for future studies to create a highly reliable validation of the qPCR assays presented in this study so they can be used as screening tools in the clinic to elucidate the biological significance of NCTRs in cancer.

8. References

Alhendi, A. S. N., & Royle, N. J. (2020). The absence of (TCAGGG)n repeats in some telomeres, combined with variable responses to NR2F2 depletion, suggest that this nuclear receptor plays an indirect role in the alternative lengthening of telomeres. *Scientific Reports*, *10*(1), 20597. https://doi.org/10.1038/s41598-020-77606-w

Baird, D. M., Britt-Compton, B., Rowson, J., Amso, N. N., Gregory, L., & Kipling, D. (2006). Telomere instability in the male germline. *Human Molecular Genetics*, *15*(1), 45–51. https://doi.org/10.1093/hmg/ddi424

Bryan, T. M., Englezou, A., Gupta, J., Bacchetti, S., & Reddel, R. R. (1995). Telomere elongation in immortal human cells without detectable telomerase activity. *EMBO Journal*, *14*(17), 4240–4248. https://doi.org/10.1002/j.1460-2075.1995.tb00098.x

Bryan, T. M., Marušić, L., Bacchetti, S., Namba, M., & Reddel, R. R. (1997). The telomere lengthening mechanism in telomerase-negative immortal human cells does not involve the telomerase RNA subunit. *Human Molecular Genetics*, *6*(6), 921–926. https://doi.org/10.1093/hmg/6.6.921

Canela, A., Vera, E., Klatt, P., & Blasco, M. A. (2007). High-throughput telomere length quantification by FISH and its application to human population studies. *Proceedings of the National Academy of Sciences of the United States of America*, *104*(13), 5300–5305. https://doi.org/10.1073/pnas.0609367104

Cawthon, R. M. (2002). Telomere measurement by quantitative PCR. *Nucleic Acids Research*, *30*(10), e47. https://doi.org/10.1093/nar/30.10.e47

Cawthon, R. M. (2009). Telomere length measurement by a novel monochrome multiplex quantitative PCR method. *Nucleic Acids Research*, *37*(3). https://doi.org/10.1093/nar/gkn1027

Chen, Y. Y., Dagg, R., Zhang, Y., Lee, J. H. Y., Lu, R., La Rotta, N. M., Sampl, S., Korkut-Demirbaş, M., Holzmann, K., Lau, L. M. S., Reddel, R. R., & Henson, J. D. (2021). The c-circle biomarker is secreted by alternative-lengthening-of-telomeres positive cancer cells inside exosomes and provides a blood-based diagnostic for alt activity. *Cancers*, *13*(21), 5369. https://doi.org/10.3390/cancers13215369

Claude, E., de Lhoneux, G., Pierreux, C. E., Marbaix, E., de Ville de Goyet, M., Boulanger, C., Van Damme, A., Brichard, B., & Decottignies, A. (2021). Detection of alternative lengthening of telomeres mechanism on tumor sections. *Molecular Biomedicine*, *2*(1), 32. https://doi.org/10.1186/s43556-021-00055-y

Conomos, D., Stutz, M. D., Hills, M., Neumann, A. A., Bryan, T. M., Reddel, R. R., & Pickett, H. A. (2012). Variant repeats are interspersed throughout the telomeres and recruit nuclear receptors in ALT cells. *Journal of Cell Biology*, *199*(6), 893–906. https://doi.org/10.1083/jcb.201207189

Dilley, R. L., & Greenberg, R. A. (2015). ALTernative Telomere Maintenance and Cancer. *Trends in Cancer*, *1*(2), 145–156. https://doi.org/10.1016/j.trecan.2015.07.007

Ehmann, U. K., Cook, K. H., & Friedberg, E. C. (1978). The kinetics of thymine dimer excision in ultraviolet-irradiated human cells. *Biophysical Journal*, *22*(2), 249–264. https://doi.org/10.1016/S0006-3495(78)85487-3

Evident Corporation. (n.d.-a). *cellSens: Deep Learning Part3. Manually Label Images to Prepare the Deep Learning Training Data* | *Olympus LS*. Retrieved May 30, 2023, from https://www.olympus-lifescience.com/en/video/cellsens_deep-learning-part3/

Evident Corporation. (n.d.-b). *cellSens:Deep Learning Part1. Preparing Training Data* | *Olympus LS*. Retrieved May 30, 2023, from https://www.olympus-lifescience.com/en/video/cellsens_dl-prepare-training-data/

Evident Corporation. (n.d.-c). *cellSens:Deep Learning Part2. Using the Training Data to Identify Nuclei* | *Olympus LS*. Retrieved May 30, 2023, from https://www.olympus-lifescience.com/en/video/cellsens_dl-use-training-data/

Frank, L., Rademacher, A., Mücke, N., Tirier, S. M., Koeleman, E., Knotz, C., Schumacher, S., Stainczyk, S. A., Westermann, F., Fröhling, S., Chudasama, P., & Rippe, K. (2022). ALT-FISH quantifies alternative lengthening of telomeres activity by imaging of single-stranded repeats. *Nucleic Acids Research*, *50*(11), e61–e61. https://doi.org/10.1093/nar/gkac113

Hammerl, D. (2021). *Wahlbeispiel Report: In vitro models for transient and stable ectopic expression of wild-type and mutant TERC (hTR) gene*. University of Vienna.

Hanahan, D. (2022). Hallmarks of Cancer: New Dimensions. *Cancer Discovery*, *12*(1), 31–46. https://doi.org/10.1158/2159-8290.CD-21-1059

Hanahan, D., & Weinberg, R. A. (2000). The hallmarks of cancer. *Cell*, *100*(1), 57–70. https://doi.org/10.1016/S0092-8674(00)81683-9

Hanahan, D., & Weinberg, R. A. (2011). Hallmarks of cancer: The next generation. *Cell*, *144*(5), 646–674. https://doi.org/10.1016/j.cell.2011.02.013

Hayflick, L. (1965). The limited in vitro lifetime of human diploid cell strains. *Experimental Cell Research*, *37*(3), 614–636. https://doi.org/10.1016/0014-4827(65)90211-9

Henson, J. D., Cao, Y., Huschtscha, L. I., Chang, A. C., Au, A. Y. M., Pickett, H. A., & Reddel, R. R. (2009). DNA C-circles are specific and quantifiable markers of alternative-lengthening-of-telomeres activity. *Nature Biotechnology*, *27*(12), 1181–1185. https://doi.org/10.1038/nbt.1587

Henson, J. D., Lau, L. M., Koch, S., Martin La Rotta, N., Dagg, R. A., & Reddel, R. R. (2017). The C-Circle Assay for alternative-lengthening-of-telomeres activity. *Methods*, *114*, 74–84. https://doi.org/10.1016/j.ymeth.2016.08.016

Henson, J. D., & Reddel, R. R. (2010). Assaying and investigating Alternative Lengthening of Telomeres activity in human cells and cancers. *FEBS Letters*, *584*(17), 3800–3811. https://doi.org/10.1016/j.febslet.2010.06.009

Ikeda, H., Aida, J., Hatamochi, A., Hamasaki, Y., Izumiyama-Shimomura, N., Nakamura, K. I., Ishikawa, N., Poon, S. S., Fujiwara, M., Tomita, K. I., Hiraishi, N., Kuroiwa, M., Matsuura, M., Sanada, Y., Kawano, Y., Arai, T., & Takubo, K. (2014). Quantitative fluorescence in situ hybridization measurement of telomere length in skin with/without sun exposure or actinic keratosis. *Human Pathology*, *45*(3), 473–480. https://doi.org/10.1016/j.humpath.2013.10.009

Kimura, M., & Aviv, A. (2011). Measurement of telomere DNA content by dot blot analysis. *Nucleic Acids Research*, *39*(12), e84–e84. https://doi.org/10.1093/nar/gkr235

Kimura, M., Hjelmborg, J. V. B., Gardner, J. P., Bathum, L., Brimacombe, M., Lu, X., Christiansen, L., Vaupel, J. W., Aviv, A., & Christensen, K. (2008). Telomere length and mortality: A study of leukocytes in elderly danish twins. *American Journal of Epidemiology*, *167*(7), 799–806. https://doi.org/10.1093/aje/kwm380

Koprowski, H., & Croce, C. M. (1977). Tumorigenicity of simian virus 40 transformed human cells and mouse-human hybrids in nude mice. *Proceedings of the National Academy of Sciences of the United States of America*, *74*(3), 1142–1146. https://doi.org/10.1073/pnas.74.3.1142

Koskinen, M. T., Holopainen, J., Pyörälä, S., Bredbacka, P., Pitkälä, A., Barkema, H. W., Bexiga, R., Roberson, J., Sølverød, L., Piccinini, R., Kelton, D., Lehmusto, H., Niskala, S., & Salmikivi, L. (2009). Analytical specificity and sensitivity of a real-time polymerase chain reaction assay for identification of bovine mastitis pathogens. *Journal of Dairy Science*, *92*(3), 952–959. https://doi.org/10.3168/jds.2008-1549

Kreilmeier-Berger, T., Aupperle-Lellbach, H., Reifinger, M., Hörstke, N. V., Holzmann, K., & Kleiter, M. (2023). Alternative Lengthening of Telomeres Is Rare in Canine Histiocytic Sarcoma. *Cancers*, *15*(17), 4214. https://doi.org/10.3390/cancers15174214

Kreilmeier, T., Sampl, S., Deloria, A. J., Walter, I., Reifinger, M., Hauck, M., Borst, L. B., Holzmann, K., & Kleiter, M. (2017). Alternative lengthening of telomeres does exist in various canine sarcomas. *Molecular Carcinogenesis*, *56*(3), 923–935. https://doi.org/10.1002/mc.22546

Lee, M., Hills, M., Conomos, D., Stutz, M. D., Dagg, R. A., Lau, L. M. S., Reddel, R. R., & Pickett, H. A. (2014). Telomere extension by telomerase and ALT generates variant repeats by mechanistically distinct processes. *Nucleic Acids Research*, *42*(3), 1733–1746. https://doi.org/10.1093/nar/gkt1117

Levsky, J. M., & Singer, R. H. (2003). Fluorescence in situ hybridization: Past, present and future. *Journal of Cell Science*, *116*(14), 2833–2838. https://doi.org/10.1242/jcs.00633

Mackay, I. M., Arden, K. E., & Nitsche, A. (2002). Real-time PCR in virology. *Nucleic Acids Research*, *30*(6), 1292–1305. https://doi.org/10.1093/nar/30.6.1292

Marzec, P., Armenise, C., Pérot, G., Roumelioti, F. M., Basyuk, E., Gagos, S., Chibon, F., & Déjardin, J. (2015). Nuclear-Receptor-Mediated Telomere Insertion Leads to Genome Instability in ALT Cancers. *Cell*, *160*(5), 913–927. https://doi.org/10.1016/j.cell.2015.01.044

Nutz, S., Döll, K., & Karlovsky, P. (2011). Determination of the LOQ in real-time PCR by receiver operating characteristic curve analysis: Application to qPCR assays for Fusarium verticillioides and F. proliferatum. *Analytical and Bioanalytical Chemistry*, *401*(2), 717–726. https://doi.org/10.1007/s00216-011-5089-x

O'Callaghan, N. J., & Fenech, M. (2011). A quantitative PCR method for measuring absolute telomere length. *Biological Procedures Online*, *13*(1), 1–10. https://doi.org/10.1186/1480-9222-13-3

Puck, T. T., & Marcus, P. I. (1955). A RAPID METHOD FOR VIABLE CELL TITRATION AND CLONE PRODUCTION WITH HELA CELLS IN TISSUE CULTURE: THE USE OF X-IRRADIATED CELLS TO SUPPLY CONDITIONING FACTORS. *Proceedings of the National Academy of Sciences*, *41*(7), 432–437. https://doi.org/10.1073/pnas.41.7.432

Rasheed, S., Nelson-Rees, W. A., Toth, E. M., Arnstein, P., & Gardner, M. B. (1974). Characterization of a newly derived human sarcoma cell line (HT-1080). *Cancer*, *33*(4), 1027–1033. https://doi.org/10.1002/1097-0142(197404)33:4<1027::AID-CNCR2820330419>3.0.CO;2-Z

Robin, T., Capes-Davis, A., & Bairoch, A. (2020). CLASTR: The Cellosaurus STR similarity search tool - A precious help for cell line authentication. *International Journal of Cancer*,

146(5), 1299–1306. https://doi.org/10.1002/ijc.32639

Rogan, E. M., Bryan, T. M., Hukku, B., Maclean, K., Chang, A. C.-M., Moy, E. L., Englezou, A., Warneford, S. G., Dalla-Pozza, L., & Reddel, R. R. (1995). Alterations in p53 and p16INK4 expression and telomere length during spontaneous immortalization of Li-Fraumeni syndrome fibroblasts. *Molecular and Cellular Biology*, *15*(9), 4745–4753. https://doi.org/10.1128/mcb.15.9.4745

Romero, A., Martín, M., Cheang, M. C. U., García-Asenjo, J. A. L., Oliva, B., He, X., De La Hoya, M., Sáenz, J. Á. G., Fernández, M. A., Rubio, E. D., Perou, C. M., & Llopis, T. C. (2011). Assessment of topoisomerase II α status in breast cancer by quantitative PCR, gene expression microarrays, immunohistochemistry, and fluorescence in Situ hybridization. *American Journal of Pathology*, *178*(4), 1453–1460. https://doi.org/10.1016/j.ajpath.2010.12.042

Samad, M. A., Saiman, M. Z., Abdul Majid, N., Yaacob, J. S., & Karsani, S. A. (2021). Berberine inhibits telomerase activity and induces cell cycle arrest and telomere erosion in colorectal cancer cell line, hct 116. *Molecules*, *26*(2). https://doi.org/10.3390/molecules26020376

Sampl, S., Pramhas, S., Stern, C., Preusser, M., Marosi, C., & Holzmann, K. (2012). Expression of telomeres in astrocytoma WHO grade 2 to 4: TERRA level correlates with telomere length, telomerase activity, and advanced clinical grade. *Translational Oncology*, *5*(1), 56–65. https://doi.org/10.1593/tlo.11202

Schindelin, J., Arganda-Carreras, I., Frise, E., Kaynig, V., Longair, M., Pietzsch, T., Preibisch, S., Rueden, C., Saalfeld, S., Schmid, B., Tinevez, J.-Y., White, D. J., Hartenstein, V., Eliceiri, K., Tomancak, P., & Cardona, A. (2012). Fiji: an open-source platform for biological-image analysis. *Nature Methods*, *9*(7), 676–682. https://doi.org/10.1038/nmeth.2019

Wright, W. C., Daniels, W. P., & Fogh, J. (1981). Distinction of seventy-one cultured human tumor cell lines by polymorphic enzyme analysis. *Journal of the National Cancer Institute*, *66*(2), 402. https://doi.org/10.1093/jnci/66.2.239

Zhang, J. M., & Zou, L. (2020). Alternative lengthening of telomeres: From molecular mechanisms to therapeutic outlooks. *Cell and Bioscience*, *10*(1). https://doi.org/10.1186/s13578-020-00391-6

9. List of Tables

Table 1: List of all cell lines and clones used in this work. 16

Table 2: Components and concentrations for 50 ml QCP lysis buffer (1x). 21

Table 3: Components and volumes of the CCA master mix for twelve reactions 23

Table 4: CCA-cycler program 24

Table 5: Chemicals/solutions needed for native ALT-FISH....25

Table 6: List of DNA-Oligomers used in this study....27

Table 7: Components & volumes of the CCA-qPCR master mixes....29

Table 8: Program for CCA-qPCR 30

Table 9: Components of telomere sequence variant-qPCR reaction....32

Table 10: Primer used for telomere sequence variant qPCRs 32

Table 11: 36B4 (SCG) qPCR program 33

Table 12: TTAGGG and NCTR qPCR program 34

Table 13: Absolute copy- respectively telomere kb numbers of the standard DNA oligomer dilutions used for absolute quantification 34

Table 14: Number of molecules of the TCAGGG cluster oligo variants in each reaction....35

Table 15: Conditions of all telomere-variant FISH experiments 38

Table 16: Chemicals/Components used for telomere-variant FISH....40

Table 17: Statistics (two-way ANOVA with Tukey's multiple comparisons follow-up test) of the ALT-spots per cell quantification of the main ALT-FISH experiment (See Figure 7, Panel A) comparing the cell lines. 57

Table 18: Statistics (two-way ANOVA with Tukey's multiple comparisons follow-up test) of the ALT-spots per cell quantification of the main ALT-FISH experiment (See Figure 7, Panel A) comparing the treatments. 58

Table 19: Statistics (two-way ANOVA with Tukey's multiple comparisons follow-up test) of the ALT-spot area quantification of the main ALT-FISH experiment (See Figure 7, Panel B) comparing the cell lines. 59

Table 20: Statistics (two-way ANOVA with Tukey's multiple comparisons follow-up test) of the ALT-spots area quantification of the main ALT-FISH experiment (See Figure 7, Panel B) comparing the treatments. 60

Table 21: Statistics (two-way ANOVA with Tukey's multiple comparisons follow-up test) of the ALT-spot intensity quantification of the main ALT-FISH experiment (See Figure 7, Panel C) comparing the cell lines. 61

Table 22: Statistics (two-way ANOVA with Tukey's multiple comparisons follow-up test) of the ALT-spot intensity quantification of the main ALT-FISH experiment (See Figure 7, Panel C) comparing the treatments. 62

Table 23: Statistics (two-way ANOVA with Sidak's multiple comparisons follow-up test) of the ALT-spots per cell quantification comparing the main and the preliminary ALT-FISH experiments (See Figure 8, Panel A). 64

Table 24: Statistics (two-way ANOVA with Sidak's multiple comparisons follow-up test) of the ALT-spot area quantification comparing the main and the preliminary ALT-FISH experiments (See Figure 8, Panel B). 64

Table 25: Statistics (two-way ANOVA with Sidak's multiple comparisons follow-up test) of the ALT-spot signal intensity quantification comparing the main and the preliminary ALT-FISH experiments (See Figure 8, Panel C). 65

Table 26: Statistics (two-way ANOVA with Tukey's multiple comparisons follow-up test) of the percentual NCTR content detected by qPCR (See Figure 9) comparing the cell lines. 69

Table 27: Statistics (two-way ANOVA with Tukey's multiple comparisons follow-up test) of the NCTRs CT of each cell line detected by qPCR compared with the NTC (See Figure 10). For CT >40 the value 40 was used for the analysis. 72

Table 28: Statistics (two-way ANOVA with Tukey's multiple comparisons follow-up test) of the SCG and NCTR standard curve concentration CTs detected by qPCR compared with the NTC (See Figure 11). For CT >40 the value 40 was used for the analysis. 75

Table 29: Statistics (two-way ANOVA with Sidak's multiple comparisons follow-up test) of the comparison of dCT values from the main and the preliminary NCTR detection qPCR experiment in gDNAs. (See Figure 12) 79

Table 30: Statistics (two-way ANOVA with Tukey's multiple comparisons follow-up test) of the comparison of variant percentages of the main and the preliminary NCTR detection qPCR experiments in gDNAs. (See Figure 12) 81

Table 31: Statistics (two-way ANOVA with Tukey's multiple comparisons follow-up test) of the percentual SCG, TTAGGG repeat and NCTR content of the polymerase-positive reaction

compared to the polymerase-negative reaction detected by qPCR (See Figure 15) comparing the CCA products of all cell lines of the second CCA.....90

Table 32: Statistics (two-way ANOVA with Tukey's multiple comparisons follow-up test) of the percentual SCG, TTAGGG repeat and NCTR content of the polymerase-positive reaction compared to the polymerase-negative reaction detected by qPCR (See Figure 15) comparing the qPCR assay results of each cell line of the second CCA. 94

Table 33: Statistics (Unpaired t-tests with Welch's correction) comparing the TTAGGG and TCAGGG SQs of uncut and LpnPI digested WI38-VA13/2RA gDNA (See Figure 16, Panel A and B). 99

Table 34: Statistics (Brown-Forsythe and Welch ANOVA test with Games-Howell's multiple comparisons follow-up test) comparing the TTAGGG and TGAGGG SQs of uncut, MnlI and HpHI digested YTBO gDNA (See Figure 16, Panel C and D). 99

Table 35: Statistics (two-way ANOVA with Tukey's multiple comparisons follow-up test) of the CTs of TCAGGG cluster variant DNA oligomers detected by qPCR (See Figure 17) comparing the CTs of all variants.....102

Table 36: Statistics (two-way ANOVA with Dunnett's multiple comparisons follow-up test) of the CTs of TCAGGG cluster variant DNA oligomers detected by qPCR (See Figure 17) comparing the CTs of each variant to the NTC.....103

Table 37: Statistics (two-way ANOVA with Sidak's multiple comparisons follow-up tests) of the TTAGGG and TCAGGG-spots per cell, spot size and spot signal intensity quantification of the first telomere variant-FISH experiment (See Figure 18) comparing the cell lines and the targets. 106

Table 38: Statistics (two-way ANOVA with Sidak's multiple comparisons follow-up tests) of the TTAGGG and TCAGGG-spots per cell, spot size and spot signal intensity quantification of the second telomere variant-FISH experiment (See Figure 19) comparing the cell lines and the targets. 109

Table 39: Statistics (two-way ANOVA with Tukey's multiple comparisons follow-up tests) of the TTAGGG and TCAGGG-spots per cell, spot size and spot signal intensity quantification of the first and second telomere variant-FISH experiment (See Figure 20) comparing the cell lines and the targets of the two experiments.....112

Table 40: STR-Marker profiles of cell lines used in this study.....135

Table 41: Phi positive values and calculations of CCA 1 137

Table 42: Phi negative values and calculations of CCA 1 139

Table 43: Normalized and raw CCA levels and status of CCA 1 142

Table 44: Standard curves of CCA 1 142

Table 45: Phi positive values and calculations of CCA 2 143

Table 46: Phi negative values and calculations of CCA 2 145

Table 47: Normalized and raw CCA levels and status of CCA 2 149

Table 48: Standard curves of CCA 2 149

Table 49: Statistics (Brown-Forsythe and Welch ANOVA with Games-Howell's multiple comparisons follow-up test) of the ALT-spots per cell quantification of the preliminary ALT-FISH experiment (See Figure 24, Panel A) comparing the cell lines. 151

Table 50: Statistics (Brown-Forsythe and Welch ANOVA with Games-Howell's multiple comparisons follow-up test) of the ALT-spot area quantification of the preliminary ALT-FISH experiment (See Figure 24, Panel B). 151

Table 51: Statistics (Brown-Forsythe and Welch ANOVA with Games-Howell's multiple comparisons follow-up test) of the ALT-spot signal intensity quantification of the preliminary ALT-FISH experiment (See Figure 24, Panel C). 152

Table 52: Statistics (Brown-Forsythe and Welch ANOVA with Games-Howell's multiple comparisons follow-up test) of the DAPI signal intensity quantification in the ALT-spot area of the preliminary ALT-FISH experiment (See Figure 25, Panel A). 154

Table 53: Statistics (two-way ANOVA with Tukey's multiple comparisons follow-up test) of the DAPI signal intensity quantification in the ALT-spot area of the main ALT-FISH experiment (See Figure 25, Panel B) comparing the cell lines. 155

Table 54: Statistics (two-way ANOVA with Tukey's multiple comparisons follow-up test) of the DAPI signal intensity quantification in the ALT-spot area of the main ALT-FISH experiment (See Figure 25, Panel B) comparing the treatments. 156

Table 55: Statistics (two-way ANOVA with Sidak's multiple comparisons follow-up test) of the DAPI signal intensity quantification in the ALT-spot area of the result comparison from the main and the preliminary ALT-FISH experiment (See Figure 25, Panel C). 157

Table 56: Raw CT values of the cell lines of the main and preliminary variant detection qPCR experiments. 158

Table 57: Raw CT values of the NTCs and standards of the main and preliminary variant detection qPCR experiments. 160

Table 58: Values of correlation analysis of WGS and qPCR data shown in Figure 14. 162

Table 59: SQ values of SCG-, canonical and variant repeats of the CCA assay products ..163

Table 60: Raw CT values of the C-circle assay product variant detection qPCR experiment. 164

Table 61: Raw CT values of the TCAGGG and TGAGGG restriction digest products variant detection qPCR experiment. 166

Table 62: Raw CT values of the TCAGGG cluster variant DNA oligomer qPCR experiment. 166

Table 63: Statistics (two-way ANOVA with Tukey's multiple comparisons follow-up test) of the DAPI signal intensity quantification in the TTAGGG- and TCAGGG-spot area of the first and second telomere-variant FISH experiment.....169

10. List of Figures

Figure 1: Scheme of the CCA process used in this study. 10

Figure 2: Scheme of the probe locations on G-circles of the native ALT-FISH method. 11

Figure 3: Scheme of the adapted primer design used for qPCR-based NCTR detection in this study. 13

Figure 4: Microscopical confocal spinning disc images at 400x magnification of the cell lines Saos-2 (A and B) and U2OS (C and D) stained using Atto 633 labeled TelC probes for ALT-spot detection and DAPI for nuclear staining used for neural network training. 42

Figure 5: Microscopical confocal spinning disc images at 400x magnification of the cell line WI38-VA13/2RA from the main native ALT-FISH experiment (Figure 7, Panel A-C) and second telomere-variant FISH experiment (Figure 19, Panel D-G) stained using Atto 633 labeled TelC probes for ALT-spot detection (A) or FITC labeled TelC PNA probes for canonical telomere repeat detection (E) and ATTO-633 labeled PNA probes for TCAGGG detection (F) and DAPI for nuclear staining (A and D) as well as the respective channels merged (C and G). 43

Figure 6: Normalized C-circle levels detected by qPCR. 49

Figure 7: Quantification of the main ALT-FISH experiment (no technical replicates). 53

Figure 8: Comparison of the main and the preliminary ALT-FISH experiment. 63

Figure 9: Average SQ-based percentage ± SEM of the analyzed NCTRs compared to the telomeric repeat SQ detected by qPCR of multiple cell lines. 67

Figure 10: Comparison of the CTs ± SEM of the analyzed NCTRs and the SCG of several cell lines with the NTC CTs ± SEM. 71

Figure 11: Comparison of the CTs ± SEM of the used NCTR- and the SCG standard curve dilutions with the NTC CTs ± SEM. 74

Figure 12: Average dCT values of telomeric repeats and NCTRs compared to the SCG detected by qPCR of the preliminary and main experiment in contrast to each other. 76

Figure 13: Average SQ-based percentage ± SEM of the analyzed NCTRs compared to the telomeric repeat SQ detected by qPCR of the preliminary and main experiment in contrast to each other. 77

Figure 14: Correlation of qPCR detected NCTR percentages shown in Figure 9 (3 technical replicates for each dot) with NCTR percentages from WGS data produced by Lee et al. (2014). 85

Figure 15: Average SQ-based percentage ± SEM of the by qPCR detected SCG, telomere repeats and NCTRs in the polymerase positive reactions compared to the SCG, telomere repeats and NCTRs in the polymerase negative reactions of the CCA products of multiple cell lines.....88

Figure 16: Comparison of the telomere repeat and NCTR SQs ± SEM from qPCRs of gDNAs of two ALT-positive cell lines after digestion with restriction enzymes specific for two NCTRs. 98

Figure 17: Average CT ± SD of TCAGGG cluster variant DNA oligomers and the NTC detected by qPCR.....101

Figure 18: Quantification of the first telomere-variant FISH experiment (no technical replicates). 105

Figure 19: Quantification of the second telomere-variant FISH experiment (no technical replicates).....107

Figure 20: Comparison of the first and second telomere-variant FISH experiment. 110

Figure 21: Microscopical images of the cell line HT-1080 hTR wt at 400x magnification on different days after starting the monoclonal cell line establishment shown as an example of the process.....115

Figure 22: Comparison of the Number of ALT spots of U2OS and HeLa cells to data reported by Frank et al. (2022). 117

Figure 23: C-circle levels detected by qPCR. 136

Figure 24: Quantification of the preliminary ALT-FISH experiment. 150

Figure 25: Quantification and comparison of the DAPI signal intensity in the ALT-spot area in the main and the preliminary ALT-FISH experiment. 153

Figure 26: Quantification and comparison of the DAPI signal intensity in TTAGGG- and TCAGGG-spot area of the first and second telomere-variant FISH experiment. 167

11. Annex

11.1. STR-Marker profiles

Table 40: STR-Marker profiles of cell lines used in this study

Markers	IIICF/c	*GM847**	HeLa	HT-1080	Saos-2	U2OS	WI38-VA13/2RA	YTBO
Amelogenin	X	X	X	X, Y	X	X	X	X,Y
CSF1PO	9,11	7,10	9,10	12	10	12,13	10,12	10,11
D3S1358	15,17	12,18	15,18	16	14,18	16	16,17	15,16
D5S818	10,13	10,11	11,12	11,13	12	8,11	10	13,14
D7S820	10,12	11,12	8,12	9,10	8,10	11,12	9,11	7,11
D8S1179	11	13,14	12,13	13,14	10,12	12,14	14	13,14
D13S317	8,10	10,12	13.3	12,14	12,13	13	11	12,13
D16S539	9,11	11,13	9	9,12	12,13	11,12	11,12	9,11
D18S51	15,18	16,17	12,16	12,18	15,22	12,14	16,18	20
D21S11	26	29	27,28	28,30	28,30	31	30,30.2	27,32.2
FGA	21,24	18,24	18,21	22,25	22,25	20	22,24	19,25
Penta D	11	9,13	8,15	9,12	11,12	9	13	9,15
Penta E	7,10	13,14	7,17	5,15	14,19	10,13	13,14	10
TH01	6,9.3	8,9	7	6	6,9	6,9.3	9.3	7,9.3
TPOX	8,11	8	8,12	8	8	11,12	8	8
vWA	16,18	17,22	16,18	14,19	18	14,18	19,20	14,16
Comment	Best match in CLASTR (Robin et al., 2020): 73.33%, No profile for IIICF/c available	Identified as HCT 116-Luc 2, Match: 93,33%	Identity 96.3%, best match	Identity 100%	Identity 100%	Identity 100%	Identity 100%	Best match in CLASTR (Robin et al., 2020): 75.86%, No public profile for YTBO available

11.2. ALT activity detection

11.2.1. C-circle assay

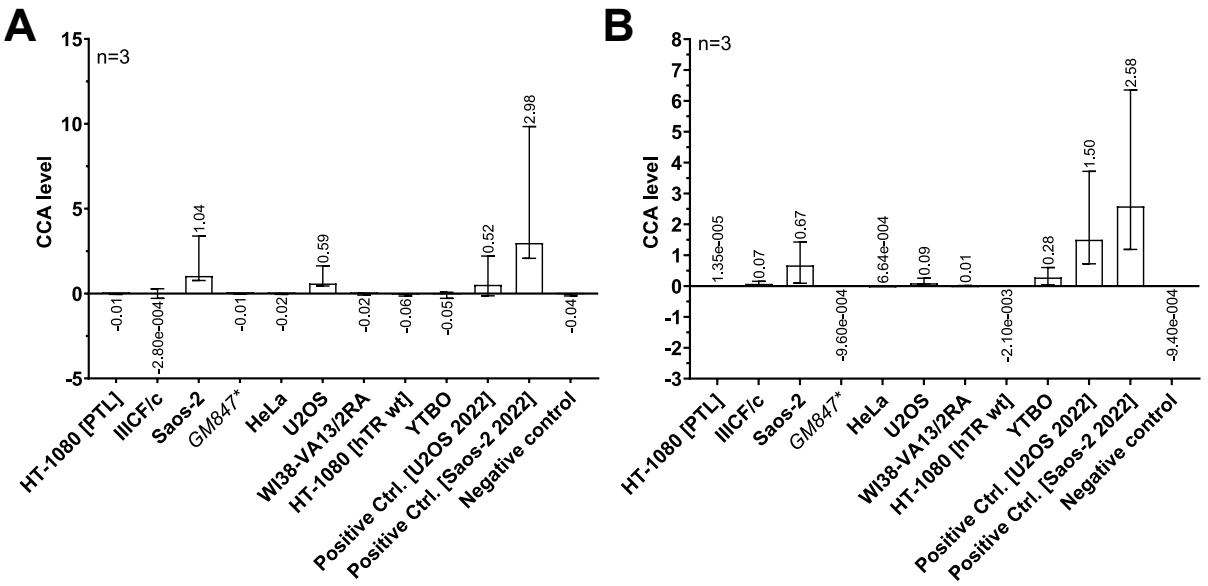

Figure 23: C-circle levels detected by qPCR. These graphs depict the averaged C-circle levels of two independent C-circle assay experiments. The qPCR experiments were performed in technical triplicates. The error bars were calculated as stated in 5.3. A: C-circle levels of the first C-circle experiment. N = 3 technical replicates. B: C-circle levels of biological replicates from cells tested in A. N = 3 technical replicates.

Table 41: Phi positive values and calculations of CCA 1

Sample Name	Target Name	CT	CT Mean	CT SD	TEL-Qty (TC)	36B4-Qty (SC)	Average-Qty	STDEV.S-Qty	Coefficient of variation (CV)	normalized TC (NTC)	NTC CV	upper error bar	lower error bar
HT-1080 PTL +	TEL	23.03	21.42	1.391	0.0026		0.0077	0.0044	0.5690	0.0090	1.3201	0.0209	-0.0029
HT-1080 PTL +	TEL	20.63	21.42	1.391	0.0101								
HT-1080 PTL +	TEL	20.61	21.42	1.391	0.0102								
HT-1080 PTL +	36B4	28.12	25.96	1.902		0.1647	0.8493	0.6380	0.7511				
HT-1080 PTL +	36B4	25.21	25.96	1.902		0.9560							
HT-1080 PTL +	36B4	24.54	25.96	1.902		1.4272							
IIICF/c +	TEL	15.86	16.67	0.785	0.1481		0.1003	0.0440	0.4390	0.1673	1.1040	0.3520	-0.0174
IIICF/c +	TEL	16.71	16.67	0.785	0.0915								
IIICF/c +	TEL	17.43	16.67	0.785	0.0613								
IIICF/c +	36B4	27.83	26.31	1.375		0.1968	0.5995	0.3988	0.6651				
IIICF/c +	36B4	25.14	26.31	1.375		0.9942							
IIICF/c +	36B4	25.96	26.31	1.375		0.6076							
Saos-2 +	TEL	12.94	14.47	1.327	0.7646		0.3954	0.3199	0.8091	1.1009	1.1629	2.3812	-0.1794
Saos-2 +	TEL	15.31	14.47	1.327	0.2018								
Saos-2 +	TEL	15.16	14.47	1.327	0.2197								
Saos-2 +	36B4	26.28	26.90	0.564		0.5016	0.3591	0.1271	0.3538				
Saos-2 +	36B4	27.38	26.90	0.564		0.2577							
Saos-2 +	36B4	27.03	26.90	0.564		0.3181							
GM847+	TEL	24.07	23.64	0.387	0.0015		0.0019	0.0004	0.2073	0.0035	0.4810	0.0051	0.0018
GM847+	TEL	23.53	23.64	0.387	0.0020								
GM847+	TEL	23.32	23.64	0.387	0.0022								
GM847+	36B4	25.70	26.18	0.439		0.7110	0.5445	0.1490	0.2737				
GM847+	36B4	26.28	26.18	0.439		0.4991							
GM847+	36B4	26.56	26.18	0.439		0.4235							
HeLa +	TEL	23.25	22.93	0.307	0.0023		0.0028	0.0005	0.1703	0.0024	0.4174	0.0035	0.0014
HeLa +	TEL	22.90	22.93	0.307	0.0028								
HeLa +	TEL	22.63	22.93	0.307	0.0033								
HeLa +	36B4	24.55	24.94	0.428		1.4181	1.1509	0.2843	0.2470				
HeLa +	36B4	24.86	24.94	0.428		1.1824							
HeLa +	36B4	25.40	24.94	0.428		0.8522							
U2OS +	TEL	14.42	14.34	0.293	0.3330		0.3506	0.0592	0.1689	1.2642	0.2013	1.5186	1.0097
U2OS +	TEL	14.59	14.34	0.293	0.3022								
U2OS +	TEL	14.02	14.34	0.293	0.4166								

U2OS +	36B4	27.30	27.26	0.053		0.2707	0.2773	0.0090	0.0324				
U2OS +	36B4	27.20	27.26	0.053		0.2875							
U2OS +	36B4	27.28	27.26	0.053		0.2738							
WI38-VA13/2RA +	TEL	20.28	19.85	0.868	0.0123		0.0171	0.0091	0.5301	0.0398	0.7406	0.0693	0.0103
WI38-VA13/2RA +	TEL	20.42	19.85	0.868	0.0114								
WI38-VA13/2RA +	TEL	18.85	19.85	0.868	0.0276								
WI38-VA13/2RA +	36B4	26.23	26.56	0.361		0.5143	0.4298	0.0905	0.2105				
WI38-VA13/2RA +	36B4	26.49	26.56	0.361		0.4408							
WI38-VA13/2RA +	36B4	26.95	26.56	0.361		0.3344							
HT-1080 hTR wt+	TEL	22.66	21.78	0.792	0.0032		0.0057	0.0022	0.3952	0.0162	0.7380	0.0282	0.0043
HT-1080 hTR wt+	TEL	21.54	21.78	0.792	0.0061								
HT-1080 hTR wt+	TEL	21.13	21.78	0.792	0.0076								
HT-1080 hTR wt+	36B4	27.34	26.93	0.579		0.2640	0.3485	0.1194	0.3428				
HT-1080 hTR wt+	36B4	26.52	26.93	0.579		0.4329							
YTBO +	TEL	18.02	18.08	0.450	0.0438		0.0433	0.0106	0.2448	0.1689	0.5592	0.2633	0.0744
YTBO +	TEL	18.56	18.08	0.450	0.0324								
YTBO +	TEL	17.67	18.08	0.450	0.0536								
YTBO +	36B4	26.98	27.45	0.567		0.3271	0.2562	0.0806	0.3145				
YTBO +	36B4	27.28	27.45	0.567		0.2729							
YTBO +	36B4	28.08	27.45	0.567		0.1686							
+ Ctrl. U2OS+	TEL	12.71	12.20	0.719	0.8711		1.2224	0.5311	0.4345	0.9028	0.8280	1.6502	0.1553
+ Ctrl. U2OS+	TEL	11.38	12.20	0.719	1.8334								
+ Ctrl. U2OS+	TEL	12.53	12.20	0.719	0.9627								
+ Ctrl. U2OS+	36B4	24.33	24.74	0.774		1.6287	1.3541	0.5328	0.3935				
+ Ctrl. U2OS+	36B4	24.26	24.74	0.774		1.6935							
+ Ctrl. U2OS+	36B4	25.63	24.74	0.774		0.7400							
+ Ctrl. Saos-2+	TEL	14.13	12.89	2.068	0.3914		1.2695	1.5029	1.1839	3.0481	1.2563	6.8775	-0.7813
+ Ctrl. Saos-2+	TEL	14.04	12.89	2.068	0.4122								
+ Ctrl. Saos-2+	TEL	10.50	12.89	2.068	3.0048								

+ Ctrl. Saos-2+	36B4	26.54	26.59	0.122		0.4275	0.4165	0.0302	0.0725				
+ Ctrl. Saos-2+	36B4	26.73	26.59	0.122		0.3823							
+ Ctrl. Saos-2+	36B4	26.49	26.59	0.122		0.4396							
neg. Control +	TEL	33.00	33.31	0.681	0.0000		0.0000	0.0000	0.3364	0.0300	1.2985	0.0689	-0.0089
neg. Control +	TEL	32.84	33.31	0.681	0.0000								
neg. Control +	TEL	34.09	33.31	0.681	0.0000								
neg. Control +	36B4	37.42	39.14	1.216		0.0006	0.0003	0.0003	0.9621				
neg. Control +	36B4	40.00	39.14	1.216		0.0001							
neg. Control +	36B4	40.00	39.14	1.216		0.0001							

Table 42: Phi negative values and calculations of CCA 1

Sample Name	Target Name	CT	CT Mean	CT SD	TEL-Qty (TC)	36B4-Qty (SC)	Average-Qty	SD Qty	Coefficient of variation (CV)	normalized TC (NTC)	NTC CV	upper error bar	lower error bar
HT-1080 PTL -	TEL	20.37	19.91	0.421	0.0117		0.0155	0.0035	0.2248	0.0225	0.4845	0.0334	0.0116
HT-1080 PTL -	TEL	19.55	19.91	0.421	0.0186								
HT-1080 PTL -	TEL	19.80	19.91	0.421	0.0162								
HT-1080 PTL -	36B4	25.32	25.78	0.408		0.8953	0.6894	0.1790	0.2597				
HT-1080 PTL -	36B4	25.97	25.78	0.408		0.6032							
HT-1080 PTL -	36B4	26.06	25.78	0.408		0.5698							
IIICF/c -	TEL	17.54	18.18	0.592	0.0574		0.0418	0.0142	0.3397	0.1676	0.5939	0.2671	0.0680
IIICF/c -	TEL	18.27	18.18	0.592	0.0382								
IIICF/c -	TEL	18.72	18.18	0.592	0.0297								
IIICF/c -	36B4	27.01	27.47	0.399		0.3223	0.2493	0.0634	0.2542				
IIICF/c -	36B4	27.66	27.47	0.399		0.2180							
IIICF/c -	36B4	27.74	27.47	0.399		0.2077							
Saos-2 -	TEL	20.55	20.04	0.795	0.0106		0.0151	0.0073	0.4847	0.0615	0.5043	0.0925	0.0305
Saos-2 -	TEL	19.13	20.04	0.795	0.0236								
Saos-2 -	TEL	20.46	20.04	0.795	0.0112								
Saos-2 -	36B4	27.43	27.46	0.033		0.2495	0.2459	0.0048	0.0195				
Saos-2 -	36B4	27.49	27.46	0.033		0.2404							
Saos-2 -	36B4	27.44	27.46	0.033		0.2477							

GM847-	TEL	22.43	22.76	0.416	0.0037		0.0031	0.0007	0.2202	0.0088	1.0441	0.0179	-0.0004
GM847-	TEL	22.62	22.76	0.416	0.0033								
GM847-	TEL	23.23	22.76	0.416	0.0023								
GM847-	36B4	25.74	27.19	1.261		0.6925	0.3550	0.2925	0.8239				
GM847-	36B4	28.02	27.19	1.261		0.1754							
GM847-	36B4	27.82	27.19	1.261		0.1971							
HeLa -	TEL	20.60	20.56	0.077	0.0103		0.0106	0.0005	0.0438	0.0245	0.0511	0.0257	0.0232
HeLa -	TEL	20.47	20.56	0.077	0.0111								
HeLa -	TEL	20.61	20.56	0.077	0.0102								
HeLa -	36B4	26.52	26.53	0.012		0.4341	0.4311	0.0032	0.0073				
HeLa -	36B4	26.54	26.53	0.012		0.4278							
HeLa -	36B4	26.53	26.53	0.012		0.4312							
U2OS -	TEL	16.40	16.63	0.201	0.1092		0.0962	0.0112	0.1167	0.6731	0.2844	0.8646	0.4817
U2OS -	TEL	16.75	16.63	0.201	0.0897								
U2OS -	TEL	16.75	16.63	0.201	0.0898								
U2OS -	36B4	28.07	28.37	0.269		0.1702	0.1430	0.0240	0.1677				
U2OS -	36B4	28.47	28.37	0.269		0.1334							
U2OS -	36B4	28.57	28.37	0.269		0.1252							
WI38-VA13/2RA -	TEL	19.28	19.44	0.140	0.0217		0.0199	0.0016	0.0803	0.0589	0.4121	0.0832	0.0346
WI38-VA13/2RA -	TEL	19.52	19.44	0.140	0.0189								
WI38-VA13/2RA -	TEL	19.52	19.44	0.140	0.0189								
WI38-VA13/2RA -	36B4	27.28	26.99	0.513		0.2731	0.3371	0.1118	0.3317				
WI38-VA13/2RA -	36B4	27.29	26.99	0.513		0.2720							
WI38-VA13/2RA -	36B4	26.40	26.99	0.513		0.4663							
HT-1080 hTR wt-	TEL	19.88	19.98	0.139	0.0154		0.0146	0.0011	0.0780	0.0741	0.2608	0.0934	0.0548
HT-1080 hTR wt-	TEL	20.08	19.98	0.139	0.0138								
HT-1080 hTR wt-	36B4	28.14	27.84	0.303		0.1631	0.1977	0.0361	0.1828				
HT-1080 hTR wt-	36B4	27.84	27.84	0.303		0.1946							
HT-1080 hTR wt-	36B4	27.53	27.84	0.303		0.2352							
YTBO -	TEL	19.69	20.06	0.334	0.0172		0.0141	0.0027	0.1942	0.2199	0.3885	0.3053	0.1345
YTBO -	TEL	20.17	20.06	0.334	0.0132								
YTBO -	TEL	20.33	20.06	0.334	0.0120								

YTBO -	36B4	29.47	29.70	0.324		0.0730	0.0641	0.0125	0.1944				
YTBO -	36B4	29.93	29.70	0.324		0.0553							
+ Ctrl. U2OS-	TEL	12.75	13.88	1.003	0.8499		0.5042	0.3024	0.5997	0.3849	1.0978	0.8074	-0.0377
+ Ctrl. U2OS-	TEL	14.21	13.88	1.003	0.3744								
+ Ctrl. U2OS-	TEL	14.67	13.88	1.003	0.2884								
+ Ctrl. U2OS-	36B4	24.20	24.88	1.054		1.7514	1.3102	0.6526	0.4981				
+ Ctrl. U2OS-	36B4	24.34	24.88	1.054		1.6188							
+ Ctrl. U2OS-	36B4	26.09	24.88	1.054		0.5605							
+ Ctrl. Saos-2-	TEL	18.88	19.01	0.461	0.0272		0.0257	0.0062	0.2433	0.0695	0.7133	0.1191	0.0199
+ Ctrl. Saos-2-	TEL	18.64	19.01	0.461	0.0311								
+ Ctrl. Saos-2-	TEL	19.53	19.01	0.461	0.0188								
+ Ctrl. Saos-2-	36B4	26.07	26.90	0.739		0.5664	0.3694	0.1736	0.4700				
+ Ctrl. Saos-2-	36B4	27.11	26.90	0.739		0.3031							
+ Ctrl. Saos-2-	36B4	27.51	26.90	0.739		0.2387							
neg. Control -	TEL	33.39	33.04	0.352	0.0000		0.0000	0.0000	0.1970	0.0703	0.3284	0.0934	0.0472
neg. Control -	TEL	33.03	33.04	0.352	0.0000								
neg. Control -	TEL	32.68	33.04	0.352	0.0000								
neg. Control -	36B4	39.64	39.88	0.172		0.0002	0.0001	0.0000	0.1314				
neg. Control -	36B4	40.00	39.88	0.172		0.0001							
neg. Control -	36B4	40.00	39.88	0.172		0.0001							

Table 43: Normalized and raw CCA levels and status of CCA 1

	CCA levels	upper error bar	lower error bar	CCA Status	norm. CCA level [norm. to 1% U2OS]	norm. upper error bar	norm. lower error bar
HT-1080 PTL	-0.0134	0.0094	-0.0363	CCA-negative	-2.27574	0.00016	-0.00061
IIICF/c	-0.0003	0.2839	-0.2845	CCA-negative	-0.04691	0.00480	-0.00481
Saos-2	1.0394	2.3507	-0.2718	CCA-negative	175.87143	397.73787	-45.99501
*GM847**	-0.0053	0.0055	-0.0161	CCA-negative	-0.89366	0.93657	-2.72389
HeLa	-0.0220	-0.0198	-0.0243	CCA-negative	-3.72894	-3.34462	-4.11326
U2OS	0.5910	1.0369	0.1451	CCA-positive	100.00000	175.44696	24.55304
WI38-VA13/2RA	-0.0191	0.0346	-0.0728	CCA-negative	-3.23304	5.85847	-12.32455
HT-1080 hTR wt	-0.0579	-0.0266	-0.0891	CCA-negative	-9.78889	-4.49465	-15.08313
YTBO	-0.0510	0.1288	-0.2309	CCA-negative	-8.63455	21.79714	-39.06624
+ Ctrl. U2OS	0.5179	1.6879	-0.6521	CCA-negative	87.62982	285.58857	-110.32893
+ Ctrl. Saos-2	2.9786	6.8576	-0.9004	CCA-negative	503.97807	1160.30596	-152.34981
neg. Ctrl.	-0.0404	0.0217	-0.1024	CCA-negative	-6.82739	3.66776	-17.32255

Table 44: Standard curves of CCA 1

Target	Efficiency %	Slope	Y-Intercept	R^2
36B4	82.89	-3.814	25.133	0.986
TEL	75.42	-4.097	12.460	0.989

Table 45: Phi positive values and calculations of CCA 2

Sample Name	Target Name	CT	CT Mean	CT SD	TEL-Qty (TC)	36B4-Qty (SC)	Average-Qty	STDEV.S-Qty	Coefficient of variation (CV)	normalized TC (NTC)	NTC CV	upper error bar	lower error bar
HT-1080 PTL +	TEL	28.88	29.01	0.195	0.00786		0.00740	0.00068	0.09133	0.00346	0.16209	0.00402	0.00290
HT-1080 PTL +	TEL	29.23	29.01	0.195	0.00662								
HT-1080 PTL +	TEL	28.92	29.01	0.195	0.00772								
HT-1080 PTL +	36B4	25.67	25.74	0.109		2.23871	2.13913	0.15137	0.07076				
HT-1080 PTL +	36B4	25.87	25.74	0.109		1.96494							
HT-1080 PTL +	36B4	25.69	25.74	0.109		2.21374							
IIICF/c +	TEL	23.96	23.93	0.102	0.08392		0.08535	0.00422	0.04943	0.07832	0.08012	0.08460	0.07205
IIICF/c +	TEL	23.82	23.93	0.102	0.09009								
IIICF/c +	TEL	24.01	23.93	0.102	0.08203								
IIICF/c +	36B4	26.81	26.76	0.047		1.05242	1.08969	0.03345	0.03070				
IIICF/c +	36B4	26.75	26.76	0.047		1.09953							
IIICF/c +	36B4	26.72	26.76	0.047		1.11711							
Saos-2 +	TEL	17.36	17.53	0.159	2.02594		1.86384	0.14476	0.07767	0.67174	0.13534	0.76265	0.58082
Saos-2 +	TEL	17.66	17.53	0.159	1.74746								
Saos-2 +	TEL	17.58	17.53	0.159	1.81811								
Saos-2 +	36B4	25.25	25.35	0.086		2.95656	2.77464	0.16002	0.05767				
Saos-2 +	36B4	25.38	25.35	0.086		2.71175							
Saos-2 +	36B4	25.41	25.35	0.086		2.65562							
GM847+	TEL	31.04	31.18	0.129	0.00278		0.00259	0.00016	0.06319	0.00182	0.07551	0.00196	0.00169
GM847+	TEL	31.24	31.18	0.129	0.00252								
GM847+	TEL	31.27	31.18	0.129	0.00248								
GM847+	36B4	26.34	26.36	0.019		1.43359	1.42141	0.01751	0.01232				
GM847+	36B4	26.38	26.36	0.019		1.40135							
GM847+	36B4	26.35	26.36	0.019		1.42930							
HeLa +	TEL	29.44	29.39	0.100	0.00600		0.00614	0.00030	0.04904	0.00274	0.13678	0.00311	0.00236
HeLa +	TEL	29.28	29.39	0.100	0.00648								
HeLa +	TEL	29.46	29.39	0.100	0.00593								
HeLa +	36B4	25.54	25.67	0.134		2.43126	2.24001	0.19656	0.08775				
HeLa +	36B4	25.66	25.67	0.134		2.25021							
HeLa +	36B4	25.81	25.67	0.134		2.03854							
U2OS +	TEL	23.13	22.79	0.464	0.12521		0.15006	0.03516	0.23428	0.15881	0.33394	0.21185	0.10578
U2OS +	TEL	22.98	22.79	0.464	0.13469								
U2OS +	TEL	22.26	22.79	0.464	0.19028								

U2OS +	36B4	26.82	26.98	0.148		1.04974	0.94488	0.09417	0.09966					
U2OS +	36B4	27.02	26.98	0.148		0.91739								
U2OS +	36B4	27.11	26.98	0.148		0.86752								
WI38-VA13/2RA +	TEL	25.12	25.07	0.174	0.04814		0.04943	0.00421	0.08513	0.01815	0.11431	0.02022	0.01608	
WI38-VA13/2RA +	TEL	25.21	25.07	0.174	0.04603									
WI38-VA13/2RA +	TEL	24.87	25.07	0.174	0.05414									
WI38-VA13/2RA +	36B4	25.38	25.37	0.044		2.70473	2.72366	0.07950	0.02919					
WI38-VA13/2RA +	36B4	25.32	25.37	0.044		2.81091								
WI38-VA13/2RA +	36B4	25.41	25.37	0.044		2.65534								
HT-1080 hTR wt+	TEL	27.87	27.89	0.047	0.01280		0.01268	0.00028	0.02229	0.00567	0.05947	0.00601	0.00533	
HT-1080 hTR wt+	TEL	27.94	27.89	0.047	0.01236									
HT-1080 hTR wt+	TEL	27.85	27.89	0.047	0.01289									
HT-1080 hTR wt+	36B4	25.71	25.67	0.056		2.17846	2.23728	0.08318	0.03718					
HT-1080 hTR wt+	36B4	25.63	25.67	0.056		2.29610								
YTBO +	TEL	19.68	19.73	0.149	0.66051		0.64509	0.04559	0.07067	0.28663	0.14378	0.32784	0.24542	
YTBO +	TEL	19.90	19.73	0.149	0.59380									
YTBO +	TEL	19.62	19.73	0.149	0.68097									
YTBO +	36B4	25.59	25.66	0.113		2.36329	2.25063	0.16455	0.07311					
YTBO +	36B4	25.61	25.66	0.113		2.32680								
YTBO +	36B4	25.79	25.66	0.113		2.06179								
+ Ctrl. U2OS+	TEL	14.83	14.43	0.790	6.82947		8.72064	3.57923	0.41043	1.54132	0.46432	2.25698	0.82566	
+ Ctrl. U2OS+	TEL	14.94	14.43	0.790	6.48369									
+ Ctrl. U2OS+	TEL	13.52	14.43	0.790	12.84875									
+ Ctrl. U2OS+	36B4	24.23	24.27	0.083		5.80488	5.65791	0.30488	0.05389					
+ Ctrl. U2OS+	36B4	24.21	24.27	0.083		5.86145								
+ Ctrl. U2OS+	36B4	24.36	24.27	0.083		5.30738								

+ Ctrl. Saos-2+	TEL	13.90	14.83	0.818	10.73144		7.22501	3.05270	0.42252	2.59011	0.45777	3.77578	1.40443
+ Ctrl. Saos-2+	TEL	15.18	14.83	0.818	5.78436								
+ Ctrl. Saos-2+	TEL	15.42	14.83	0.818	5.15923								
+ Ctrl. Saos-2+	36B4	25.39	25.34	0.054		2.68419	2.78946	0.09834	0.03525				
+ Ctrl. Saos-2+	36B4	25.29	25.34	0.054		2.87895							
+ Ctrl. Saos-2+	36B4	25.33	25.34	0.054		2.80526							
neg. Control +	TEL	40.00	39.75	0.000	0.00004		0.00004	0.00001	0.22134	0.00184	0.48767	0.00274	0.00094
neg. Control +	TEL	39.24	39.75	0.000	0.00005								
neg. Control +	TEL	40.00	39.75	0.000	0.00004								
neg. Control +	36B4	32.27	32.64	0.426		0.02876	0.02308	0.00615	0.26633				
neg. Control +	36B4	32.54	32.64	0.426		0.02394							
neg. Control +	36B4	33.10	32.64	0.426		0.01655							

Table 46: Phi negative values and calculations of CCA 2

Sample Name	Target Name	CT	CT Mean	CT SD	TEL-Qty (TC)	36B4-Qty (SC)	Average-Qty	STDEV.S-Qty	Coefficient of variation (CV)	normalized TC (NTC)	NTC CV	upper error bar	lower error bar
HT-1080 PTL -	TEL	28.72	28.54	0.188	0.00849		0.00930	0.00085	0.09097	0.00345	0.11751	0.00385	0.00304
HT-1080 PTL -	TEL	28.55	28.54	0.188	0.00923								

HT-1080 PTL -	TEL	28.34	28.54	0.188	0.01018								
HT-1080 PTL -	36B4	25.34	25.39	0.040		2.78102	2.69834	0.07163	0.02655				
HT-1080 PTL -	36B4	25.41	25.39	0.040		2.65503							
HT-1080 PTL -	36B4	25.41	25.39	0.040		2.65898							
IIICF/c -	TEL	29.25	29.23	0.023	0.00658		0.00665	0.00007	0.01103	0.00504	0.05113	0.00529	0.00478
IIICF/c -	TEL	29.23	29.23	0.023	0.00665								
IIICF/c -	TEL	29.20	29.23	0.023	0.00672								
IIICF/c -	36B4	26.41	26.47	0.061		1.37403	1.32040	0.05294	0.04010				
IIICF/c -	36B4	26.53	26.47	0.061		1.26817							
IIICF/c -	36B4	26.47	26.47	0.061		1.31901							
Saos-2 -	TEL	29.24	29.16	0.107	0.00662		0.00686	0.00036	0.05247	0.00314	0.10770	0.00348	0.00280
Saos-2 -	TEL	29.21	29.16	0.107	0.00669								
Saos-2 -	TEL	29.04	29.16	0.107	0.00727								
Saos-2 -	36B4	25.62	25.71	0.083		2.32082	2.18341	0.12058	0.05522				
Saos-2 -	36B4	25.77	25.71	0.083		2.09524							
Saos-2 -	36B4	25.74	25.71	0.083		2.13418							
GM847-	TEL	29.82	30.14	0.279	0.00499		0.00431	0.00060	0.13857	0.00278	0.17314	0.00327	0.00230
GM847-	TEL	30.26	30.14	0.279	0.00403								
GM847-	TEL	30.34	30.14	0.279	0.00389								
GM847-	36B4	26.24	26.23	0.052		1.53312	1.54655	0.05346	0.03457				
GM847-	36B4	26.28	26.23	0.052		1.50110							
GM847-	36B4	26.17	26.23	0.052		1.60545							
HeLa -	TEL	29.83	29.84	0.054	0.00496		0.00494	0.00013	0.02611	0.00207	0.04702	0.00217	0.00198
HeLa -	TEL	29.90	29.84	0.054	0.00480								
HeLa -	TEL	29.79	29.84	0.054	0.00506								
HeLa -	36B4	25.54	25.58	0.031		2.43778	2.38075	0.04978	0.02091				
HeLa -	36B4	25.59	25.58	0.031		2.35842							
HeLa -	36B4	25.60	25.58	0.031		2.34604							
U2OS -	TEL	23.41	23.73	0.285	0.10940		0.09460	0.01329	0.14048	0.06628	0.23111	0.08160	0.05096
U2OS -	TEL	23.97	23.73	0.285	0.08370								
U2OS -	TEL	23.80	23.73	0.285	0.09069								
U2OS -	36B4	26.21	26.36	0.136		1.56879	1.42719	0.12934	0.09063				
U2OS -	36B4	26.48	26.36	0.136		1.31527							
U2OS -	36B4	26.38	26.36	0.136		1.39752							
WI38-VA13/2RA -	TEL	26.05	26.04	0.057	0.03068		0.03086	0.00086	0.02781	0.00991	0.06901	0.01060	0.00923
WI38-VA13/2RA -	TEL	26.09	26.04	0.057	0.03011								

WI38-VA13/2RA -	TEL	25.98	26.04	0.057	0.03180								
WI38-VA13/2RA -	36B4	25.24	25.17	0.063		2.96587	3.11396	0.12830	0.04120				
WI38-VA13/2RA -	36B4	25.14	25.17	0.063		3.18444							
WI38-VA13/2RA -	36B4	25.13	25.17	0.063		3.19158							
HT-1080 hTR wt-	TEL	27.30	27.26	0.052	0.01685		0.01715	0.00043	0.02510	0.00777	0.06133	0.00825	0.00729
HT-1080 hTR wt-	TEL	27.22	27.26	0.052	0.01746								
HT-1080 hTR wt-	36B4	25.73	25.69	0.054		2.14885	2.20739	0.07997	0.03623				
HT-1080 hTR wt-	36B4	25.71	25.69	0.054		2.17481							
HT-1080 hTR wt-	36B4	25.63	25.69	0.054		2.29850							
YTBO -	TEL	26.87	27.00	0.252	0.02070		0.01955	0.00228	0.11688	0.00800	0.14523	0.00916	0.00684
YTBO -	TEL	26.84	27.00	0.252	0.02103								
YTBO -	TEL	27.29	27.00	0.252	0.01692								
YTBO -	36B4	25.50	25.54	0.043		2.50348	2.44427	0.06930	0.02835				
YTBO -	36B4	25.53	25.54	0.043		2.46128							
YTBO -	36B4	25.58	25.54	0.043		2.36805							
+ Ctrl. U2OS-	TEL	21.68	21.56	0.203	0.25241		0.26788	0.02690	0.10043	0.04236	0.10739	0.04690	0.03781
+ Ctrl. U2OS-	TEL	21.33	21.56	0.203	0.29894								
+ Ctrl. U2OS-	TEL	21.68	21.56	0.203	0.25227								
+ Ctrl. U2OS-	36B4	24.08	24.10	0.011		6.37477	6.32446	0.04401	0.00696				
+ Ctrl. U2OS-	36B4	24.10	24.10	0.011		6.29311							
+ Ctrl. U2OS-	36B4	24.10	24.10	0.011		6.30551							
+ Ctrl. Saos-2-	TEL	26.81	26.47	0.312	0.02127		0.02525	0.00369	0.14602	0.00724	0.19829	0.00868	0.00581
+ Ctrl. Saos-2-	TEL	26.20	26.47	0.312	0.02855								
+ Ctrl. Saos-2-	TEL	26.40	26.47	0.312	0.02593								
+ Ctrl. Saos-2-	36B4	25.04	25.00	0.078		3.39043	3.48625	0.18222	0.05227				
+ Ctrl. Saos-2-	36B4	24.91	25.00	0.078		3.69638							
+ Ctrl. Saos-2-	36B4	25.05	25.00	0.078		3.37192							
neg. Control -	TEL	40.00	0.00	0.000	0.00004		0.00004	0.00000	0.00000	0.00278	0.24342	0.00346	0.00210

neg. Control -	TEL	40.00	0.00	0.000	0.00004				
neg. Control -	TEL	40.00	0.00	0.000	0.00004				
neg. Control -	36B4	33.06	33.46	0.350		0.01704	0.01331	0.00324	0.24342
neg. Control -	36B4	33.63	33.46	0.350		0.01168			
neg. Control -	36B4	33.69	33.46	0.350		0.01121			

Table 47: Normalized and raw CCA levels and status of CCA 2

	CCA levels	upper error bar	lower error bar	CCA Status	norm. CCA level [norm. to 1% U2OS]	norm. upper error bar	norm. lower error bar
HT-1080 PTL	0.00001	0.00098	-0.00095	CCA-negative	0.00090	1.05835	-1.02914
IIICF/c	0.07329	0.07982	0.06675	CCA-positive	4.88907	5.32489	4.45324
Saos-2	0.66860	0.75985	0.57735	CCA-positive	44.60406	50.69178	38.51633
*GM847**	-0.00096	-0.00034	-0.00158	CCA-negative	-0.06408	-0.02273	-0.10543
HeLa	0.00066	0.00114	0.00019	CCA-negative	0.04431	0.07581	0.01280
U2OS	0.09253	0.16088	0.02418	CCA-positive	6.17300	10.73295	1.61306
WI38-VA13/2RA	0.00824	0.01100	0.00548	CCA-negative	0.54959	0.73363	0.36554
HT-1080 hTR wt	-0.00210	-0.00129	-0.00291	CCA-negative	-0.14011	-0.08582	-0.19439
YTBO	0.27863	0.32100	0.23626	CCA-positive	18.58828	21.41507	15.76150
+ Ctrl. U2OS	1.49896	2.21917	0.77875	CCA-positive	100.00000	148.04723	51.95277
+ Ctrl. Saos-2	2.58286	3.76997	1.39575	CCA-positive	172.31002	251.50542	93.11462
neg. Ctrl.	-0.00094	0.00063	-0.00252	CCA-negative	-0.06285	0.04213	-0.16783

Table 48: Standard curves of CCA 2

Target	Efficiency %	Slope	Y-Intercept	R^2
36B4	93.52	-3.488	26.890	0.995
TEL	61.90	-4.779	18.821	0.991

11.2.2. Native ALT-FISH

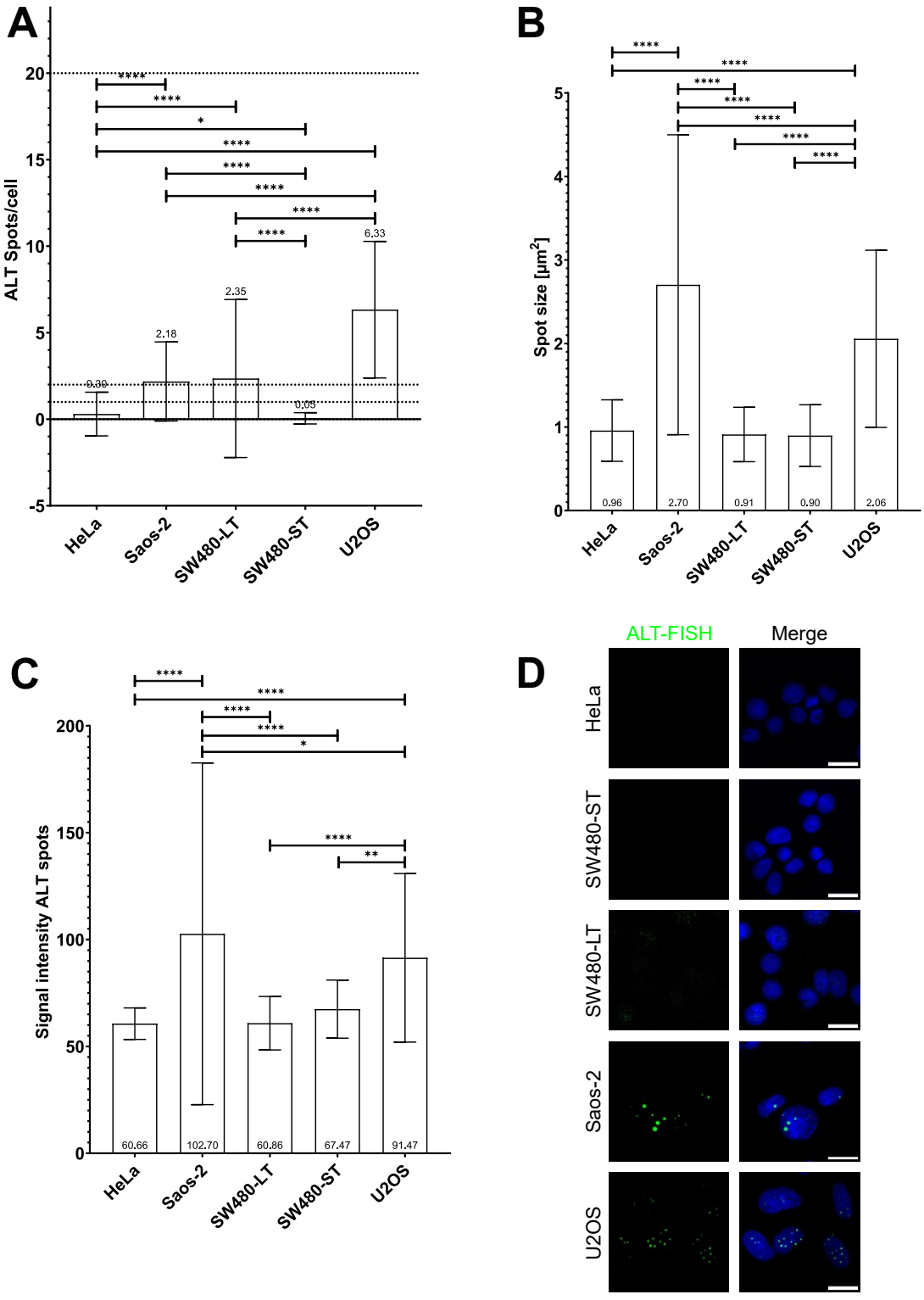

Figure 24: Quantification of the preliminary ALT-FISH experiment. No technical replicates. A: Comparison of the mean ALT spots per cell ± SD of five different cell lines. The dotted lines depict thresholds for ALT levels: 1-2: low ALT, 2-20 ALT, >20 super ALT. Statistics are shown in Table 49. B: Depiction of the mean area of ALT-spots ± SD in the analyzed cell lines. Both experiments are biological replicates of each other. Statistics can be found in Table

50. C: Portrayal of the mean ALT-Spot signal intensity ± SD of the analyzed cell lines. Statistics are presented in Table 51. D: Microscopical confocal spinning disc images at 400x magnification of the analyzed cell lines stained using Atto 633 labeled TelC probes for ALT-spot detection and DAPI for nuclear staining. Scale bar: 20 µm.

Table 49: Statistics (Brown-Forsythe and Welch ANOVA with Games-Howell's multiple comparisons follow-up test) of the ALT-spots per cell quantification of the preliminary ALT-FISH experiment (See Figure 24, Panel A) comparing the cell lines.

DAPI + TelC					
	HeLa	Saos-2	SW480-LT	SW480-ST	U2OS
n Cells	249	238	351	175	570
Mean ALT spots/cell	0.30	2.18	2.35	0.05	6.33
SD spots/cell	1.26	2.29	4.57	0.33	3.95
Range	1	1	36	10	20
			P values		
HeLa		**** (<0.0001)	**** (<0.0001)	* (0.0253)	**** (<0.0001)
Saos-2	**** (<0.0001)		ns (0.9746)	**** (<0.0001)	**** (<0.0001)
SW480-LT	**** (<0.0001)	ns (0.9746)		**** (<0.0001)	**** (<0.0001)
SW480-ST	* (0.0253)	**** (<0.0001)	**** (<0.0001)		**** (<0.0001)
U2OS	**** (<0.0001)	**** (<0.0001)	**** (<0.0001)	**** (<0.0001)	

Table 50: Statistics (Brown-Forsythe and Welch ANOVA with Games-Howell's multiple comparisons follow-up test) of the ALT-spot area quantification of the preliminary ALT-FISH experiment (See Figure 24, Panel B).

DAPI + TelC					
	HeLa	Saos-2	SW480-LT	SW480-ST	U2OS
n ALT spots	75	519	826	9	3610
Mean Area [µm^2]	0.96	2.70	0.91	0.90	2.06
SD Area	0.37	1.80	0.33	0.37	1.06
			P values		
HeLa		**** (<0.0001)	ns (0.8187)	ns (0.9891)	**** (<0.0001)
Saos-2	**** (<0.0001)		**** (<0.0001)	**** (<0.0001)	**** (<0.0001)
SW480-LT	ns (0.8187)	**** (<0.0001)		ns (>0.9999)	**** (<0.0001)
SW480-ST	ns (0.9891)	**** (<0.0001)	ns (>0.9999)		**** (<0.0001)
U2OS	**** (<0.0001)	**** (<0.0001)	**** (<0.0001)	**** (<0.0001)	

Table 51: Statistics (Brown-Forsythe and Welch ANOVA with Games-Howell's multiple comparisons follow-up test) of the ALT-spot signal intensity quantification of the preliminary ALT-FISH experiment (See Figure 24, Panel C).

	DAPI + TelC				
	HeLa	Saos-2	SW480-LT	SW480-ST	U2OS
n ALT spots	75	519	826	9	3610
Mean ALT spot Intensity	60.66	102.70	60.86	67.47	91.47
SD ALT spot Intensity	7.37	79.92	12.49	13.60	39.43
			P values		
HeLa		**** (<0.0001)	ns (0.9996)	ns (0.6008)	**** (<0.0001)
Saos-2	**** (<0.0001)		**** (<0.0001)	**** (<0.0001)	* (0.0149)
SW480-LT	ns (0.9996)	**** (<0.0001)		ns (0.6156)	**** (<0.0001)
SW480-ST	ns (0.6008)	**** (<0.0001)	ns (0.6156)		** (0.0045)
U2OS	**** (<0.0001)	* (0.0149)	**** (<0.0001)	** (0.0045)	

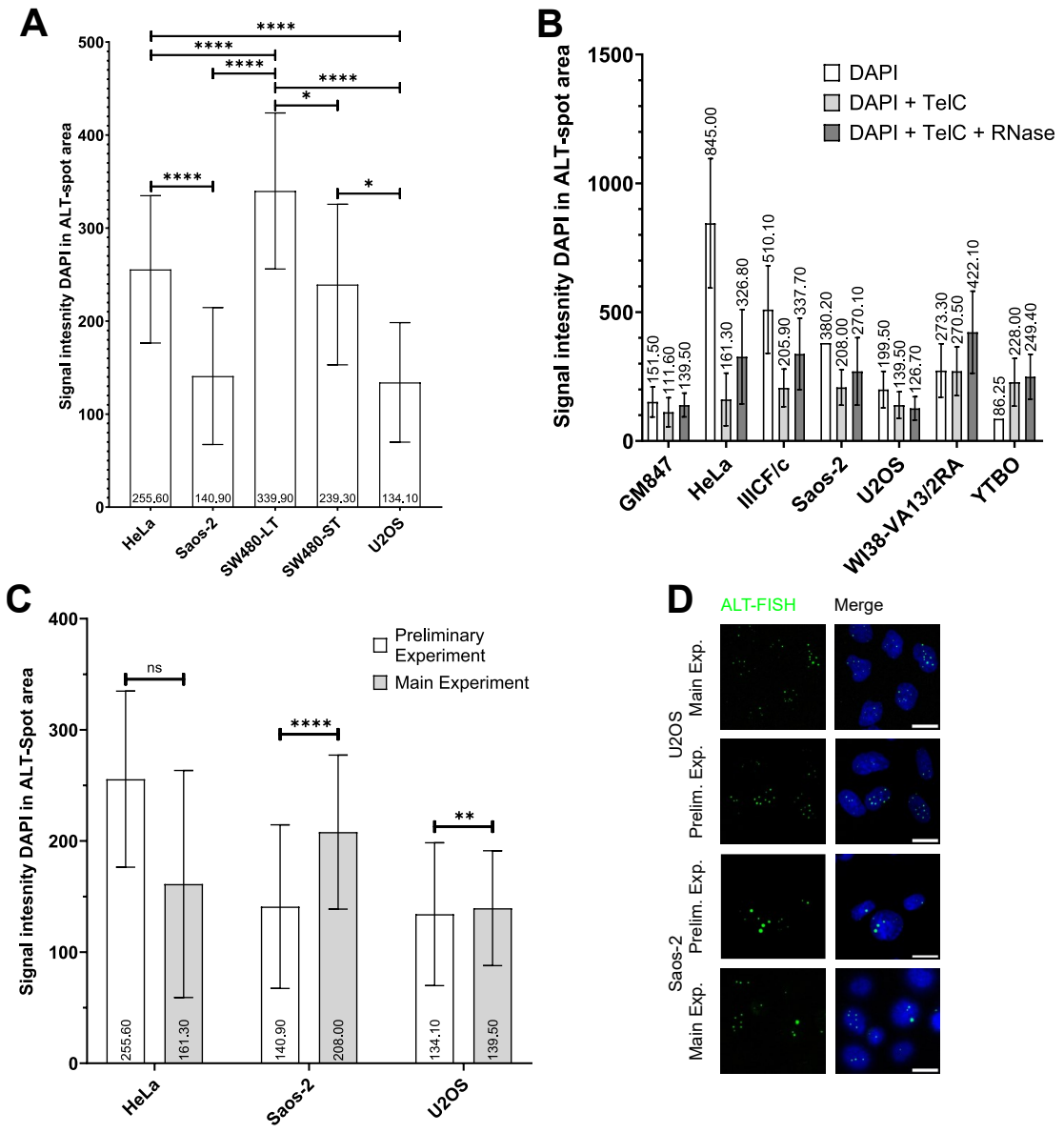

Figure 25: Quantification and comparison of the DAPI signal intensity in the ALT-spot area in the main and the preliminary ALT-FISH experiment. Both experiments are biological replicates of each other. No technical replicates for each. A: Quantification of the mean DAPI signal intensity in ALT-spot area ± SD of five different cell lines of the preliminary ALT-FISH experiment stained using Atto 633 labeled TelC probes for ALT-spot detection and DAPI for nuclear staining. Statistics are shown in Table 52. B: Quantification of the mean DAPI signal intensity in ALT-spot area ± SD of seven different cell lines of the main and the preliminary stained using Atto 633 labeled TelC probes for ALT-spot detection and DAPI for nuclear staining. The cells have undergone three different treatments. Statistics can be found in Table 53 and Table 54. C: Portrayal of the mean DAPI signal intensity in ALT-Spot area ± SD of the analyzed cell lines of the main and the preliminary experiment. Statistics are presented in Table 55. D: Microscopical confocal spinning disc images at 400x magnification of two ALT-positive cell lines (Saos-2 and U2OS) of the main and preliminary experiment

stained using Atto 633 labeled TelC probes for ALT-spot detection and DAPI for nuclear staining. Scale bar: 20 µm.

Table 52: Statistics (Brown-Forsythe and Welch ANOVA with Games-Howell's multiple comparisons follow-up test) of the DAPI signal intensity quantification in the ALT-spot area of the preliminary ALT-FISH experiment (See Figure 25, Panel A).

DAPI + TelC					
	HeLa	Saos-2	SW480-LT	SW480-ST	U2OS
n ALT spots	75	519	826	9	3610
Mean DAPI Intensity	255.60	140.90	339.90	239.30	134.10
SD DAPI Intensity	79.20	73.61	83.90	86.35	64.27
			P values		
HeLa		**** (<0.0001)	**** (<0.0001)	ns (0.9807)	**** (<0.0001)
Saos-2	**** (<0.0001)		**** (<0.0001)	ns (0.0526)	ns (0.2681)
SW480-LT	**** (<0.0001)	**** (<0.0001)		* (0.0474)	**** (<0.0001)
SW480-ST	ns (0.9807)	ns (0.0526)	* (0.0474)		* (0.0381)
U2OS	**** (<0.0001)	ns (0.2681)	**** (<0.0001)	* (0.0381)	

Table 53: Statistics (two-way ANOVA with Tukey's multiple comparisons follow-up test) of the DAPI signal intensity quantification in the ALT-spot area of the main ALT-FISH experiment (See Figure 25, Panel B) comparing the cell lines.

DAPI only

		*GM847**	HeLa	IIICF/c	Saos-2	U2OS	WI38-VA13/2RA	YTBO
Mean DAPI Intensity		151.50	845.00	510.10	380.20	199.50	273.30	86.25
SD DAPI Intensity		58.25	251.10	170.00	0.00	70.87	104.00	0.00
n ALT spots		7	3	6	1	33	6	1
*GM847**	P values		**** (<0.0001)	**** (<0.0001)	ns (0.4629)	ns (0.9451)	ns (0.4333)	ns (0.9981)
HeLa	P values	**** (<0.0001)		*** (0.0004)	** (0.0054)	**** (<0.0001)	**** (<0.0001)	**** (<0.0001)
IIICF/c	P values	**** (<0.0001)	*** (0.0004)		ns (0.9333)	**** (<0.0001)	** (0.0042)	** (0.0075)
SAOS-2	P values	ns (0.4629)	** (0.0054)	ns (0.9333)		ns (0.6806)	ns (0.974)	ns (0.4995)
U2OS	P values	ns (0.9451)	**** (<0.0001)	**** (<0.0001)	ns (0.6806)		ns (0.7468)	ns (0.9532)
WI38-VA13/2RA	P values	ns (0.4333)	**** (<0.0001)	** (0.0042)	ns (0.974)	ns (0.7468)		ns (0.7086)
YTBO	P values	ns (0.9981)	**** (<0.0001)	** (0.0075)	ns (0.4995)	ns (0.9532)	ns (0.7086)	

TelC

		*GM847**	HeLa	IIICF/c	Saos-2	U2OS	WI38-VA13/2RA	YTBO
Mean DAPI Intensity		111.60	161.30	205.90	208.00	139.50	270.50	228.00
SD DAPI Intensity		56.42	102.10	73.13	69.26	51.69	94.64	92.59
n ALT spots		4	2	1762	993	2633	2094	296
*GM847**	P values		ns (<0.0001)	ns (<0.0001)	ns (<0.0001)	ns (0.9894)	ns (<0.0001)	ns (<0.0001)
HeLa	P values	ns (<0.0001)		ns (>0.9999)	ns (0.676)	ns (<0.0001)	ns (0.0958)	ns (0.299)
IIICF/c	P values	ns (<0.0001)	ns (>0.9999)		ns (<0.0001)	**** (<0.0001)	**** (<0.0001)	* (<0.0001)
SAOS-2	P values	ns (<0.0001)	ns (0.676)	ns (<0.0001)		**** (<0.0001)	**** (<0.0001)	ns (<0.0001)
U2OS	P values	ns (0.9894)	ns (<0.0001)	**** (<0.0001)	**** (<0.0001)		**** (<0.0001)	**** (<0.0001)
WI38-VA13/2RA	P values	ns (<0.0001)	ns (0.0958)	**** (<0.0001)	**** (<0.0001)	**** (<0.0001)		**** (<0.0001)
YTBO	P values	ns (<0.0001)	ns (0.299)	* (<0.0001)	ns (<0.0001)	**** (<0.0001)	**** (<0.0001)	

TelC + RNase treatment

		*GM847**	HeLa	IIICF/c	Saos-2	U2OS	WI38-VA13/2RA	YTBO
Mean DAPI Intensity		139.50	326.80	337.70	270.10	126.70	422.10	249.40
SD DAPI Intensity		46.05	183.00	138.50	130.60	45.47	159.20	87.08
n ALT spots		43	10	3188	1789	2296	4013	1069
*GM847**	P values		**** (0.9986)	**** (0.6187)	**** (0.5942)	ns (0.9988)	**** (0.0645)	**** (0.3635)
HeLa	P values	**** (0.9986)		ns (0.9977)	ns (0.997)	**** (>0.9999)	ns (0.8076)	ns (0.98)
IIICF/c	P values	**** (0.6187)	ns (0.9977)		**** (0.9991)	**** (<0.0001)	**** (<0.0001)	**** (0.0258)
SAOS-2	P values	**** (0.5942)	ns (0.997)	**** (0.9991)		**** (<0.0001)	**** (<0.0001)	**** (0.0935)
U2OS	P values	ns (0.9988)	**** (>0.9999)	**** (<0.0001)	**** (<0.0001)		**** (<0.0001)	**** (<0.0001)
WI38-VA13/2RA	P values	**** (0.0645)	ns (0.8076)	**** (<0.0001)	**** (<0.0001)	**** (<0.0001)		**** (<0.0001)
YTBO	P values	**** (0.3635)	ns (0.98)	**** (0.0258)	**** (0.0935)	**** (<0.0001)	**** (<0.0001)	

Table 54: Statistics (two-way ANOVA with Tukey's multiple comparisons follow-up test) of the DAPI signal intensity quantification in the ALT-spot area of the main ALT-FISH experiment (See Figure 25, Panel B) comparing the treatments.

	DAPI	DAPI + TelC	DAPI + TelC + RNase treatment
		*GM847**	
Mean DAPI Intensity	151.50	111.60	139.50
SD DAPI Intensity	58.25	56.42	46.05
n ALT spots	7	4	43
		P values	
DAPI only		ns (0.8345)	ns (0.962)
DAPI + TelC	ns (0.8345)		ns (0.8805)
DAPI + TelC + RNase treatment	ns (0.962)	ns (0.8805)	
		HeLa	
Mean DAPI Intensity	845.00	161.30	326.80
SD DAPI Intensity	251.10	102.10	183.00
n ALT spots	3	2	10
		P values	
DAPI only		**** (<0.0001)	**** (<0.0001)
DAPI + TelC	**** (<0.0001)		ns (0.132)
DAPI + TelC + RNase treatment	**** (<0.0001)	ns (0.132)	
		IIICF/c	
Mean DAPI Intensity	510.10	205.90	337.70
SD DAPI Intensity	170.00	73.13	138.50
n ALT spots	6	1762	3188
		P values	
DAPI only		**** (<0.0001)	*** (0.0004)
DAPI + TelC	**** (<0.0001)		**** (<0.0001)
DAPI + TelC + RNase treatment	*** (0.0004)	**** (<0.0001)	
		Saos-2	
Mean DAPI Intensity	380.20	208.00	270.1
SD DAPI Intensity	0.00	69.26	130.6
n ALT spots	1	993	1789
		P values	
DAPI only		ns (0.2679)	ns (0.5826)
DAPI + TelC	ns (0.2679)		**** (<0.0001)
DAPI + TelC + RNase treatment	ns (0.5826)	**** (<0.0001)	
		U2OS	
Mean DAPI Intensity	199.50	139.50	126.7
SD DAPI Intensity	70.87	51.69	45.47
n ALT spots	33	2633	2296
		P values	
DAPI only		** (0.0058)	*** (0.0005)
DAPI + TelC	** (0.0058)		*** (0.0002)
DAPI + TelC + RNase treatment	*** (0.0005)	*** (0.0002)	
		WI38-VA13/2RA	
Mean DAPI Intensity	273.3	270.5	422.1
SD DAPI Intensity	104	94.64	159.2
n ALT spots	6	2094	4013
		P values	
DAPI only		ns (0.9979)	** (0.003)
DAPI + TelC	ns (0.9979)		**** (<0.0001)
DAPI + TelC + RNase treatment	** (0.003)	**** (<0.0001)	
		YTBO	
Mean DAPI Intensity	86.25	228	249.4
SD DAPI Intensity	0	92.59	87.08
n ALT spots	1	296	1069
		P values	
DAPI only		ns (0.4099)	ns (0.3063)
DAPI + TelC	ns (0.4099)		** (0.0094)
DAPI + TelC + RNase treatment	ns (0.3063)	** (0.0094)	

Table 55: Statistics (two-way ANOVA with Sidak's multiple comparisons follow-up test) of the DAPI signal intensity quantification in the ALT-spot area of the result comparison from the main and the preliminary ALT-FISH experiment (See Figure 25, Panel C).

DAPI + TelC

				HeLa Prelim. Exp.	Saos-2 Prelim. Exp.	U2OS Prelim. Exp.
			n ALT spots	75	519	3610
			Mean DAPI Intensity	255.60	140.90	134.10
	n ALT spots	Mean DAPI Intensity	SD DAPI Intensity	79.20	73.61	64.27
					P values	
HeLa Main Exp.	2	161.30	102.10	ns (0.0971)		
Saos-2 Main Exp.	993	208.00	69.26		**** (<0.0001)	
U2OS Main Exp.	2633	139.50	51.69			** (0.002)

11.3. qPCR-based variant detection

11.3.1. gDNA samples

Table 56: Raw CT values of the cell lines of the main and preliminary variant detection qPCR experiments.

		*GM847** (ALT)			IIICF/c (ALT)			HeLa (TA)			U2OS (ALT)			Saos-2 (ALT)			WI38-VA13/2RA (ALT)			HT-1080 [PTL] (TA)			YTBO (ALT)		
Prelim. Exp.		23.09	23.26	23.18	22.88	22.84	22.94	23.42	23.31	23.42	23.70	23.62	23.56	23.77	23.77	23.87	21.32	21.36	21.27	22.40	22.43	22.54	23.56	23.57	23.58
Main Exp.	36B4	21.55	21.60	21.70	21.73	21.63	21.72	21.53	21.71	21.67	21.56	21.60	21.59	21.47	21.49	21.67	21.70	21.61	21.62	21.73	21.74	21.69	21.70	21.64	21.79
Prelim. Exp.	TTA	14.37	14.51	14.62	15.65	15.63	15.61	17.58	17.81	17.85	13.48	13.50	13.58	16.99	17.05	17.11	12.15	12.13	12.18	17.55	17.58	17.56	16.81	16.68	16.63
Main Exp.	TTA	19.18	19.22	19.25	15.71	15.60	15.64	18.41	18.19	18.28	13.19	12.27	12.73	16.20	16.05	16.01	15.09	15.07	15.12	17.52	17.47	17.47	16.09	15.96	15.97
Prelim. Exp.	TCA	18.66	18.66	18.84	23.38	23.31	23.38	24.40	24.73	24.45	22.36	22.39	22.49	23.20	23.29	23.28	15.07	15.25	15.02	23.33	23.28	23.62	20.75	20.74	20.76
Main Exp.	TCA	23.37	23.44	23.22	23.28	23.44	23.43	23.77	23.69	23.44	21.13	21.12	21.10	22.08	22.24	22.11	17.66	17.80	19.87	23.21	23.32	23.45	19.58	19.52	

Prelim. Exp. TGA	22.48	22.44	22.51	21.66	21.66	21.76	23.56	23.62	23.59	22.03	22.00	22.12	23.39	23.51	23.49	19.80	20.10	20.08	22.35	22.23	22.34	18.91	18.81	18.84
Main Exp. TGA	22.82	22.68	22.60	21.54	21.53	21.57	23.07	23.02	23.03	20.69	20.61	20.72	22.62	22.30	22.35	22.03	21.89	21.88	22.01	22.04	21.95	18.20	17.81	17.78
Prelim. Exp. TAA	24.27	24.11	24.23	24.84	24.59	24.57	26.18	26.37	26.44	23.20	23.28	23.28	26.07	26.08	26.15	22.26	22.20	22.33	25.42	25.45	25.48	24.81	24.71	24.77
Main Exp. TAA	26.55	26.45	26.53	24.55	25.10	24.56	25.88	25.69	26.01	22.31	22.55	22.07	24.54	24.61	24.96	24.19	24.16	24.38	25.38	25.42	25.48	23.82	23.91	23.71
Prelim. Exp.	23.09	23.26	23.18	22.88	22.84	22.94	23.42	23.31	23.42	23.70	23.62	23.56	23.77	23.77	23.87	21.32	21.36	21.27	22.40	22.43	22.54	23.56	23.57	23.58

Table 57: Raw CT values of the NTCs and standards of the main and preliminary variant detection qPCR experiments.

	CT values																			
	NTC			Std. 1			Std. 2			Std. 3			Std. 4			Std. 5			Std. 6	
Prelim. Exp. 36B4	40	40	40	11.15	11.14	11.16	14.37	14.28	14.36	18.05	18.01	17.92	21.28	21.29	21.36	25.03	24.91	25.01	28.43	28.30	28.58
Main Exp. 36B4	37.71	40	40	11.49	11.35	11.37	14.85	14.82	14.77	18.3	18.31	18.22	21.61	21.62	21.61	25.44	25.08	25.07	28.66	28.9	28.56
Prelim. Exp. TTA	27.52	27.55	27.17	5.80	6.26	6.12	10.20	10.22	10.33	13.41	13.38	13.55	17.07	16.88	17.09	20.15	20.15	20.22			
Main Exp. TTA	23.48	23.27	23.25	6.49	6.53	6.24	9.9	9.93	10.62	14.2	14.1	14.05	17.42	17.68	17.45	20.72	20.87	21.09	22.78	23.25	23.16
Prelim. Exp. TCA	27.23	27.47	27.45	11.52	11.52	11.57	14.80	14.88	15.05	18.03	18.18	18.23	21.48	21.65	21.67	24.69	24.83	24.88	26.77	26.86	27.00
Main Exp. TCA	28.58	28.89	28.91	12.86	13.23	13.43	17.17	17.07	17.03	20.55	20.26	20.43	24.22	24.11	24.82	27.1	27.1	27.12	29.63	29.15	29.01

Prelim. Exp. TGA	28.49	28.58	28.50	13.18	13.18	13.26	16.45	16.37	16.47	20.07	19.94	20.04	23.25	23.28	23.33	26.32	26.35	26.42		
Main Exp.	26.51	24.39	28.12	14.94	14.81	14.93	18.17	18.29	18.52	21.69	21.71	21.39	24.67	22.93	22.95	24.76	24.99	25.55	28.35	27.65	24.9
Prelim. Exp. TAA	30.46	30.62	30.61	12.54	12.48	12.58	15.88	15.77	15.84	19.22	19.19	19.25	22.68	22.72	22.87	26.1	26.13	26.18	28.79	28.86	29.07
Main Exp. TAA	28.42	26.08	26.84	14.63	15.16	14.75	18.21	18.31	18.34	22.02	21.59	22.02	24.81	24.71	25.08	26.75	26.81	26.49	30.79	26.7	29.35

11.3.2. Correlation with whole genome sequencing data

Table 58: Values of correlation analysis of WGS and qPCR data shown in Figure 14.

TCAGGG		
	log% WGS	log% qPCR
IIICF/c (ALT)	0.10	-0.78
HeLa (TA)	0.33	-0.04
U2OS (ALT)	-0.57	-0.98
Saos-2 (ALT)	-0.07	-0.25
Wi38-VA13/2RA (ALT)	1.40	0.85
HT-1080 [PTL] (TA)	0.35	-0.19
HT-1080 hTR wt (TA)	0.02	-0.51

TGAGGG		
	log% WGS	log% qPCR
IIICF/c (ALT)	0.38	0.23
HeLa (TA)	0.61	0.61
U2OS (ALT)	-0.24	-0.43
Saos-2 (ALT)	0.25	0.11
Wi38-VA13/2RA (ALT)	0.52	-0.05
HT-1080 [PTL] (TA)	0.66	0.67
HT-1080 hTR wt (TA)	0.28	0.24

TGAGGG				
	% WGS	% qPCR	SEM %qPCR	n % qPCR
IIICF/c (ALT)	0.41	0.22	0.02	3
HeLa (TA)	0.52	0.68	0.05	3
U2OS (ALT)	0.12	0.13	0.03	3
Saos-2 (ALT)	0.26	0.30	0.03	3
Wi38-VA13/2RA (ALT)	0.64	0.20	0.01	3
HT-1080 [PTL] (TA)	0.66	0.50	0.01	3
HT-1080 hTR wt (TA)	0.32	0.27	0.02	3

11.3.1. C-circle assay products

Table 59: SQ values of SCG-, canonical and variant repeats of the CCA assay products

Treatments and cell lines	36B4			TTAGGG			TCAGGG			TGAGGG			TAAGGG		
	Avg. SQ	SEM	n	Avg. SQ	SEM	n	Avg. SQ	SEM	n	Avg. SQ	SEM	n	Avg. SQ	SEM	n
Phi+ *GM847**	2685.43	92.26	3	46172.55	2139.28	3	1501.06	99.44	3	4243.96	451.20	3	140.23	29.51	3
Phi- *GM847**	2523.21	24.51	3	63522.13	2003.32	3	1624.05	20.70	3	4356.15	106.14	3	166.16	11.74	3
Phi + WI38VA13	5310.52	197.54	3	2063961.22	53911.78	3	132608.78	11928.50	3	11057.78	762.92	3	1334.17	185.73	3
Phi - WI38VA13	3387.63	123.95	3	1438479.92	10407.74	3	74680.65	4068.74	3	5651.42	321.52	3	545.15	128.04	3
Phi+ IIICF/c	2414.48	35.17	3	4716473.55	186591.46	3	4960.83	353.71	3	28001.68	3203.10	3	1027.04	288.96	3
Phi- IIICF/c	1327.84	38.37	3	812997.58	86437.76	2	1495.29	32.35	3	6016.32	121.32	3	273.59	6.45	3
Phi + HT1080 PTL	3988.33	137.89	3	234921.92	23149.33	3	2360.99	57.94	3	9015.05	93.04	3	346.71	45.04	3
Phi -HT1080 PTL	3025.76	42.56	3	187422.32	6822.41	3	1823.92	119.32	3	6477.12	499.37	3	215.76	43.41	3
Phi+ HeLa	4351.23	125.91	3	158408.39	12420.28	3	2678.02	293.06	3	6581.76	285.35	3	305.44	9.64	3
Phi- HeLa	2764.76	63.89	3	162593.79	1575.70	3	1867.49	26.65	3	3933.84	97.75	3	222.87	16.08	3
Phi +HT1080 hTR wt	4060.92	352.97	3	866152.19	72667.81	3	2783.82	98.52	3	8108.61	190.26	3	518.24	25.14	3
Phi -HT1080 hTR wt	3254.85	184.66	3	905153.20	68761.54	3	2571.00	158.96	3	7252.92	109.82	3	427.22	28.05	3
Phi+ U2OS	1936.69	36.37	3	7391712.77	474553.61	3	5783.35	425.74	3	13951.62	1059.84	3	1786.77	300.15	3
Phi- U2OS	1502.40	37.75	3	4420640.54	216353.19	3	2912.31	79.88	3	8083.07	233.57	3	989.45	38.69	3
Phi+ YTBO	3945.35	133.54	3	12104128.15	666065.45	3	162736.10	8096.46	3	1991927.38	52430.82	3	11519.49	1710.11	3
Phi- YTBO	2586.61	44.52	3	606967.30	13252.18	3	11981.88	312.56	3	94324.17	7402.41	3	510.17	28.37	3
Phi+Saos-2	5396.57	56.04	3	65947162.01	3348067.53	3	63303.28	3240.18	3	48046.20	5400.92	3	20179.32	226.76	3
Phi- Saos-2	2382.07	19.72	3	622923.87	16652.56	3	2560.91	44.52	3	3714.37	122.99	3	321.16	6.80	3
Phi+ Positive Ctrl. [U2OS]	9034.22	87.77	3	113447201.30	8697483.86	3	47443.11	4999.10	3	150382.16	7421.97	3	24830.89	2407.09	3
Phi- Positive Ctrl. [U2OS]	6488.14	477.31	3	15341059.79	966500.47	3	7215.56	649.71	3	30071.88	933.50	3	2954.13	238.19	3

Phi+ Positive Ctrl. [Saos-2]	4790.96	161.53	3	132985581.25	7860540.37	3	103673.21	14230.52	3	95874.31	3709.63	3	29093.97	4766.62	3
Phi- Positive Ctrl. [Saos-2]	3295.11	156.74	3	824934.35	30128.70	3	3632.54	479.70	3	4756.23	199.52	3	350.01	32.05	3
Phi+ negative Ctrl.	6.86	2.38	3	2137.36	142.18	3	1022.85	30.28	3	1141.72	27.20	3	58.62	6.22	3
Phi- negative Ctrl.	3.46	0.00	1	1677.47	88.89	3	1062.12	62.49	3	960.51	95.08	3	64.21	5.84	3

Table 60: Raw CT values of the C-circle assay product variant detection qPCR experiment.

Treatments and cell lines	CT values														
	36B4			TTAGGG			TCAGGG			TGAGGG			TAAGGG		
Phi+ *GM847**	25.28	25.12	25.28	23.10	22.93	23.15	27.30	27.52	27.15	26.21	25.95	25.68	30.82	30.57	29.86
Phi- *GM847**	25.30	25.35	25.31	22.63	22.52	22.67	27.22	27.15	27.20	25.89	25.84	25.96	29.95	30.11	30.30
Phi + WI38-VA13/2RA	24.30	24.15	24.10	17.60	17.66	17.73	20.58	20.11	20.16	24.70	24.64	24.38	27.09	26.82	27.53
Phi - WI38-VA13/2RA	24.80	24.84	24.98	18.16	18.17	18.19	21.01	21.29	21.22	25.39	25.53	25.67	27.86	28.63	28.94
Phi+ IIICF/c	25.43	25.35	25.38	16.59	16.39	16.49	25.65	25.43	25.26	23.00	23.57	23.21	28.19	27.75	26.86
Phi- IIICF/c	26.35	26.35	26.22	18.84	19.14		27.36	27.26	27.35	25.49	25.40	25.41	29.36	29.37	29.46
Phi + HT1080 PTL	24.72	24.54	24.60	20.85	20.94	20.49	26.54	26.60	26.68	24.89	24.85	24.84	29.10	28.75	29.39
Phi - HT1080 PTL	25.04	25.01	25.08	20.97	21.08	21.15	26.84	27.01	27.20	25.16	25.30	25.55	29.27	29.85	30.26
Phi+ HeLa	24.42	24.47	24.57	21.44	21.40	21.10	26.71	26.44	26.12	25.43	25.28	25.22	29.31	29.16	29.25
Phi-HeLa	25.17	25.13	25.25	21.27	21.24	21.29	26.96	27.02	26.94	26.05	25.98	26.10	29.57	29.91	29.61
Phi +HT1080 hTR wt	24.71	24.75	24.35	19.07	18.96	18.68	26.37	26.24	26.42	25.07	25.01	24.95	28.34	28.52	28.57
Phi -HT1080 hTR wt	24.77	24.97	25.07	18.85	18.65	19.02	26.31	26.46	26.65	25.20	25.17	25.13	28.59	28.78	28.91
Phi+ U2OS	25.73	25.78	25.68	15.87	15.69	16.00	25.44	25.05	25.11	24.09	24.18	24.46	27.18	26.71	26.32
Phi- U2OS	26.16	26.14	26.04	16.50	16.53	16.72	26.20	26.27	26.35	25.04	24.93	25.07	27.54	27.65	27.46
Phi + YTBO	24.57	24.74	24.61	15.08	15.31	15.07	19.83	20.10	19.91	17.17	17.21	17.09	23.72	23.94	24.48
Phi - YTBO	25.29	25.23	25.32	19.46	19.39	19.35	23.97	24.10	24.08	21.72	21.49	21.33	28.35	28.59	28.57
Phi+Saos2	24.13	24.15	24.19	12.77	12.61	12.85	21.28	21.55	21.47	22.63	22.18	22.65	23.24	23.20	23.18
Phi- Saos2	25.40	25.40	25.43	19.29	19.37	19.43	26.42	26.51	26.50	26.03	26.18	26.15	29.18	29.11	29.21

Phi+ Positive Ctrl. [U2OS]	23.36	23.40	23.35	12.00	12.15	11.78	22.04	22.08	21.58	20.77	20.99	20.78	23.16	22.93	22.68
Phi- Positive Ctrl. [U2OS]	23.88	23.69	24.08	14.65	14.95	14.86	24.61	24.86	25.11	23.10	23.23	23.09	25.88	25.84	26.22
Phi+ Positive Ctrl. [Saos-2]	24.41	24.37	24.24	11.62	11.72	11.91	20.28	20.98	20.79	21.49	21.58	21.39	22.27	22.95	22.93
Phi- Positive Ctrl. [Saos-2]	24.88	24.81	25.06	19.00	18.86	19.03	25.59	25.97	26.30	25.66	25.87	25.79	28.93	28.90	29.33
Phi+ negative Ctrl.	33.58	34.77	35.30	27.41	27.60	27.27	28.01	27.87	27.87	27.87	27.81	27.75	31.35	31.69	31.85
Phi- negative Ctrl.		35.42		27.62	27.86	27.82	27.69	27.93	27.98	27.81	28.10	28.29	31.27	31.73	31.48
10mMTris+H2O1:3	36.29	34.49	36.49	28.03	27.87	27.71	28.22	27.79	27.64	28.35	28.29	28.31	30.06	28.79	29.71
Std. 1	15.14	15.06	15.16	11.42	11.52	11.76	12.98	12.98	12.91	14.26	14.24	14.29	13.57	14.20	13.83
Std. 2	18.58	18.61	18.65	15.06	14.61	15.04	16.64	16.64	16.66	17.67	17.65	17.89	16.91	16.92	17.14
Std. 3	22.15	22.18	22.23	18.39	18.23	18.80	20.14	20.14	20.09	21.04	21.11	21.15	20.43	20.32	20.41
Std. 4	25.87	25.79	25.86	21.69	21.76	22.01	23.38	23.38	23.46	24.54	24.62	24.75	24.05	23.99	24.08
Std. 5	29.35	29.03	29.30	24.35	24.47	24.75	27.66	27.66	27.79	27.21	27.32	27.41	27.35	27.52	27.46
Std. 6													30.05	30.11	30.31

11.3.2. TCAGGG and TGAGGG restriction digest products

Table 61: Raw CT values of the TCAGGG and TGAGGG restriction digest products variant detection qPCR experiment.

Treatments and cell lines	CT values								
	TTAGGG			TCAGGG			TGAGGG		
WI38-VA13 LpnPI	16.56	16.32	16.12	18.09	18.15	18.06			
WI38-VA13 uncut	16.74	16.40	16.39	17.88	17.99	18.03			
YTBO MnlI	17.50	17.56	17.52				20.86	20.77	20.83
YTBOHpHI	17.44	17.24	17.28				20.02	20.09	20.09
YTBO Uncut	17.65	17.52	17.50				18.56	18.71	18.59
NTC	28.54	28.39	27.95	28.47	27.80	28.94	28.73	28.99	28.10
Std. 1	11.46	11.26	11.54	13.14	12.88	12.97	13.97	14.03	14.27
Std. 2	14.84	14.83	14.71	16.63	16.53	16.85	17.44	17.50	17.66
Std. 3	17.56	18.29	18.48	20.27	20.09	20.40	21.03	21.16	21.17
Std. 4	21.74	21.54	21.67	23.53	23.26	23.47	24.43	24.39	24.58
Std. 5	24.74	24.79	24.98	26.38	26.49	26.56	27.14	27.39	27.57

11.3.3. TCAGGG cluster variant DNA oligomer qPCR

Table 62: Raw CT values of the TCAGGG cluster variant DNA oligomer qPCR experiment.

Molecules	CT values																	
	Telg-C_1x (13 Hex)			Telg-C_2x (14 Hex)			Telg-C_4x (16 Hex)			Telg-C_8x (20 Hex)			Telg-C_7xL (13 Hex)			Telg-C_7xR (13 Hex)		
NTC	28.89	28.58	28.77	28.89	28.58	28.77	28.89	28.58	28.77	28.89	28.58	28.77	28.89	28.58	28.77	28.89	28.58	28.77
10^8	12.62	12.46	13.89	13.45	12.83	12.92	14.91	14.07	13.88	15.01	15.35	15.46	14.3	14.21	14.37	15.76	15.66	16.16
10^7	16.06	15.89	15.74	16.19	16.71	16.39	17.17	17.09	17.42	18.34	18.36	18.62	17.57	17.41	17.87	19.06	19.01	19.29
10^6	19.18	18.95	19.12	20.04	19.51	19.81	20.76	20.73	20.46	21.32	22.00	22.9	20.64	20.64	20.88	22.36	23.03	
10^5	22.47	22.43	22.77	23.64	23.45	23.14	24.10	24.05	23.95	24.77	24.92	25.22	24.13	24.11	24.27	25.48	25.68	26.23
10^4	25.59	25.44		25.78	26.06	26.06	26.79	27.04	26.82	27.52	27.75	28.11	26.99	27.11	27.31	27.96	29.01	

11.4. Telomere-variant FISH

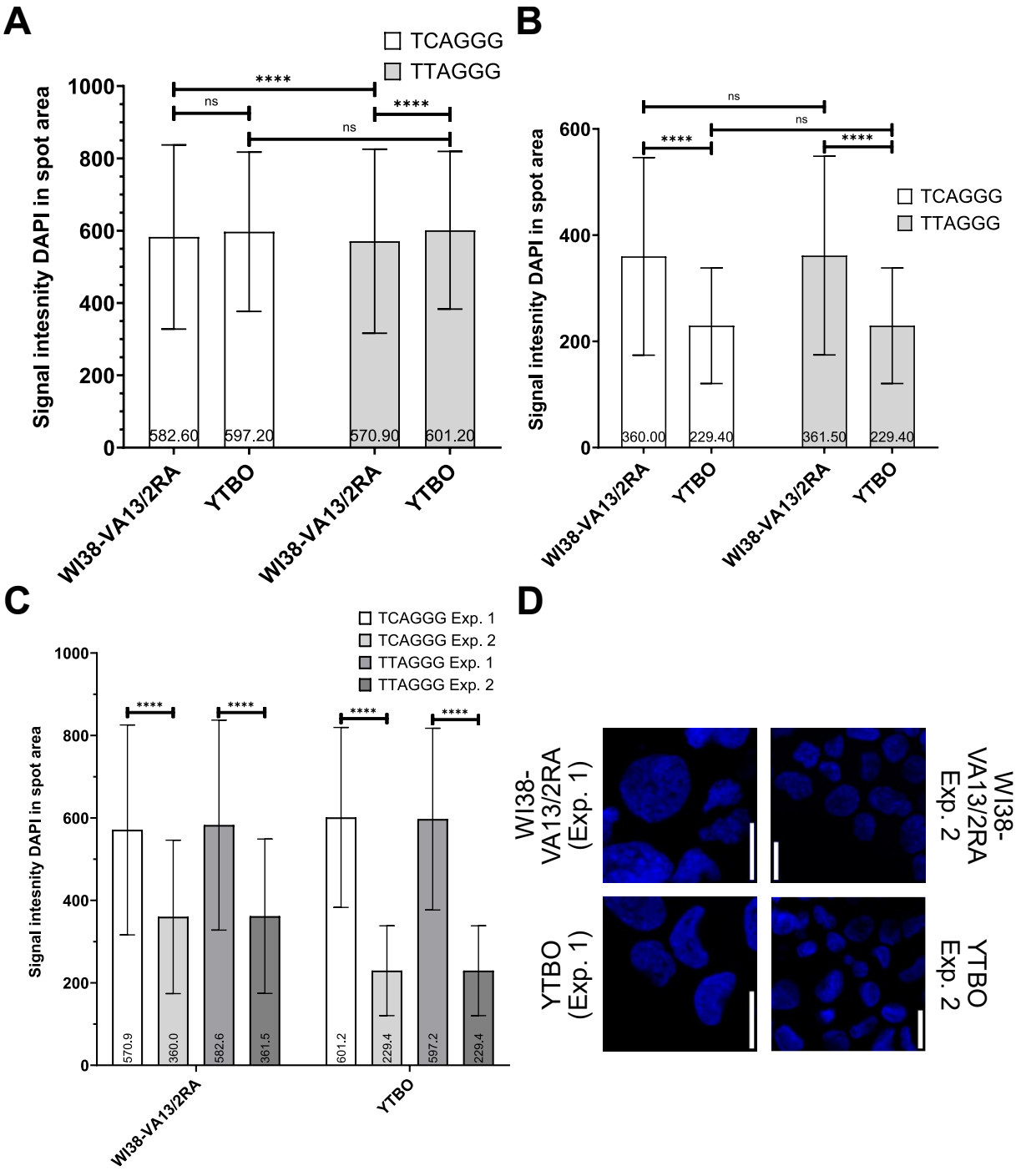

Figure 26: Quantification and comparison of the DAPI signal intensity in TTAGGG- and TCAGGG-spot area of the first and second telomere-variant FISH experiment. Both experiments are biological replicates of each other. No technical replicates for each. Statistics are presented in Table 63. A: Quantification of the mean DAPI signal intensity in TTAGGG- and TCAGGG -spot area ± SD of the cell lines WI38-VA13/2RA and YTBO of the first telomere-variant FISH experiment. B: Quantification of the mean DAPI signal intensity in TTAGGG- and TCAGGG -spot area ± SD of the cell lines WI38-VA13/2RA and YTBO of the second telomere-

variant FISH experiment. C: Comparison of the mean DAPI signal intensity in TTAGGG- and TCAGGG -spot area ± SD of the analyzed cell lines of the main and the Prelim. experiment. D: DAPI channel of microscopical confocal spinning disc images at 600x (Exp.1.), respectively 400x (Exp. 2.) magnification of two ALT-positive cell lines (WI38-VA13/2RA and YTBO) from Experiment 1 and 2, stained using FITC labeled TelC PNA probes for canonical telomere repeat detection, Cy3 labeled PNA probes for TCAGGG detection and DAPI for nuclear staining. Scale bar: 20 µm.

Table 63: Statistics (two-way ANOVA with Tukey's multiple comparisons follow-up test) of the DAPI signal intensity quantification in the TTAGGG- and TCAGGG-spot area of the first and second telomere-variant FISH experiment

Signal intensity DAPI									
			Wi-38-VA13/2RA				YTBO			
		Experiment	1		2		1		2	
		Target	TCAGGG	TTAGGG	TCAGGG	TTAGGG	TCAGGG	TTAGGG	TCAGGG	TTAGGG
		Mean Signal intensity DAPI	582.60	570.90	361.50	360.00	597.20	601.20	229.40	229.40
		SD	254.60	254.60	187.20	186.10	220.40	218.20	108.90	108.90
		n	22418	30541	29353	27053	1117	10255	608	10922
	Experiment	Target	p-values							
Wi-38-VA13/2RA	1	TCAGGG		**** (<0.0001)	**** (<0.0001)	**** (<0.0001)				
		TTAGGG	**** (<0.0001)		**** (<0.0001)	**** (<0.0001)				
	2	TCAGGG	**** (<0.0001)	**** (<0.0001)		ns (0.8401)				
		TTAGGG	**** (<0.0001)	**** (<0.0001)	ns (0.8401)					
YTBO	1	TCAGGG						**** ns (0.9345)	**** (<0.0001)	**** (<0.0001)
		TTAGGG					ns (0.9345)		**** (<0.0001)	**** (<0.0001)
	2	TCAGGG					**** (<0.0001)	**** (<0.0001)		ns (>0.9999)
		TTAGGG					**** (<0.0001)	**** (<0.0001)	ns (>0.9999)	